The Electrosynthesis and Characterisation of Functionalised Poly(indoles)

Alastair David Thomson

Degree of Doctor of Philosophy

University of Edinburgh

1997

"Truth is like a lizard, just when you think you've grasped it, it leaves its tail in your fingers and runs away, knowing full well it will grow a new one in a twinkling."

Ivan Sergeyevich Turgenev

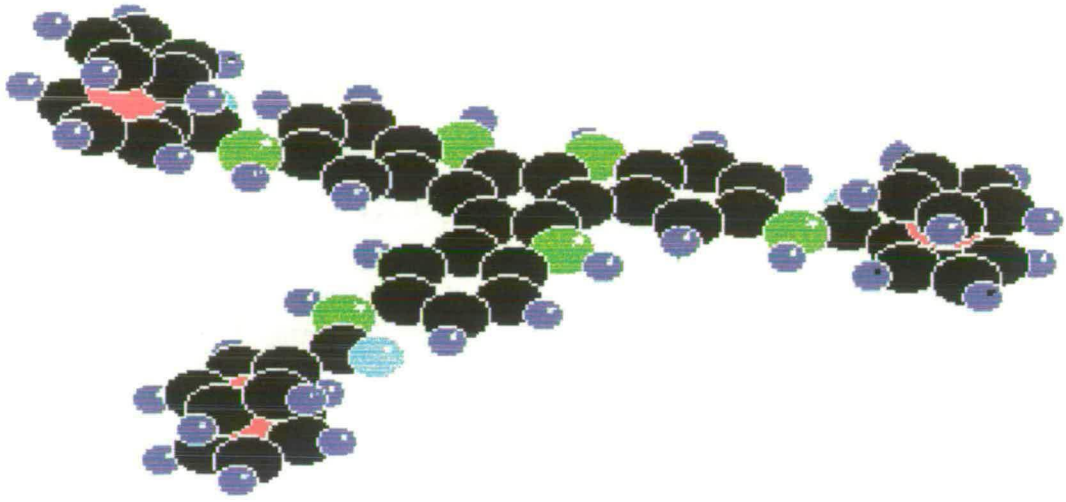

N-(5'-indole)ferroceneamide asymmetric cyclic trimer

Declaration

I hereby, declare that the work presented in this thesis is my own unless otherwise stated by reference.

Alastair David Thomson

April 1997

Acknowledgements

I would like to express my gratitude to the following people for their help in carrying out the work described in this thesis and for making the past three and a bit years so enjoyable :-

Firstly I would like to express my appreciation to my supervisor Dr Andy Mount for his unwavering enthusiasm, eternal optimism, excellent suggestions and help beyond the call of duty throughout my PhD.

In the Lab, Dr Gordon Mackintosh for his assistance with the polymerisation studies, Mark Robertson for his help with computing, and Pete Jennings and Dr Jones for their support with the Flourescence experiments.

The mass spectroscopy studies were carried out in conjuction with Drs' Pat Langridge-Smith, Mike Dale, Scott Wright, Craig Redpath, Ian Mowat and Anita Jones.

The synthesis of the NIFA compound was carried with suggestions and help from Dr Ian Fallis and Dr Steve Ross.

The XRD, SQUID and EPR studies were carried out with help from Dr Andrew Harrison, Dr Gavin Whittaker, Gareth Oakley, and Binbing Zha

I would like to thank the University of Edinburgh for the funding of my PhD through a Faculty of Science and Engineering Scholarship.

Of course, not all of my time here was spent hard at work, and a big reason that it was so enjoyable was due to many of the people that I met here; so a big thanks to, Dave B, Nick, Steve, Lynne, Ian F, Dave D, Gideon, Ali B, Scott, Carole, the neds at Argyle Park Terrace, and all past and present in the "condensed matter" groups for helping me continue the student life-style for as long as possible.

I would like to thank my family for their encouragement and support, and finally I owe a huge amount to Kathy for her enlivening go-getting attitude, support, love and friendship which have made my life so much more rewarding.

Postgraduate courses and lectures

1) Modern aspects of electrochemistry

2) Advanced materials

3) Colloids

4) Colloquia and physical section meetings

5) Unilever

6) ICI

7) Chemical aspects of biotechnology

8) EPSRC "Insight into management" course

9) Mass spectrommetry in action

10) I.R. Spectroscopy

Conferences and meetings

Irvine review lectures, University of St. Andrews 1993

Butler meeting '94, University of St. Andrews 1994

Electrochem '94, University of Edinburgh 1994

Butler meeting '95, University of Strathclyde 1995

Butler meeting '96, University of Edinburgh 1996

Electrochem '96, University of Bath 1996

Firbush physical section meetings, 1993-1996

Publications

P. Jennings, A.C. Jones, A.R. Mount, A.D. Thomson, Electrooxidation of 5-substituted indoles, *J. Chem. Soc. Faraday. Trans.* In Press.

List of Abbreviations

CI	5-Cyanoindole
NI	5-Nitroindole
I	Indole
I5CA	Indole-5-carboxylic acid
Poly(CI)	Poly(5-Cyanoindole)
Poly(NI)	Poly(5-Nitroindole)
Poly(I5CA)	Poly(indole-5-carboxylic acid)
TEA	Tetraethyl ammonium
RDE	Rotating disc electrode
RRDE	Rotating ring-disc electrode
CV	Cyclic voltammetry
LSV	Linear Sweep voltammetry
IR	Infra-red
Equ^n	Equation
:	Indicates a copolymer
/	Indicates the concentration of starting monomer concentrations for production of copolymer
~	Indicates an electrodeposited layer formed on top of a pre-formed polymer layer

Contents

Abstract

The aim of the work presented in this thesis was to investigate the electropolymerisation of indole and various substituted indole monomers, with the objective of electrosynthesising, characterising and functionalising indole-based conducting polymers for possible use as sensor devices.

It was found that on electropolymerisation, all of the substituted indole monomers studied formed asymmetric cyclic trimer species. A mechanism was proposed invoking a 3-3' dimer intermediate to explain the nature of the trimer formed. These trimers were believed to initially form in solution and then deposit on to the electrode surface where they could link to form a polymer film consisting of linked trimer units. The polymer film then facilitated the formation of trimers on the film surface. The electronic nature of the substituents was found to control the reactivity of the trimers, and a correlation was found between the electron withdrawing / donating nature of the substituent and the observed potential of the trimer one electron redox reaction. The lyophilicity of the trimer substituents was found to affect the relative solubility of the trimers which controlled the rate of initial adsorption of trimers on to the electrode surface and the rate of desorption of free trimers from the polymer film. It was discovered that for the electropolymerisation of indoles with highly solubilising substituents, a pre-formed polymer layer could be used to encourage the deposition of trimers on to the film and decrease their desorption rate, this was also used to limit any passivation effects noted for electropolymerisation on Platinum.

The linking mechanism of all the substituted cyclic trimers studied is believed to be very similar. This was tested by studies carried out on the electropolymerisation of N-methylindole. These studies showed that the major product of the N-methylindole electropolymerisation was a highly soluble cyclic trimer species, in addition there was also an appreciable amount of linear polymer produced from the energetically destabilised sterically hindered 3-3'dimer. The absence of any linking of the N-methylindole trimers suggested that the Nitrogen positions in the trimer

are involved in the linking reaction observed for all of the other substituted indoles studied.

To probe the electronic communication between a substituent and the trimer centre, a ferrocene derivatised indole was synthesised, (N-5'-indole)ferroceneamide, and copolymerised with indole-5-carboxylic acid to form a conducting copolymer film containing covalently bound redox active ferrocene groups.

To test whether a substituted polyindole could be used as a sensor device, 5-aminoindole was copolymerised with 5-cyanoindole to produce a conducting polymer film which was potentiometrically sensitive to changes in pH. A similar film was produced which showed selective potentiometric changes to varying concentrations of aqueous Cu^{II} ions which suggests possible use as a simple electrochemical copper ion sensor device.

Chapter 1 - Introduction

1.1 - Polymers.

A polymer is a chain consisting of one or more types of linked chemical units. They were first discovered and characterised in the 1920's and the study of them has since grown into one of the most diverse and important areas of science.

Polymers appear in nature and are indeed the basis of life itself where natural nucleotides link to form large complex polymers termed DNA, but they can also be synthetically produced to form new materials, such as plastics, which represent one of the most important revolutions of the 20^{th} century. They often posses highly useful properties such as strength, elasticity, plasticity, toughness and a low frictional resistance comparable with metals. However they also tend to be lighter, cheaper and more resistant to corrosion. As a result these materials have pervaded every area of modern life with a range of products extending from everyday consumer goods to highly specialised applications in the space and aeronautical industries.

1.2 - Conducting Polymers.

Most of the synthetic polymers produced have been solely electrically insulating materials with conductivities around 10^{-14} Scm^{-1}. However in 1977 it was found that the simple organic compound acetylene, C_2H_2, could be chemically oxidised to form polyacetylene $(CH)_n$ which was found to be electrically conductive[1]. The conductivity of this film was found to be in the semi-conductor range, being considerably less than that for a metal, but it was shown that on oxidatively doping the polyactylene, the conductivity could reach levels comparable with the metals (10^4 Scm^{-1}). Not surprisingly this generated a great deal of interest due to the possibility of combining the useful physical properties of a synthetic organic polymer with the electrical conductivity of a metal. This

was hoped to create an entirely new field of materials research, leading to the development of exciting novel applications and related technologies.

Originally research focused on polyacetylene (PA) although it was found to be air and moisture sensitive (suffering an irreversible loss of conductivity) which has limited its usefulness for practical applications. Research in this area then rapidly expanded to examine other related organic polymers and since then conducting polymers (CPs) have been produced from a multitude of organic molecules. Most of the research workers have concentrated on studying the polyheterocycles such as polypyrrole (PP) and polythiophene (PT), which can be thought of as analogous to the cis form of polyactylene (fig. 1.1). The polyheterocycles are much more stable to oxidation by O_2 in the environment than PA and are therefore better suited for many applied technologies.

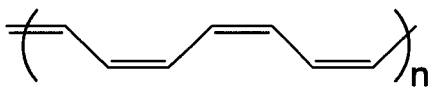

Fig. 1.1 PA -cis form.

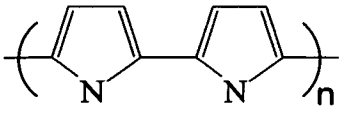

Fig. 1.2 - Polypyrrole benzoid form.

Although research today still focuses mainly on polypyrrole and polythiophene, conducting polymers can be produced from many cyclic benzenoid and non-benzenoid hydrocarbons, the essential characteristic being that the monomers must link together to form a conjugated π-electron system which allows an efficient conduction of charge. The term "conducting polymer" is often now extended to include the whole group of organic aromatic polymers even though not all of them are electrically conducting. Conducting polymers often show many structural similarities, although their resultant physical, mechanical and conductive properties are highly dependent upon the particular nature of the monomer used. Substantial investigation is therefore currently underway on the molecular engineering of novel organic polymers with tailor made conduction, physical and mechanical properties.

1.3 - Synthesis of conducting polymers.

Conducting polymers are generally produced by the oxidation of the monomers which leads to a radical-type polymerisation. The oxidation can be achieved by a number of ways, the main routes being chemical oxidation and electrochemical oxidation which are discussed in turn below.

1.3.1 - Chemical oxidation.

Polyacetylene was originally produced chemically by the oxidation of acetylene by I_2 [2] , although a variety of chemical and electrochemical routes have been employed[3]. The chemically produced polyacetylene was formed in a non-conducting neutral state; however on exposure to a further oxidising agent (X) such as $FeCl_3$ or $CuCl_2$ the polyacetylene formed a complex where positive charges on the polymer backbone were balanced by the reduced (X^-) form of the oxidising agent. The "doping" process is more correctly described as a redox process; this is not directly analogous to the n- and p-type doping observed for inorganic semi-conductors where the dopant is incorporated into fixed sites in the lattice creating electron rich and deficient sites. This general method of chemical oxidation of the monomer and polymer, using simple oxidising agents, has been used by other workers as one route to the formation of many organic CPs as removal of π-electrons from these unsaturated polymers is relatively facile. Others have also used various catalysts[4] and complexes[5] to achieve the chemical oxidation. Polymers produced by chemical oxidation are often far less conductive than those produced by other methods as precise control of the polymerisation process is often difficult to achieve and the results hard to reproduce. This is due to the lack of control of transport of reactants for the initial formation of both oxidant and monomer. This can lead to local depletion effects resulting in areas that have widely differing concentrations of the oxidised monomers resulting in an uncontrolled polymerisation with differing local rates of reaction. After formation it is also necessary to "work the reaction up" to get rid of any remaining reactants and by-products which often proves laborious.

1.3.2 - Electrochemical oxidation.

A much more controllable technique is the use of electrochemical oxidation, where the monomer is placed in a suitable solvent with supporting electrolyte. An electrode directly oxidises the monomer to form radical species which sustain the polymerisation reaction at the electrode. The electrochemical approach contains several inherent advantages over the chemical synthesis and it can in principle produce more regular, homogeneous and reproducible polymers. This can be achieved by precise control of the concentration of monomer radicals at the electrode surface. The polymerisation rate can in principle be easily controlled and maintained by controlling the electrochemical conditions and hydrodynamic flow at the electrode. In practise though, the rate is often controlled by the rate of nucleation of the film at the surface and is insensitive to the electrode rotation rate. Other advantages are that the polymer is produced in an oxidised and electrically conducting state where it is charge balanced (or doped) by incorporation of anions from the supporting electrolyte. The conductivities of CPs produced electrochemically tend to be higher than those produced by the corresponding chemical synthesis, this being due to their more homogeneous and regular form which allows a greater conjugation length and a more facile charge transport. Electrochemical synthesis is usually much cleaner than the corresponding chemical routes as there are no biproducts or catalysts to eliminate from the reaction. It is also much easier to monitor the progress of the polymerisation with *in-situ* analysis using electrochemical methods.

It is generally thought[6, 7] that the electrochemical polymerisation reaction is initiated by electrooxidation at the electrode to form radical cation species. These can then couple and undergo further electrooxidation and coupling steps resulting in chain growth and polymer formation. If, as is normally the case, the electron transfer reaction is faster than diffusion of monomer to the electrode, then a high concentration of radical cation species is maintained at the electrode surface which allows the coupling and electrooxidation reactions to be maintained at a controlled rate. The radical cation concentration is

maintained and controlled by diffusion of the monomer from the bulk of solution to the electrode surface. The growth of the polymer film is often believed to follow a nucleation process on specific sites on the electrode surface similar to that observed for the deposition of metals[8]. This electrooxidation-coupling process is shown schematically for a polyheterocycle such as polypyrrole or polythiophene in fig. 1.3.

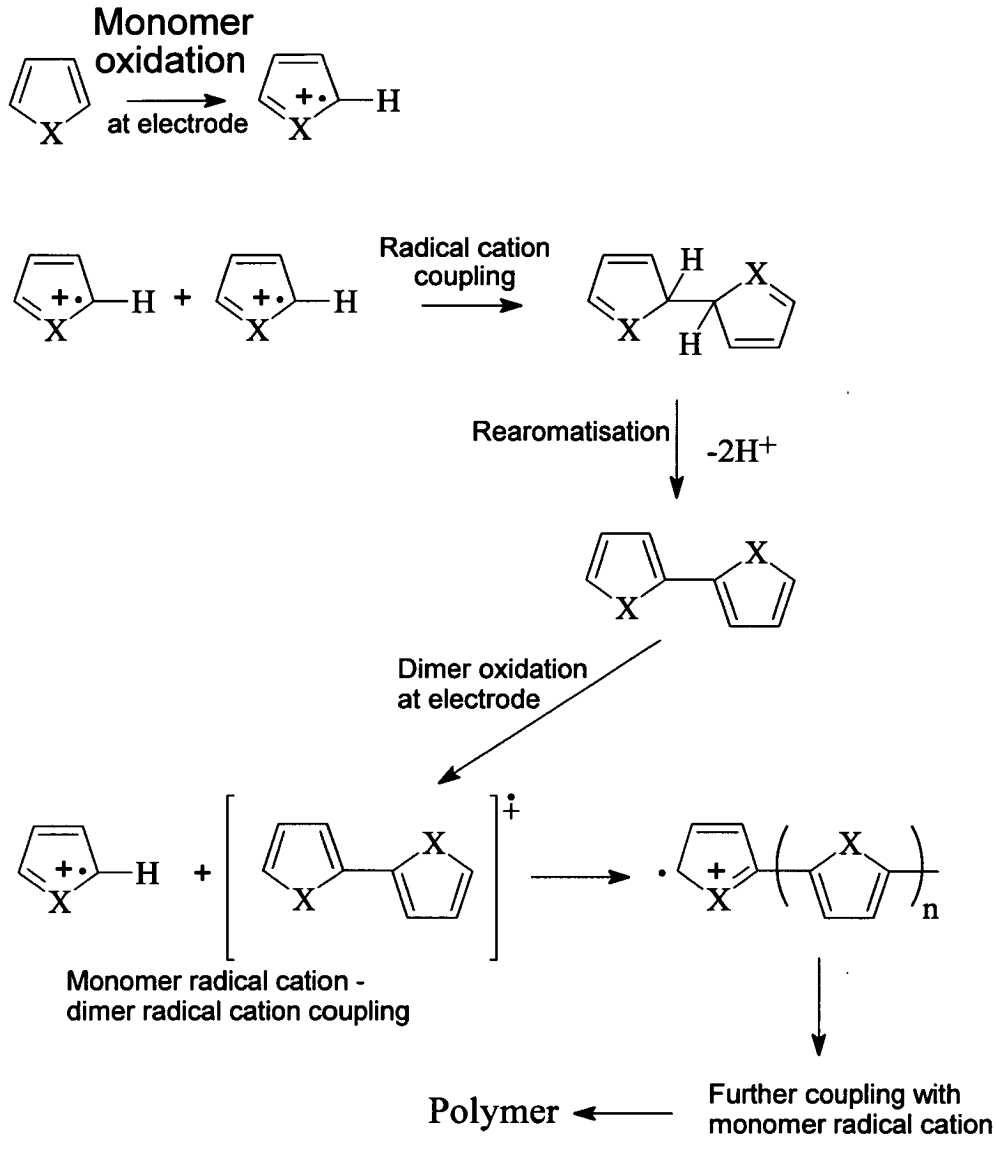

Fig. 1.3 - Electrooxidation - coupling process. X = O, NH or S.

This process is often termed an $E(CE)_n$ polymerisation as the first step of the polymerisation is electrochemical (E) which is then followed by a series of chemical and electrochemical steps $(CE)_n$. The first (E) step results in the creation of radical cations at the electrode. This is then followed by a chemical reaction (C) consisting of the linking together of two of the radical cations which immediately undergo chemical rearomatisation and is the driving force of the chemical step. Owing to the applied potential at the electrode, the dimer (and later oligomers), which are more easily oxidised than the monomer because of the extra aromatic stabilisation, undergo further electrooxidation (E). The polymerisation reaction continues with a series of further $(CE)_n$ steps where the oxidised dimer (and oligomers) link with additional monomeric radical cations followed by rearomatisation and re-oxidation of the resultant oligomers. This process continues for as long as the oxidation potential is maintained at the electrode. The long chain polymers produced are inherently insoluble so the polymer chains often deposit on to the electrode surface as a polymeric film which, owing to its electrical conductivity, can oxidise further monomer arriving at the conducting surface of the growing polymer film, fig. 1.4.

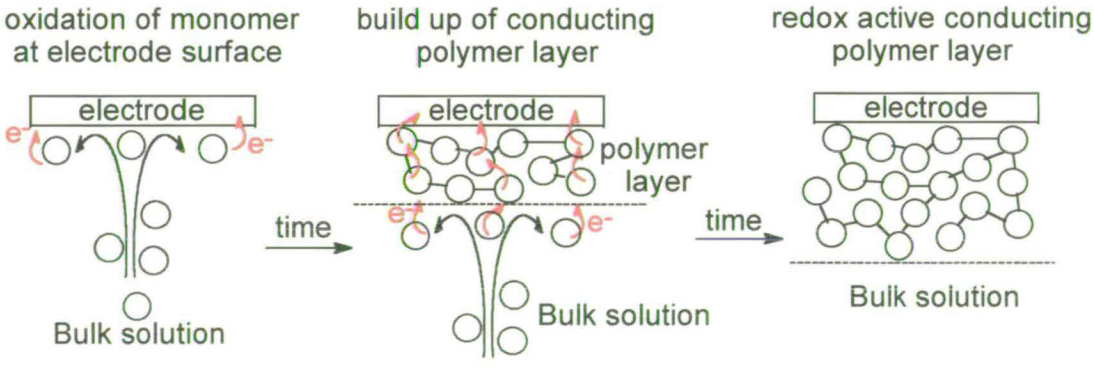

Fig.1.4 - Build up of film on electrode. o = monomer unit.

This E(CE)n mechanism is supported by a number of pieces of evidence including ultra fast cyclic voltammetry[9], rotating disc studies[10] and pH measurements[11] which have observed the presence of the radical

cations, oligomers and protons produced. Chronoabsorptometric techniques[12] have also showed that the rate-limiting step is the radical cation linking step which is consistent with the $E(CE)_n$ mechanism proposed. A number of the steps however are not fully characterised and some experiments have implied the presence of conflicting mechanisms. These are still a point of debate, hence continued research in this area is necessary to elucidate the processes fully.

The polymer films are usually produced in a conducting oxidised form, the charge of which is balanced by the uptake of a counterion from the electropolymerising solution. As the films are adsorbed on to the electrode surface, they can therefore often be reversibly cycled between a neutral reduced state where the counterions are expelled back in to solution, and an oxidised (doped) state where the counterions diffuse back in to balance the charge in the polymer film, fig. 1.5. Many of the important properties that CPs posses arise from this process. Thicker films can often be peeled off the electrode to give free standing conducting polymer discs.

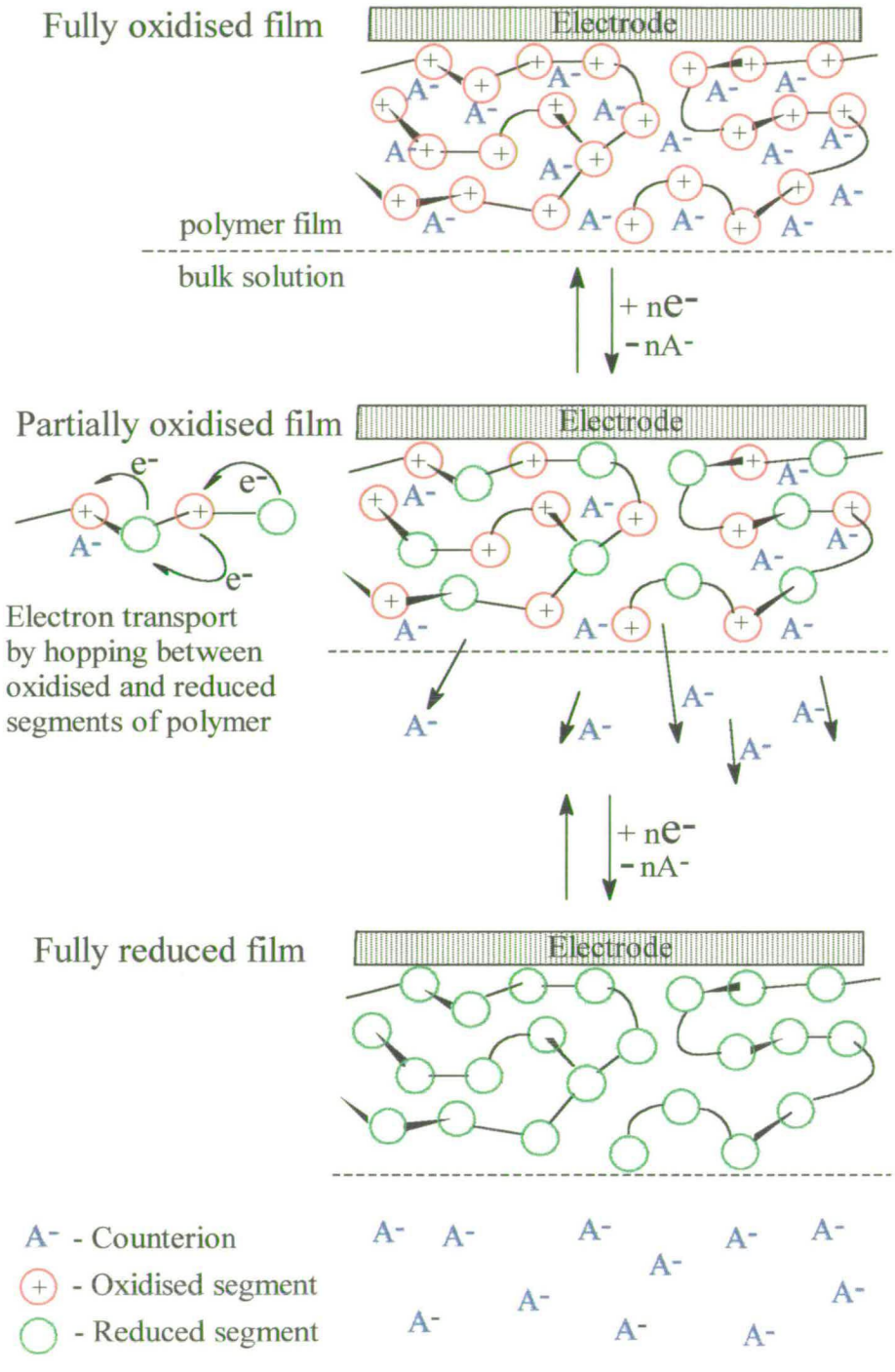

Fig. 1.5 - Reversible uptake of counterions by conducting polymer film.

1.4 - Mechanism of conduction.

Electrical conductivity in solids, such as metals and silicon type semi-conductors, have generally been described by band theory where electrons and/or holes moving in or between the highest occupied π-electron band (valence band) and the lowest unoccupied π-electron band (conduction band) are responsible for the conduction properties. The energy gap between these bands is responsible for the degree of conductivity observed in the solid. A modified version of this theory was one model proposed for the observed conduction properties in organic conducting polymers[13].

This model suggests that in a polymer the interaction of a monomer unit with all its intra- and inter-chain neighbours leads to the formation of electronic valence and conduction bands similar to a metal. In a typical metal the valence band is only half filled, so on application of an electric field electrons are free to move within this band giving rise to electrical conductivity, fig. 1.6A. In a neutral conducting polymer, the valence band is completely filled and there is a large band gap (usually 1 - 4 eV[14]) to the conduction band which is completely empty, fig. 1.6B. The formation of holes in the valence band is not possible for CPs as it is in inorganic semi-conductors, so another charge transfer mechanism was proposed for organic conducting polymers.

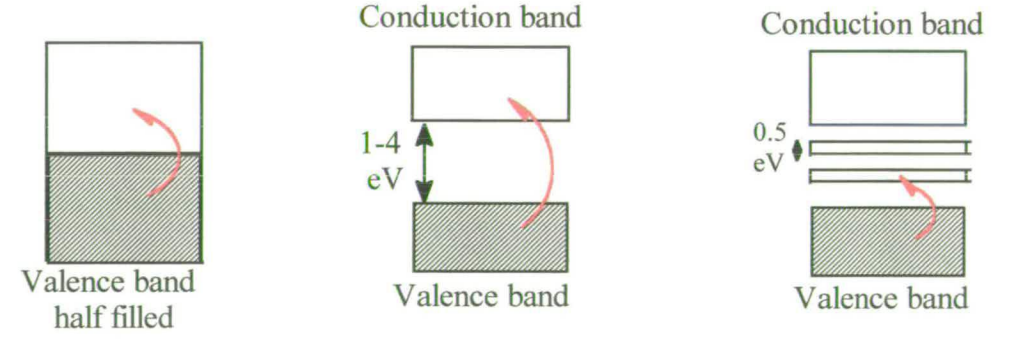

A - Metal band. B - Neutral CP. C - Doped CP.

Fig. 1.6 - Conduction mechanism by band theory.

1.4.1 - Charge carriers in organic conducting polymers.

It is thought that on subsequent oxidation (doping) of a conducting polymer, such as polypyrrole[15], the loss of one electron from a monomer unit results in the formation of a radical cation (often termed a polaron). It is then energetically favourable for the polymer chain to locally distort around this charge, transforming from a benzenoid to a quinoid structure which is more easily able to accommodate the charge, fig. 1.7. On further oxidation a second electron can be removed from the polaron to form a dication state termed a bipolaron which has no electronic spin. This is energetically more favourable than forming a second polaron. It is believed that this benzoid ↔ quinoid structural rearrangement causes new electronic bands to appear in the band gap (fig. 1.6C) which permits a more facile charge transport from the filled valence band allowing conduction to take place. The charge carriers are believed to be bipolarons, as at high oxidation (doping) levels the EPR signal, arising from the electronic spin of polarons, is seen to disappear but the polymer retains its electrical conductivity[16]. This model is supported by optical measurements[17] and theoretical considerations[18].

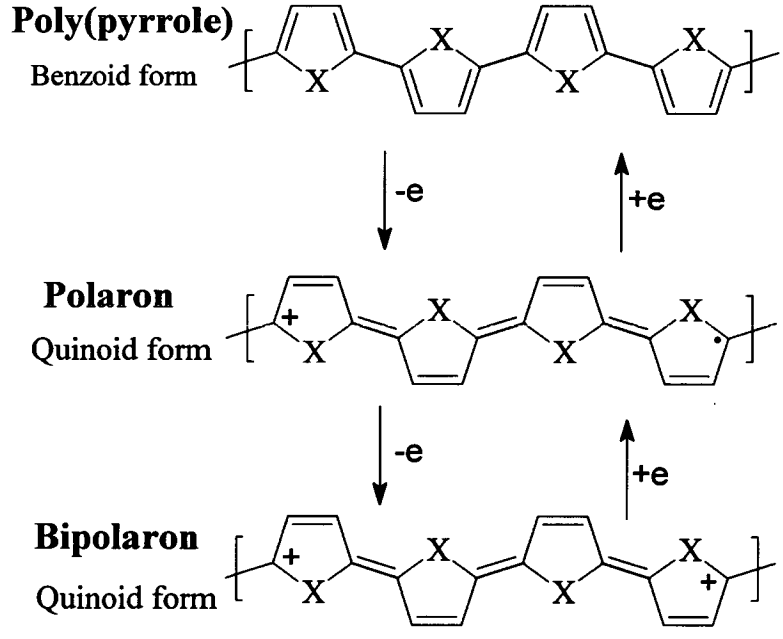

Fig. 1.7 - Benzoid-Quinoid rearrangement.

This localisation means that the charge carriers can also be considered to be localised chemical species which transport through the polymer system. There are those who argue that that a redox hopping model is more appropriate than a delocalised model.

1.4.2 - Charge transport mechanisms.

It is generally accepted that the bipolarons are the charge carriers in many CPs, but the precise mechanism of their transport is currently a matter of controversy. Transport of the bipolarons by movement along the polymer chain is sufficient to explain conduction only along an individual polymer chain. In reality, however, it is known that the polymer films are made up of an array of many polymer stands of varying lengths and orientations which contain many intra-chain defects, geometric disruptions and cross-links. The effects of these disorders on the transport of bipolarons is not fully understood and various models have been proposed to explain the transport of charge across these defects. It also seems unlikely that at very high polymer oxidation levels bipolarons are the sole charge carriers.

1.4.2.1 - Variable range hopping.

This is a model derived from studies on inorganic semi conductors. It is based on an assumption that spatial fluctuations in potential, due to the lack of atomic ordering in these materials, leads to a localisation of electronic states. It was thought that CPs containing polymer chains with short conjugation lengths, due to a high concentration of defects and disorders, may also lead to a similar localisation of electronic states where charge carriers move between the states by thermally assisted tunnelling, often termed hopping[19]. Others have argued that this localisation can be thought of as islands of metal-like states separated by potential barriers which can be overcome by quantum mechanical tunnelling[20].

1.4.2.2 - Inter chain hopping.

The charge carriers (bipolarons) also have to move from chain to chain to achieve efficient macroscopic conduction. Chance *et al*[21] have shown that the transfer rate of this process is dependent upon the combined possibility of finding a bipolaron on one chain and a sufficiently long segment free of excitation on the neighbouring chain, fig. 1.8.

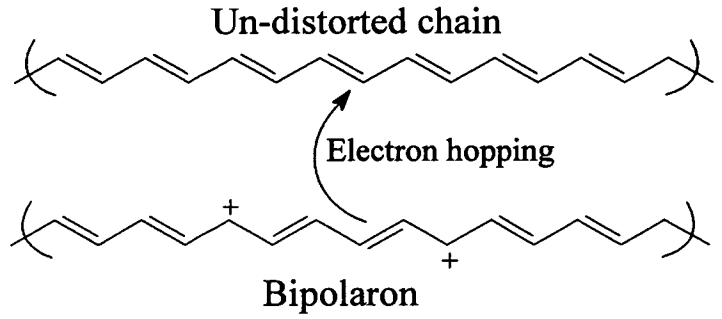

Fig. 1.8 - Inter-chain charge transport in polyactylene.

Xie *et al*[22] have found that hopping of the order of 5-10Å between localised sites associated with the counterion was the dominant effect in Polypyrrole. Others have found that as the counterion is changed to a larger more diffuse ion, the sites become less localised and charge transport is more facile leading to higher conductivity levels[23].

1.4.2.3 - Localised Redox chemical model.

Another model which has been proposed suggests that charge is transferred by electrons hopping between localised oxidised and reduced sites[24]. They suggest that polypyrrole undergoes a two electron redox reaction to cycle between a fully reduced form (A), a polaron form (B) and a bipolaron form (C), fig.1.9. This is accompanied by a phase change from a tightly packed, lyophobic reduced form to a more diffuse oxidised conducting form which incorporates the counterions, possibly in a helical structure[25, 26].

This chemical redox model has also been applied to other conducting polymer films[27, 28, 29]. In reality a single model is probably not sufficient to explain the conduction mechanisms in all the organic conducting polymers at different doping levels formed by various polymerisation conditions. It is most likely that a general mechanism cannot be found to explain the observed conductivity in all of the CPs studied and it is most likely that a combination of the charge transport mechanisms occurs in many of them.

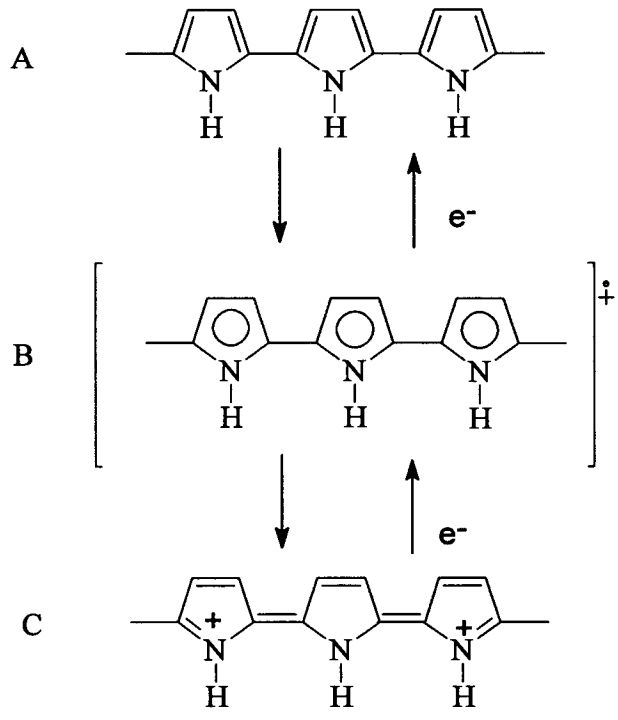

Fig. 1.9 - Reduced (A), polaron (B), and bipolaron(C) redox structures of polypyrrole.

1.5 - Molecular engineering of conducting polymers.

Conducting polymer films have now been prepared from a wide variety of organic compounds such as heterocycles, cyclic benzoid type

compounds and complex fused aromatic systems. The resultant electronic, physical and mechanical properties of the polymer films are highly dependent upon the structure of the monomer and the polymerisation conditions employed. In view of their multiple potential technological applications which, to be realised, require a greater understanding, versatility and a tailoring of their properties, a review follows which includes some of the more important and interesting organic conducting polymers produced. This will concentrate on how their properties relate to their structure and some of the methods employed to produce them.

1.5.1 - Polymer structure and substituent effects.

Among the various possible strategies for modification of conducting polymers, the polymerisation of monomers modified by substitution with functional groups represents the most straightforward method of achieving a molecular control of the structure and properties of the functionalised conducting polymers. This approach is more complex than first imagined as the substitution has to be compatible with both the polymerisation process and the conservation of an extensively conjugated π-system, which is required in order to maintain the required conduction, electrochemical and physical properties. The substituents affect the polymers on various levels of organisation, i.e.

Molecular level	Reactivity of monomer and stability of the radical cation. Propagation of the polymerisation process.
Macromolecular	Planarity of the polymer backbone. Conjugation length - intra-chain conductivity. Physical properties.
Macroscopic	Morphology and porosity of the film. Macroscopic conductivity. Mechanical properties.

The resultant properties of the polymer are related to its structure and can be influenced by the presence of substitutents which affect the polymer mainly through two ways, these are :-

i) **Electronic effects**, i.e. by its effect on the distribution of electrons at the reactive site of the monomer and over the polymer chain.

ii) **Steric effects**, the effects due to spatial crowding at the reactive sites and the way this influences the geometry and packing of the polymer chains.

For the majority of substituents, both these effects have to be taken into consideration. A number of conducting polymers are discussed below with reference to how their structure and substituents affect their resultant properties.

1.5.2 - Conducting polymers produced from heterocycles.

By far the most studied type of conducting polymers are those produced from heterocyclic monomers which show relatively high conductivities (10^{-3} - 10^{3} Scm^{-1}) and high environmental stabilities relative to PA. The heterocyclic CPs also offer a greater opportunity for the tailoring of their properties by derivitisation, and a greater scope exists for the examination of how their properties arise.

1.5.2.1 - Polypyrrole.

Polypyrrole (PP) was first electropolymerised in 1979 by Diaz *et al*[30] and can now be produced with conductivities as high as 10^{2} Scm^{-1}. From various studies[31, 32, 33] it is generally thought that pyrrole links through the α-positions (fig. 1.10). Indirect evidence for this is supplied by the fact that film formation is not observed for α-substituted pyrroles. It was found that longer PP chains show an increased propensity for a small amount of α-β linkage. This is due to the increase in electron density in

the β-position of the oligomers formed. The films produced generally have relatively poor mechanical properties (such as lack of elasticity, *etc.*) although are much more stable to oxidation by oxygen than PA. Substituted pyrroles were also examined in an attempt to examine how the substituents affected the properties of the film. As electropolymerisation of α-substituted pyrroles does not lead to the formation of a polymer film, then substitution is only possible at the β-position and at the nitrogen atom (1-position).

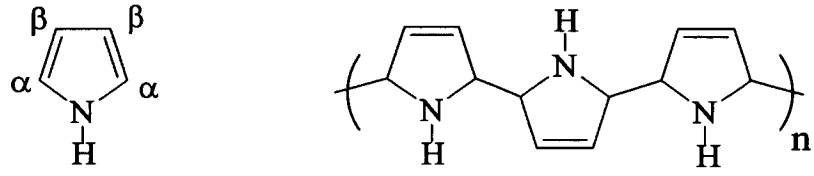

Pyrrole Polypyrrole

Fig. 1.10 - Pyrrole and polypyrrole.

1.5.2.1.1 - β-substitution.

Substitution by one or more methyl groups on the β-position(s) on the pyrrole ring leads to a conducting polymer with a slightly lower conductivity than the unsubstituted parent pyrrole[34]. This has been attributed to a steric effect of the methyl substituent forcing the pyrrole chain into a less planar conformation which disrupts the propagation of charge along the chains. This hypothesis is backed up by the observation that an increase in the steric bulk of the substituent (e.g. with a phenyl group) decreased the conductivity further. The effect being presumably due to an even greater distortion of the polymer chain. PPs substituted with longer alkyl groups tend to show a decrease in conductivity. However, it was found that their solubility in organic solvents was increased with the length of the alkyl chain. It has been observed that poly(3-octyl-pyrrole)[35] has a much better electrochemical activity in organic solvents compared with that in water, whereas polypyrrole is fully active in water but not in organic solvents. Poly(3-ethyl-pyrrole) was synthesised and has been shown to have intermediate characteristics, thus the lipophilic nature of

the films can be manipulated by substitution with the required length of alkyl group.

1.5.2.1.2 - 1-substitution.

Various polypyrroles substituted with an alkyl chain in the 1-position have been synthesised and their conductivity was again observed to decrease with an increasing size of the alkyl chain[36]. This has been described as solely a steric effect of the substituent which decreases chain planarity limiting efficient charge transport along the chain. The quality (i.e. homogeneity, electroactivity, *etc.*) of the film was also seen to decrease with substitution at the one position.

1.5.2.2 - Polythiophene.

Polythiophene (fig. 1.11) (PT) is similar in structure to polypyrrole and it is therefore not surprising that it was found to electropolymerise in a similar way[37]. It is believed that polythiophene similarly links primarily through α-α coupling of the monomers leaving the β-positions free for substitution although a less favourable competing α-β coupling mechanism has been noted for longer chains[38]. Polythiophene itself was found to have a conductivity that was slightly less than that observed for polypyrrole (10^{-1} – 10^{1} Scm^{-1}) although it has very similar macroscopic properties. The reduced form of PT has been found to be more stable than polypyrrole to oxidation by O_2 and has therefore attracted a considerable amount of research.

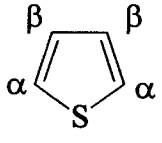

Thiophene

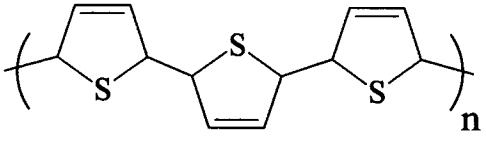

Polythiophene

Fig. 1.11 - Thiophene and polythiophene.

1.5.2.2.1 - Mono β-substitution.

Similarly to polypyrrole, polythiophenes substituted with alkyl groups have been produced and show a decrease in their conductivity with an increase in the linear alkyl chain length, although this is a relatively small effect[39]. 3-methyl thiophene actually showed an increased conductivity over unsubstituted thiophene. This was accounted for by the statistical lowering of any side α–β coupling reactions, which were blocked at one of the β-positions by the methyl substituent. This leads to a longer effective mean conjugation length and a more facile conduction of charge. PTs substituted with branched alkyl chains were also studied but led to much less dense films with a corresponding much greater decrease in the conductivity of the films. This effect was attributed to the greater steric bulk of the branched alkyl chain forcing the polymer backbone out of plane. PTs substituted with alkyl groups however were found to be advantageously much more soluble in common organic solvents than that found for unsubstituted polythiophene[40, 41]. This was thought to be a result of weaker inter-chain interactions and less rigid conjugated backbones arising from the steric bulk of the alkyl chains. Solubility in organic solvents is a very useful property to impart as characterisation of conducting polymers from solution is much easier than the typically insoluble and intractable films produced.

Polythiophenes substituted with fluroalkyl chains have also been produced in an effort to create polymers exhibiting properties similar to those of PTFE such as chemical inertness, hydrophobicity and a low coefficient of friction. It was hoped to combine these properties with the electrical conductivitiy of a CP resulting in a polymer which exhibited all of these desirable properties. This work resulted in a polymer which showed highly elastomeric properties combined with a good electroactivity[42].

1.5.2.2.2 - Di–β–substitution.

Thiophenes substituted at both the β- positions e.g. 3,4-dimethylthiophene, have been produced and were hoped to exhibit an

increased conductivity due to the complete hindrance of any side α–β couplings. This would in turn lead to a much greater mean conjugation length. It was noted, however, that conductivities were appreciably lower than for unsubstituted thiophene, which was ascribed to the effect of the increased steric bulk of having two β-substituents leading to the disruption of the polymer chain planarity[43]. Many fused ring systems containing the thiophene unit have been synthesised and polymerised and can be thought of as a particular case of disubstitution. Isothianaphtene (fig. 1.12) has been polymerised[44] and when doped with iodine has been found to have the lowest band gap (at ≈1eV) of any thiophene conducting polymer yet produced, giving a correspondingly high conductivity (50 Scm^{-1}). Many other such fused thiophene ring systems have been produced but none of them were found to produce PTs with superior electronic or mechanical properties over unsubstituted thiophene[45,46].

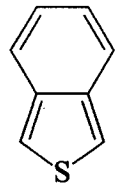

Fig. 1.12 - Isothianaphtene.

1.5.2.2.3 - Electronic effects of substituents observed in polythiophenes.

β-substituted PTs were found to show a strong electronic substituent effect[47] in addition to the steric effects discussed above. Various thiophene monomers substituted at the β-position with a number of simple substituents such as halides, amino and nitro groups were studied and there was found to be a linear correlation between the oxidation half-wave potential of these PT monomers and the Hammett substituent constant, σ^+, of the substituent. The Hammett substituent constant describes the relative electron donating or withdrawing nature of a substituent. The linear correlation shows that a purely electronic (inductive) influence was controlling the oxidation potential of the

substituted monomer. The magnitude of the oxidation potential indicates the ease with which the monomer can be oxidised to form radical cations, and their resultant relative stability. Thiophenes substituted with strong electron donating substituents were found not to produce a polymer film. This was suggested to have been due to the strong inductive influence of the substituents which stabilised the monomer radical cation to such a great extent that they drifted away from the electrode without linking. Strong electron withdrawing substituents, however, were found to destabilise the radical cations to such an extent that they reacted with nucleophiles in the solvent before they could link together to form a polymer. Thus it can be seen that a careful balance must often be struck between the steric and electronic effects of a substituent when attempting to manipulate the properties of a conducting polymer by substitution.

1.5.2.2.4 - Polythiophenes substituted with other functional groups.

1.5.2.2.4.1 - Ethers.

Some interesting properties such as hydrophilicity, and increased solubility in aqueous solvents have been observed in polythiophenes substituted with polyether groups[48]. Polythiophenes containing ion selective functional groups,such as crown ethers have also been synthesised. However due to the large steric bulk of such groups, long spacer chains between the crown ether groups and the polythiophene backbone are needed to decrease the deleterious steric effects imparted by such bulky substituents. This drastically limits the conjugation between the functional group and the backbone, hindering the electronic communication between the crown ether functional group and the polymer backbone[49].

1.5.2.2.4.2 - Aryl.

PTs have been produced containing pendant phenyl groups which are important as these substituents can act as anchoring sites for further functionalisation at the phenyl groups. It was found, however, that phenyls

substituted with electron donating groups hindered electropolymerisation, which was ascribed to parasitic side reactions at the stabilised phenyl ring. It was also found that spacer groups (alkyl or ether chains) limited the adverse steric effects of the bulky phenyl ring, thus allowing relatively high conductivities to be maintained[50].

1.5.2.2.4.3 - Chiral.

Chiral polythiophenes, which contain optically active substituents, have been synthesised[51] as they have potential applications as enantioselective modified electrodes. Fig. 1.13 shows this type of substituted PT and was found to have an enhanced reversible doping for an optically active (+) anion over its (-) enantiomer which constitutes evidence for enantioselective molecular recognition.

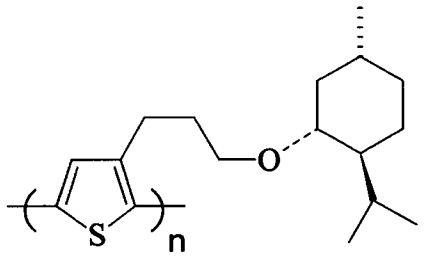

Fig. 1.13 - Enantioselective poly(thiophene).

1.5.3 - Self-doped conducting polymers.

As previously discussed in section 1.3.2, the electrochemical oxidation of a polymer leads to the formation of a positive charge on the polymer backbone which is balanced by the uptake of counterions from solution. However, electroneutrality can also be maintained by a counter charged species covalently bound to the polymer backbone. This is achieved by the expulsion from the film of a cation which was previously bound to the substituent. Oxidation leads to the expulsion of the cation from these substituents allowing the resultant substituent anion to balance the positive charge on the polymer backbone. Subsequent reduction

releases the covalently attached anion from the charged polymer site and the free cations diffuse back into the polymer film to charge compensate the anion. Poly(3-carboxypyrrole) (fig. 1.14) has been shown to exhibit self-doping behaviour and has been identified for use as a cation-exchange polymer[52] and a pH sensor[53].

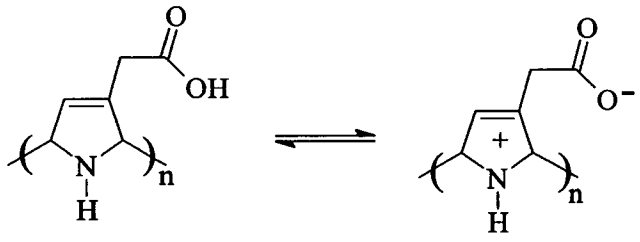

Fig. 1.14 - Self-doping behaviour of poly(3-carboxypyrrole).

1.5.4 - Conducting polymers produced from fused aromatic systems.

Hydrocarbons consisting of fused aromatic rings such as pyrene[54], azulene[55], fluorene[54], triphenylene[54] (fig. 1.15), poly(*p*-phenylene) and polynaphthylene[56] have also been studied. They offer an alternative route to obtaining CP's with interesting properties.

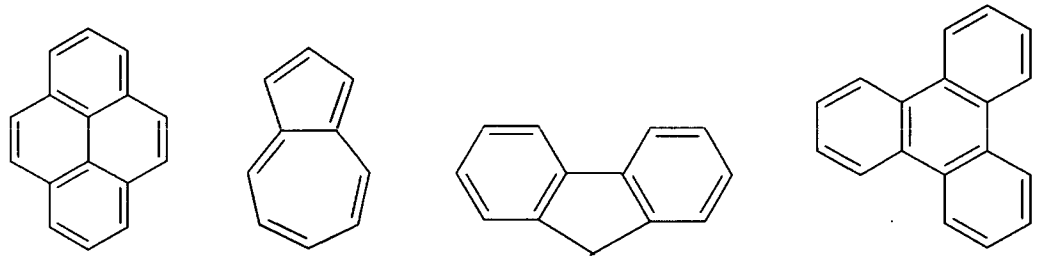

Pyrene Azulene Fluorene Triphenylene

Fig. 1.15 - Fused ring systems.

Most of the conducting polymers produced from fused ring-systems have conductivities in the same range as the polythiophenes, but due to the larger size of the monomers which hinder close packing, they tend to produce polymers that are less elastomeric and more diffuse, limiting their scope for certain applications. Little extensive work has been carried out to fully characterise these systems although it is likely that they polymerise in a similar way to the polyheterocycles, with a linear coupling of monomers through the positions containing greatest electron density.

1.5.4.1 - 1-D Graphite.

Polyacene and polyphenanthene can be thought of as being made up of strands of cis or trans polyactylene, fig 1.16. If successive strands of polyacetylene are added to these structures then ultimately a 1-dimensional graphite type structure can be obtained displaying similar conduction properties to graphite[57].

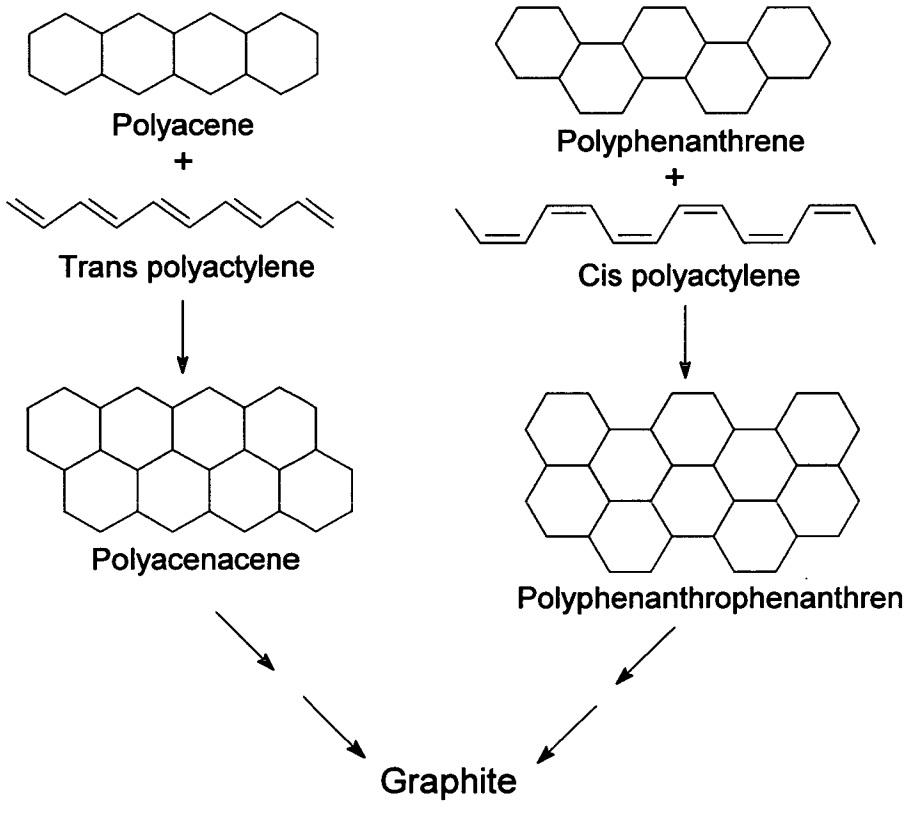

Fig. 1.16 - 1-D Graphite.

1.5.5 - Polymers containing redox active groups.

Various conducting polymers have been produced which are covalently bonded to redox active functional groups such as ferrocene,[58] viologens[59] and bipyridyls[60]. These derivitisations are very useful as they can be used to produce polymers that are catalytically active or that can mediate transfer of electrons to large biological molecules.

With most electrode materials (e.g. platinum, gold, etc.) electron transfer to enzymes is not possible as the active redox site is usually embedded in the centre of the enzyme. These electrodes also often show irreversible adsorption of the enzyme and protein denaturing effects. However, electrodes modified by a conducting polymer film containing specific redox active groups tailored to the outer shell of the biological species, have been used for molecular recognition and electron transfer to enzymes. The reason that this is possible is that the functional group is thought to mimic the natural partner of the biological species. Conducting polymers containing such redox active groups that undergo these electron transfer and molecular recognition processes are highly desirable, as small biologically active peptides are known to control a large number of biological functions and direct therapeutic properties such as receptor antagonists and inhibitors. Thus, novel biosensors and biospecific electroactive materials can be manufactured for the extraction and delivery of enzymes and for directing their biological functions.

Polypyrrole substituted with a dipeptide deriviative [Phe[Hea]Pro] has been produced and has been proposed as a potent and selective inhibitor of HIV-1 protease[61], fig. 1.17.

Electron transfer has been obtained between a poly(3-methyl, 4-carboxy-pyrrole) modified electrode (fig. 1.18) and the redox protein cytochrome c[62].

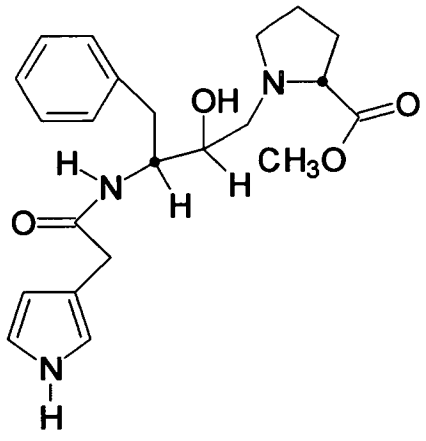

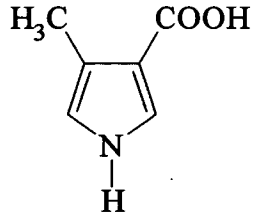

Fig. 1.17 - HIV inhibitor molecule

Fig. 1.18 - Electron transfer mediator

1.5.6. - Towards zero band gap polymers.

Some attempts have been made to synthesise molecules containing very low band gaps so that their conductivities can reach the high levels of a metal, even in their undoped state. Havinga *et al*[63] have found that by synthesising a polymer (fig. 1.19) that contains alternate electron withdrawing and donating groups then they can create a conducting polymer with a band gap of 0.5eV. This, they believe, is due to the broadening of the energy bands which leads to a smaller band gap and a corresponding conductivity of 10^{-5} Scm^{-1} in the undoped state. This is still 7 orders of magnitude less than a typical metal but is far greater than has been previously produced for a CP.

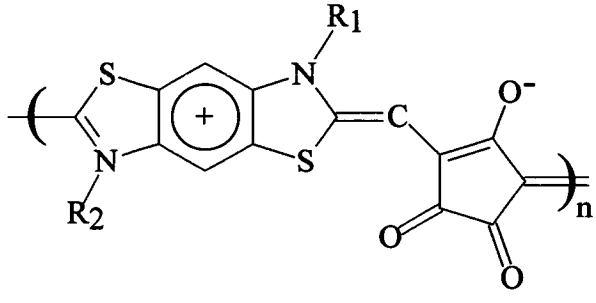

Fig. 1.19 - Polysquarine/croconaine low band gap polymer. R=alkyl group.

1.5.7 - Copolymerisation and composite polymers.

The formation of copolymers and composites is one of the most useful tools in polymer science in that the physical, electronic and mechanical properties of two or more polymers can be combined and enhanced to produce a copolymer or composite with many highly useful properties. The formation of copolymers has also been used to study the conduction properties and effects of substituents allowing a more detailed examination of the processes involved[64, 65]. For instance, copolymers have been produced from a combination of pyrrole and n-methylpyrrole monomers.[66] By varying the relative amounts of the monomers a precise evaluation of the steric effects of the methyl group on the macroscopic conductivity of the copolymer film has been elucidated. Similarly, copolymers of acetylene and methylacteylene have been produced with varying compositions showing conductivities from 10^{-3} to 10^{3} Scm^{-1} allowing a tailoring of the resultant conductivity over a wide range.

Copolymers have also been produced which aim to combine the differing physical properties of two or more monomers, for instance the high conductivity of poly(3-methylthiophene) has been combined with the high solubility of poly(3-octylthiophene) to produce a random copolymer of poly(3-octylthiophene-co-3-methylthiophene). This copolymer is both soluble in aqueous media and exhibits a high conductivity[67]. Copolymerisation has also been used to limit the detrimental steric effects of bulky substituents by spacing them out along the polymer backbone. The spatial locations and concentration of chelation centres can also be tailored in this way giving much greater control of the copolymer properties.

Composites of conducting polymers in a non-conducting matrix have been used to useful effect and can show practical advantages over homogenous materials such as higher environmental stability[68] and much improved mechanical properties such as good elasticity and a high tensile strength[69]. Often the advantages of the properties gained in this way far outweigh any decrease in conductivity of the composite, indeed a composite of polypyrrole in the typically highly insulating polyethylene

actually showed an increased conductivity compared with pure PP[70]. This was ascribed to the much greater elasticity of the composite which allowed stretching of the polymer chains resulting in greater chain alignment and conductivity. Similarly, polypyrrole has been electrochemically incorporated in to both polyvinylchloride (PVC)[71] and Nafion[72] to form composites that exhibit superior mechanical properties without any decrease in electroactivity. It was found, however, that it was often difficut to reproduce a morphologically similar composite in this way and fundamental studies of the conduction mechanisms and structural effects are limited.

1.5.8 - Effects of electropolymerisation conditions.

To date there is no use of standard electropolymerising conditions which often make comparisons between different polymers produced in differing ways (and therefore the effects of structural differences on properties) troublesome. The electropolymerisation involves many experimental variables such as choice of solvent, concentrations and type of reagents and electrolyte, temperature, amount of degassing, cell geometry, nature of electrodes and applied electrical conditions. These all affect the electropolymerisation reaction and therefore the properties of the resulting polymer, however due to their interdependence the analysis of their independent effects constitutes a complex problem.

1.5.8.1 - Solvent.

The choice of solvent has a large effect on the quality of polymer films produced. It has been found that the solvent must have a high dielectric constant, low nucleophicity, and usually be anhydrous and aprotic with a large potential window, such as acetonitrile, benzonitrile and nitrobenzene[73]. This limits any deleterious side reactions of water and aprotic solvents on the polymerisation reaction.

1.5.8.2 - Electrolyte.

Supporting electrolytes are required for the electropolymerisation reaction to pass the current efficiently through the solution and for the anion "doping" of the oxidised polymer. Various electrolytes have been used but the most studied, which are suitably inert at the potentials used, are small anions such as ClO_4^-, PF_6^-, BF_4^- and AsF_6^- associated with lithium or tetraalkylammonium cations. It has been found that the nature of the anion strongly affects the morphology and electrochemical properties of the prepared polymers, for instance a partial crystallinity has been observed in polymethylthiophene grown in acetonitrile with $CF_3SO_3^-$ [74]. From diffraction studies performed on the crystalline areas a helical structure of the polymer is observed with the counterions in-between neighbouring helixes, fig. 1.20. The reason for the adoption of this structure has been attributed to the size of the counterion fortuitously being exactly the same size as the distance between two thiophene units. Others[75] have found that differing tetraalkylammonium ions affect the rate of electropolymerisation at varying potentials.

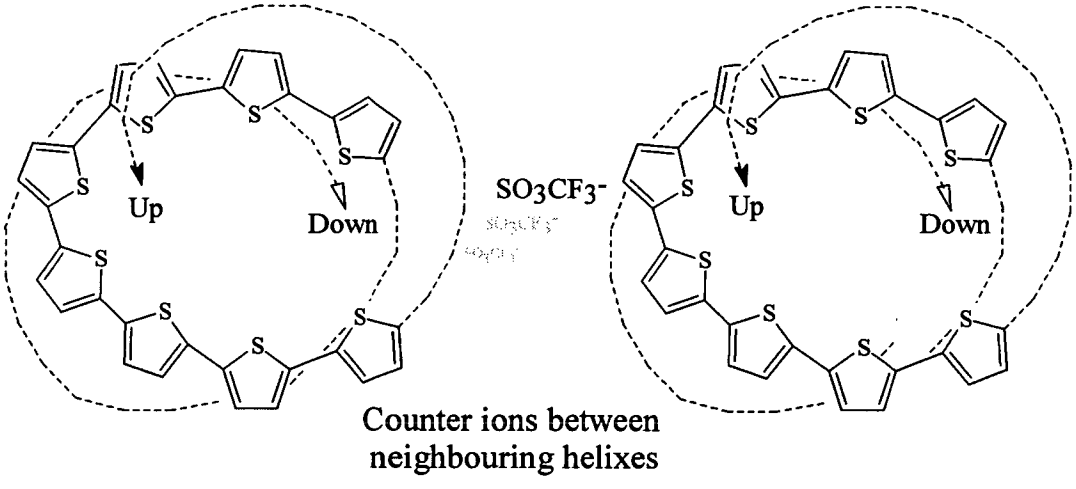

Fig.1.20 - Helix structure of polythiophene formed with $SO_3CF_3^-$ counter ion.

1.5.8.3 - Temperature.

The temperature at which electropolymerisation is carried out has been reported to affect the extent of conjugation, higher temperatures producing a shorter mean conjugation length[76]. For many CPs it has been observed that as the temperature is lowered, the conductivity of the film also decreases. This is the opposite effect than for a metal where the conduction increases with a lowering of the temperature and indicates that a different form of conduction is taking place. It has been observed that more highly doped samples show a reduced temperature dependence. This observation is more consistent with a redox-hopping model

1.5.8.4 - Electrode material.

The electrode material exerts an influence over the quality of films produced with materials such as platinum[54] gold[77], indium tin oxide[78], coated glass[79], titanium[80] and iron[81] all being studied. Most, however, have been produced on bulk platinum which seems to present a larger number of active nucleation sites which lead to a more compact and homogeneous film. The type of hydrodynamic flow imparted on the electrode has also been studied with more compact and less porous films being produced at a rotating disc electrode compared to a stationary one[82]. This has been ascribed to the relative rate of deposition of oligomers produced in solution that deposit on to the electrode surface compared with the rate of addition of radical cation monomer units to the ends of deposited polymer chains. Thus electropolymerisation is often more controllable with the use of a rotating disc electrode as the relative rates of these reactions can be varied with the rotation speed of the electrode.

1.5.8.5 - Applied electrical conditions.

Perhaps the greatest control of film morphology and properties come from the applied electrical conditions. CPs have been deposited using potentiostatic, galvanostatic, potential sweep and current pulse

methods which produce differing qualities of films. Generally the techniques which use a high overpotential produce the best quality films which has been explained by the production of a large number of nucleation sites which improve the compactness of the film and its resultant conductivity.

1.5.8.6 - Concentration.

The concentration of monomer has a large effect on the electropolymerisation reaction. It has been found that most CP's have a threshold concentration (which is solvent dependent) below which a polymer film is not obtained[83]. High concentrations of monomer also tend to produce loose, poorly conducting films containing significant amounts of soluble oligomers[84].

1.6 - Characterisation of conducting polymers.

The characterisation of conducting polymers is necessary to achieve an understanding of the processes and development of properties in the polymers produced. For potential applications, the length of the conducting polymer chain, its degree of conjugation, porosity, macroscopic morphology, physical, electrochemical and mechanical properties, and molecular level structure all have to be determined and controlled. In addition, the variation of the properties and structure of the polymers with polymerisation conditions have to be elucidated. Polymers, due to their inherent insolubility, intractability and amorphous structure are notoriously difficult to characterise, hence it has been necessary to employ a wide variety of classical and novel techniques to study them. Their full characterisation can only come from the piecing together of information from a variety of methods to obtain a full picture of the processes at work and their effects on the polymers' structure and properties.

Many classical techniques have been employed to study polymers that have solubilising groups which make characterisation much simpler. Structural features have been elucidated using NMR, IR, RAMAN, XPS, UPS and EXAFS spectroscopies which can yield information on the linking sites and morphology of the polymer chains. Chain and conjugation lengths have been determined by various direct and indirect techniques such as gel permeation chromatography (GPC), and viscosity and light scattering experiments. Problems with these, however, have been identified due to differing interactions between CPs and the reference materials that were used to calibrate the systems[85]. A novel technique to infer chain lengths was developed using radiochemical techniques to determine the amount of terminal protons in a polypyrrole film[86].

Charge transport mechanisms have been examined both theoretically using INDO (Intermediate Neglect of Differential Overlap) calculations[87] and practically using EPR which can be used to study species with electronic spin such as polarons or radicals.

Macroscopic properties such as conductivity, porosity, layer roughness, tensile strength, etc., have been examined using various microscopies such as scanning electron microscopy (SEM), scanning tunneling microscopy (STM), Atomic force spectroscopy (AFS) and with thermal neutrons. Electronic and optical properties have been studied using various spectroscopies such as UV-vis, infra-red and fluorescence.

Classical mass spectroscopies do not lend themselves well to the study of conducting polymers as the CPs tend to fragment to such a great extent that little information can be obtained. Various novel mass spectroscopies have been developed to overcome this by using "soft" ionisation and desorption methods which can be used to obtain both mass distributions and some structural information. These include MALDI and L^2TOFMS (Chapter 3 for definitions).

A fuller description of these techniques and their use for the characterisation of CPs are found in various reviews[88,89,90].

1.7 - Applications of conducting polymers.

A considerable research effort has been directed at the elucidation of the structure, physical, mechanical and electronic properties of the many conducting polymers produced, which has largely been motivated by their multiple potential technological applications. So far only a few commercial devices using CPs have been produced which has mainly been due to their lack of processability and environmental stability. Recently however, considerable progress has been made to improve their solubility, and easily processable materials can now be produced from composites of CPs with conventional thermoplastics such as polyethylene. Most of the heterocylic CP's can now be prepared with high environmental stabilities by using pure reagents and the appropriate conditions. The technological applications take advantage of a variety of different properties that the CPs posses and in all the redox forms that they appear. For instance, applications have been identified for their undoped insulating state (such as microelectronic transistors), the fully doped conducting state (molecular wires) and many applications which use the reversibility process between the two states. A tremendous amount of applications have been proposed for CPs therefore only the main areas are discussed in this section to give some insight into the wide variety and importance of their applications.

1.7.1 - Rechargeable batteries.

The reversible doping-undoping behaviour of CPs make them a good candidate for secondary batteries which is perhaps the most widely discussed application for CPs that display a reversible doping behaviour. Early work using doped PA in conjunction with Zn electrodes and a liquid electrolyte have produced a reversible cell that has shown relatively high voltages and good energy and power densities[91]. Other similar batteries using conducting polymers such as polyaniline have also been produced, but problems such as self-discharge and low reversibility have been encountered.[92] Solid state secondary batteries have also been studied,[93] for instance PA doped with iodine in direct contact with a Lithium disc was studied where the LiI produced during cell reaction acts as a solid

electrolyte. This battery has shown a good reliability and durability. There are many advantage of these batteries over standard lead acid cells; one such advantage is their much lighter weight which makes the realisation of battery powered vehicles a more viable goal. Another advantage is that they are much less toxic, making disposal an easier process.

1.7.2 - Display devices and smart windows.

A wide range of display devices have been proposed which use the electrochromic properties of some conducting polymers. Electrochromism is broadly defined as a reversible colour change induced in a material by an applied electric field or current. Many conducting polymers exhibit considerable spectral changes in the visible region associated with changes in the oxidation levels, e.g. films of polythiophene change from a deep blue colour to red on oxidation of the film. The particular colour produced by the film is highly dependent on the particular conducting polymer used, its substituents, the counterion present, the method of preparation and the film thickness, with many spectral colours having been observed. To be useful for display devices such materials have to exhibit fast switching times between the two states (<150ms) and be able to do this over a large number of cycles ($>10^7$). Some polythiophenes have been produced which have switching times of around 30ms and can be cycled around a million times retaining 75% of their activity[94]. These displays have been used to replace existing liquid crystal type displays (LCD's) in such devices as digital watches and calculators and offer a number of advantages over them. CP electrochromic devices do not have any limited visual angle, they may be constructed in large dimensions, they use less power in low switching applications and contain optical memory. This is because power is only needed to switch the CPs between the differently coloured states leaving the final form to remain displayed without the need for any additional power.

The electrochromic properties exhibited by some CPs can also be used to manufacture "smart windows". These consist of very thin polymer layers which can be embedded, with a colourless electrolyte, between two panes of a glass coated with a conducting transparent material eg. ITO

(Indium Tin oxide). On application of an electric potential the CP can be made to change from complete transparency to a darkened layer within the window by the electrochromic redox reaction of the polymer. If this technology is linked to a light sensitive device then the windows can be programmed to automatically tint with an increase in sunlight, the degree of darkening being controlled by the amount of charge passed. Indeed smart windows are already in operation in some office blocks that have the benefit of seeing some summer sun.

1.7.3 - Sensor devices.

Perhaps the most promising area of technology so far exploited by conducting polymers has been that of sensor devices, as a number of sensors have already reached commercial use. Sensors are used for detecting and measuring concentrations of various chemical species in the solution or gas phases that interact with CP films. These films can use changes in conductivity and potential to detect adsorbed or absorbed species because their conductivity is dependent upon their electronic structure which can undergo changes due to redox, polar or chelation interactions between the polymer and the detected species, fig. 1.21. Polythiophene has been suggested for use in humidity and radiation detectors as its conductivity changes considerably on exposure to moisture and radiation[95]. Devices using derivatised polypyrroles have been studied for use as gas sensors[96], for instance a reversible response has been noted for ammonia from which it is possible to infer its concentration. One problem with these sensors is that their selectivity is often rather poor, this can be tackled with the use of more sophisticated polymer films that are tailored to the specific atom/ion that is required to be detected.

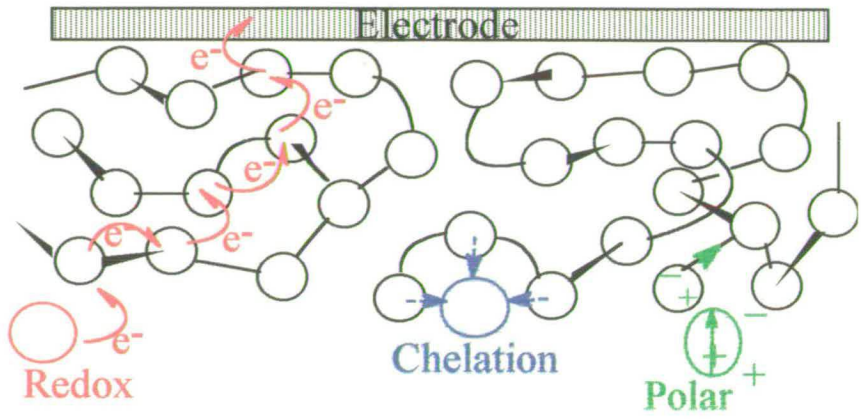

Fig. 1.21 - Redox, chelation and polar effects of detected molecules in polymer sensor film.

Some commercial devices have been developed such as the "electronic nose" which has found use in the monitoring of fermentation brews in the brewing industry[97]. This device consists of an array of approximately twelve different conducting polymers which interact differently with various volatile reaction products produced during the brewing process. As the volatile components permeate the polymer matrices, they change the resistivity of the polymer arrays through their polar interactions and by monitoring the resistivity changes, it is possible to develop a fingerprint reading from the different volatile components. Comparing the sensor readings to the behaviour of previous "perfect" brews, the optimal fermentation level can be reached. The brewing company Bass for instance, have used a similar sensor to monitor the build-up of diacetyl which gives the beer a buttery off-taste. Once the diacetyl is detected the fermentation is allowed time to give the yeast a chance to convert the diacetyl to a tasteless alcohol. This type of approach has also been used in sensors for the monitoring of pollutants in water and soil, and is set to play an increasingly important role in environmental monitoring.

1.7.4 - Microelectronics.

The undoped semi-conducting or insulating state of the CPs has led to them being proposed for use in the microelectronics industry. It is

possible to construct very small field effect transistors using a conducting polymer film in place of silicon which is more difficult to deposit in very thin films. When linked to liquid crystal displays this is hoped to be useful for the production of ultra thin flat screen televisions. Polymer based light emitting diodes (LEDs) have been produced using poly(p-phenylenevinylene) as the emitting layer.[98] The range of conducting polymers that show this electroluminescence property is so wide now that any colour in the visible spectrum can be obtained by variation of the electronic properties through substituent effects. These applications may be increasingly useful in the future as they offer a lower production cost and an easier fabrication than existing technologies. Displays with large surface areas will then be more feasible and economically viable than the standard GaAs LEDs.

1.7.5 - Solar cells.

Some considerable research has been carried out on the production of photo-voltaic cells from conducting polymers. Undoped polythiophene has been used as the photo-active constituent of a solar cell. This has been reported as having a relatively long life producing a constant photovoltaic current over a number of hours[99]. However, the currents produced were found to be relatively small compared with standard Si devices. Most conducting polymers used in solar cells have therefore been utilised as protection against the photocorrosion and photopassivation of Si or GaAs devices by grafting thin films on to the surface of the semiconductor[100].

1.7.6 - Other technologies.

Many additional technologies have been proposed with diverse applications over a wide range of fields. In the medical field for instance a drug-delivery system has been produced where the drug anion is pre-doped in to the polymer matrix and can be released with very fine control on application of a reduction potential. CPs have also been identified for use in information storage devices as it has been shown that polypyrrole

can be grown on an anode with a finely etched surface. Removal of the film reveals the reverse of the etched surface on the underside of the polymer film. The reading of these patterns by a capacitative method has been shown to be feasible which allows the possibilty of producing an information storage and retrieval system[101]. The electronics industry has recently been concerned with electromagnetic interference from the increased density of electronic circuitry in everday life and CPs have been found to be useful as an electromagnetic radiation shielding coat for the protection of sensitive micro-chips. They may also be useful as protection against the large electromagnetic pulses produced in nuclear explosions. Even more imaginative applications have been proposed such as electronically heated wallpapers and clothes but there are many competing technologies for all these applications so intensive research in the conducting polymer field is still necessary for the realisation of this promise.

1.8 - Indole and its derivatives.

Conducting polymers can be produced from the heterocycle indole, Fig. 1.22, and a number of its derivatives. It is not surprising indole electropolymerises as it can be thought of as a pyrrole ring fused to a benzene ring. This section describes the main findings of the research previously carried out on the electropolymerisation of indole and its derivatives.

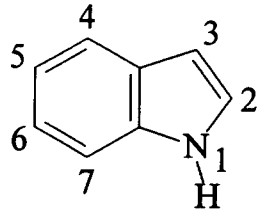

Fig. 1.22 - Indole with the position numberings indicated.

Indole was first electropolymerised in 1982 by Tourillon *et al*[102] resulting in the deposition of a polyindole layer on the electrode. The layer was found to be electroactive but it exhibited a conductivity of approximately 10^{-2} Scm^{-1} which is one hundred fold less than that for polyfuran (PF), polypyrrole and polythiophene. The conductivity level is therefore in the semi-conducting range, but is still relatively high and is sufficient for use in most of the proposed applications. PF, PP and PT have all been found to polymerise in very similar ways, mainly through α–α couplings. However this is not possible for indole as one of the α-positions in the pyrrole ring is fused to the benzene-type ring. A number of other groups have since studied the electropolymerisation of indole and a variety of its derivatives[103,104,105,106,107,108,109] and have used many different spectroscopic techniques in an attempt to characterise the nature of the electropolymerisation reaction. They have put forward several conflicting mechanisms and possible polymer structures, postulating that the linking of the monomers occurs through different sites. Some of these previously proposed structures are shown in fig. 1.23.

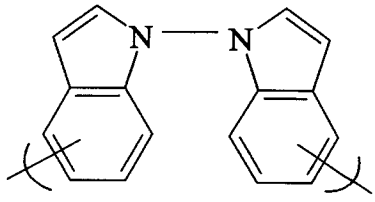

(A) N-N bonded

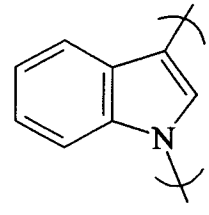

(B) 1-3 bonded

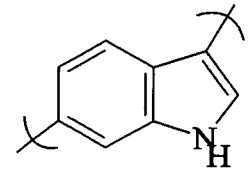

(C) 1-6 bonded

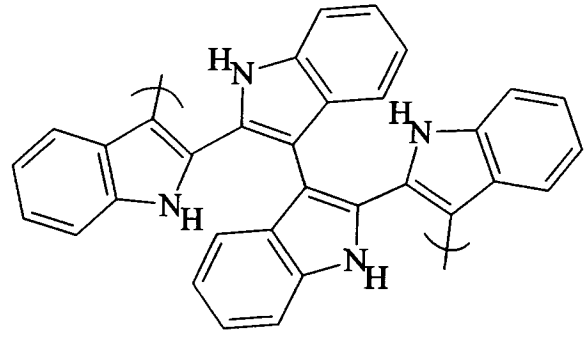

(D) 2,2 -3,3 bonded

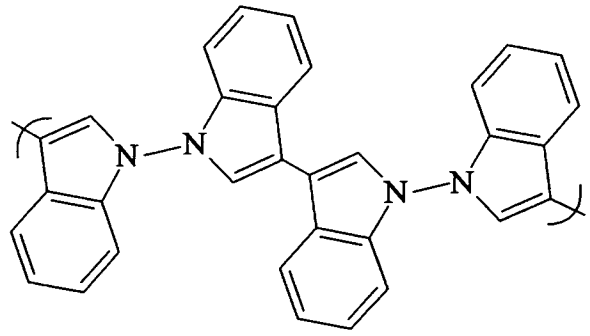

(E) 1,1-3,3 bonded

Fig. 1.23 - Proposed structures of poly(indole). (A) - Tourillon and Garnier[102], (B) - Waltman *et al* [106], (C) - Bukowska *et al* [110], (D) - Zotti *et al*[109] and (E) - Tabli *et al*[111].

1.8.1 - Steric effects.

It is agreed by most workers that the linking of indole monomers occurs through sites in the pyrrole ring of the indole monomer as infra-red spectroscopy studies have shown that the aromatic C-H stretches remain undiminished on electropolymerisation. Tourillon *et al*[102] have also found that the N-H stretch in the infra-red spectrum was considerably diminished on electropolymerisation of indole. This evidence taken together with their observance that the electropolymerisation of N-methylindole did not result in a polymer film, led them to propose that the indole polymer was linked through the 1-positions in the monomers. The second linkage site was not suggested. Later Waltman *et al*[106] studied the substitution effects of derivatised indoles and determined that the electropolymerisation of indole monomers substituted in any of the pyrrole ring positions (1,2 or 3) did not form polymer films on electropolymerisation. Combined with INDO molecular orbital calculations, which showed that the one and three positions showed greatest electron density, they postulated that the linkage of monomers was through the 1 and 3 positions. To the contrary

Zotti *et al*[109] using FTIR, UV and electrochemical measurements indicated that the monomers were linked through the 2 and 3 positions and that the polymer is made up of a regular alternation of 2,2-3,3 couplings. Indeed this year Tabli *et al*[111] have examined polyindole by HREELS, XPS and FTIR and have concluded that polyindole consists of yet another alternative structure, i.e. a regular alternation of 1,1-3,3 couplings. It is obvious that the electropolymerisation mechanism of indole and linking sites in the monomer is anything but clear with many of the results seemingly to conflict with each other. This problem has partly arisen due to the belief that indole would polymerise in a similar way to the other heterocycles, i.e. through a linear chain of monomers linked together through two sites.

1.8.2 - Electronic effects.

Waltman *et al*[106] and later Mount *et al*[112] have examined a number of substituted indoles and have concluded that on electropolymerisation only some of the 5-substituted indoles produce a polymer film on the electrode. They claim that this is are due to electronic effects and not steric interactions as they observed that electropolymerisation of 5-bromoindole, which contains a bulky bromine substituent, results in a polymer film whereas the electropolymerisation of indoles with some smaller substituents (such as hydroxy) did not. They suggested that the polymer formation is dependent upon the overall stability of the radical cation monomer produced on oxidation which is controlled solely by the electronic nature of the substituent. They indicated that indole monomers substituted with electron withdrawing groups tended to produce good quality polymer films. This was explained by the destabilisation of the radical cation to an extent where their linking with one another was encouraged. They also found that electron-donating substituents tended to stabilise the monomer radical cations to such an extent that they diffused away from the electrode surface without linking. The electronic effect of the 5-substituents was shown in a plot of the oxidation peak potential of a number of the 5-substituted indole monomers against the Hammett substituent constant ,σ^+, of the 5-substituent. A Hammett plot showing the oxidation peak potentials of the monomers relative to the

reference electrode used in this thesis is reproduced in fig. 1.24. The box included in the Hammett plot indicates the 5-substituted indole monomers that Waltman *et al* claimed could be electropolymerised to form a conducting polymer film.

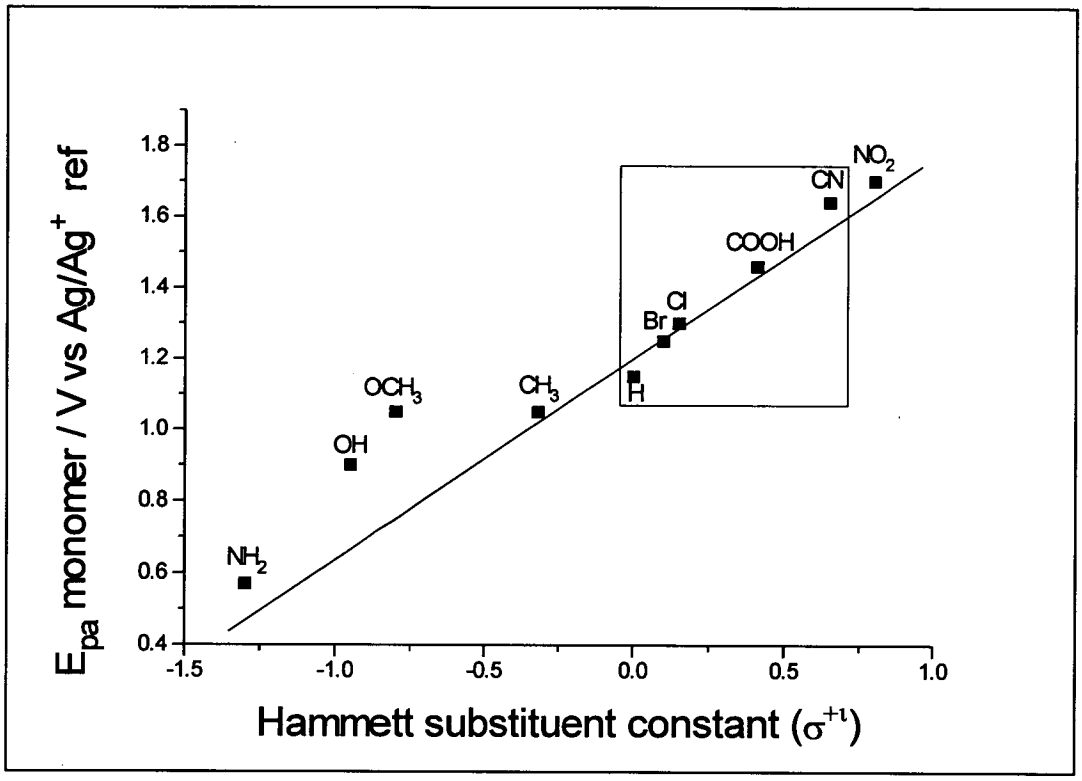

Fig. 1.24 - Oxidation peak potential of 5-substituted indole monomers *vs* Hammett substituent constant of 5-substituents.

1.8.3 - Recent work on the electropolymerisation of 5-substituted indoles.

Recent work has been carried in Edinburgh to study the electropolymerisation mechanism of, and linking sites in, indole and some 5-substituted indoles in an attempt to address the conflicting results found previously by other workers described above. Mount *et al* have shown that electropolymerised films of poly(5-cyanoindole)[113] and poly(5-

carboxyindole)[114] consisted of two distinct products which could be separated by their differential solubility in dimethylformamide (DMF). One fraction consisted of a polymer and the other fraction consisted of an asymmetric cyclic trimer structure (fig. 1.25) which was characterised by NMR.

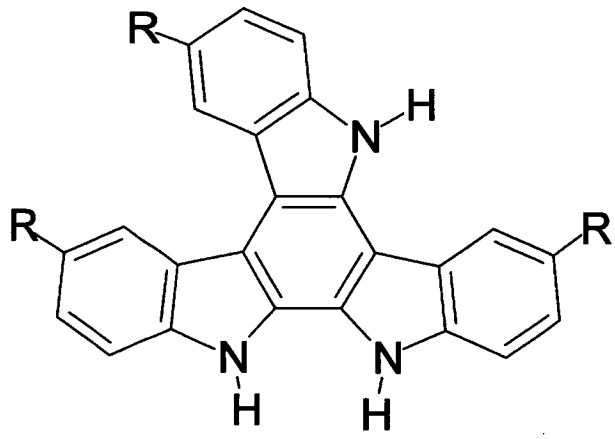

Fig. 1.25 - Asymmetric cyclic trimer species, R = CN, H or COOH.

The asymmetric cyclic trimer can be thought of as three monomers linked through their 2 and 3 positions to form a stable delocalised aromatic ring. This observation accounts for the previous findings by Zotti[109] and Tabli[111] who observed evidence of coupling at the 2 and 3 positions. Electrochemical measurements and mass spectrometry, fluorescence, UV-vis and IR spectroscopies undertaken by Mount *et al*[113] have shown that the polymer is made up of linked cyclic trimers with the linkage probably occurring through two of the 1(N)-positions on each trimer. This is consistent with the apparent decrease in intensity of N-H stretches in the infra-red spectrum on electropolymerisation observed Waltman[107] and Tourillon[102].

Mount *et al*[112] have proposed that the electropolymerisation of 5-cyanoindole, 5-carboxyindole, indole and tentatively some other 5-substituted indoles proceeds as in fig. 1.26. This mechanism is consistent with the observations found by other workers but invokes a novel two-step polymerisation where the formation of asymmetric cyclic trimer species is

followed by their linking to form a polymer consisting of linked trimers. The conflicting mechanisms proposed by other workers have arisen due to their *a priori* belief (wrongly) that indole would polymerise in the same way to the other heterocycles studied such as PP and PT.

$$3nIn_{(aq)} \xrightarrow{-7ne,-6nH^+} nIn^+_{3(aq)}$$

$$nIn^+_{3(s)} \xrightarrow{-2ne,-2nH^+} -(In^+_3)-_{n(s)}$$

Fig. 1.26 - Electropolymerisation mechanism of the 5-substituted indole monomers. Where In, In_3^+ and $-(In_3^+)-_n$ represent indole monomer, oxidised trimer and oxidised polymer consisting of linked trimer respectively.

The reason that these cyclic trimers are believed to form is that the greatest electron density in the majority of 5-substituted indole radical cations is in the 2 and 3 positions, with the formation of a delocalised system around a 6-membered aromatic ring being the driving force. These trimers, that are believed to form on the surface of the electrode, undergo a further linking step with neighbouring trimers to form a conductive polymer chain on the surface of the electrode, although this step is believed to be considerably slower than the trimer formation. Polyindole has also been produced chemically,[115] but the polymer formed was found to be less conductive and homogeneous than those produced by electrochemical methods. Similar trimers (symmetric and asymmetric) have previously been manufactured by two chemical syntheses, although both routes involved complex syntheses producing low yields[116, 117].

A doping process similar to that for the other heterocyclic CPs has been observed for polyindole and its derivatives with the incorporation of a counterion such as ClO_4^-, PF_6^-, BF_4^- or AsF_6^- into the polymer film on

oxidation being noted[118]. The conduction of charge is believed to occur by a redox hopping mechanism, with polarons as the charge carriers. The conductivity has been found to vary between 10^{-3} and 10^{-1} Scm^{-1} depending on the applied polymerisation conditions. Bartlett *et al*[119] have proposed that poly(Indole-5-carboxylic acid) could be used for a micro pH sensor device as they have found that the polymer film is potentiostatically sensitive to pH changes. This they ascribe to the loss of protons from the acid groups which attenuates the electronic nature of the polymer backbone which can be detected as a change film potential. Later studies have indicated that it is probably the labile N-H proton in the trimer that causes the observed pH-potential dependence.

There are a number of advantages in studying polyindole and its derivatives for the possible development of sensor devices compared to the other heterocycles which have been studied to a greater extent. Poly(indole) has been found to be thermally much more stable than PT, PP or PA and exhibits a superior resistance to oxidation by oxygen in the environment[120]. Due to the asymmetry of the trimer and polymer molecule, it has a greater number of sites available for substitution and thus offers an increased scope for the tailoring of properties through substitution. Many of the substituted indoles are commercially available or are relatively easy to manufacture, giving the opportunity for further derivitisation. They have also been identified as being useful for the study of biopolymers such as melanin, as the amino acid tryptophan contains the indole unit.

1.9 - Aim of work presented in this thesis.

This thesis is concerned with the investigation of the electropolymerisation of indole and various substituted indole monomers. The main objectives include the electrosynthesis, characterisation and functionalisation of indole-based conducting polymers for the possible use as sensor devices. Chapters 4 - 8 describe the studies undertaken and discuss the results obtained in light of these aims. Chapter 2 examines some of the theory behind the techniques used in this thesis and describes the information that can be obtained from them. Chapter 3 describes the experimental details of the equipment, chemicals and methods used to obtain the results in chapters 4 - 8.

Chapter 2 - Theory

2.1 - Potential sweep voltammetry

Voltammetry techniques are probably the most widely used techniques in electrochemistry as they can provide information on a number of processes such as the potentials at which redox reactions occur, the coupling of homogenous reactions, kinetic information, presence of the adsorption of species and detection of products produced at the electrode.

The simplest of these techniques is linear sweep voltammetry (LSV) where the potential of the working electrode in a stagnant solution is swept linearly at a pre-set and constant rate (the sweep rate, v) between two fixed potential limits E_1 and E_2. On reaching E_2 the sweep is reversed and the potential swept back towards E_1 where the sweep is terminated. The current produced by electro-active species in solution in response to this potential sweep is measured and plotted against the applied (time-dependent) potential to produce a linear sweep voltammogram.

This technique can be expanded by repeating the linear sweep a number of times and monitoring any changes in the voltammogram on successive sweeps which is termed cyclic voltammetry (CV).

In both LSV and CV the solution is stagnant so transport of species to the electrode surface is achieved solely by diffusion and uncontrolled thermal convection hence these studies can be described as dynamic i.e. non steady-state. Techniques such as LSV and CV are often very useful for obtaining information on the presence of electrochemical reactions and their E^0 values; however precise quantitative information on specific reaction steps and mechanisms is often difficult to extract so other more direct techniques, such as those employing forced convection, are often used to complement these. A full mathematical discussion of the theory of LSV and CV is described elsewhere[1 21]

2.2 - Electrochemical studies at the Rotating Disc Electrode.

The Rotating disc electrode (RDE) can be used to obtain more precise information on the kinetics of an electrode and the role of mass transport to it by its controllable hydrodynamic system.

The RDE consists of a platinum disc electrode surrounded by an insulating mantle of PTFE as shown in fig. 2.1. The RDE is suspended in a suitable solvent containing the species of interest with a supporting electrolyte. The electrode can then be rotated at a controlled rate and the rotation acts as a hydrodynamic pump pulling the solution up towards the electrode surface and out radially across it as shown in fig. 2.2.

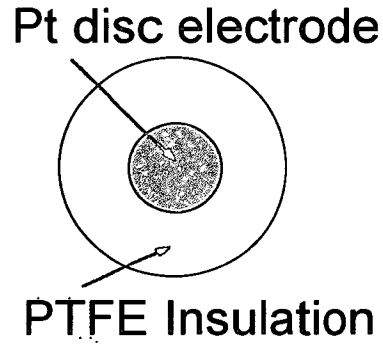

Fig. 2.1 - Rotating Disc Electrode

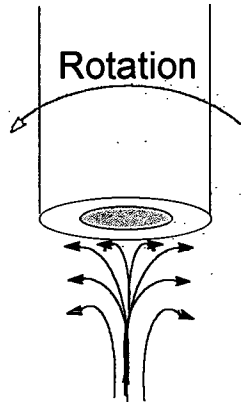

Fig. 2.2 - Hydrodynamic flow.

The RDE system is known as a forced convection-diffusion method as mass transport of electroactive species to the electrode surface can be described by a combination of forced convection and diffusion. Convection, the movement of species due to rotation of the electrode, becomes less important in the direction perpendicular to the electrode as one approaches the electrode, and is zero at the electrode surface, thus a boundary layer can be defined near the electrode in which the only significant form of mass transport in this direction is diffusion. This is termed the Nernst diffusion layer which is shown schematically in fig. 2.3

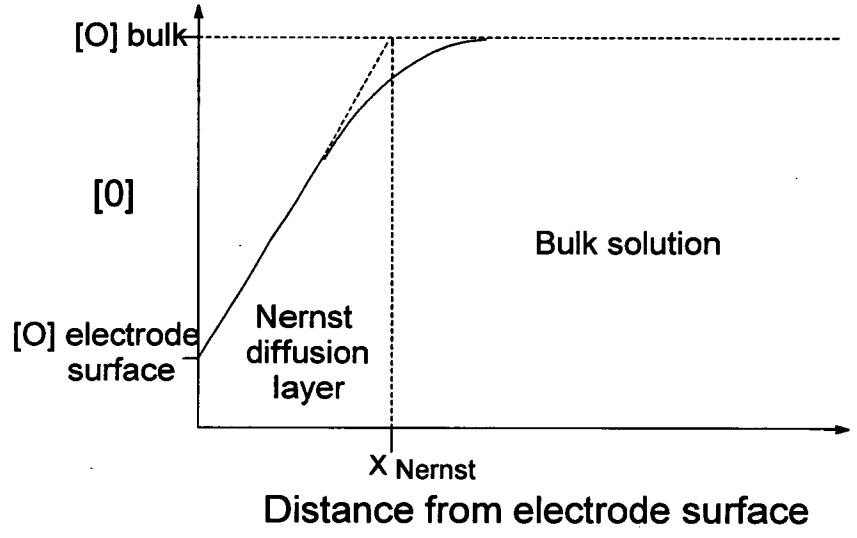

Fig. 2.3 - Concentration-distance profile of reactant. Nernst diffusion layer.

Outside this layer convection is strong enough to maintain the concentration of all species at their bulk values; however inside the diffusion layer the concentration of electroactive species varies essentially linearly with distance producing a uniform concentration gradient. This concentration gradient can be varied by decreasing or increasing the Nernst diffusion layer thickness which is dependent upon the force of convection. Mass transport by diffusion is directly proportional to this concentration gradient, hence the mass transport can be controlled by the rotation speed of the electrode. The potential of the electrode can be independently controlled and by varying the rate of mass transport at a given potential the current data obtained can yield information on the kinetic parameters of the system.

For potentials where the surface concentration is zero, reaction is limited by mass transport and the equation relating the limiting current density I_L and the rotation rate W (in Hz) is the Levich equation (Equ^n 2.1).

$$I_L = 1.554\ n\ F\ A\ D^{2/3}\ \upsilon^{-1/6}\ C_\infty\ W^{1/2} \quad \text{--- Equ}^n\ 2.1 \text{ - Levich Equation}$$

Where :- n = number of electrons,
F = Faraday's constant,
D = Diffusion coefficient,

υ = Kinematic viscosity,
A = Area of electrode,
and C_∞ is the bulk concentration of species.

Derivation of this equation has been described elsewhere[122]. In a mass transport controlled regime, a plot of I versus $W^{1/2}$ should be linear and pass through the origin and thus be used as a test to elucidate whether the current density is entirely mass transport controlled. The gradient of the plot can be used to estimate the number of electrons transferred in the process if the diffusion coefficient is known.

However there is often a mass transport independent step at the electrode, i.e.

$$C_O \xrightarrow[-ne^-]{K_{ox}} C \qquad \text{--- Equ}^n\ 2.2$$

The overall reaction mechanism can then be described as :-

$$C_{bulk} \xrightarrow[\text{mass transport}]{k_d} C_O \xrightarrow[-ne^-]{k_{ox}} C \qquad \text{--- Equ}^n\ 2.3$$

Where :- k_d = Rate constant for mass transport step,
k_{ox} = rate constant for electrode reaction,
and C_0 is surface concentration of species.

For the electrode reaction, $I = n F A k_{ox} C_0$ --- Equ^n 2.4

The mass transport step in the diffusion layer,

$$I = n F A k_d (C_{bulk} - C_0) \qquad \text{--- Equ}^n\ 2.5$$

As the currents are equal $C_O = \{k_d / (k_d + k_{ox})\} C_{bulk}$ --- Equ^n 2.6

Hence when $k_d >> k_{ox}$ the reaction at the electrode is limiting and when $k_d << k_{ox}$ the reaction is limited by mass transport only.

If k_{ec} = observed electrochemical rate constant then

$$I = n F A k_{ec} C_\infty \quad \text{--- Equ}^n \text{ 2.7}$$

and $$1 / k_{ec} = 1 / k_d + 1 / k_{ox} \quad \text{--- Equ}^n \text{ 2.8}$$

So that, $$1 / I_{obs} = 1 / (nFAC_\infty [1/ k_d + 1/ k_{ox}]) \quad \text{--- Equ}^n \text{ 2.9}$$

This leads to, $1 / I_{obs} = 1 / (nFAC_\infty [(0.643) / D^{2/3}\nu^{-1/6}W^{1/2} + 1 / k_d])$ Equ^n 2.10

Therefore a plot of $1 / I_{obs}$ versus $1 / W^{1/2}$ should be linear if n (the number of electrons passed) is invariant. The intercept, i_∞, can be used to calculate k_{ox} at a given potential and the gradient can be used to calculate the number of electrons passed if the diffusion coeffiecient is known. This is termed a Koutecky-Levich plot[123] .

2.3 - Rotating ring-disc electrode studies.

Reversal techniques, such as CV to detect products produced at an electrode, are obviously not available to a RDE since the product of reaction is continuously being swept away from the surface of the disc and out in to the bulk of solution by the radial flow across it. However addition of a ring electrode surrounding the disc electrode can yield information of products that are being swept radially out from the disc to be intercepted (collected) by the ring electrode. The potentials of the ring and disc electrodes can be independently controlled to facilitate the study of specific processes of interest. Figs. 2.4 (a) & (b) & (c) show a rotating ring-disc electrode (RRDE) and its hydrodynamic flow.

The operation of the RRDE is essentially the same as for the RDE with the addition of one important parameter, the collection efficiency of the ring electrode, N_0, defined as :-

$$N_0 = |I_{ring}| / |I_{disc}| \quad \text{--- Equ}^n\ 2.11$$

I_{ring} must be a transport limited current for product and there must be a 100% efficient reaction.

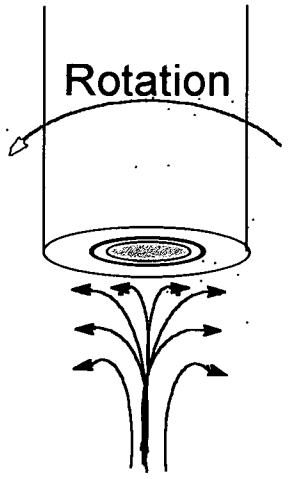

Fig. 2.4 (a) - Hydrodynamic flow.

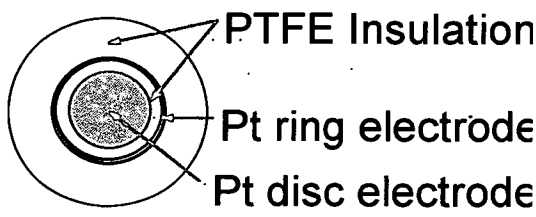

Fig. 2.4 (b) - Rotating ring-disc electrode.

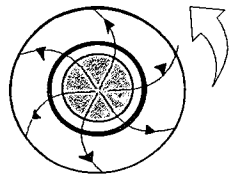

Fig. 2.4 (c) - Radial flow pattern across ring-disc electrode.

For a reversible reaction $O + e^- \Leftrightarrow R$

Where I_{ring} indicates the mass transport limited ring current expected for any disc current, I_{disc}, so long as the number of electrons passed in both ring and disc reactions are the same.

If O is reduced at the disc and the ring set at a potential for the re-oxidation of R then not all of the R produced at the disc will reach the ring to be oxidised back to O (collected). This is because not all of the R is swept directly past the ring and some is lost to the bulk of solution. Hence a fraction of the disc current is observed at the ring and this fraction (collection efficiency, N_0) is dependent solely on the specific electrode geometry. The effect of electrode geometry on the collection efficiency has been described theoretically elsewhere[124].

Soluble products can be detected at the ring by setting the potential of the disc to that at which the electrochemical reaction at the disc takes place, then by sweeping the potential of the ring while monitoring the ring current, a ring polarogram of electro-active soluble products that have been produced at the disc electrode can be plotted.

Some useful information can be obtained from RRDE experiments by considering the transit time for a species produced at the ring electrode to cross the gap and be detected at the ring electrode. The transit time, t, has been described theoretically[152] as :-

$$t = 3.58\ (\nu/D)^{1/3}\ [\log\ (r_2/r_1)\ ]^{2/3} \qquad \text{--- Equ}^{n}\ 2.12$$

Where r_2 and r_1 are the radii of the disc electrode and the gap respectively.

Quantitative kinetic measurements can also be obtained by monitoring the disc and ring currents when holding the ring and disc at specific potentials where reactions of interest occur. A full explanation of the theory behind RDE and RRDE experiments can be found elsewhere[4].

2.4 - Fluorescence spectroscopy.

It has been observed that indole, some substituted indoles and conducting polymers produced from them are highly fluorescent and are therefore suitable for study by fluorescence spectroscopy[112].

Fluorescence spectroscopy is used to detect the emission of radiation due to the relaxation of an electronically excited molecule to the ground state. Transitions that can lead to fluorescence are shown in the Jablonski diagram in fig. 2.5.

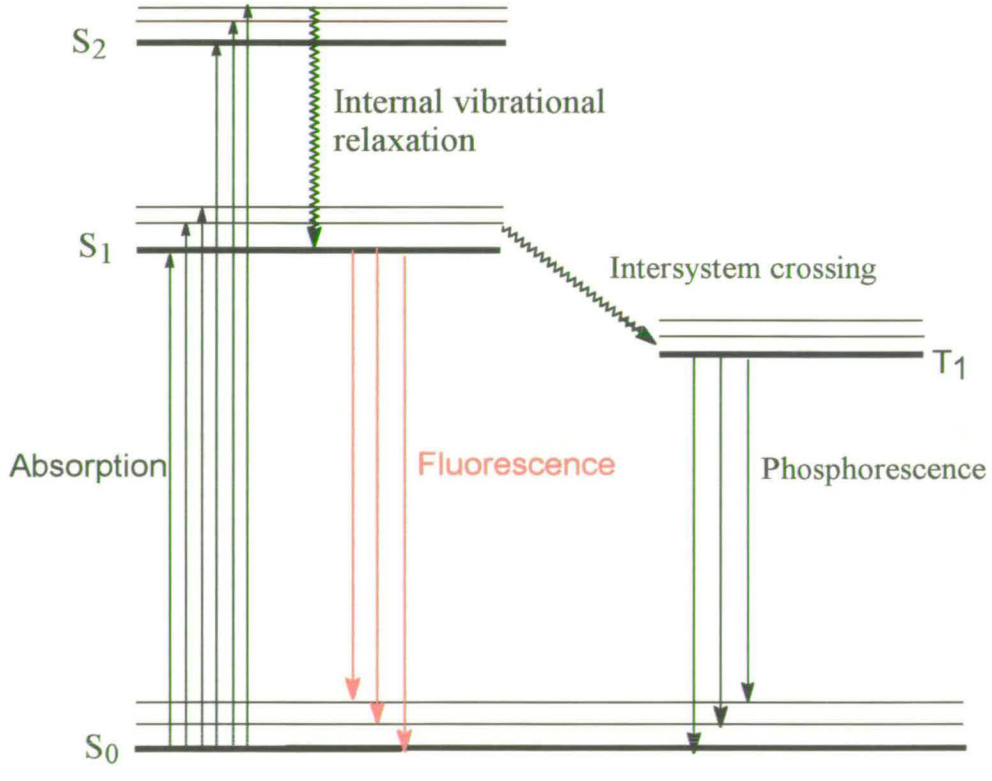

Fig. 2.5 - Jablonski diagram

In the absence of any electromagnetic radiation most molecules will occupy the lowest electronic state (ground state), S_0, and have a Boltzman distribution of vibrational levels. The molecule can absorb electromagnetic radiation, typically in the ultaviolet or visible region of the

spectrum, which induces promotion of an electron from the ground state to an electronically and vibrationally excited state.

In solution, molecules constantly collide with solvent which induces a very fast non-radiative decay of states higher than the S_1 electronically excited state down to the lowest vibrational level of the S_1 state; this is termed vibrational relaxation.

From this electronically excited S_1 state a number of processes can occur. The molecule can undergo spontaneous emission of radiation and relax back to the vibrational sub-levels of the electronic ground state S_0 which is termed fluorescence. Thus detection of the emission (fluorescence) spectrum can yield information on the S_1 state and the vibrational sub-levels of the S_0 state of the molecule under study. The electronically excited molecule can also undergo decay to the electronic ground state through further vibrational relaxation, chemical reaction or undergo phosphorescence via the forbidden transition of inter-system crossing by inversion of the excited electron to a triplet state.

Fluorescence spectroscopy is a very useful tool for the study of conducting polymers as it can yield important information on the transitions between the excited S_1 state of a molecule to its ground state S_0. This in turn can tell us about the vibrational energy distributions which can produce some structural information and about additional effects due to solvents etc. Full theoretical considerations of fluorescence spectroscopy has been decribed elsewhere[125]

2.5 - Electron Paramagnetic Resonance spectroscopy.

Electron paramagnetic resonance (EPR) spectroscopic methods can be used for the study of species that have unpaired electrons and therefore a net electronic spin. The spectrometer detects the magnetic fields at which they come in to resonance with microwave radiation. An EPR spectrum consist of monitoring the microwave absorption as the magnetic field is changed. Some conducting polymers when in their charged oxidised state contain unpaired electrons and can therefore be studied by EPR.

A spinning electron acts as a magnet and takes up a quantised spin angular momentum in an applied magnetic field either with its spin parallel to the applied magnetic field (M_s = -1/2) or anti-parallel (M_s = +1/2). In this field the spins split in to separate energies and transitions between these two spin states can be observed by EPR, fig. 2.6.

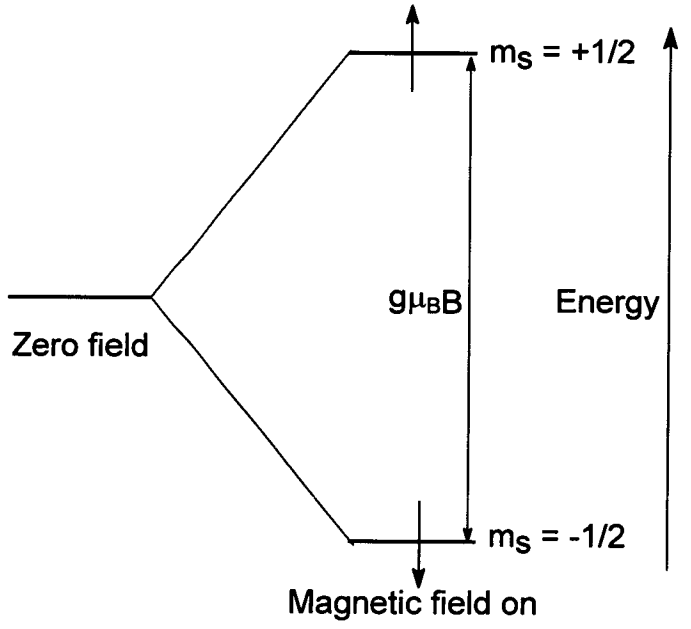

Fig. 2.6 - Electron spin levels in a magnetic field

The spin magnetic moment interacts with the local magnetic field where the resonance condition is given as :-

$$h\nu = g\mu_B B \quad \text{--- Equ}^n\ 2.13$$

Where :- B = The applied magnetic field
μ_B = The magnetic moment
g = The g-factor

The local magnetic field experienced by a particular atom is dependent upon the local field effects due to other neighbouring atoms in the molecule and this is indicated by the g-factor in the epr spectrum. The deviation of g from g_e, the electron g value, depends on the ability of the applied field to induce local electron currents in the radical and therefore its value gives some indication about electronic structure.

Hyperfine splitting arises from the interaction of the electron spin with nuclear spin present and is indicated in the epr spectrum by further splittings of the m_s transitions. The hyperfine structure can be used to fingerprint the type of radical present, moreover it can be used to map the molecular orbital occupied by the unpaired electron. A full description of the theoretical consideration is described elesewhere.[126]

2.6 - Super Conducting Quantum Interference Device.

The super conducting quantum interference device (SQUID) magnetometer is essentially a very sensitive device for measuring magnetic fields The sample is moved through superconducting detection coils at the centre of a magnetic field and the magnetic moment of the sample induces an electric current in the detection coils. This current is converted linearly in to a voltage which is directly proportional to the magnetic flux of the sample. The technique is related to epr in that it can

be used to measure the paramagnetism of the charged state in some conducting polymers. The SQUID magnetometer can measure the magnetisation of the sample (M) as a function of temperature (T) and/or the applied magnetic field (H). The magnetism and applied magnetic field can be related by a simple equation (Equ^{n} 2.14).

$$B = H + 4\pi M \qquad \text{--- Equ}^{n}\ 2.14$$

Where B is the flux density, this can be thought of as the net local field. Another important relationship is called the magnetic susceptibility, χ

$$\chi = M / H \qquad \text{--- Equ}^{n}\ 2.15$$

A plot of M Vs H for a paramagnet shows a simple linear relationship that intersects the origin. The magnetisation is usually reversible. The magnetic susceptibility, χ, is an important parameter for such a paramagnet. Two features are often used to describe such paramagnets, the magnitude of χ and its temperature dependence, i.e. $\chi(T)$. A plot of $1/\chi$ vs T is useful to characterise paramagnets and should result in a straight line. The slope of this line is equivalent to :-

$$1 / b\ \mu_{eff}^{2} N \qquad \text{--- Equ}^{n}\ 2.16$$

Where b = a universal constant μ_{eff} is the effective magnetic moment.

N = the concentration of magnetic atoms with that moment.

Hence this kind of $\chi(T)$ plot can be used to determine the product of the effective moment of an atom and the number of magnetic atoms present. If one of them is known the other can be determined. A full review of the uses and theory behind the use of SQUID is described elsewhere.[127]

Chapter 3 - Experimental

The following chapter details the apparatus and experimental methods used in order to achieve the results discussed in chapters 4-8.

3.1 - Circuitry

Rotating disc and ring-disc electrode studies were carried out using a modular potentiostat/galvanostat with combined wave-form generator and voltage sources (Oxford Electrodes).

Other electrochemical measurements were recorded using a Ministat potentiostat (Sycopel), combined with a PPRI Waveform generator (Hi-Tek Instruments).

An x-y-t chart recorder (Bryans Instruments 60000) was used to record the electrochemical data.

3.2 - Electrodes

3.2.1 - Working and Counter Electrodes

The working rotating ring-disc electrode consisted of a platinum disc electrode (Oxford Electrodes) with a disc area of = 0.387cm^2 (diameter of 7.0mm). The platinum disc was surrounded by in an insulating gap of PTFE (diameter of 7.5mm) which was in turn surrounded by a platinum ring electrode (diameter of 8mm). The platinum ring electrode was in turn surrounded by a PTFE insulating mantle.

The counter electrode consisted of a 2cm^2 platinum gauze (Oxford Electrodes).

The working electrodes were hand polished using 25μm Alumina (Büehler Limited) in a water slurry followed by polishing in 3 μm Alumina (Büehler Limited) also in a water slurry and then rinsed thoroughly in doubly deionised water.

The working electrode was further cleaned electrochemically by cycling past the anodic and cathodic solvent limits in aqueous sulphuric acid (50mM).

Counter electrodes were cleaned using a nitrating mix of 1:1 nitric acid (BDH) and sulphuric acid (BDH) and then subsequently rinsed with doubly deionised water and flamed unitil red hot over a micro bunsen burner.

3.2.2 - Reference Electrode

For non-aqueous work, a Ag/Ag^{+} reference electrode was used. Constructed in-house, it consisted of a silver wire dipping into a solution of silver perchlorate ($AgClO_4$, 99%, Aldrich, 0.01mol dm^{-3}) in acetonitrile[112].

All potentials for non aqueous work are reported with respect to this electrode. This electrode has a potential of +0.437V with respect to a saturated calomel reference electrode and a potential of +0.681V against a normal hydrogen electrode, NHE.

All potentials quoted in Chapters Four, Five, Six, Seven, and Eight are given with respect to this electrode.

For aqueous work a saturated calomel reference electrode (Russell Electrodes) was employed.

3.3 - Rotation System & Cell Assembly.

For rotating disc and ring-disc electrode studies a motor controller supplied by Oxford Electrodes was employed. Such an assembly has been described elsewhere[128].

3.4 - Chemicals

3.4.1 - Purification

Indole-5-carboxylic Acid (I5CA, 99%, Aldrich) was recrystallised twice from deionised water and dried in an oven at 130°C for two days prior to use. 5-Cyanoindole (5CI, 99%, Aldrich), was recrystallised from ethanol and dried in *vaccu* before use.

3.4.2 - Other Chemicals

Indole (Aldrich,99+% GC), 5-Methylindole (Aldrich,99%), 5-Bromoindole (Aldrich,99%), 5-Chloroindole (Aldrich,98%), 5-Methoxyindole (Aldrich,99%), 5-Nitroindole (Aldrich,98%), 5-Aminoindole (Aldrich,97%), 5-Hydroxyindole (Aldrich,97%) and 5-Benzyloxyindole (Aldrich,95%) were all used as received.

Lithium Perchlorate ($LiClO_4$, Aldrich 99%+) was dried in *vaccu* before use. Sodium Perchlorate ($NaClO_4$, Fluka), Tetraethylammonium perchlorate ($TEAClO_4$, Fluka 99%), Tetraethylammonium tetrafluoroborate ($TEABF_4$, Fluka 99%), Tetraethylammonium hexafluorophosphate ($TEAPF_6$, Fluka 99%), Sodium Chloride (NaCl, BDH, 99.9%), Pottasium ferricyanide ($K_3Fe(CN)_6$, Fissons, 98%), Ferrocene ($FeC_{10}H_{10}$, Fluka, 98%), Ferrocene-carboxylic acid ($FeC_{11}H_{10}O_2$, Alrdich, 98%), 1,2-Dichloro-etha-1,2-dione ($C_2Cl_2O_2$, Aldrich), and Pyridine (C_5H_5N, Aldrich, 99%) were all used as recieved.

3.5 - Solvents

Acetonitrile (MeCN, Fisons, dried doubly distilled), N,N-Dimethylformamide (DMF, Aldrich 99%), Tetrahydrofuran (THF, Labscan), Dimethylsulfoxide (DMSO, Aldrich 99+% anhydrous), Diethyl Ether (Rathburn), Ethyl Acetate (Rathburn) and Acetone (Prolabo) were all used as received.

Sulphuric Acid (H_2SO_4, Fisons), Hydrochloric Acid (HCl, Fisons), Nitric acid (HNO_3, Fisons) and were all used as received.

3.6 - Mass Spectrometry

3.6.1 - L^2TOF

Laser Time-of-flight mass spectrometry was carried out in conjunction with Dr P.P.R. Langridge-Smiths' research group within the Department of Chemistry, University of Edinburgh.

The mass spectrometer system used in these studies has been described in detail elsewhere[129]. The mass spectra of the polymeric species was recorded using two-step laser desorption laser photo-ionisation time-of-flight mass spectrometry (L^2TOFMS).

The sample (given as a concentrated solution) was deposited onto a stainless steel rod by drop-coating the material in a suitable solvent followed by evaporation. A pulsed CO_2 laser (wavelength 10.6μm) was used to vaporise the species as intact neutral molecules which were photo-ionised by multiphoton absorption using 198 nm or 248nm laser radiation.

In L^2TOFMS, the desorption and entrainment steps are separated both spatially and temporally which allows for the independent optimisation of each process with respect to laser power and wavelength. The resulting ions were mass analysed using a time-of-flight mass spectrometer. The ions were detected by a microchannel plate detector and the signals were amplified then digitised with a Jöerger TR200 (200 MHz) transient recorder. The data were processed using a Dell microcomputer connected to the spectrometer *via* a CAMAC interface.

3.6.2 - MALDI

The MALDI mass spectroscopy was carried out by Dr Ian Mowat in the chemistry department in the University of Edinburgh. The mass spectrometer has been described fully elsewhere[130]. The sample was mixed in to a solution of the matrix (1,8,9-trihydroxyanthrocene-dithanol) and Potassium/sodium salts. This solution was then droped on to the sample holder (stainless steel) and the solvent evaporated. The sample was then placed in to the mass-spec system and ionised and desorbed using a Nitrogen laser with a wavelength of 337.1nm (Lambda Physik excimer laser, model EMG102). The polymer fragments were then detected by a dual microchannel plate (Galileo Electro-Optics Corp) and their time of flight analysed. The data were then transferred to a Personal Computer and analysed in MicroCal Origin software.

3.7 - Spectroscopy

3.7.1 - UV/visible Absorption Spectroscopy

UV-visible spectroscopic measurements were recorded using a Shimadzu UV-160A recording spectrophotometer with 1cm silica transmission cells.

3.7.2 - Fluorescence Spectroscopy

Fluorescence experiments were carried out and recorded on a Jobin Yvon Spex Fluoromax spectrometer. Spectra were recorded using poly(methyl methacrylate) (PMMA) UV disposable 1cm cuvettes (Fisons).

3.7.3 - Infra Red Spectroscopy

IR spectra were collected on a Bio-Rad FTS-7 FTIR spectrometer. Samples were recorded either in Nujol cast on NaCl plates or in DMF or DMSO solution.

3.7.4 - ^{1}H NMR Spectroscopy

^{1}H NMR experiments were carried out by the High Field NMR Spectroscopy Service at the Department of Chemistry, University of Edinburgh. All ^{1}H NMR spectra were obtained at 360.13 MHz, using a Brücker AM 360 NMR Spectrometer. Spectra were referenced to internal TetraMethylSilane (TMS) at 0 ppm.

Samples were dissolved in either d_6-DMSO (Aldrich), d_8-THF (Aldrich), d_6-Acetone (Aldrich) or as otherwise indicated.

3.7.5 - X-ray diffraction

The crystal structure of the NIFA molecule was obtained on a Stoe-Stadi 4-circle diffractometer by Dr Simon Parsons at the University of Edinburgh.

3.7.6 - EPR

The EPR data was recorded on a ESR model ER 200D from Brucker using a ER 041 MR Microwave bridge, Brucker.

3.7.7 - SQUID

The SQUID data were recorded on a Quantum Design $MPMS_2$ model by Dr G. Whittaker.

3.8 - Experimental details

All of the electrochemical measurements in this thesis were recorded in background electrolyte 0.1M $LiClO_4$ unless otherwise stated.

3.8.1 - Chapter Four - Polymerisation of 5-substituted indoles.

3.8.1.1 - RRDE experiments

The rotating ring-disc experiments described in chapter 4 were carried out using a modular potentiostat/galvanostat with combined wave-form generator and voltage sources (Oxford electrodes). The experiments were run with the following circuit which allowed both the ring and disc electrodes to be potentiostated (fig. 3.1).

In fig. 3.1, terminal 2 is connected to the disc bias, terminal 3 is connected to the ring bias, terminal 4 is connected to the scan input, terminal 5 is the ring output and terminal 6 is the disc output. This allowed the ring electrode potential to be scanned with the ring current output being recorded at the chart recoder. The disc voltatge was set with the d.c. voltage source and the disc current monitored on a dual voltmeter. To maintain a constant disc current, the d.c. voltatge source was manually increased or decreased over a small potential range and the disc current noted. The ring current-time transients described in section 4.6 were obtained by setting the scan unit (and therefore ring potential) to hold at 0V and the current recorded with the time base input on the x-y-z chart recorder.

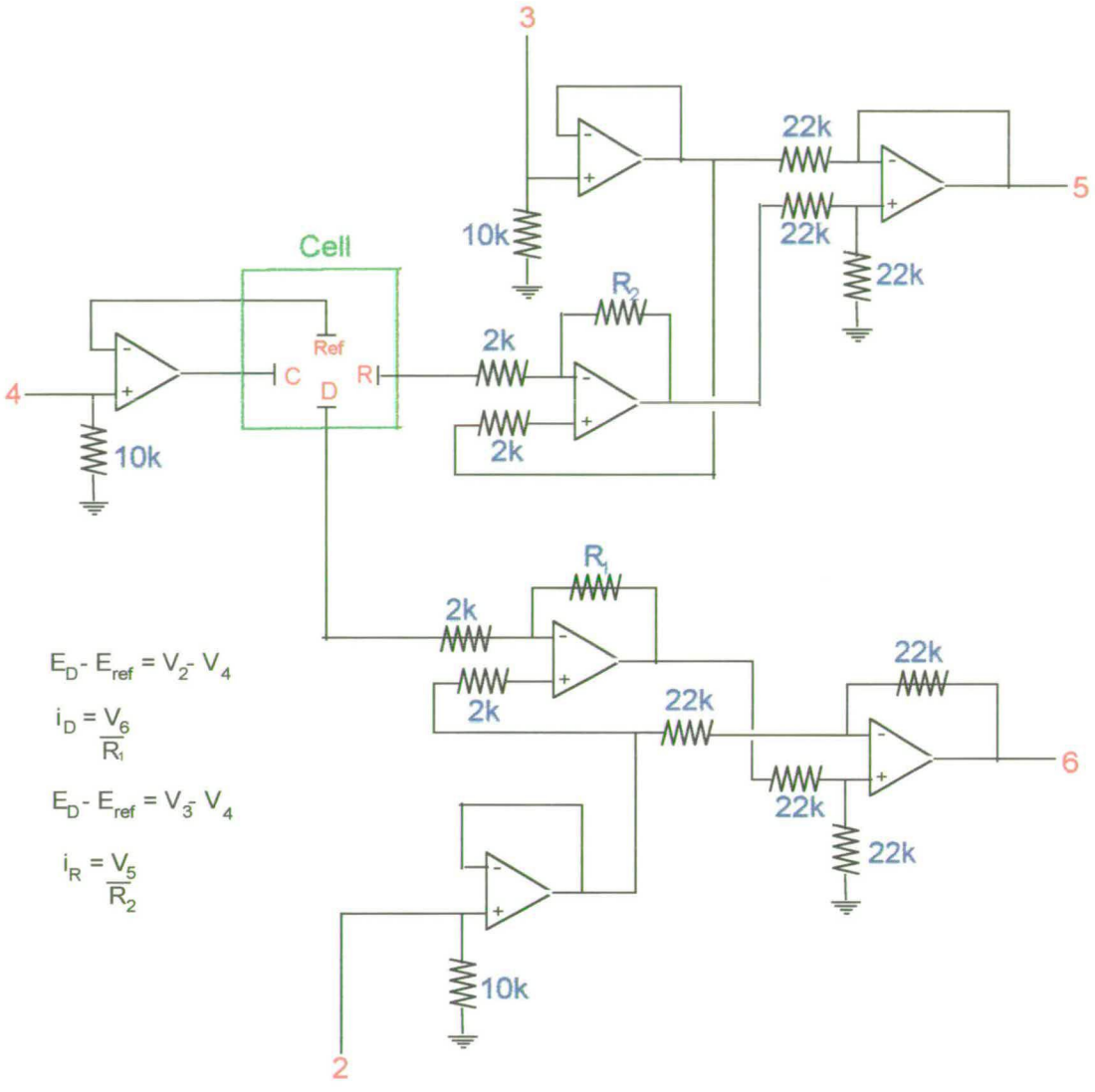

Fig. 3.1 - Circuit diagram of bipotentiostat set-up.

3.8.1.2 - Fluorescence experiments in 4.3.1 and 4.5.

These fluorescence experiments were carried out by dissolving a pipette drop of the sample in spectroscopic grade Ethanol (Aldrich) and placed in a disposable UV cuvette (Aldrich). The specta were recorded at room temperature and analysed by the datamax software.

3.8.1.3 - EPR

The EPR data was recorded from a 36mg of an oxidised poly(CI) solid sample. This was recorded at a frequency of 9.81Ghz.

3.8.1.4 - SQUID

15.58 mg of a poly(CI) sample was placed in a silica sample holder (which does not have a significant magnetic moment) and the resultant magnetic behaviour observed with varying temperature.

3.8.2 - Chapter Five - Electrooxidation of N-methylindole

3.8.2.1 - Molecular modelling

The molecular modelling calculations were obtained using a "Desk top molecular modeller" version 1.2, Oxford University Press.

3.8.2.2 - Fluorescence

The Fluorescence spectra were recorded in specroscopic grade Ethanol at room temperature.

3.8.2.3 - MALDI mass spectroscopy

The MADLI mass spectrum was recorded by mixing together the electrooxidised N-methylindole product with the 1,8,9-trihydroyanthracen-dithanol matrix and allowing the actetonitrile solvent to evaporate.

3.8.3 - Chapter Six - Electrooxidation of 5-aminoindole

3.8.3.1 - Fluorescence

The fluorescence spectra were all recorded at room temperature in spectroscopic grade Ethanol.

3.8.3.2 - pH studies

The pH studies were recorded using a zero-current potentiometric method in 0.1M NaCl / H_2O. These were carried out using a patchable potentiostat/galvanostat with combined wave-form generator and voltage sources (Oxford Electrodes) with the following connections:-

Saturated calomel electrode reference electrode ↔ Buffer A input
Disc electrode ↔ Buffer B input
Buffer A output ↔ Top difference input
Buffer B output ↔ Bottom difference input
Difference output ↔ Dual voltmeter readout.

The DVM readout gave a zero-current potential reading of the copolymer film. The pH probe was a standard glass pH electrode (Russel electrodes) and was used to measure the pH of the aqueous solution. The electrode was rotated at 2 Hz to mix the solution thouroughly.

3.8.4 - Chapter Seven - Copper ion sensor

3.8.4.1 - Potential responses to Cu^{II}

The potential responses were carried out using the same technique as that for the pH measurements in Chapter 6 and are desribed in section 3.8.3.2

3.8.5 - Chapter Eight - Ferrocene incorporation

3.8.5.1 - Synthesis of NIFA

0.5 g of Ferroecene-mono-carboxylic acid was dissolved in 20 mls of dry CH_2Cl_2 in a Shlenk tube. 1:1 $C_2O_2Cl_2$ was added under Nitrogen with 1 drop of DMF as a catalyst. Red crystals of Ferrocene-mono-carboxylic acid chloride immediatley began to form. The solvent was evaporated off and more added repeatedly to remove the DMF, HCl (that had formed) and the solvent. 1:1 of the 5-aminoindole was added (280mg). A red / brown ppt immediately started to form. The product was columned (silica 60 (Aldrich) in CH_2Cl_2) under pressure. Two bands were collected. Acetone was added to the column to increase the polarity. A large third band was produced. This was collected and the solvent taken off by a rotary evaporator leaving orangey-red crystals. This product (NIFA) was recrystallised from hot toluene and spectroscopic measurements taken.

Chapter 4 - Polymerisation of 5-substituted indoles

4.1 - Introduction

Indole was first electropolymerised in 1982 by Tourillon et al;[102] since then many workers have attempted to characterise the mechanism of polymerisation and the molecular structures of polyindole and some substituted indoles. As described in Section 1.8, much ambiguity remains on the precise polymerisation mechanism and the linking positions in the indole monomers. Waltman *et al*[106] and Mount *et al*[123] have examined a number of substituted indoles and have observed that indoles substituted in the 1, 2, or 3 positions do not form polymer films, whereas the electropolymerisation of some 5-substituted indoles produced high quality electroactive polymer films. Mount *et al*[123] suggested that 5-cyanoindole (CI), indole-5-carboxylic acid (I5CA) and indole (I) itself electropolymerise via an asymmetric trimer species (fig. 1.27) which link to form a polymer consisting of linked trimer units. These asymmetric trimers have been characterised spectroscopically. They proposed that the polymerisation mechanism of CI, I5CA and indole follows two main steps. The first is the linking of three monomers through their 2 and 3 positions to form the asymmetric trimer, the driving force of which is the formation of the delocalised aryl ring. The second step involves the linking of these cyclic trimers on the electrode surface to form a polymer with the loss of two protons per trimer unit. The proposed mechanism for the electropolymerisation of CI, I5CA and I is shown in Equations 4.1 and 4.2.

$$3nIn_{(aq)} \xrightarrow{-7ne,-6nH^+} nIn^+_{3(aq)} \quad \text{--- Equ}^n\ 4.1$$

$$nIn^+_{3(s)} \xrightarrow{-2ne,-2nH^+} -(In^+_3)-_{n(s)} \quad \text{--- Equ}^n\ 4.2$$

Where In, In_3^+ and $-(In_3^+)-_n$ represent indole monomer, oxidised trimer and oxidised polymer consisting of linked trimer respectively.

This thesis is concerned with the study of polyindoles for their potential uses as sensor devices and related technologies. For many of these applications, it is desirable to produce electroactive indole layers containing a wide variety of substituents. The most obvious method for achieving this would be the electopolymerisation of a wide variety of 5-substituted indole monomers.

This chapter seeks to expand on the previous research discussed above; results are presented on the study of the electropolymerisation of a wide variety of 5-substituted indoles and on insights gained on the mechanism of polymerisation.

4.2 - Characterisation of electroactive products from the electropolymerisation of 5-substituted indoles.

The first part of this chapter is concerned with the study of soluble products produced in the electropolymerisation of indole and 5-substituted indoles. The polymerisation mechanism proposed by Mount *et al* (Equ^{n}s 4.1 & 4.2) involves a loss of protons and electrons to facilitate the linking of the monomers and trimer units. More sepecifically it takes the loss of 6 protons and 7 electons to form an oxidised cyclic trimer and the loss of 8 protons and 9 electrons (per trimer) to link the trimers to form an oxidised polymer consisting of linked trimer units.

Some obvious questions arise about what happens to the protons produced in the polymerisation, and if the protons can be detected electrochemically. Moreover are there any other soluble products, and is there any additional evidence to validate the proposed reaction mechanism ? It was decided to use a rotating ring-disc electrode (RRDE) to probe the mechanism of polymerisation further, and to attempt to address these questions. The theory of RRDE experiments is decribed fully in section 2.3.

An important parameter for the ring-disc electrode is its collection efficiency (N_0), which relates the proportion of products produced at the disc electrode to that which is transported to the ring electrode by the hydrodynamic regime caused by rotation. This parameter is highly dependent upon the exact geometry of the electrode and can be determined experimentally and theoretically.

4.2.1 - Determination of collection effieciency of the RRDE used.

The most facile way to determine the collection efficiency of an RRDE, is to monitor the current produced at the ring electrode by the rereduction (or reoxidation) of a characterised reversible species, which has been oxidised (or reduced) at the disc electrode with a known disc current. The ratio of ring current observed to the disc current applied when the species (produced at 100% efficiency) is detected at the ring under mass transport control is known as the collection efficiency (N_0).

The collection efficiency was determined for the RRDE used in this work by obtaining ring reduction polarograms at a number of different disc currents for the oxidation of ferrocene at the disc. A plot of the disc current produced by the oxidation of ferrocene, against the ring current "collected" by the reduction of the ferrocinium ion, is shown in fig. 4.1.

From the slope of the best-fit line in this plot, the collection efficiency was calculated to be 0.21 ± 0.005. A similar experiment was carried out using $K_3Fe(CN)_6$ to eliminate the possibility of a spurious result due to any adverse adsorption of ferrocene on the platinum disc electrode that has been previously noted[131]. However the $K_3Fe(CN)_6$ experiment gave a collection efficiency of 0.205 ± 0.005 which is within experimental error of the ferrocene experiment.

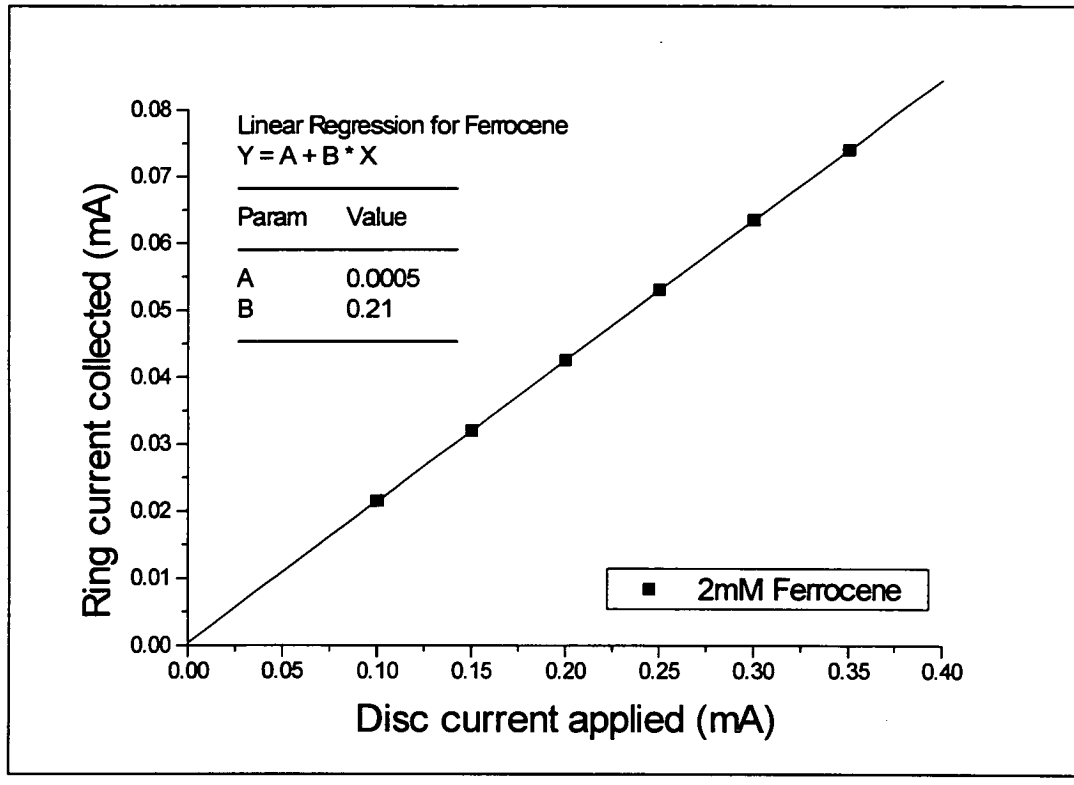

Fig. 4.1 - Collection efficiency determination of RRDE using ferrocene.

4.2.2 - Effective proton collection efficiency for electropolymerisation of indole and 5-substituted indoles.

Having obtained the theoretical collection efficiency of the RRDE, N_0, from the ferrocene/ferrocinium redox reaction, it was now possible to study the electropolymerisation of indole and its derivatives. These RRDE experiments consisted of rotating the ring-disc electrode in a solution consisting of the indole monomer under study in acetonitrile which contained background electrolyte (0.1M $LiClO_4$). The rotation of the electrode acted as a pump which pulled the solution up to the disc electrode and threw it out radially past the ring electrode and out in to the bulk. A potential was chosen at the disc electrode to electropolymerise the indole monomer reaching the disc electrode surface and the current produced by this electropolymerisation reaction was monitored. A dark

green film was observed to form on the disc electrode and any soluble products formed by this reaction were swept out past the ring electrode by the radial flow of the solution. The potential of the ring electrode was scanned to detect any electroactive products being swept past it.

The potentials at where the electropolymerisation reaction of indole and the substituted indoles occur, have been determined by other workers[112]. These have been reproduced by determining the oxidation peak potentials from the cyclic voltammograms of the monomers. Typically around 50mV greater than the monomer oxidation peak potentials were used to ensure that electrochemical oxidation was not the rate determining step and that mass transport or radical cation coupling was rate limiting. However for some experiments described in this chapter, electropolymerisation potentials corresponding to part of the way up the monomer oxidation wave have been employed so that only thin polymer films were formed. This reduced any adverse effects due to thick film formation which would disrupt the theoretical collection efficiencies of the RRDE. However at these lower potentials electrochemical oxidation may be rate determining.

4.2.2.1 - Indole

A typical ring polarogram produced for the electropolymerisation of 20mM indole at the disc electrode is shown in fig. 4.2. As the ring potential was swept more negatively from +0.10V to -1.4V, a classical reversible reduction wave in the ring polarogram was observed. This was obtained with a galvanostatic disc current of 0.2mA. This wave is suggested to have been due to the reduction of protons at the ring electrode that had been released by the linking of indole radical cations and trimers. The ring reaction is therefore :-

$$H^+ + e^- \Rightarrow 1/2\ H_2 \quad \text{--- Equ}^n\ 4.3$$

The limiting ring reduction current ,I_L, was found to be 33μA at a disc current of 0.2mA. A number of ring polarograms were recorded at

disc currents ranging between 0.1mA to 0.35mA and the limiting ring currents noted. These limiting ring currents were plotted against the applied disc currents for each polarogram, fig. 4.3. This shows a good straight line, the gradient of which is equivalent to the ratio of the mass transport limited ring current due to the reduction of protons to the number of electrons passed for the electropolymerisation reaction at the disc electrode. In this work, this ratio is termed the effective proton collection efficiency or N_H.

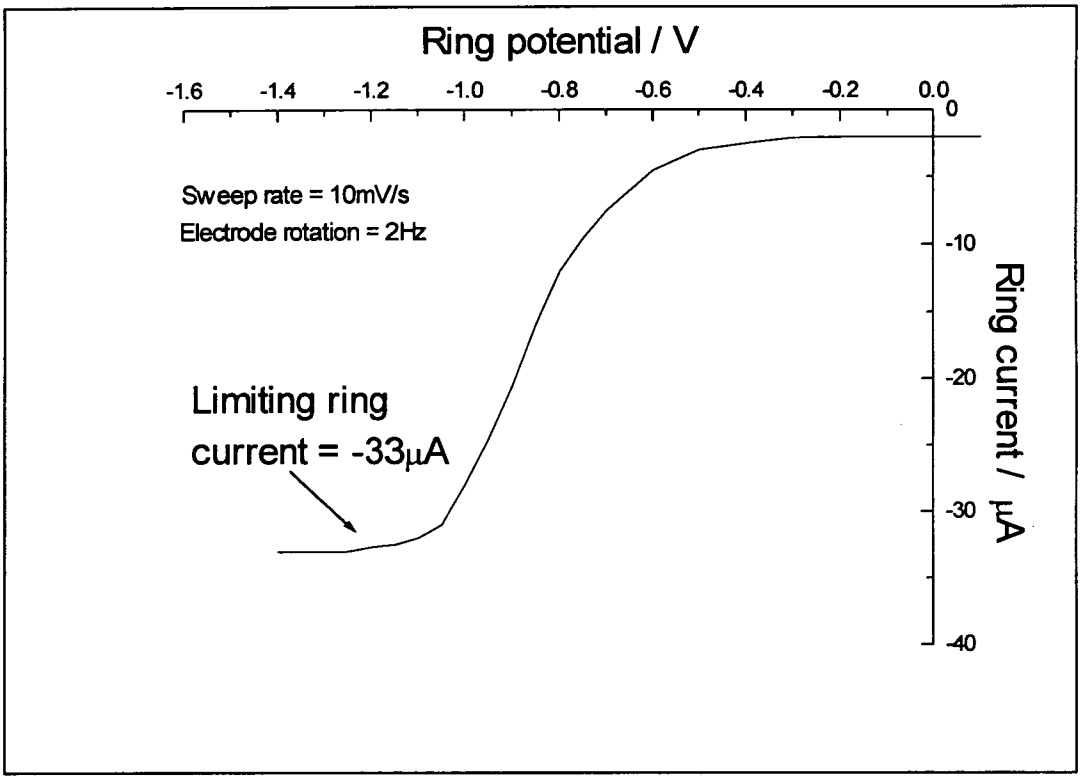

Fig. 4.2 - Ring polarogram from electropolymerisation of indole.

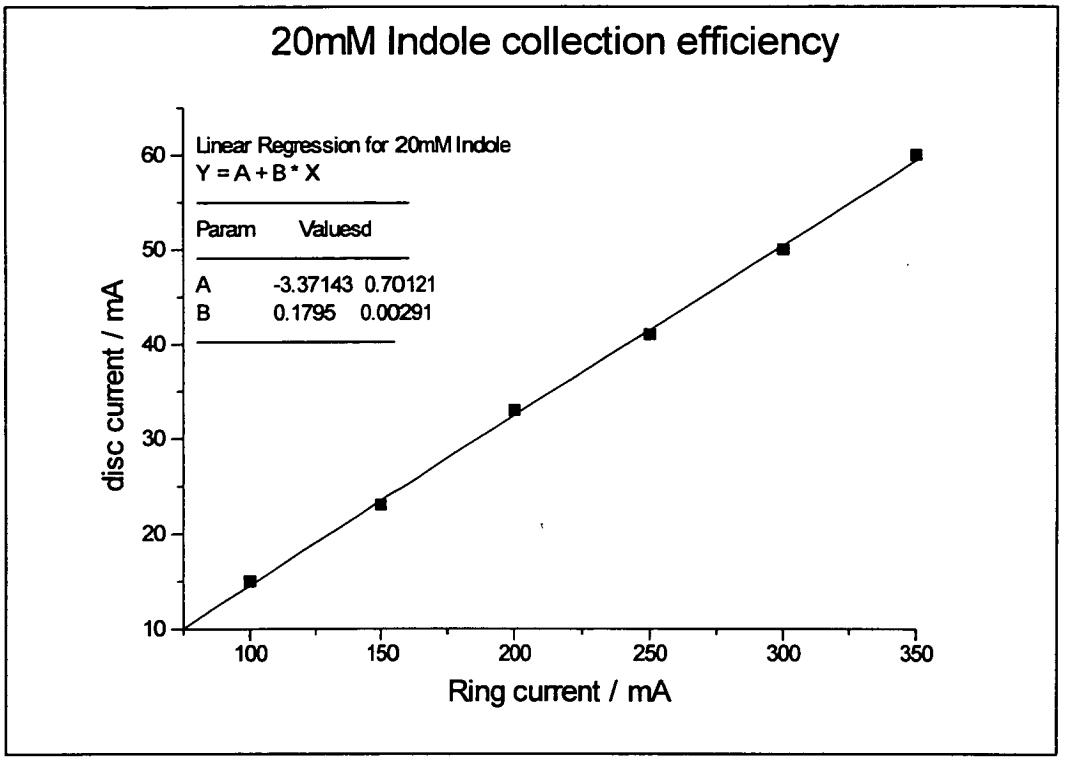

Fig. 4.3 - Plot of proton ring current *vs* disc current applied for electropolymerisation of 20mM indole polaragrams.

Equation 4.4 shows the dependence of the observed ring current on the disc current applied for a soluble species produced at the disc electrode. It can be seen that the ring current observed is dependent upon the disc current passed and the collection efficiency (N_0) of the electrode (in this case $N_0 = 0.21$).

$$|I_{ring}| = |I_{disc}| N_o \quad \text{--- Equ}^n\ 4.4$$

This equation must be modified to describe the detection of protons produced in the electropolymerisation reaction. If the proposed polymerisation mechanism by Mount *et al* was correct, then the formation an oxidised trimer would be expected to result in the observation of six protons for every seven electrons at the disc electrode (Equ^n 4.1). For the formation of an oxidised polymer it would be expected observe eight

protons at the ring for every nine electrons passed at the disc during the electropolymerisation (Equ^{n} 4.2). Thus if Equ^{n} 4.1 dominates the electropolymerisation reaction, the effective proton collection efficiency, N_H, would be equal to :-

$$N_H = 6/7\ N_0 \quad \text{---} \quad \text{Equ}^{n}\ 4.5$$

If Equ^{n} 4.2 dominates the electropolymerisation then the effective proton collection efficiency would be :-

$$N_H = 8/9\ N_0 \quad \text{---} \quad \text{Equ}^{n}\ 4.6$$

Therefore if the proposed polymerisation mechanism was correct, it would be expected to observe an effective proton collection efficiency of between 0.18 and 0.187 depending upon the degree of trimer linkage. Mount *et al*[112] have previously examined the ratio of unlinked trimer to polymer formation in the electropolymerisation of CI, and have found that a greater amount of unlinked trimer is formed at higher monomer concentrations and faster electrode rotation speeds. In principle the value of the effective proton collection efficiency would be able to directly calculate this, however it proved difficult to determine as the experimental errors were such that reproducible significant differences were hard to observe.

For the electropolymerisation of 20mM indole, fig. 4.3, an effective collection efficiency of 0.179 ± 0.005 was observed. This is in good agreement with what was expected from the proposed reaction mechanism and is good evidence to support the reaction mechanism. It also indicates that in acetonitrile, the protons produced in the electropolymerisation are released from the polymer film and can be swept past the ring electrode in to the bulk of solution, where they will react with nucleophiles in the solvent.

4.2.2.2 - Effective proton collection efficiency determination for the electropolymerisation of 5-substituted indoles.

It was decided to examine the effective proton collection efficiencies for a number of 5-substituted indoles, namely 5-cyanoindole (CI), indole-5-carboxylic acid (I5CA), 5-nitroindole (NI) and 5-bromoindole (BI) . Very similar ring polarograms to that in fig. 4.2 were obtained for the electropolymerisation of all the 5-substituted indoles studied.

Fig. 4.4 shows the effective proton collection efficiencies caluclated from RRDE experiments for the electropolymerisation of these 5-substituted indoles. It can be seen that, with the exception of 5-cyanoindole, (which has an N_H of 0.21 ± 0.005) the effective proton collection efficiencies are in the range of about 0.18 ± 0.05. This suggests that the same polymerisation mechanism, consisiting of cyclic trimer and polymer formation, is occuring for the 5-substituted indoles to that of indole. The atypical behaviour shown by the electropolymerisation of 5-cyanoindole suggests that N_H is approximately equal to N_0. Three possible reasons for this difference were proposed; it was suggested that it maybe due to an extra proton being released during the electropolymerisation, or that one electron less is passed at the disc resulting in the formation of a neutral polymer, or that the polymerisation of CI was not occuring evenly over the whole disc electrode.

5-substituted indole	Effective collection efficiency, N_H
Indole	0.180 ± 0.005
5-cyanoindole	0.210 ± 0.005
5-cyanoindole *	0.190 ± 0.005
Indole-5-carboxylic acid	0.185 ± 0.005
5-nitroindole	0.175 ± 0.005
5-bromoindole	0.175 ± 0.005

Fig. 4.5 - Collection efficiencies of protons from RRDE experiments on 5-substituted indoles. * Denotes electropolymerisation carried out on pre-formed polymer layer (see below).

Experiments were carried out to test these proposed reasons for the observed anomaly. If an extra proton was released during the polymerisation, a neutral oxidised trimer/polymer, which could be reduced to an anionic trimer/polymer, would probably result, fig. 4.6.

$$3nCI_{(aq)} \Rightarrow n(CI)_3^{\bullet} + 7e^- + 7H^+$$

Fig. 4.6 - Hypothetical formation of neutral oxidised CI trimer.

If this hypothesis was correct then it would be expected that a disc CV of the 5-cyanoindole would show differences upon changing the cation size of the electrolyte, as a cation would need to be incorporated on the reductive sweep of the CV to retain film electroneutrality. This was tested by forming a 5-cyanoindole polymer (poly(CI) film and obtaining CVs in solutions containing $LiClO_4$, $NaClO_4$, $TEAClO_4$ and $TMAClO_4$. However, no difference was observed between the CVs which suggests that the oxidised neutral trimer does not form.

The poly(CI) film showed a difference in CVs from changing the electrolyte anion from ClO_4^- to BF_4^- and PF_6^-, fig. 4.8. This suggests that the poly(CI) was being cycled between a neutral state and an oxidised cationic state, with the anions being taken up on the oxidative sweep to maintain film electroneutrality. It can be seen that the polymer redox reaction peaks moved to a more positive potential on increasing the anion size from ClO_4 to BF_4 and PF_6 which indicates that it is more difficult (requires a greater overpotential) to insert the larger anions in to the film, fig. 4.7. This reaction is consistent with the polymerisation mechansim proposed in Equ^{n}s 4.1 & 4.2, and has been noted for the other 5-substituted indoles (except I5CA).

$$(CI)_3^+ + e^- \Leftrightarrow (CI)_3$$

Fig. 4.7 - Reduction of oxidised trimer.

The formation of an oxidised poly(CI) layer is reinforced by the observation that on reconnecting the polymer coated electrode circuit at 0V, a large reduction current spike was noted.

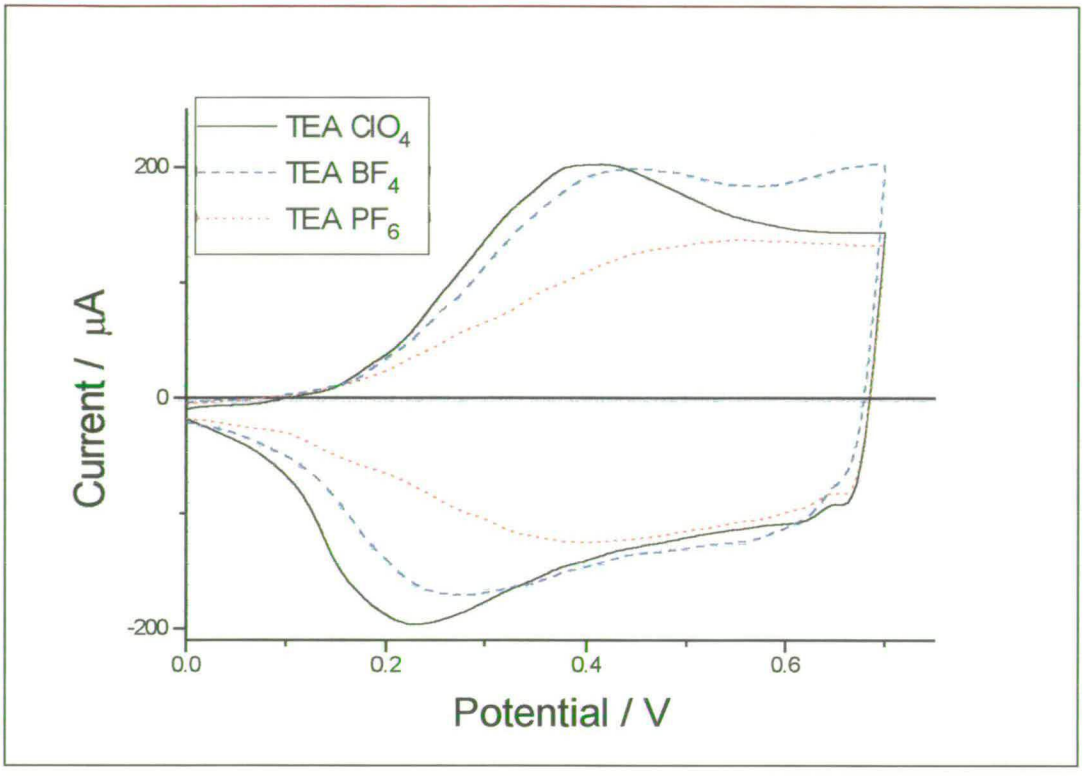

Fig. 4.8 - Poly(CI) anion dependence of CVs. Sweep rate = 10mV/s.

Finally, the atypical N_H value obtained for CI was proposed to be due to the formation of poly(CI) only around the edges of the platinum disc electrode. This had previously been observed by eye which shows a much darker colouration of polymer around the edges of the disc electrode than in the centre. This would have the effect of increasing the observed effective proton collection efficiency, as the protons released from the polymerisation reaction around the edges of the disc electrode have a smaller electrode gap to the ring electrode and would disrupt the theoretical N_0 value. This was tested by recording ring polarograms with polymerisation of the 5-cyanoindole monomer on a pre-formed poly(CI) layer. The pre-formed poly(CI) layer was hoped to facilitate the

electropolymerisation of the 5-cyanoindole monomer across the whole film surface leading to a more accurate value of N_H. The use of a pre-formed polymer layer is explained in greater detail in chapter 6 and 7). The resultant effective proton collection efficiency was found to be 0.190 ± 0.05 using this technique. This value is in experimental error of the 0.18-0.187 range that suggested the validity of the proposed polymerisation mechanism.

The N_H values observed for all the 5-substituted indoles studied indicate that they all appear to be undergoing the polymerisation mechanism proposed in Equ^{n}s 4.1 & 4.2.

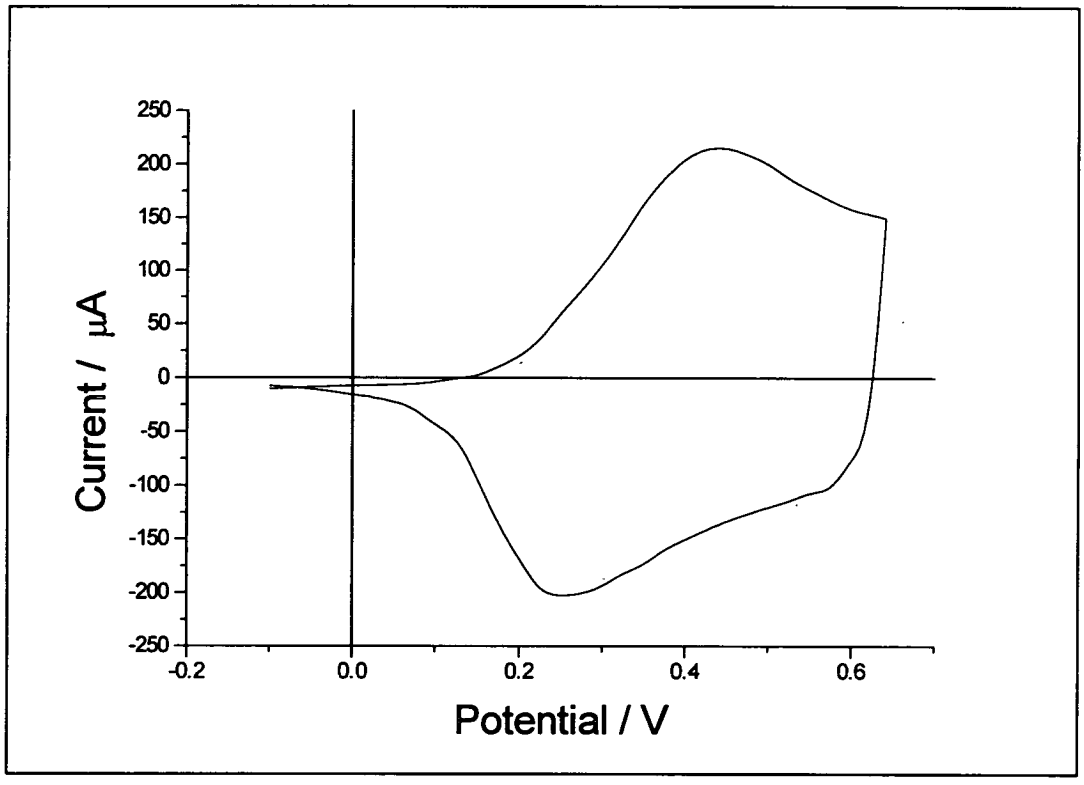

Fig. 4.9. - Disc CV of poly(CI)layer deposited in RRDE electropolymerisation. Sweep rate = 10mV/s.

Cyclic voltammograms of the polymer layers produced on the disc during the ring-disc experiments were very similar to CVs of the polymers observed by other workers[112]. This indicates that the ring electrode was "collecting" protons from the proposed electropolymerisation reaction and not a side-reaction which was leading to some other product. A CV of the polymer formed on the disc obtained from the electropolymerisation of 5-cyanoindole in an RRDE experiment is shown in fig. 4.9.

The proton collection efficiencies for the 5-substituted indoles were recorded out at a number of different monomer concentrations, electrolytes, disc currents and potentials, fig. 4.10. These, however did not show any significant differences on changing the concentration of monomer or the type of electrolyte, which indicates a similar polymerisation mechanism.

Monomer	Concentration of monomer	Electrolyte	$N_H \pm 0.005$
5-cyanoindole	60mM	$LiClO_4$	0.210
	50mM	$LiClO_4$	0.210
	50mM	$NaClO_4$	0.205
	20mM	$LiClO_4$	0.210
	20mM *	$LiClO_4$	**0.190**
	5mM	$LiClO_4$	0.210
Indole-5-caboxylic acid	60mM	$LiClO_4$	0.185
	20mM	$LiClO_4$	0.184
	5mM	$LiClO_4$	0.180
	5mM	$TEAClO_4$	0.175
Indole	60mM	$LiClO_4$	0.185
	20Mm	$LiClO_4$	0.179
	5Mm	$LiClO_4$	0.180

Fig. 4.10 - Table of N_H values for 5-substituted indoles. (* denotes collection efficiency on a preformed 5-cyanoindole layer)

4.2.3 - Evidence that RRDE wave is due to protons.

It has been suggested that the ring polarogram obtained from the electropolymerisation of the 5-substituted indoles is due to the reduction of protons at the ring electrode. These protons were thought to have been lost by the linking of monomer radical cations and trimers to form a polymer. Evidence for this is suggested for a number of reasons.

The wave shows a variation in the observed $E_{1/2}$ value with the addition of trace amount of water or base (for instance the amino group in 5-aminoindole). This was expected as these stabilise protons in acetonitrile. Proton waves have been noted previously in acetonitrile at similar potentials.[132]

An experiment was carried out where protons were added to a solution of 0.1M $LiClO_4$ in acetonitrile by addition of a drop of concentrated HCl. The ring electrode was rotated in the solution under the same experimental conditions to the above RRDE experiments used to study the 5-substituted indoles. The potential of the ring electrode was swept negatively from 0V to -1.60V. The resultant ring polarogram is shown in fig. 4.11. It can be seen that the potential of this wave is very similar to that observed for the waves produced by the electropolymerisation of the 5-substituted indoles. above RRDE. The magnitude of the ring wave is such that it must be due to a species that is produced in almost the same extent as the electrons passed to form it. The only candidates for products of this magnitude are protons and soluble radical cations. The reduction of soluble radical cations would be expected to have a similar potential dependence to that of the monomer oxidation potential and occur at higher potentials than where the wave was observed. As film formation was observed during the polymerisation,most of the radical cations produced must be linking to form the polymer film leaving only a negligible amount to diffuse away from the disc electrode. From these pieces of indirect evidence it seems very likely that the observed waves on the ring electrode were due to the production of protons from the electropolymerisation of the 5-substituted indoles.

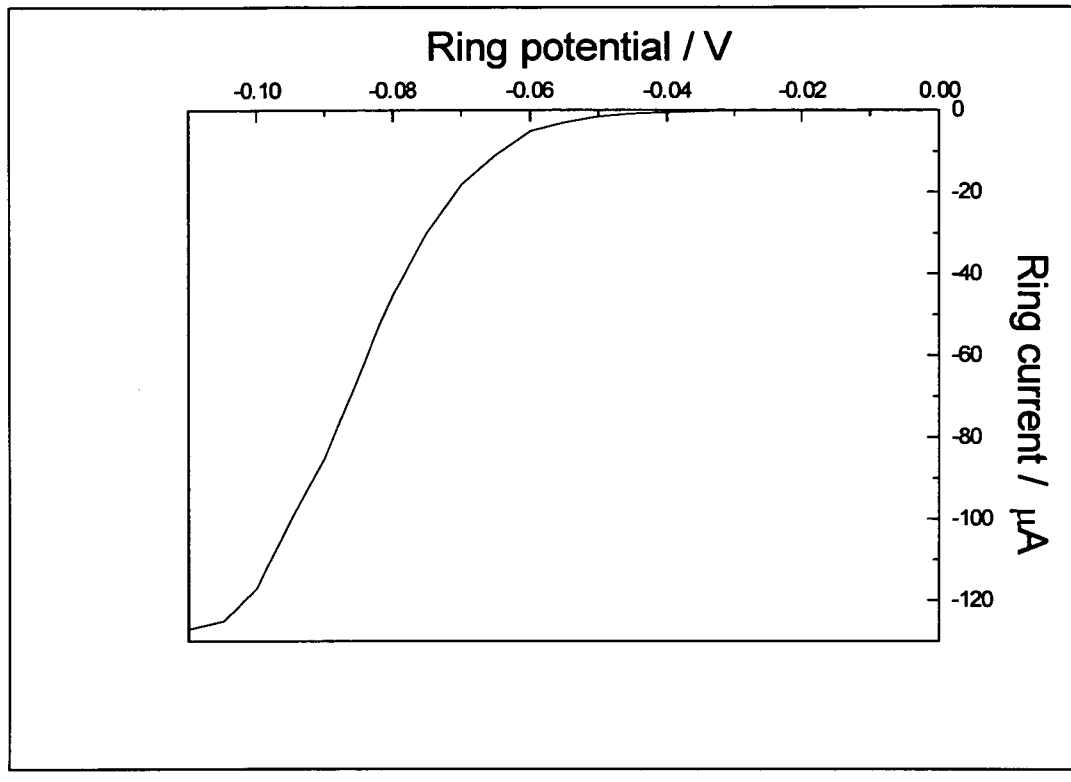

Fig. 4.11 - Ring polarogram produced by the addition of HCl. Sweep rate = 10mV/s. Electrode rot^{n} = 2Hz.

4.3 Detection of soluble trimers.

It has been shown that it is possible to observe the protons released during the electropolymerisation reaction of 5-substituted indoles. In addition to the observation of a proton wave, another electroactive product was observed as a wave at potentials more positive than the proton wave.

4.3.1 - Electrochemistry - RRDE studies.

The RRDE was rotated in a solution of the indole monomer under study and a galvanostatic current applied to the disc. The ring electrode potential was scanned at more negative at a higher potential range to that

of the proton wave. The potential range was found to have a positive potential limit due the oxidation of monomer on the ring electrode, at a negative limit due to the reduction of protons.

The ring polarogram for the electropolymerisation of 0.1M indole is reproduced in fig. 4.12. This shows a well defined reduction wave at potentials lower than the oxidation of the monomer but higher than the reduction of protons. It is proposed that this wave is due to soluble cyclic trimer produced on (and partly in the diffusion layer) the surface of the disc electrode which has been transported to the ring electrode by the hydrodynamic regime of the electrode, where it was reduced (or collected).

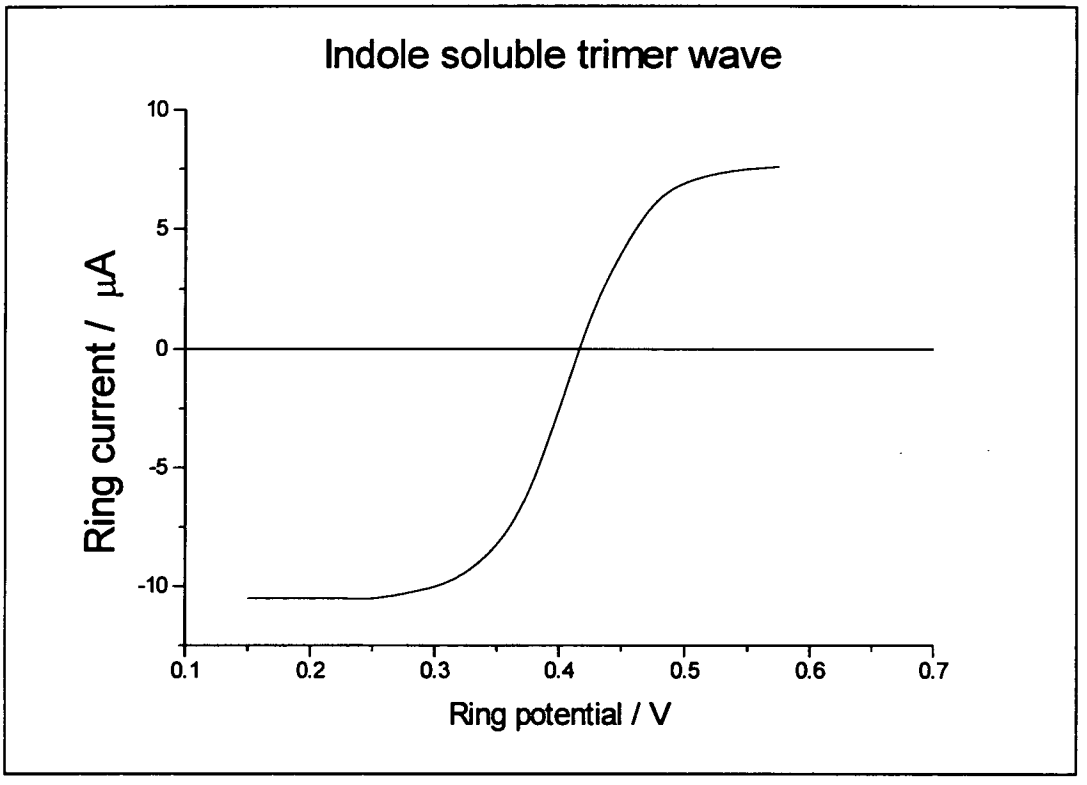

Fig. 4.12 - Ring polarogram of soluble indole cyclic trimer produced by the electropolymerisation of 0.1M indole at start of electropolymerisation. Sweep rate = 10mV/s. Electrode rotation = 2 Hz. Disc I = 1.5 mA.

It was observed that almost half of the current observed on the ring was an oxidation current; this is proposed to be due to the oxidation of neutral trimers that may have formed in the diffusion layer close to the disc electrode and were swept away from the disc before further oxidation. The formation of neutral reduced cyclic trimers is shown in Equ^{n} 4.7.

$$3n\ In^{+\bullet} \Rightarrow n(In)_{3\ (aq)} + 6H^{+} \quad \text{--- Equ}^{n}\ 4.7$$

The other half of the ring current was observed as a reduction current which is believed to be the reduction of oxidised trimers formed from radical cation monomers on the disc electrode (where further oxidation would have taken place), these would then have desorbed from the polymer / electrode surface and been swept past the ring electrode. It is suggested that the reduction wave observed on the ring electrode is due to the reduction of soluble indole cyclic trimers, i.e.

$$(In)_3^{+} + e^{-} \Rightarrow (In)_3 \quad \text{--- Equ}^{n}\ 4.8$$

Experiments were carrried out to elucidate the mechanism of formation of the oxidisable and reducible trimers and are described further in section 4.6.

After indole film formation had taken place on the disc (or at low indole monomer concentrations) it was observed that the oxidised part of the ring trimer wave disappeared to leave only a reduction wave. This suggests that once film deposition has occured, all the cyclic trimer formed is produced on the electrode surface in its oxidised state and not in the diffusion layer, i.e. Equ^{n} 4.8 dominates.

In this case, assuming that free trimer is produced in the polymerisation, the apparent trimer collection efficiency (which is equal to the I_{ring}/ I_{disc}) for this trimer wave would be :-

$$N_{tri} = x/7\ N_0 \quad \text{--- Equ}^{n}\ 4.9$$

In this equation, x, refers to the fraction of trimer formed at the disc electrode which does not remain in the electrodeposited film, but rather desorbs from the film into solution and is detected by the ring.

For the electropolymerisation of 0.1M indole, using Equ^{n}s 4.4 & 4.9 and the observed values of the disc and ring currents, x is calculated to be 0.41 (including both oxidised and reduced trimers) initially which rapidly reduces to 0.25 with the onset of a polymer film. At lower concentrations of indole, x reduces considerably to values of around 0.1. In other words, at the high concentration of 0.1M, the electropolymerisation of indoles results in approximately 1/4 of the trimers formed desorbing from the film surface and entering the bulk of solution. This is not entirely unexpected, as the $(In)_3^+$ were expected to be relatively stable and soluble as it has been noted previously that indole trimer films dissolve completely in MeCN that does not contain any electrolyte[112] .

4.3.2 - Evidence for cyclic trimer formation.

It was observed during the RRDE experiments decribed in section 4.3.1 that the electropolymerising solution became increasingly red / brown coloured and showed a distinct purple fluorescent appearance when held up to sunlight. The colouration was suggested to have been due to soluble species entering the bulk solution produced by the electropolymerisation reaction at the disc electrode. It was thought most likely that these coloured species were the soluble cyclic trimers observed at the ring electrode, and was decided to attempt to characterise these species further.

A solution of 20mM indole monomer was electropolymerised for a relativley long period of time (3hours) with a large area platinum gauze as the working electrode. It was calculated that this pass enough electrons to electropolymerise around 3/4 of the monomer which would allow a relatively large amount of the soluble products of the reaction to enter in to

to the bulk solution where they could be studied. The resultant solution was deep red in colour and highly fluorescent under a UV-light. It has previously been observed that indole, CI and I5CA monomers, trimers and polymers are highly fluorescent, it was therefore decided to study these solution products by fluorescence spectroscopy.

4.3.2.1 - Fluorescence spectroscopy.

The electropolymerised solution was examined by fluorescence spectroscopy. Fig. 4.13 shows highly characteristic cyclic trimer type fluorescence and excitation spectra. This spectrum is very similar to those observed by Mount et al for the fluorescence spectra of 5-cyanoindole and I5CA[114]. This is very strong evidence that soluble trimers were produced in the polymerisation reaction. The fluorescence spectra show very little of any other products in solution apart from some of the remaining unreacted monomer.

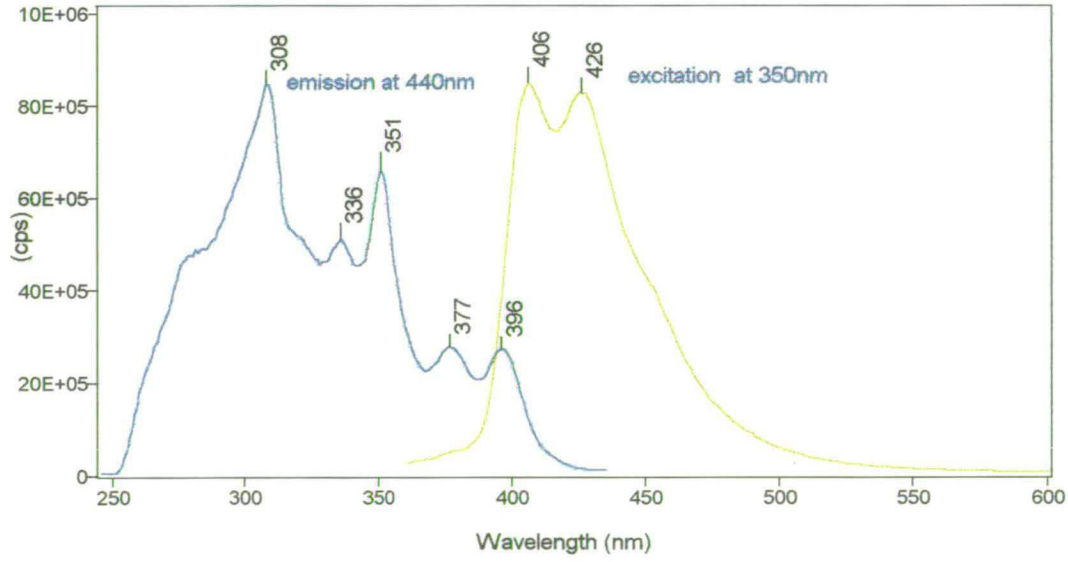

Fig. 4.13 - Fluorescence and excitation spectra of soluble products produced from the electropolymerisation of 20mM indole.

4.3.2.2 - Tafel plot.

A Tafel plot, fig. 4.14, of the ring polarogram produced in the indole RRDE experiment (fig. 4.12) shows that the species observed on the ring undergoes a fully reversible 1-electron redox reaction. This is what would be expected for the reversible one electron oxidation of a delocalised cyclic trimer species (Equ^{n} 4.8). Tafel theory (chapter 2) predicts a slope of 39mV^{-1} for a fully reversible wave. The observed Tafel plot exhibits a gradient of 35mV^{-1} which is reasonably close to the theoretical slope. Similar Tafel plots for some of the trimer ring polarograms produced from the electropolymerisation of 5-substituted indoles, have exhibited gradients closer to the theoretical plot with 5-methylindole producing a plot with a gradient of exactly 39 mV.

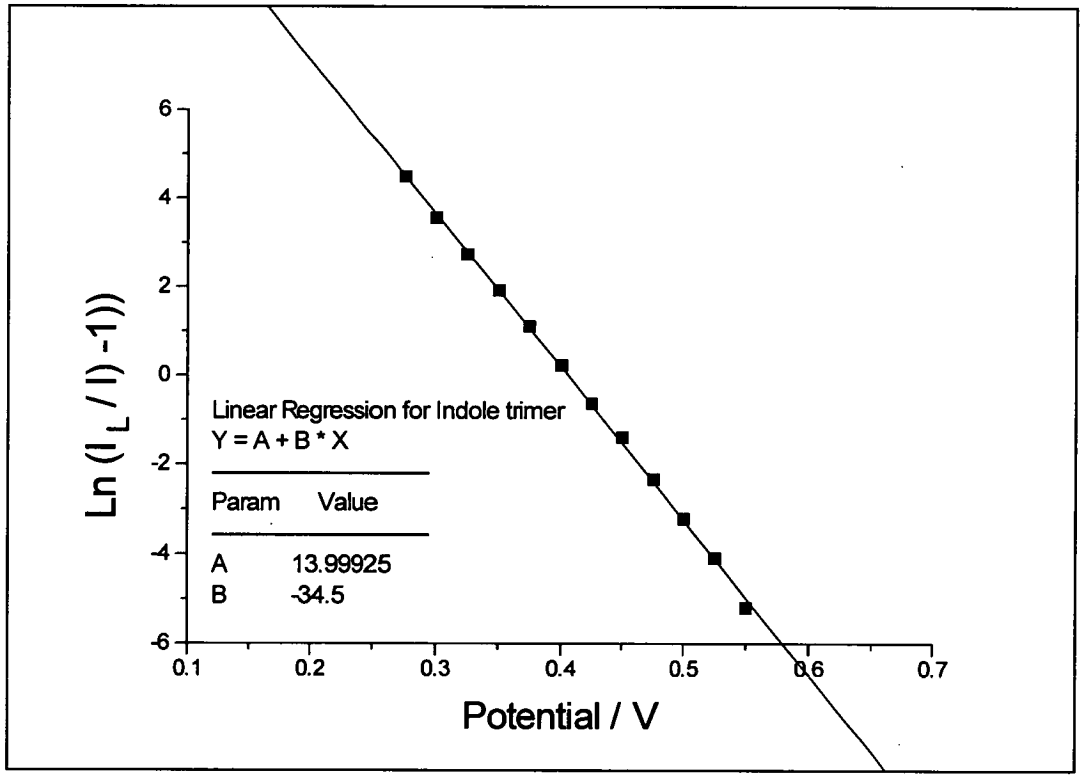

Fig. 4.14 - Tafel plot of ring polarogram of soluble indole trimer.

4.3.2.3 - Potential of trimer wave.

The potential at which the indole trimer wave is observed (0.410V) is less than the oxidation potential of the indole monomer (+1.10V) but greater than the potential of the redox peaks of the indole polymer observed from CV experiments (0.350V)[112]. The magnitude of the oxidation potential is dependent upon the ease of oxidation of the species; the lower the potential the easier it is to oxidise, hence the more delocalised a species the lower will be its oxidation potential, all other factors being equal. This suggests that wave is due to a species that is more delocalised than the monomer but is not as delocalised as the polymer. Therefore the potential at which the wave was observed in the RRDE is consistent with that predicted for a cyclic trimer species.

4.3.3 - Soluble trimers produced from the electropolymerisation of 5-substituted indoles.

In section 4.3.1, evidence was found that a portion of the indole cyclic trimers produced at the disc electrode was soluble, and could be detected at a ring electrode downstream from the disc. It was decided to extend these experiments to the electropolymerisation of a wide variety of 5-substituted indoles in an attempt to observe soluble cyclic trimer waves formation. This would constitute good evidence to suggest that all of the 5-substituted indoles polymerise via the same mechanism as CI, I5CA and indole outlined in Equ^{n}s 4.1 & 4.2.

Similar RRDE experiments to that for indole in section 4.3.1 were carried out on a number of commercially available 5-substituted indoles. Similar reduction waves to that for indole were observed on the ring electrode for all the 5-substituted indoles studied at potentials more postive than the proton waves. The main difference between the waves were the potentials at which the waves were observed. It was believed that this difference was due to the substituent imparting an electronic

influence on the trimer which either stabilised or destabilised the trimers accordingly. This stabilisation or destabilisation was noted by a corresponding lowering or raising of the trimers redox reaction potentials.

The half wave potential, $E_{1/2}$, can be related to the standard potential, E^0, for the trimer redox reaction which is electrochemically reversible[8] (Equ^n 4.8) by :-

$$E_{1/2} = E^0 + RT/F \; Ln \{ (D_R/D_O)^{2/3} \} \quad \text{--- Equ}^n \; 4.10$$

Where D_R and D_O are the diffusion coefficients of $(In)_3$ and $(In)_3^+$ respectively.

For these relatively large aromatic molecules, it is reasonable to assume that $D_R \approx D_O$, and hence from Equ^n 4.10, that $E_{1/2} \approx E^0$. Therefore, the half wave potentials of the observed soluble trimer waves for the 5-substituted indoles studied are listed in fig. 4.15. This table includes trimer $E_{1/2}$ values observed for the electropolymerisation of 5-aminoindole and 5-hydroxyindole using a preformed poly(CI) layer, this technique is explained in further detail in section 4.5 and Chapter 6. The trimer $E_{1/2}$ values could not be accurately obtained for 5-cyanoindole and 5-nitroindole as the monomer oxidation reaction occurs on the ring at potentials lower than the $E_{1/2}$ of the trimer waves.

The trimer potential values for CI and NI recorded in figs 4.15 & 4.16 are the highest potentials observed for the trimer waves before entering the monomer oxidation wave. In other words, the $E_{1/2}$ potentials of the NI and CI trimers must be higher than the foot of the oxidation wave. The CI and NI $E_{1/2}$ values recorded, can therefore be thought of as a lower limit of the true $E_{1/2}$ for these trimers.

5-substituted indole	Potential of trimer wave / mV vs ref	Hammet substituent constant
Indole	410	0.00
5-methylindole	260	- 0.32
5-bromoindole	480	+ 0.15
Indole-5-carboxylic acid	600	+ 0.41
5-chloroindole	440	+ 0.10
5-methoxyindole	260	- 0.80
5-nitroindole	> 690 $^{\diamond}$	+ 0.80
5-aminoindole *	-250	- 1.32
5-hydroxyindole *	220	- 0.95
5-cyanoindole	> 650 $^{\diamond}$	+ 0. 65

Fig 4.15 - Hammet substituent constants and $E_{1/2}$ values of the soluble trimer waves for the 5-substituted indoles studied. * Denotes electropolymerisation on poly(Cl) layer, $^{\diamond}$ denotes lowest limit for trimer $E_{1/2}$.

4.3.4 - Hammet plot.

The $E_{1/2}$ values of the 5-substituted indole trimers in fig. 4.15, were plotted against the respective Hammett substituent constants (σ^+ or σ^-) for their functional group, fig. 4.19. The Hammett equation (Equ^n 4.4) describes the relative rate of reaction of the substituted indole relative to unsubstituted indole. This can be written mathematically as :-

$$\log (k_{sub} / k_{indole}) = \rho\sigma^+ \quad \text{--- Equ}^n \text{ 4.11 - Hammett equation}$$

Where K_{sub} refers to the reaction of the substituted indole, K_{indole} refers to the reaction of indole, ρ is the reaction constant and σ^+ is the Hammett substituent constant. The Hammett substituent constant (σ^+ or σ^-) indicates the relative electron withdrawing or electron donating nature of a particular substitutent. It is used to correlate the electronic effect of the direct conjugation of the π-electron density of a para-substituent into the reactive centre of a delocalised system on the equilibrium constant of reaction.

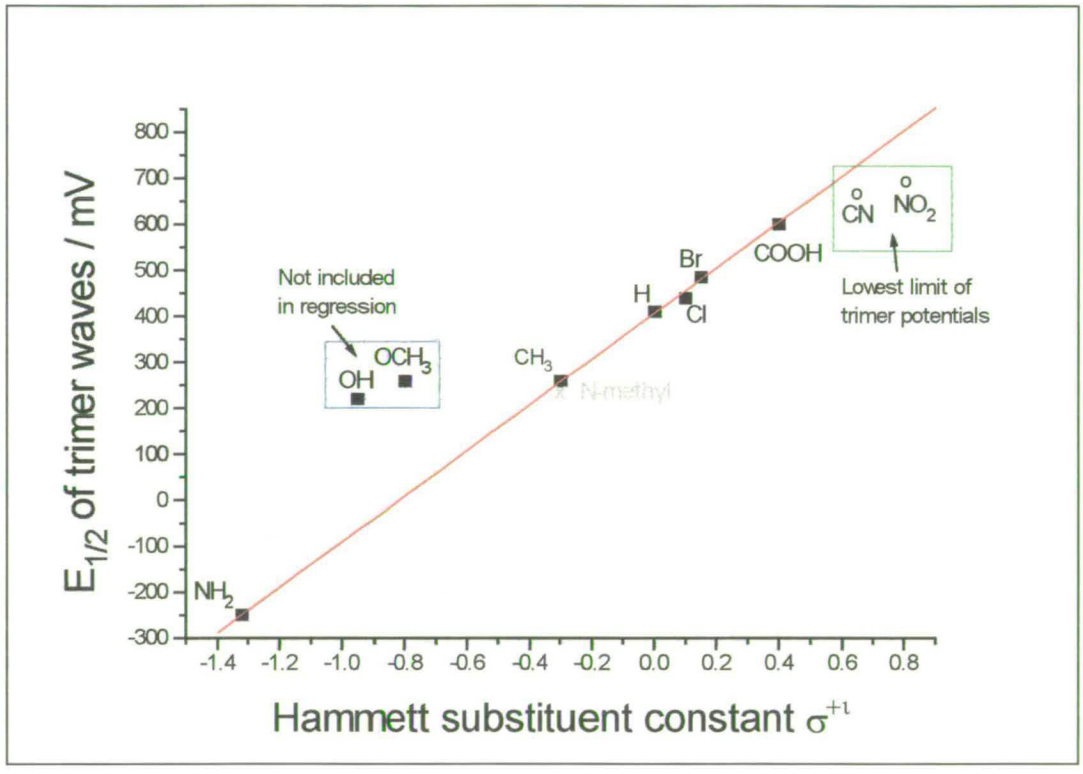

Fig. 4.16 - Hammett plot.

The Hammett plot shows a good straight line which indicates that the redox potential of the 5-substituted indoles is solely controlled by the electronic effects of their substituents. The 5-hydroxyindole and 5-methoxyindole trimer potentials are somewhat higher than that predicted by the rest of the plot. However this trend is in good agreement with the observed variation of the peak monomer oxidation potentials for both σ^+ and σ^- (fig. 1.24), which suggests that similar conjugation is observed in the monomer and the difference in the behaviour of the OX substituents is

not solely limited to the trimer. For the OX substituents, the observed oxidation potentials for the trimer and monomer are much closer to those expected for a *meta*-substituent. This suggests that that the π-electronic delocalisation between the OX substituent and the trimer is much reduced in these systems. This effect may have arisen due to aggregation of the OX monomers in MeCN due to hydrogen bonding which is supported by the findings of anomalously high diffusion coefficients calculated for these OX monomers from RDE experiments. The other 5-substituents however lie very close to the line in fig. 4.16 suggesting that there is a great deal of π-delocalisation between the redox centre (the delocalised π-system of the trimer) and the substitutent. This is a very important result, as the building of tailored sensor devices using substituents as the active "sensing" site, will need to exhibit efficient conjugation between the functional group and the polymer backbone.

4.3.5 - SQUID and EPR measurements.

It was decided that it would be interesting to examine the EPR spectrum and SQUID behaviour of some of the 5-substituted indole trimers and polymers. It was thought, from the electrochemical evidence discussed previously in this chapter, that the cyclic trimers could undergo a one electron redox reaction between an oxidised radical species, containing an unpaired electron, and a reduced neutral species. If this is the case, it would be expected to observe the spin of the unpaired electron in trimer and polymer EPR and SQUID measurements.

4.3.5.1 - EPR

An EPR (electron paramagnetic resonance) spectrum of a solid sample of oxidised poly(CI) was recorded. This showed a simple Lorentzian shaped spectrum with a g factor of 2.0126. This value is considerably larger than the g values observed for other poly(heteroaromatics) such as polythiophene and polypyrrole which both

have values of 2.0028 [133]. The deviation, Δg, of the g factor from the free electron spin, g_e (2.0023), arises from spin-orbit coupling of the excited state to the electronic ground state[11].

$$\Delta g = \frac{\lambda}{D} \quad \text{--- Equ}^{n}\ 4.12$$

Where λ is the spin-orbit coupling and D is the energy difference between the ground state and the excited state.

The value of D can be obtained from the fluorescence spectra (in this case around 420nm) and λ is 76 cm^{-1} for the p-electrons in a nitrogen atom. This calculation holds if the trimers indole-ring nitrogen atom orbitals are involved with the unpaired electron. The theoretical Δg value for a 5-cyanoindole trimer is calculated to be approximately 0.01 which is consistent with the g-factor observed in the EPR spectrum. This result suggests that the unpaired electron in the oxidised 5-cyanoindole trimer unit is delocalised over the whole trimer system including the three indole ring Nitrogen atoms. This is consistent with a polymer that is made up of linked delocalised trimer units.

The magnitude of the EPR signal produced is consistent with approximately one unpaired electron per trimer unit. An electrochemically reduced sample of poly(CI) showed a much less intense EPR signal indicating the presence of fewer unpaired electrons. This result is consistent with the trimer units in the polymer undergoing a one electron redox reaction between a oxidised radical cyclic trimer units containing delocalised unpaired electrons and reduced trimer units without any electron spin.

4.3.5.2 - SQUID

Poly(CI) was also studied by a SQUID (superconducting quantum interference device) magnetometer. Fig. 4.17 shows a plot of $1/\chi$ *vs* T for a solid sample of 15.58 mg of poly(CI). This plot shows a straight line

which is indicative of a paramagnet. There is a small positive intercept due to a diamagnetic contribution from the silica sample holder.

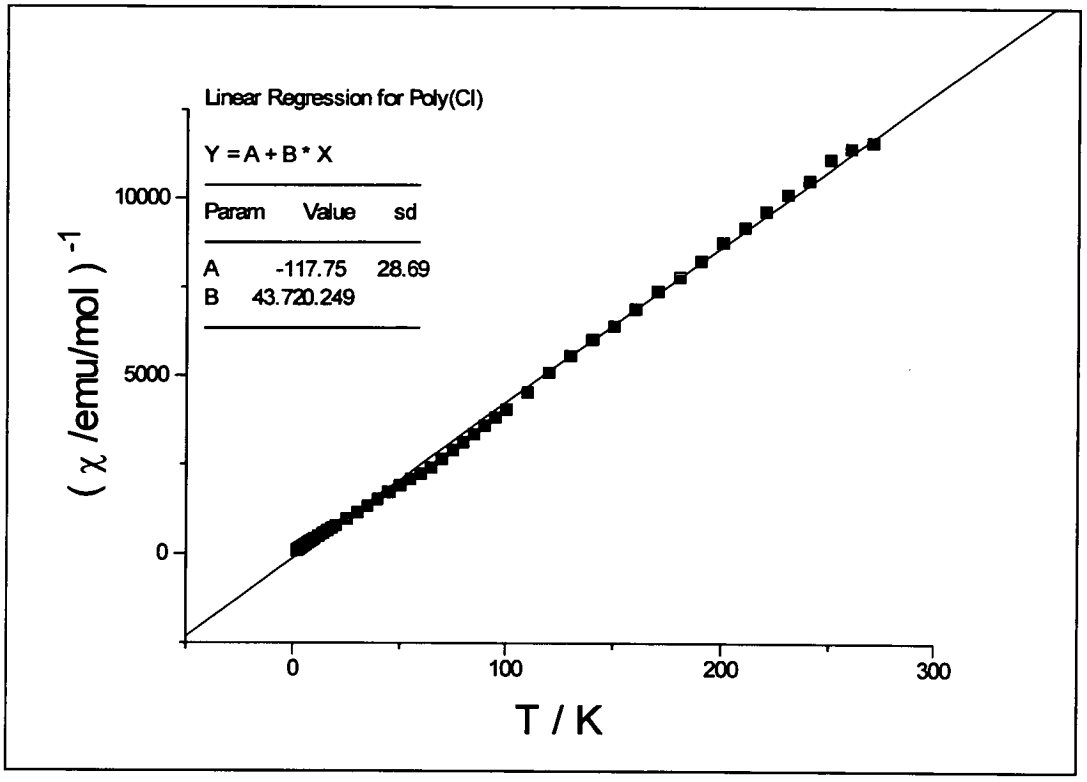

Fig. 4.17 - Plot of $1/\chi$ *vs* T for poly(CI) sample

From the slope of this plot, the effective magnetic moment, μ_{eff}, can be calculated. For this poly(CI) sample μ_{eff} = 1.14 ± 0.01 Bohr magnetons. For a spin 1/2 sample, it would be expected to observe a μ_{eff} of 1.73 (as $\mu_{eff} = 2\,[s(s+1)]^{1/2}$), therefore the obseved μ_{eff} indicates that approximately 66 % of the trimer units are oxidised and contain an unpaired electron.

4.4 - Copolymers

It has previously been found that it is possible to form a copolymer from the electropolymerisation of a solution consisting of two differently 5-substituted indole monomers (I5CA and 5-cyanoindole)[112]. It was believed

that the monomer radical cations produced at the electrode by the electrooxidation linked to form a series of co-trimers that contained both types of substituent on each trimer. Co-trimers containing 3:0, 2:1, 1:2 and 0:3 ratios of the two substituent groups were observed to form. The four different types of co-trimers formed are shown in fig. 4.18. If geometrical and structural isomerism occurs, the number of possible bifunctional trimers is theoretically eight. These co-trimers would only be expected to form on a statistical basis if the electrode is set at a potential to ensure the oxidation of both types of monomer at the electrode surface. This is because both monomer oxidise at different potentials, so at insufficient potentials to oxidise all the monomers, this may result in a skew towards an increased concentration of one type of monomer radical cation and a non-statistical amount of the trimers formed.

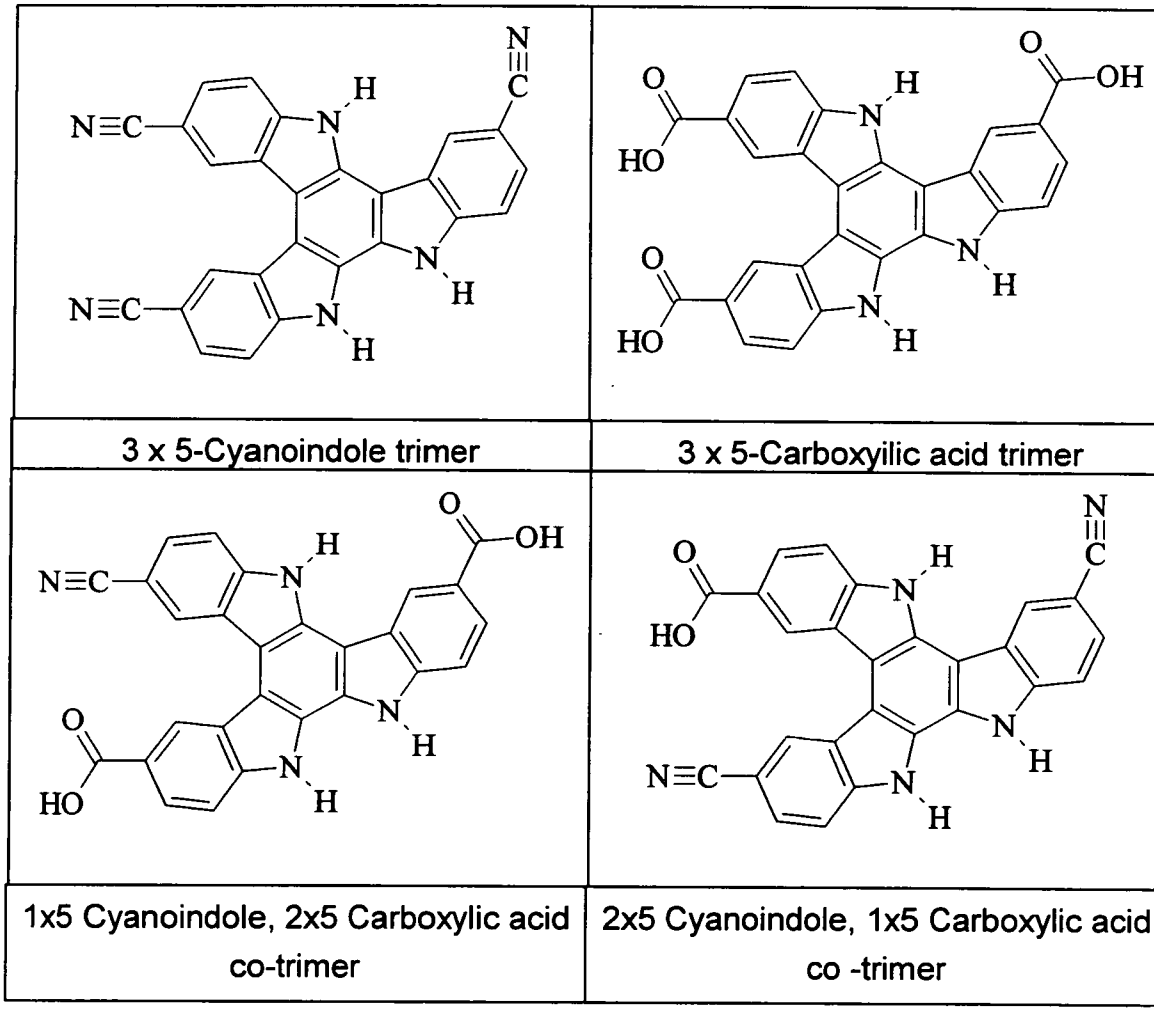

Fig. 4.18 - Co-trimer products produced in the copolymerisation reaction of 1:1 5-cyanoindole and I5CA[150].

It was hoped that this type of copolymerisation could be extended to other 5-substituted indoles as it has been shown here that all of them can be directed towards cyclic trimer formation. If this were possible, then it was expected to be able to observe the soluble portion of any co-trimers that formed at the ring electrode during the electropolymerisation of a solution containing two of 5-substituted indole monomers. The Hammett plot (fig. 4.16) showed that the $E_{1/2}$ (which is related to reactivity) of the 5-substituted trimers is dependent upon the electronic delocalisation of the substituent. Therefore a co-trimer species consisiting of a trimer unit with two types of functional groups would be expected to have electron-donating / withdrawing characteristics of the combination of all three 5-substituents. The co-trimer would therefore be expected to have an $E_{1/2}$ value between that of the potentials of the trimers formed during the electropolymerisation of either of the monomers on their own.

This hypothesis was tested by recording a ring polarogram during the electropolymerisation of a solution containing both 20mM indole and 20mM 5-methylindole at the disc. It was decided to study indole and 5-methylindole, as a large portion of the trimers formed from the electropolymerisation are soluble. This was carried out at an electrode potential sufficient to fully electropolymerise both types of monomers arriving at the electrode surface (1.1V). The resultant ring polarogram (fig. 4.19), is displayed with ring polarograms produced by the electropolymerisation of separate solutions of pure 40mM indole and pure 40mM 5-methylindole.

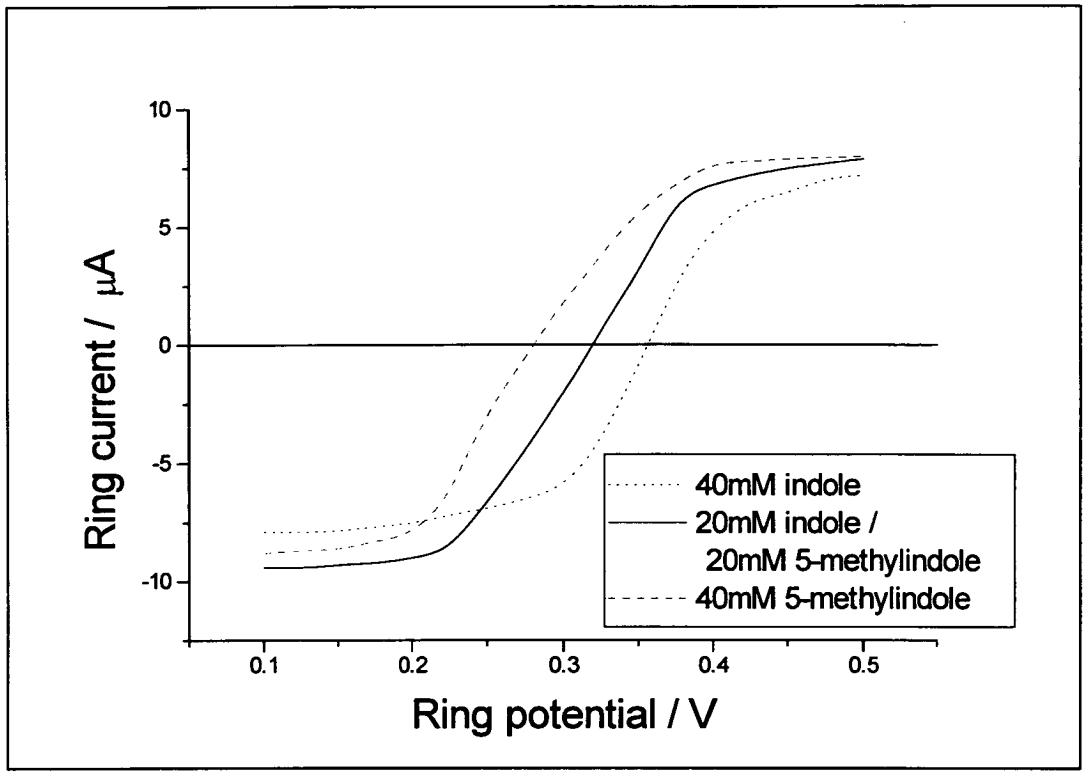

Fig. 4.19 - Ring polarogram produced from the copolymerisation of 20mM indole and 20mM 5-methylindole. Sweep rate = 10mV/s. Electrode rotation = 2Hz.

The ring polarogram from the coelectropolymerisation of indole and 5-methylindole shows a reduction wave at potentials consistent with being a co-trimer species. The $E_{1/2}$ of this wave was observed at intermediate potentials to the polarograms obtained for the electropolymerisation of pure 40mM indole and pure 40mM 5-methylindole. This is good evidence to suggest the formation of soluble co-trimers containing both 5-methyl and 5-H substituents. Similarly for the copolymerisation of I5CA and 5CI, which produced a series of differently substituted co-trimers, it was hoped to have observed a series of waves for all the 3:0, 2:1, 1:2 and 0:3 indole : 5-methylindole co-trimers and geometric isomers that were expected to have formed. However the Hammett substituent constants (and therefore $E_{1/2}$ potentials) of these two monomers are relatively close to one another (0.3 apart). This made it difficult to identify separate waves for all the different co-trimers formed which would be expected to have $E_{1/2}$ values intermediate to the indole and 5-methylindole trimers. However, a single

broad wave at intermediate potentials (≈ 0.315mV) was observed which is good evidence for the formation of soluble co-trimers containing 5-methyl and H-substituents.

This study was extended to the copolymerisation of I5CA and N-methylindole in order to attempt to produce co-trimers containing substituents with a greater difference in Hammett substituent constants and therefore $E_{1/2}$ potentials. In this way it was hoped to be able to observe a series of cotrimers and possibly geometrical isomers at the ring electrode on co-electropolymerisation.

A ring polarogram was recorded during the copolymerisation of 20mM N-methylindole and 20mM I5CA. These were chosen for their relatively high degree of trimer solubility and relatively large variation in Hammett substituent constant value (approximately 0.8). Again the electrode potential was set at a value sufficient to electropolymerise all the monomers reaching the electrode surface, (1.46V). The polarogram is reproduced in fig. 4.20.

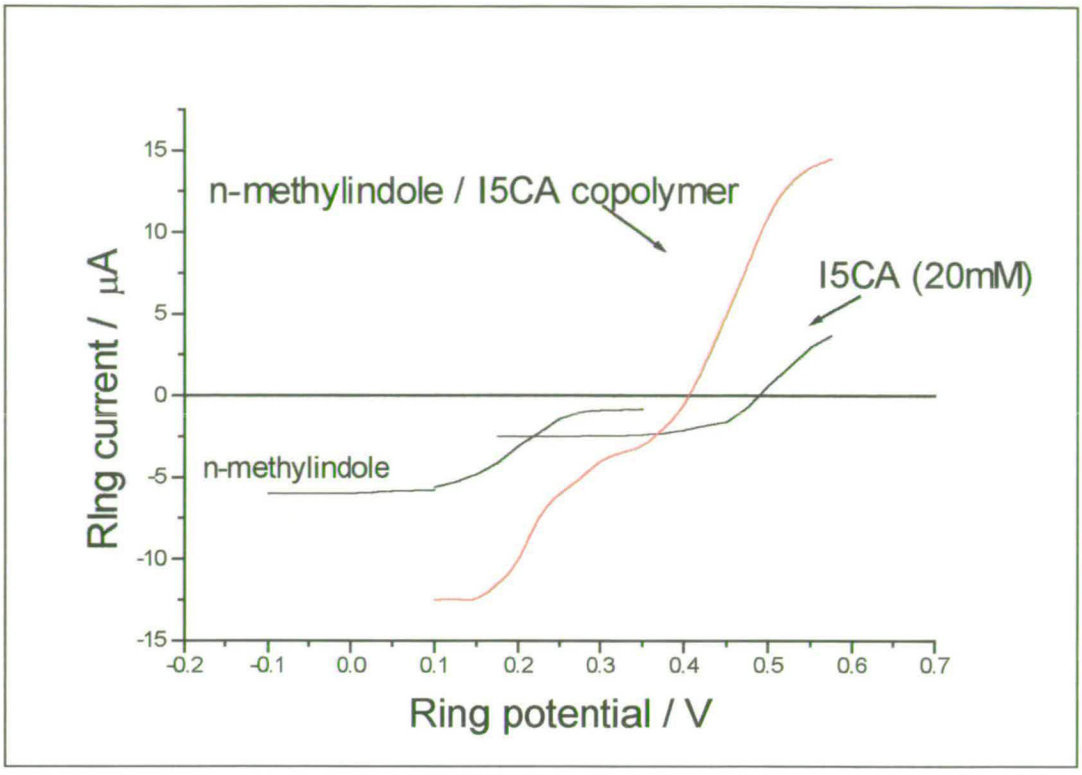

Fig. 4.20 - Ring polarogram produced from the the copolymerisation of 20mM N-methylindole and 20mM I5CA. Sweep rate = 10mV/s. Electrode Rotation = 2 Hz.

The ring polarogram for the copolymerisation reaction of N-methylindole and I5CA shows the prescence of three distinctive waves with a hint of a fourth. This is suggesed to be due to the reduction of a series of I5CA/N-methylindole co-trimers. It is reasonable to assume, that as all of the 5-substituted indoles form cyclic trimers, then copolymerisation of any of the indole monomers studies in this thesis would result in the production of co-trimers and copolymers. Moreover, these copolymers would be expected to have a redox reaction that was dependent upon the electronic nature of the substituents in the copolymer. This indicates that with the judicious choice of monomers, in theory copolymers could be produced with $E_{1/2}$ values over a very wide (1.5V) potential range.

Previously Waltman *et al*[106] observed the production of electroactive polymer films with the electropolymerisation a only few 5-

substituted indole monomers, these are shown by inclusion in a box in fig. 1.24. They concluded that the reason the other 5-substituted indoles did not form polymer films was due to the electron-donating nature of the substituents stabilising the radical cations sufficiently so that they drift away from the electrode without reacting. Also they did not observe polymer film formation for the strong electron withdrawing substituent in 5-nitroindole. They proposed that this was due to its highly destabilising influence on the monomer radical cation which was thought to react with nucleophiles in the solvent which hindered the polymerisation.

In light of the results discussed here, the above conclusions reached by Waltman are believed to be inaccurate. Electroactive film formation has been observed here and elsewhere[112] for some of the 5-susbstituted indoles for which they did not observe film formation. For instance, a CV of a film produced by the electropolymerisation of 5-Nitroindole is shown in fig. 4.21. This is a highly electroactive polymer which exhibits an unusual and highly intense reversible colour change from light green to orange / red on reduction from the oxidised form.

An electroactive polymer film was also produced from the electropolymerisation of 5-methylindole which was previously not observed. It is suggested the reason Waltman *et al* did not observe polymer film formation for these indoles, was due to the low concentration of monomer which was not sufficient to create a high enough radical cation concentration in the diffusion later which would hinder efficient coupling of the radical cations.

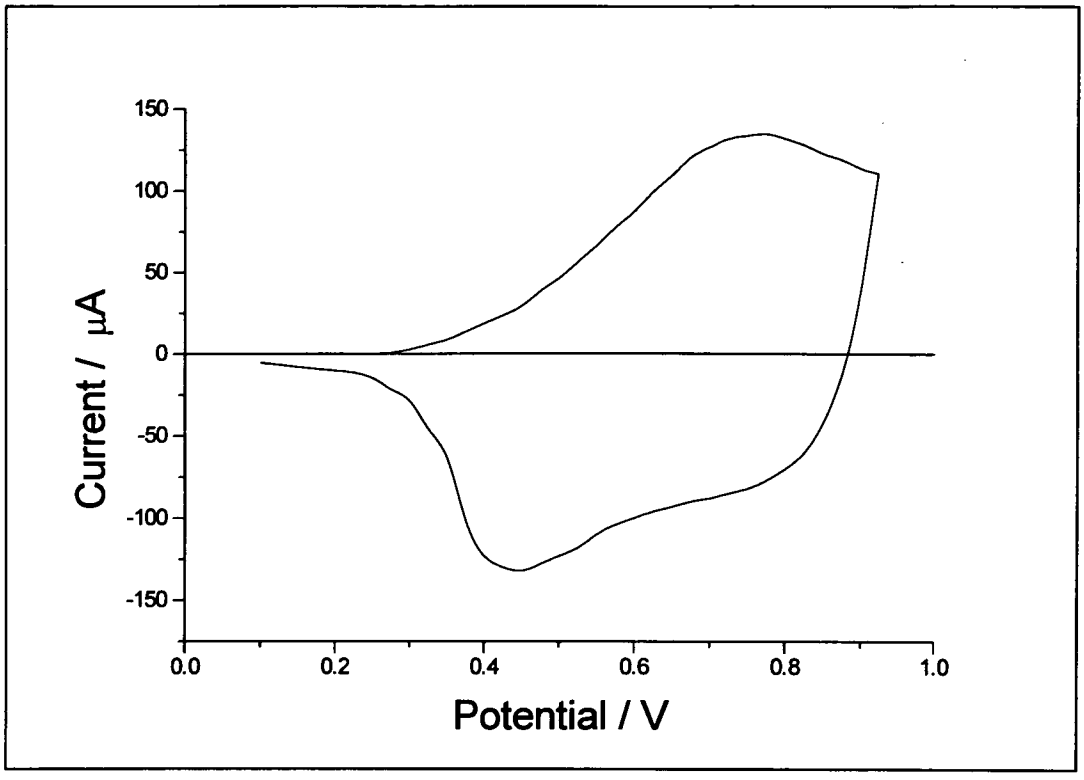

Fig. 4.21 - CV of poly(NI) produced from 50mM 5-nitroindole (1.70V). Sweep rate = 10mV/s

It was suggested by Waltman *et al* that on application of a sufficient potential 5-methyl-, 5-hydroxy-, 5-methoxy- and 5-amino-indole, which all have electron-donating groups, form stable radical cations that drift away from the electrode surface without reacting. Evidence presented here however indicates that all of these indoles, can with the correct procedures, be directed to produce soluble trimers that can be observed on the ring electrode in an RRDE experiment. Therefore it is suggested that the reason that a polymer film was not readily electrodeposited for these substituted indoles was because of the increased stability of the trimers due to the electron-donating groups and the lyophilic nature of the substituents. This increases the solubility of the trimers and slows the linking rate of the radical cations which hinders efficient polymer formation.

4.5 - Electropolymerisation of indoles with electron-donating substituents using a thin pre-formed polymer layer.

It would be very useful for the creation of a range of sensor devices to be able to form polymer films from indole monomers that contain electron-donating substituents, such as 5-aminoinodle, 5-hydroxyindole and 5-methoxyindole. Electroactive polymer films containing such functional groups may exhibit useful and interesting properties, although attempts by other workers to form indole-based polymer films from these indoles have previously failed. In light of the results discussed in this chapter where some soluble trimer formation was observed for these indole, it was decided that polymer film formation should be theoretically possible. What was needed was a technique to encourage the deposition and linking of these soluble trimers to form conducting polymer films containing electron donating groups.

It was suggested that these soluble trimers may have a greater affinity for formation and linking on top of a pre-fomed polymer layer than for that on a clean platinum surface. This was considered likely due to the fact that the trimers contain an extensive delocalised π-system which may be able to interact with other trimer units in the polymer layer. This would have the the effect of "holding" the trimers on the polymer surface slowing the rate of their desorption and allowing them to link to form polymer. Monomer arriving at the surface of the polymer surface deposits and is oxidised on this polymer film leading to a more facile trimer formation.

4.5.1 - XRD.

Evidence for π-stacking interactions between trimer/polymer layers has been found from X-ray powder diffraction (XRD) studies on I5CA trimer and polymer and 5-methylindole trimer samples which show strong peaks at approximately 3.34 Å. This is a very similar distance to that observed between layers in graphite (3.35 Å)[153], and is consistent with layers of trimer units π-stacking in these indole polymers.

4.5.2 - Electrodeposition of 5-hydroxyindole.

It was decided to attempt to electropolymerise 5-hydroxyindole (which typically does not form a polymer film) on top of a pre-formed poly(5-cyanoindole) film. This technique was hoped to encourage the deposition and linking of the 5-hydroxyindole radical cation monomers on the surface of the poly(CI) layer and to lower the rate of desorption of any cyclic 5-hydroxyindole trimers that formed on the polymer surface.

Fig. 4.22 shows a cyclic voltammogram of 50mM 5-hydroxyindole in background electrolyte on a clean platinum surface. The CV on Pt shows an oxidation peak at approximately 800mV, however no polymer film formation was observed with successive sweeps.

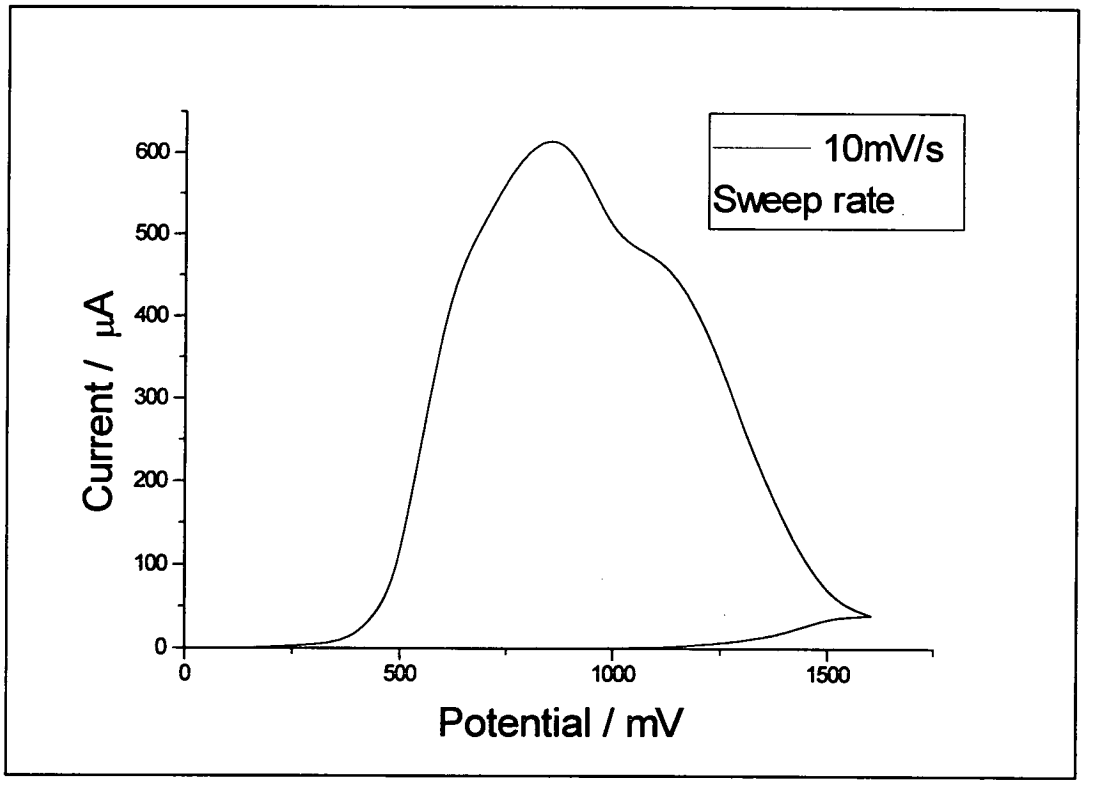

Fig. 4.22 - CV of 50mM 5-hydroxyindole on platinum disc electrode.

Fig. 4.23, shows a CV of the same 50mM 5-hydroxyindole solution on an electrode coated with a thin poly(CI) layer. This CV is markedly

different to that on a platinum surface and shows oxidation peaks at ca. 700mV and 900mV. Successive sweeps re-produce this CV.

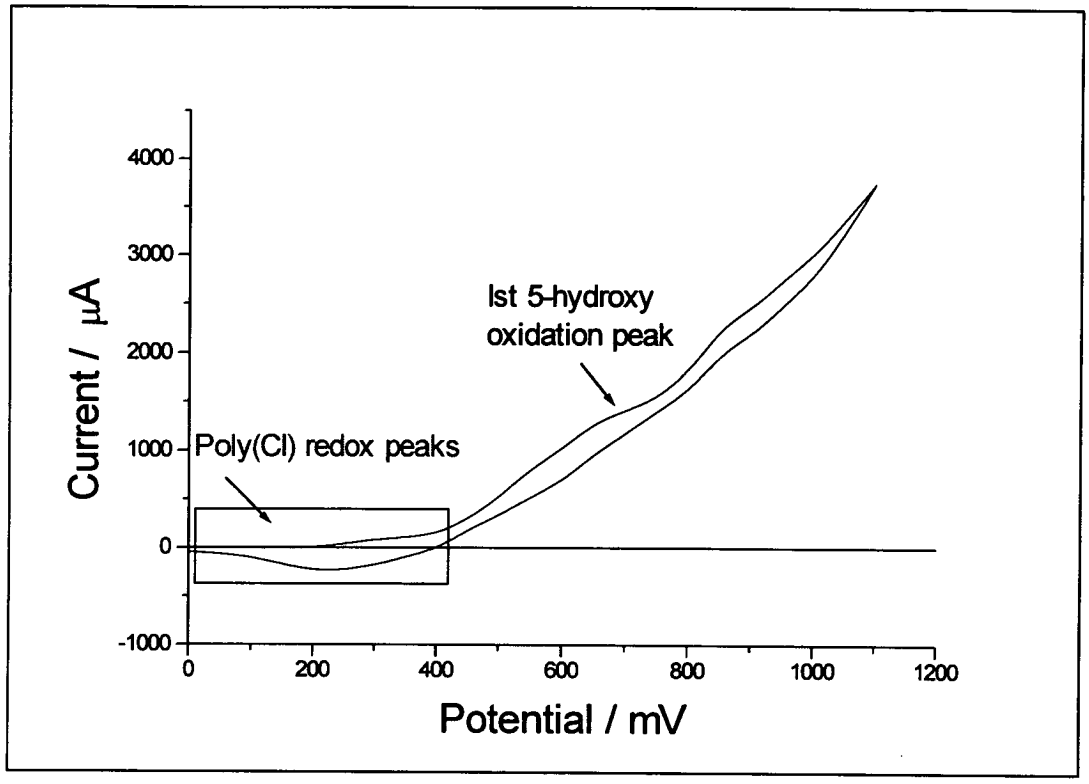

Fig. 4.23 - CV of 50mM 5-hydroxyindole on poly(Cl) layer.

A CV in background electrolyte of the polymer film produced on the electrode after carrying out the CV in fig. 4.23, was compared with a CV of the poly(Cl) film before carrying the 5-hydroxyindole CV. This is plotted in fig. 4.24. It can be seen that there is additional charge under the CV in 4.24 after carrying out the CV in fig 4.23 than the CV of the as-formed poly(Cl) layer . The extra charge suggests that there was deposition of a 5-hydroxyindole trimer/polymer layer on top of the poly(Cl) film due to the oxidation of the 5-hydroxyindole monomer on the poly(Cl) surface during the 5-hydroxyindole CV.

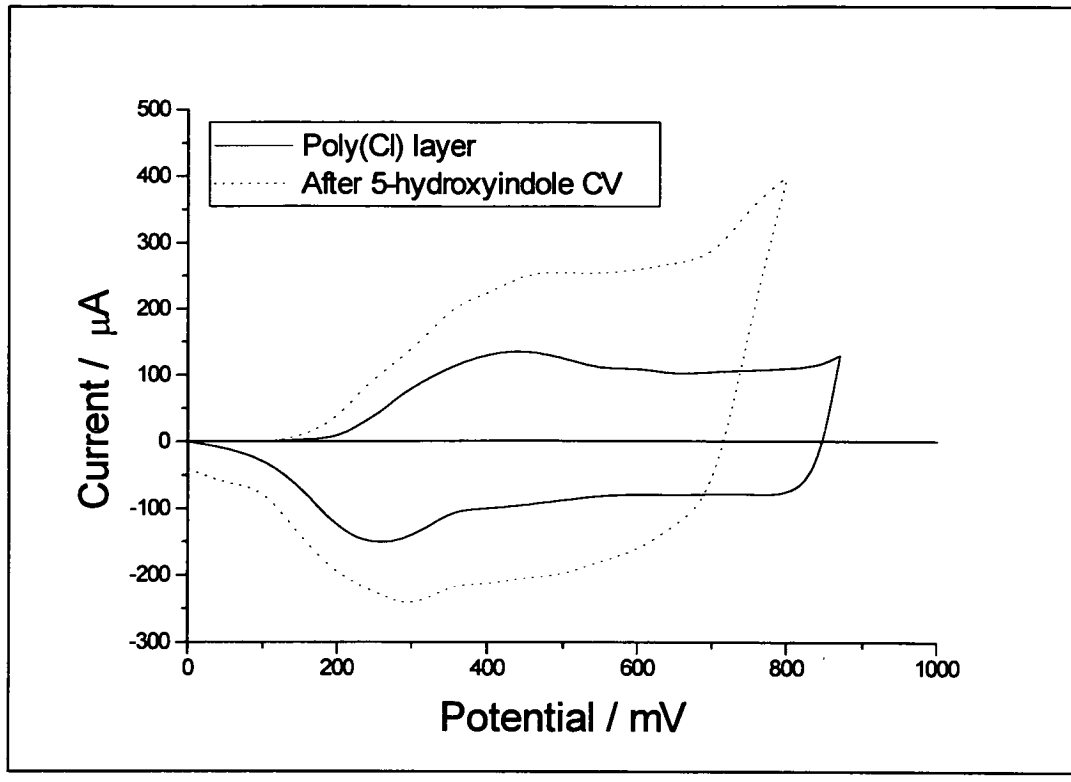

Fig. 4.24 - CV showing build up of 5-hydroxyindole trimer/polymer on poly(Cl) layer. Sweep rate = 10mV/s.

The current-time transient for the electropoylmerisation of 50mM 5-hydroxyindole on a poly(Cl) layer shows a steady-state current of approximately 3.8mA (fig. 4.25). This is consistent with the mass transport controlled oxidation at the electrode observed for the other 5-substituted indoles.

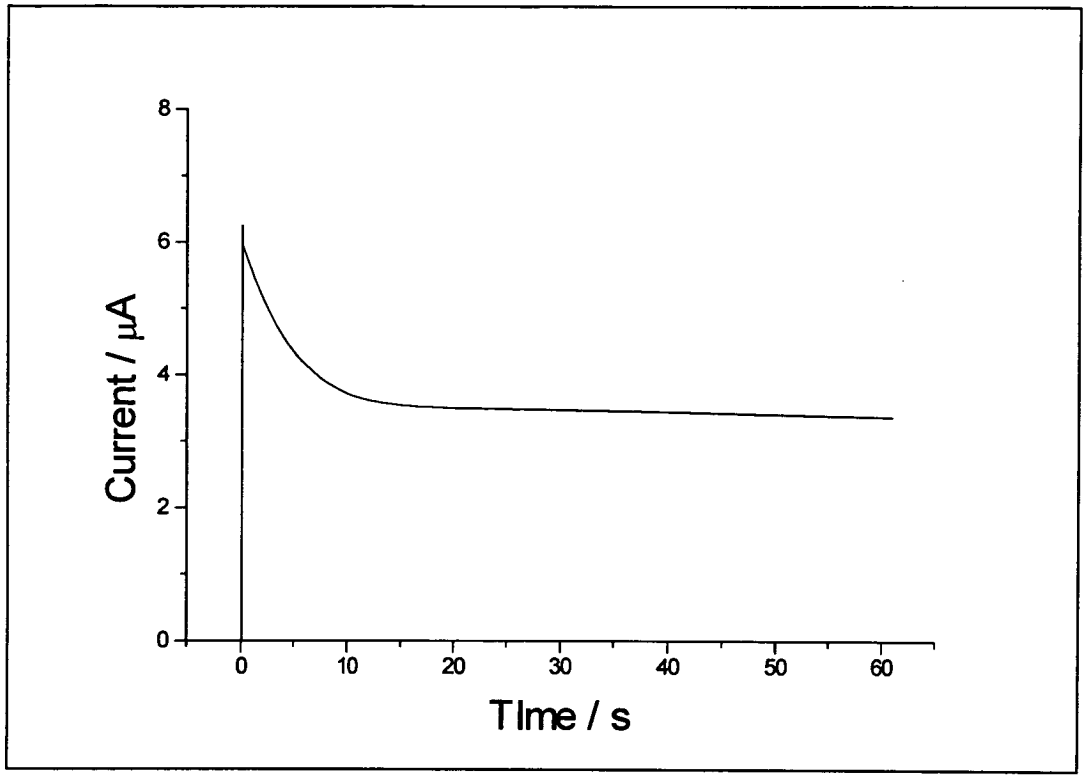

Fig. 4.25 - Current-time transient of 50 mM 5-hydroxyindole on poly(Cl) film. Potential = 0.75V, electrode rotation = 1Hz.

4.5.3 - Trimer wave produced in the electropolymerisation of 5-hydroxyindole on a pre-formed poly(Cl) layer.

To test whether 5-hydroxyindole trimer was being formed on the poly(Cl) layer, a ring polarogram was recorded while electropolymerising 10mM 5-hydroxyindole on a pre-formed poly(Cl) film at a potential of 0.75V, fig. 4.26.

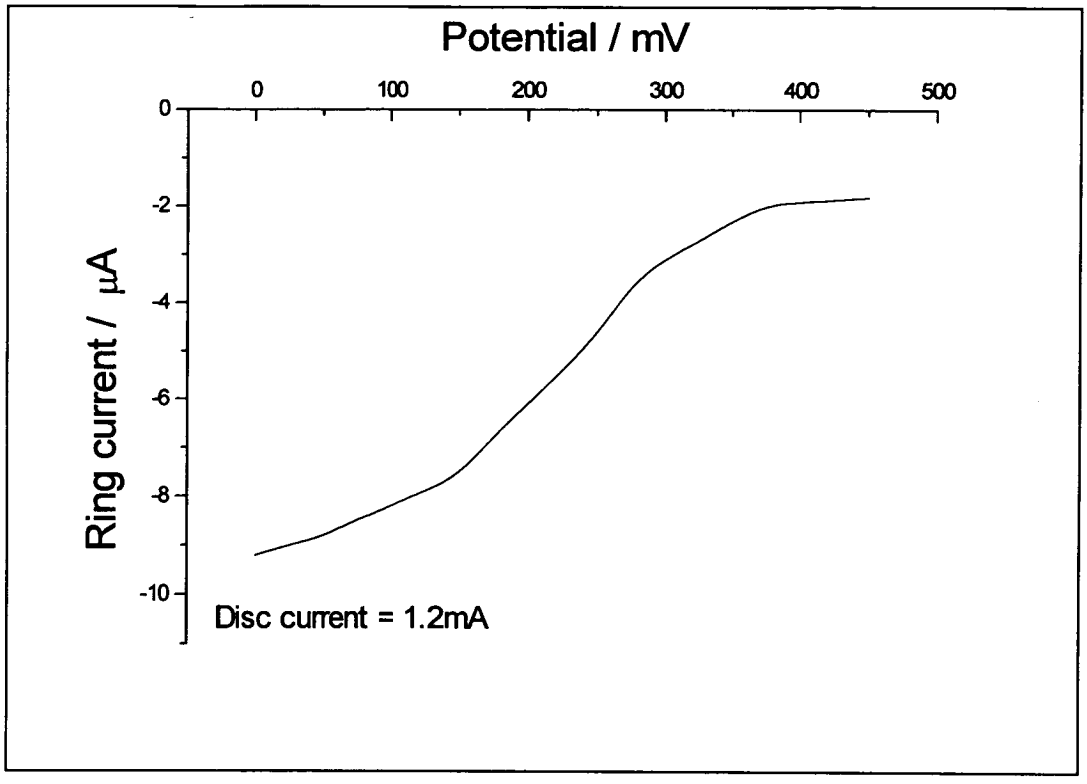

Fig. 4.26 - Ring polarogram of 10mM 5-hydroxyindole on a poly(CI) layer. Electrode rotation = 2 Hz. Sweep rate = 20 mV/s.

This technique of using a thin pe-formed poly(CI) layer to facilitate the formation of 5-hydroxyindole trimers was used to obtain the $E_{1/2}$ values for the trimer waves observed in the electropolymerisation of 5-hydroxyindole and 5-aminoindole. These values were used in the Hammett plot in fig. 4.16.

Further characterisation of the electro-deposited 5-hydroxyindole layer by techniques such as fluorescence spectroscopy proved difficult, as separation of the poly(CI) and 5-hydroxyindole layers could not readily be achieved. The layer could not be studied as a whole as the poly(CI) layer is highly fluorescent, creating problems in distinguishing between fluorescence produced by poly(CI) layer, and that from the electro-deposited 5-hydroxyindole layer. Fortuitously it has been found that the trimers and polymer formed from the electropolymerisation of 5-nitroindole do not show any fluorescence. Hence it was decided to attempt to electrodeposit a 5-hydroxyindole layer on top of a poly(NI) layer in a

similar way to that on the poly(CI) layer. Similar RRDE ring polarograms and current time transients to that obtained on the poly(CI) layer were observed with the electropolymerisation on the poly(NI) layer. This was accompanied with a similar build up of a dark secondary layer on top of the green poly(NI) layer.

4.5.4 - Fluorescence of electrodeposited 5-hydroxyindole layer.

Fluorescence spectroscopy was used to study the poly(NI)~5-hydroxyindole layer. The fluorescence and excitation specta are shown in fig. 4.27.

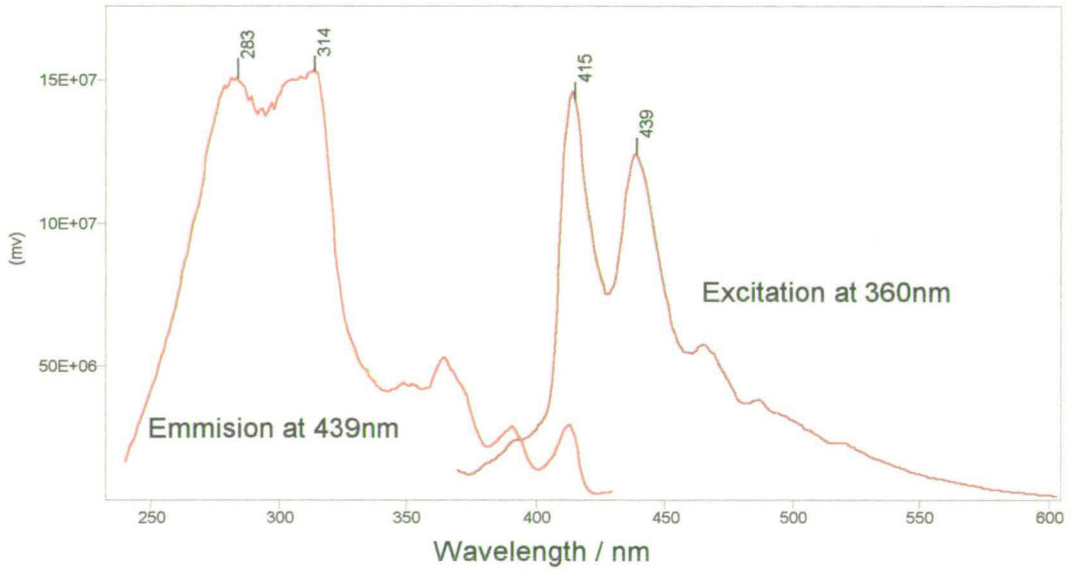

Fig. 4.27 - Fluorescence and excitation spectra for 5-hydroxyindole~ poly(NI) layer. Recorded at room temp.

The excitation and fluorscence spectra in fig. 4.27 are very similar to those observed previously for 5-cyanoindole trimers[113] and I5CA trimers.[114] It shows the charactersitics of a cyclic trimer species which

must be due to the formation 5-hydroxyindole cyclic trimers. Thus this is good evidence that 5-hydroxyindole was directed towards cyclic trimer formation and deposition by facilatating the formation and deposition of trimers using a pre-formed poly(CI) or poly(NI) layer. This novel use of a thin pre-formed layer to promote cyclic trimer formation, is a very important technique as it allows a much greater variety of functional groups to be incorporated in a indole polymer / trimer film.

4.6. Formation of oxidised and neutral cyclic trimers.

In light of the results presented in section 4.5 where it was shown that a polymer layer could be used to facilitate the formation and deposition of cyclic trimer, it was decided to address the question of why both oxidisable and reducible components were observed for the many of the soluble cyclic trimer waves. It was suggested that the soluble cyclic trimers were formed in two ways. The first is that they were formed in the diffusion layer near the electrode surface, where linking of the radical cations may occur due to the high concentration of radical cations. i.e. :-

$$3n\ In^{+\bullet} \Rightarrow n\ (In)_{3\ (aq)} + 6H^{+} \quad \text{--- Equ}^{n}\ 4.13$$

These neutral trimers could then be swept away from the electrode surface without being further oxidised, and reach the ring electrode in an oxidisable neutral state. It is suggested that the larger portion of soluble trimers observed is due to the oxidation and linking of monomers on the disc electrode surface. On formation, these trimers would be expected to be immediately oxidised. It is then thought that a portion of these trimers may desorb from the electrode surface before linking to form polymer (which is relatively slow). These would then be swept past the ring electrode as oxidised cyclic trimer species. i.e. These trimers are formed according to Equ^{n} 4.1 and desorb from the electrode surface.

4.6.1 - RRDE experiments of indole on platinum *vs* pre-formed polymer layer.

To investigate this further, ring polarograms were recorded during the electropolymerisation of 0.1M indole on both a polished platinum disc electrode, and on a pre-formed indole polymer layer, fig 4.28. They were both recorded at a galvanostatic current of 1mA

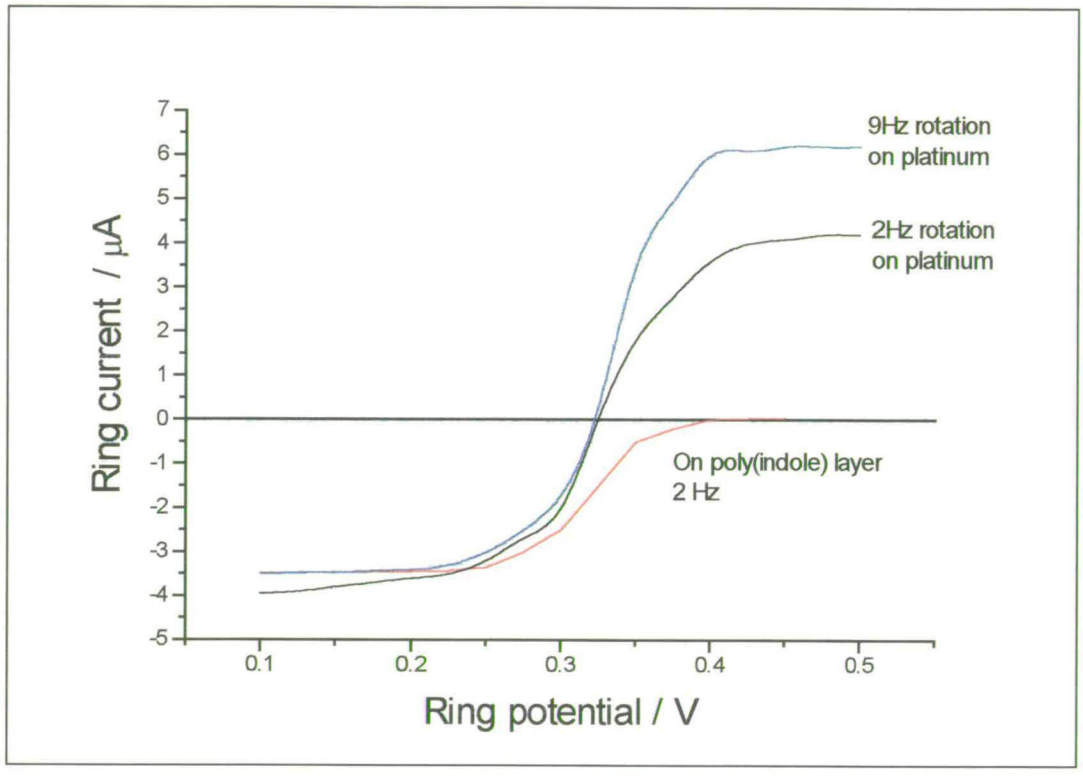

Fig. 4.28 - Ring polarograms produced form the electrpolymerisation of 0.1M indole on platinum and on poly(indole)

The ring polarogram produced from the electropolymerisation of 0.1M indole on a clean platinum surface shows a wave due to trimers that are both oxidisable and reducible ie. neutral and oxidised trimers were being produced. However the ring polarogram produced on a pre-formed indole polymer layer, shows a wave due to only (reducible) oxidised

trimers at the ring. This suggests that on pure platinum the trimers are being formed both in solution close to the electrode as neutral species and also on the surface of the platinum disc electrode as oxidised species. When the electropolymerisation is carried out on a pre-formed indole layer, however, the trimers are produced solely as (reducible) oxidised species, which suggests that they are formed on the pre-formed indole layer and not in the diffusion layer. This indicates that the indole monomers adsorb and trimerise (on oxidation) on top of a polymer film in the same way as the other 5-substituted indoles. Fig. 4.28 shows that there is a rotation speed dependence upon the amount of neutral trimer produced but not on the amount of oxidised trimer produced. This can be explained by the fact that, at a faster rotation speed the diffusion layer thickness is decreased which increases the concentration of radical cations near to the electrode surface. The higher concentration of radical cations in the diffusion layer allows an increase in the formation of neutral trimers (Equ^{n} 4.13). The amount of oxidised trimer produced is not rotation speed dependent as the oxidised trimer formed is only dependent upon the likelihood of the trimer to desorb from the electrode surface. This is not affected by the concentration of the radical cations in the diffusion layer.

4.6.2 - Trimer current - time transients on ring.

The formation of soluble trimers was studied further, by recording the change of ring current at a fixed potential (0V) with time, while passing a galvanostatic disc current. In this way any oxidised soluble trimer that was produced would be reduced at the ring electrode. The variation of the ring current was plotted against time for during the electropolymerisation of 5-cyanindole at a number of disc potentials both on a clean platinum electrode and on a pre-formed layer.

The collection efficiency of the RRDE is assumed to remain at 0.21 at all disc currents, hence the trimer ring current can be displayed as an effective trimer collection efficiency, N_{tri} (Equ^{n} 4.9). This can be used to calculate the soluble portion, x, of trimer arriving at the ring electrode.

The time taken for a species produced at the disc to take to travel across the gap to the ring electrode is termed the transit time (t'). This transit time is dependent upon a number of factors and is described by theory, Equ^{n} 2.12.

A rotation rate of 2Hz was used for all these ring-transit experiments. This taken along with the Diffusion coefficient (D), the viscosity of acetonitrile (υ), and the radii of the disc and ring electrodes (r_2 and r_1), gives a transit time of approximately 0.2 seconds for the start of the detection and approx 0.9 seconds to reach the steady state value. This transit time is useful in determining adsorption of a disc generated species at the disc, since this will cause a delay in the appearance of the species at the ring.

Fig. 4.29 shows the current-time transients at the ring with the application of a constant potential of 0V measured with various disc potentials pulses to a solution of 20mM 5-cyanoindole. At t = 0, the disc electrode potential is jumped from 0V to the various potentials included in the plot. These potentials correspond to, the foot of the monomer oxidation peak noted in a CV, half way up the oxidation wave, and at the top of the peak. It can be seen that a number of reduction current-time transients are produced by the electrooxidation of the CI at the disc electrode. It is suggested that the "burst" of reduction current corresponds to the reduction of cyclic CI trimer at the ring electrode. The transit time for the on-set of the reduction current is consistent with a soluble species produced at the disc electrode. It can be seen that as the disc potential is increased (increasing the disc electropolymerisation current), the ring reduction current increases which suggests the production of an increased amount of cyclic trimer. The maximum height of the ring reduction current, the steady state value of the ring current, the disc current applied, and the amount of soluble trimer observed relative to the maximum amount (x), for both the maximum and steady state ring currents are displayed in fig. 4.30.

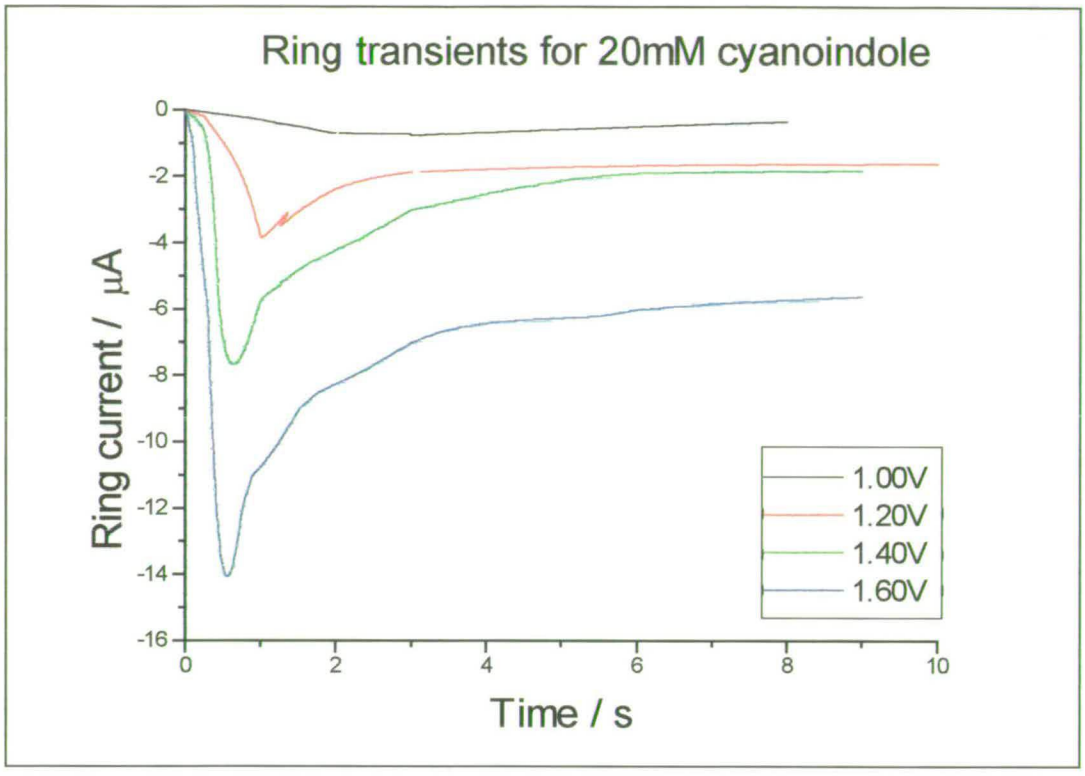

Fig. 4.29 - Trimer ring reduction current - time transients for the electropolymerisation of 5-cyanoindole.

Potential applied / V	Disc current / μA	Peak ring current / μA	x at peak current	Steady state ring current / μA	x at steady state current
1.00	55	0.8	0.48	0.6	0.36
1.20	280	3.9	0.46	1.5	0.18
1.40	840	7.8	0.31	2	0.08
1.60	2200	14	0.21	6	0.08

Fig. 4.30 - Table showing amount of trimer produced in 5-cyanoindole electropolymerisation. $x = 7\ (I_{ring}) / N_0\ (I_{disc})$

It can be seen that as the potential of the electropolymerisation reaction is increased, the amount of soluble 5-cyanoindole trimer

observed at the steady state ring current decreases from 36% of the total trimer formed to around 8%. The peak ring current also decreases from collecting around 48% of the total trimer produced to about 21%. In other words as the electropolymerisation reaction is "switched on" the amount of poly(CI) that deposits is around 92% during steady state polymerisation and approximately 79% at the start of the polymerisation.

4.6.2.1 - Trimer current - time transients on pre-formed polymer film.

Fig. 4.31 presents the trimer ring reduction current for the polymerisation of CI on a polished platinum surface. It was decided to examine similar ring current-time transient for the polymerisation on a poly(CI) coated electrdoe. Fig. 4.28 shows current-time transients taken one after another without cleaning the disc electrode surface between the experiments. This had the effect of allowing a thin poly(CI) layer to build up on the disc electrode surface between runs 1 and 2, and runs 2 and 3. It can be seen that the ring transients produced on the thin polymer layer show a progressively delayed transit time as the disc layer becomes thicker. This is suggested to be due to the time taken to oxidise the poly(CI) layer on the disc before any further electrooxidation of monomer can take place at the surface. As the polymer layer becomes thicker, it takes longer to re-oxidise the layer and so the trimer burst is further delayed. It can also be seen that the magnitude of the trimer reduction current is decreased on a pre-formed poly(CI) layer compared to that on a clean platinum surface. This indicates that less soluble trimer desorbs from the preformed poly(CI) layer than desorbs from a clean platinum surface at the start of the electropolymerisation This is consistent with the RRDE findings discussed previously, that showed that a reduction in the amount of trimer produced on a polymer layer compared to that on clean platinum electrode. Very similar ring current-time transients to these were obtained with experiments on I5CA and 5-bromoindole.

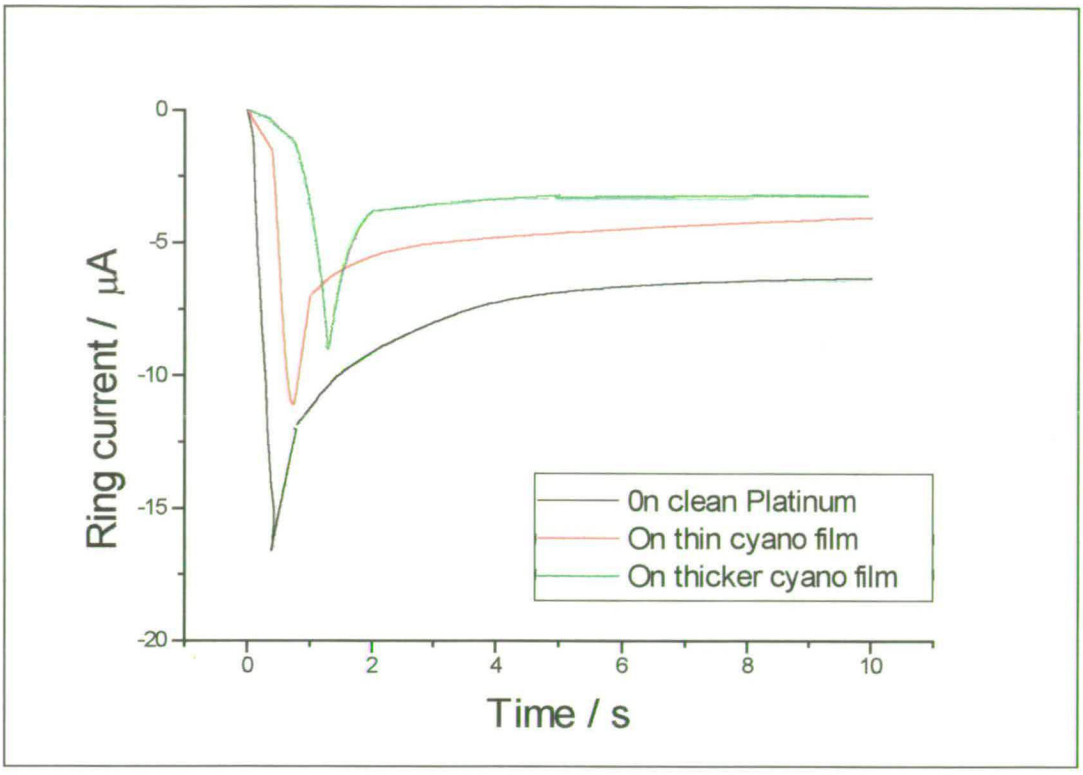

Fig. 4.31 - Ring current time-transient during the electropolymerisation of 50mM 5-cyanoindole on platinum surface and on a pre-formed poly(CI) layer.

4.6.2.3 - Trimer ring current - time transients for the polymerisation of N-methylindole.

It was decided that it would be interesting to compare the current - time transients produced from the electropolymerisation of CI with the electropolymerisation of a monomer which does not form a polymer film. In this case it was expected that the trimer current would not peak but rise to a plateau. Ring current-time transients were obtained for the electropolymerisation of N-methylindole at a clean platinum disc electrode at a number of different disc potentials (therefore disc currents) (fig. 4.32). The electropolymerisation of N-methylindole results in the production of soluble cyclic trimers but does not form a polymer. The reasons for this are explained fully in chapter 5 which studies the electropolymerisation of N-methylindole.

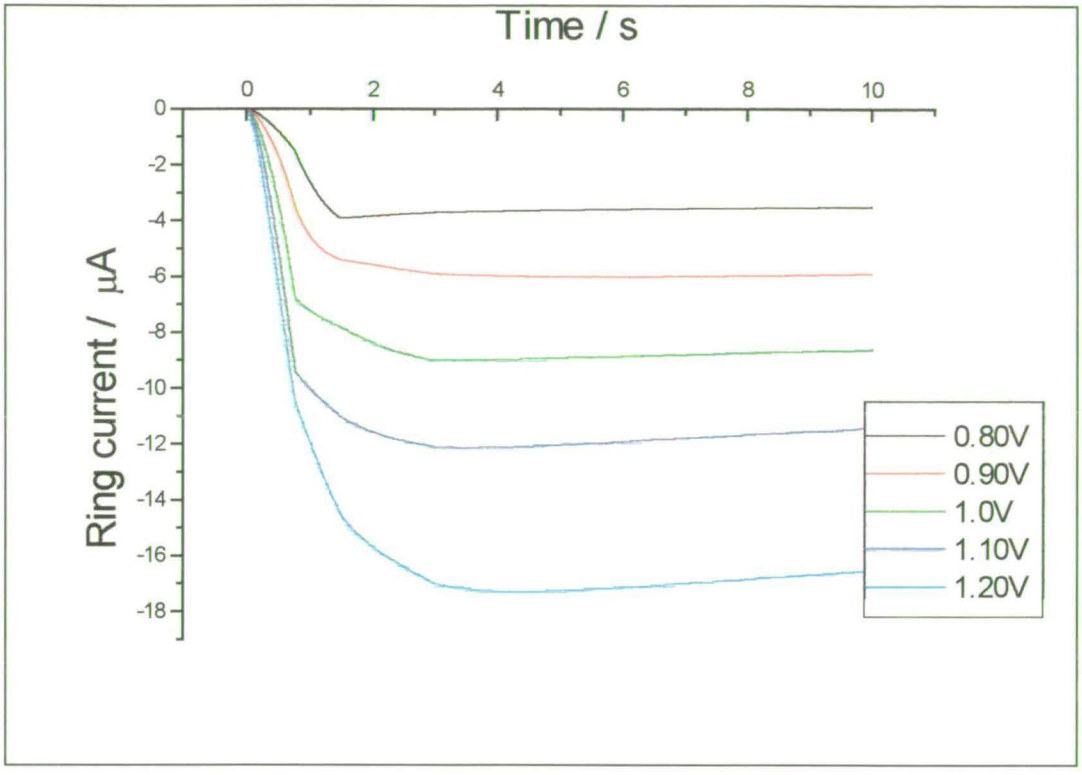

Fig. 4.32 - Trimer ring current - time transients for the electropolymerisation of 50mM N-methylindole.

The ring current-time transients in fig. 4.29 show trimer reduction currents due to the production of soluble trimer at the disc electrode. These ring currents are considerably larger than those observed for the electropolymerisation of 5-cyanoindole, 5-bromoindole or I5CA. This was expected as film formation (or deposition of trimers) is not observed for the electropolymerisation fo N-methylindole (therefore x is nearer to one). It can also be seen that ring current does not peak, as for the other indoles studied, but is maintained at a steady state level. This can also be explained by the fact that as polymer deposition does not occur for N-methylindole, the amount of soluble trimer produced remains constant as the polymerisation continues to occur on the platinum disc. The ring current produced is tabulated with the disc current applied at each potential in fig. 4.33.

Potential / V	Disc current / μA	Ring current / μA	x at steady state
0.8	162	3.8	0.78
0.9	270	6.0	0.74
1.0	385	9.0	0.78
1.1	520	12.0	0.77
1.2	840	17.4	0.69

Fig. 4.33 - Table of degree of soluble trimer observed from the electropolymerisation of N-methylindole.

It can be seen that the amount of soluble N-methylindole observed at the ring remains at around 70-80% of the maximum possible theoretical amount produced at the disc. This value is consistent with the amount of trimer produced in studies carried out in chapter 5. The electropolymerisation of N-methylindole is examined in detail in the following chapter.

4.7 - Conclusions

A number of important results have been described in this chapter; these are summarised below.

(1) It was found that protons released during the electropolymerisation of several 5-substituted indoles could be detected at the ring electrode during an RRDE experiment. These were suggested to have been released during the linking of monomer radical cations to form cyclic trimers and the linking of trimers to form polymer. The amount of protons released suggests that the all 5-substituted indoles studied polymerise via the same mechanism suggested by Mount *et al*[112]

(2) During the electropolymerisation of the 5-substituted indoles, it was found that a proportion of the cyclic trimers formed were soluble (i.e. did not deposit to form a film) and could be detected electrochemically using a rotating ring-disc electrode. A linear relationship between the $E_{1/2}$ value of the soluble trimers and the Hammett substituent constant of the trimers 5-substituents was found, which showed there to be a great deal of π-electron delocalisation between the substituent and the trimer redox centre.

(3) On copolymerisation of two 5-substituted indole monomers, it was found that a series of co-trimers could be formed that possesed $E_{1/2}$ values intermediate between the trimers formed by the polymerisation of the two individual indole monomers. This suggests that copolymerisation of two or more selected 5-substituted indoles may result in the formation of a copolymer with a tailored redox potential over a wide range of potentials (almost 1.5V).

(4) It was found that electropolymerisation of 5-substituted indoles with electron donating groups, often resulted in only soluble trimer / polymer fomation. The rate of desorption of these cyclic trimers was decreased and the rate of linking of the trimers on the surface was increased by using a pre-formed polymer layer. This layer was believed to facilitate the deposition of oxidised monomer and formation of trimers by coupling of these monomer radical cations to form cyclic trimers on the surface. This resulted in the formation of an electrodeposited layer of 5-hydroxyindole trimer on poly(Cl) layer, which would not be possible on platinum. This technique is an important discovery as it allows a much greater variety of substituents to be incorporated in to a substituted indole polymer film.

(5) It was found that electropolymerisation of the 5-substituted indoles on a platinum surface at first resulted in the production of both neutral trimers, formed in the diffusion layer, and oxidised trimers formed on the platinum electrode surface. A soluble proportion of both types of neutral and oxidised trimers were observed at a ring electrode during electropolymerisation. As the polymerisation proceeds, with film deposition

taking place on the electrode surface, almost all of the soluble trimer observed at that ring was in an oxidised state and was apparent in a lesser amount. Neutral trimer was not observed as trimer formation on the polymer film was immediately followed by oxidation. Thus this switch in mechanism indicates that the monomer radical cations have a greater affinity for adsorption on the polymer layer, and after linking to form trimer, their rate of desorption is reduced relative to that at the start of polymerisation where there was no polymer surface to facilitate the deposition and growth of the polymer film.

Chapter 5 - Electrooxidation of N-methylindole

5.1 - Introduction

The previous chapter has shown that the formation of asymmetric cyclic trimers can be observed for all the 5-substituted indoles studied in this thesis. It was suggested that these trimers can then link together to form a polymer consisting of linked trimers on the electrode surface. Due to the fact that diminished N-H IR bands are observed in the polymer compared with the monomer and trimer,[115] it is believed that these trimers may link via the indole ring nitrogens. This linking process, however, is not well understood or characterised and the participation by the nitrogen atoms remains as conjecture. This chapter seeks to increase the understanding of the linking process of indole and derivatised indoles by analogy to studies undertaken on the electropolymerisation of N-methylindole. It also seeks to examine the polymerisation mechanism of N-methylindole itself. N-methylindole, which is also sometimes known as 1-methylindole, is shown in fig. 5.1.

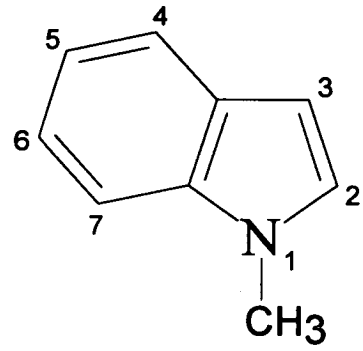

Fig. 5.1 - N-methylindole

Previously, Waltman *et al*[106] have briefly studied the electropolymerisation of N-methylindole, and have claimed that although they see an oxidation wave consistent with radical cation formation, they do not observe the formation of a polymer film. They attributed this to the blocking of the primary linking position which hindered the coupling of the

radical cations. This would allow them to drift away from the electrode into the bulk of solution without coupling to form polymer. The lack of N-methylindole polymer film formation, led them to propose that indole and many substituted indoles polymerised linearly via the indole ring nitrogen position and one other unspecified position.

In light of the results presented in chapter 4 which contradict some of their findings, it was decided to study the electropolymerisation of N-methylindole further. It was considered that the formation of an N-methylindole cyclic trimer may be possible as the 2 and 3 positions are free for linking allowing the formation of an asymmetric cyclic trimer. Equ^{n} 4.2 suggested that cyclic trimers formed by CI, I5CA or indole link together to form a polymer. The most likely linking positions of the trimers were thought to be through two of the indole ring nitrogen atoms. In an N-methylindole trimer, the methyl substituents on the nitrogen position were expected to hinder the linking of the trimers in forming a polymer consisting of linked trimers.

5.2 - Molecular modelling calculations

The likelihood of N-methylindole cyclic trimer formation was predicted by the use of a molecular modelling computer program (Desk top molecular modeller, v1.2, Oxford Universiy Press). This was used to compare the molecular energy of a model of an N-methylindole asymmetric cyclic trimer molecule with its isomer, a 5-methylindole asymmetric cyclic trimer. An unsubstituted indole asymmetric cyclic trimer was also studied to examine the steric effects due to substituents on the conformation of the molecules. The final, energy minimised, structure of the N-methylindole trimer is shown in figs. 5.2 (a) & (b).

The N-methylindole trimer molecular model was compared with a similar, energy minimised, model of its isomer a 5-methylindole asymmetric cyclic trimer and unsubstituted indole cyclic trimer, fig. 5.3 (a) & (b). Comparison of the N-methylindole and the indole models showed that there is considerable steric hindrance between the two closest methyl

groups in the N-methyindole trimer. This forces these two methyl groups out of the plane of the almost flat cyclic trimer. The third methyl substituent is also forced out of the plane due to a steric clash with a hydrogen substituent on the 4-position. The final energies of the energy minimised structures are shown in fig. 5.4. This shows that the N-methylindole trimer is approximately 7 $KJmol^{-1}$ less stable than its 5-methylindole trimer, although this energy difference is of the ground state which is relatively small compared with the overall energy of the system. The energy of the transition state, however, would be expected to be greater than the ground state, as the methyl substituents would interact as the cyclic trimer is formed. It can be seen that much of this difference is due to the higher torsional strain of the N-methylindole molecule imparted by the methyl groups being forced out of the plane of flat trimer. It was predicted that the increase in energy of the system due to the steric clash of the methyl groups was probably small enough to allow the formation of the N-methylindole cyclic trimer. It should be remembered that that the energy values calculated by the molecular modeller for these systems are not absolute energy values and are only useful for comparing isomers.

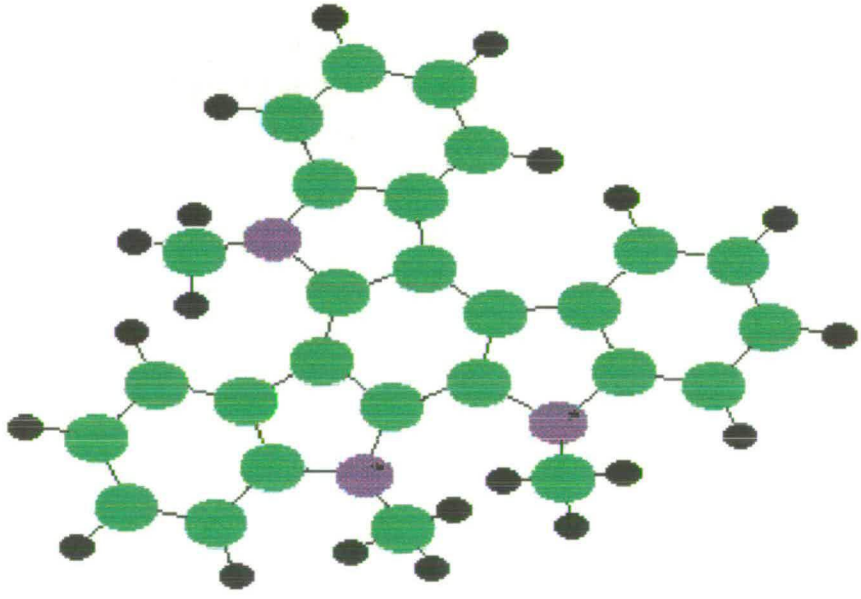

Fig. 5.2(a) - Energy minimised structure of N-methylindole asymmetric cyclic trimer. Carbon, Nitrogen and Hydrogen atoms are represented by green, blue and black respectively.

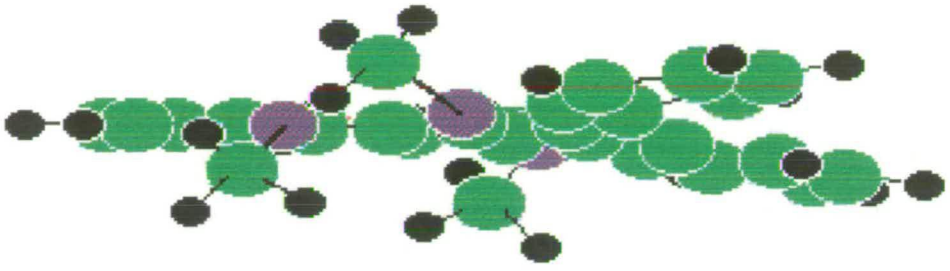

Fig. 5.2(b) - Plane view of N-methylindole asymmetric cyclic trimer. Key as in fig. 5.2(a).

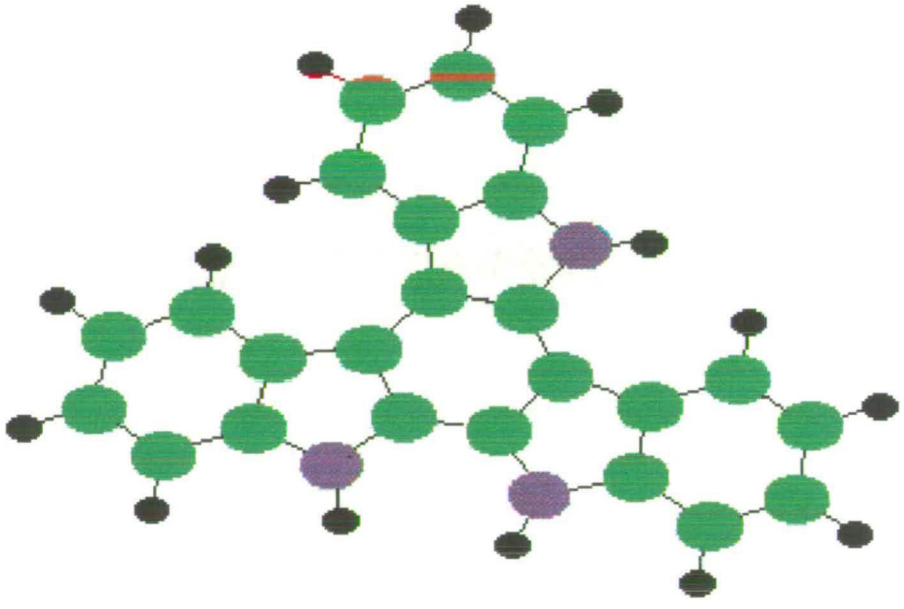

Fig. 5.3 (a) - Energy minimised structure of indole asymmetric trimer. Carbon, Nitrogen and Hydrogen atoms are represented by green, blue and black respectively.

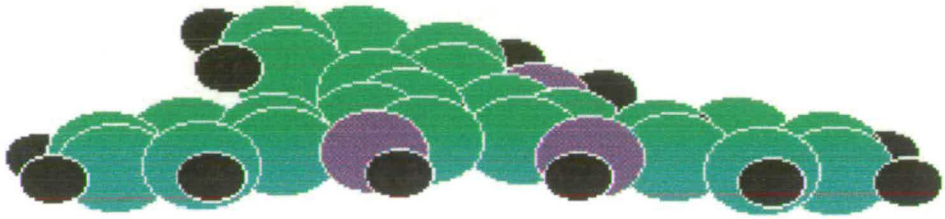

Fig. 5.3 (b) - Space-filled view of indole asymmetric cyclic trimer. Key as for fig 5.3 (a).

Energy minimisation / KJ/mol	Indole trimer	N-methylindole trimer	5-methylindole trimer
Bond	2.971	2.178	3.384
Angle	294.092	281.028	295.059
Torsional strain	15.052	53.852	17.638
Van der Waals	-20.809	-44.669	-31.646
Total	**291.305**	**292.390**	**284.436**

Fig. 5.4 - Energy minimisation calculations from OUP DTMM Molecular modelling program.

5.3 - Production of N-methylindole cyclic trimer.

It was decided to electropolymerise a solution of 50mM N-methylindole in an attempt to form the predicted asymmetric cyclic trimer. On the application of a potential (1.1V) to a stationary platinum disc electrode, a brown colouration was observed to form around the disc and drift away from the electrode surface in plumes. On rotation of the electrode, the brown species was mixed in to the bulk of solution and on continuation of the applied potential, the solution turned progressively darker. Removal of the electrode from solution showed that a polymer film

had not formed on the electrode surface. It was suggested, however, that the dark brown colour observed in solution was due to soluble products produced from an electrooxidation at the disc electrode. It was decided to study these soluble products by electrogenerating a large amount in solution, followed by spectroscopic and electrochemical analysis. The 50mM N-methylindole solution was electropolymerised for approximately 90 minutes with a large area platinum gauze passing a charge which was calculated to have electropolymerised approximately 2/3 of the monomer. The resultant solution containing the electropolymerisation product was observed to be fluorescent, therefore it was decided to examine the solution by fluorescence spectroscopy.

5.3.2 - Fluorescence spectroscopy.

A fluorescence and excitation spectrum recorded from a sample of the electroxidised N-methylindole solution is shown in fig. 5.5.

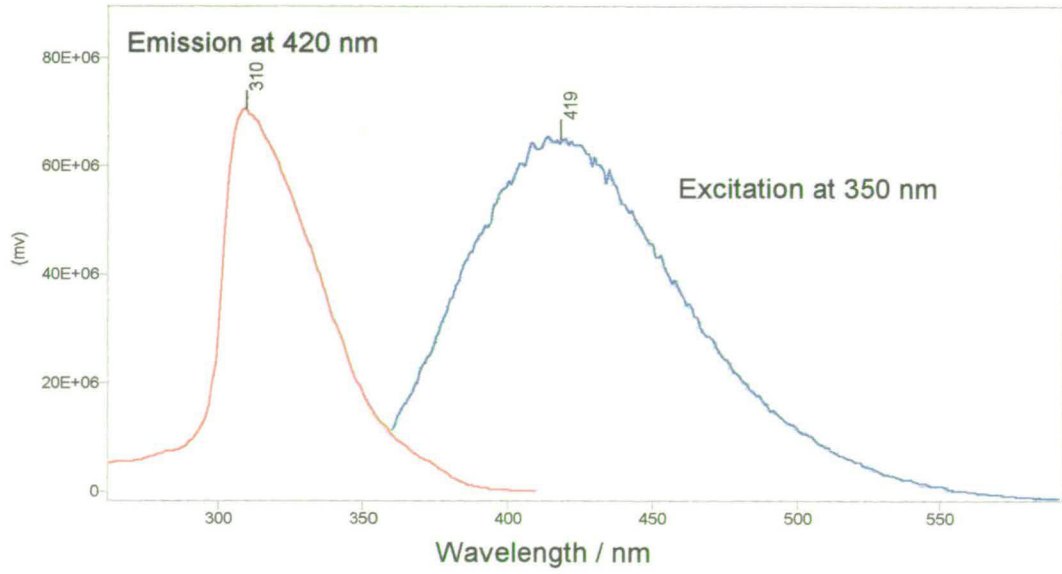

Fig. 5.5 - Fluorescence and excitation spectra of electroooxidised N-methylindole solution.

The fluorescence and excitation spectra show the characteristic peaks associated with a cyclic trimer species[112], although the fluorescence spectrum reveals a broad shoulder to longer wavelengths. This suggests that N-methylindole cyclic trimer formation is taking place. The shoulder to longer wavelengths suggests that another species is also present in solution and is more delocalised than the cyclic trimer species. This was tentatively thought to be a small amount of polymer.

5.3.3 - Electrochemistry

5.3.3.1 - Cyclic voltammetry

It was decided to examine the electrooxidised N-methylindole solution by cyclic voltammetry. The resultant CV is shown in fig. 5.6.

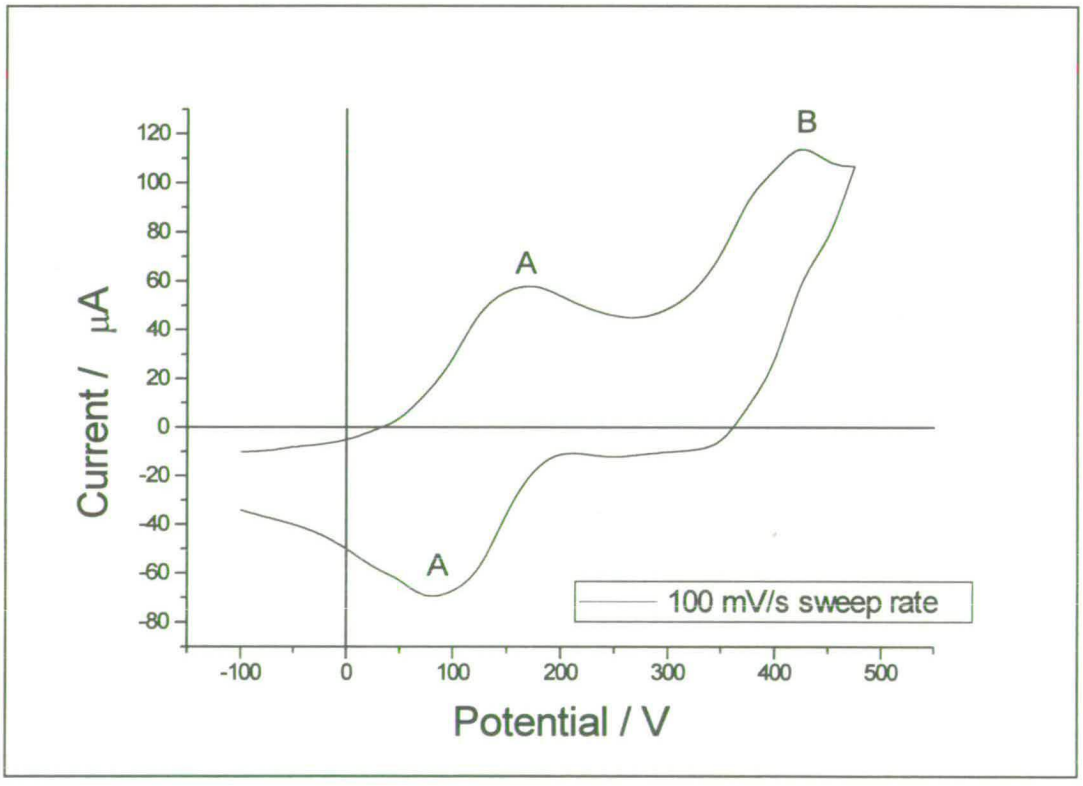

Fig. 5.6 - CV of electrooxidised N-methylindole solution.

The CV in fig. 5.6 shows an electrochemically reversible peak (A), and an electrochemically irreversible peak (B), both at lower potentials to that of the N-methylindole monomer oxidation. No electroactivity was observed in this potential region prior to electrooxidation of the N-methylindole monomer. It is suggested that the peaks noted in the CV are due to the electrochemical response of soluble products produced in the electrooxidation reaction at the disc electrode. It can be seen that there was an appreciable amount of both oxidised and reduced species in solution at the beginning of the CV sweep; this can be explained by the probability that the soluble products may have visited both the working and the counter electrodes where they can be oxidised and reduced respectively, or that some of the trimer formed in solution, where it would form in its reduced state.

5.3.3.2 - Rotating disc electrode experiments.

A rotating disc electrode (RDE) study was carried out on the electrooxidised N-methylindole solution in order to try and elucidate the electrochemical processes (at A and B) further. This experiment consisted of monitoring the current produced by a disc potential sweep at various rotation rates of the electrode. The resultant limiting currents produced in the polarograms were analysed by Levich theory and are plotted against the (electrode rotation speed)$^{1/2}$, fig. 5.7.

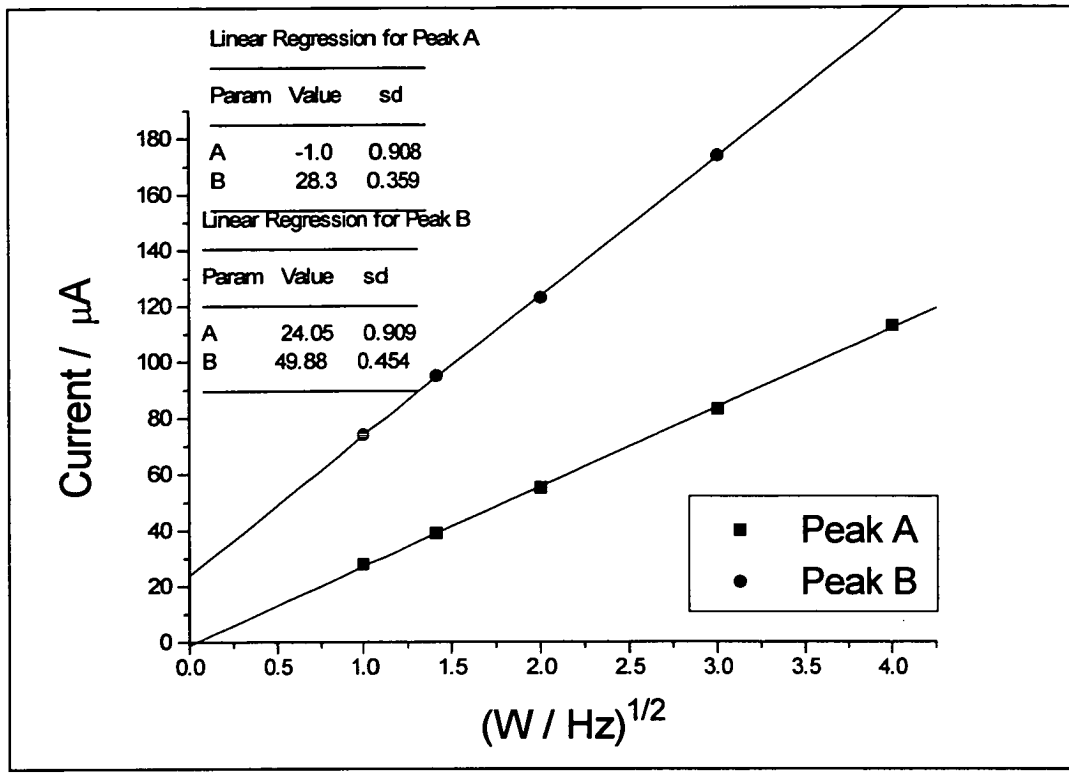

Fig. 5.7 - Levich plots for the electroxidised N-methylindole solution products.

It can be seen that the oxidation process observed at peak A in fig. 5.6 produces a Levich plot with a good straight line of gradient $28\mu A/s^{1/2}$. The straight line plot is indicative of a simple mass transport controlled oxidation process where the oxidation is first order in the species' concentration. Assuming D, the diffusion coefficient of the monomer, to be $2x10^{-5}$ cm^2/s, this gradient corresponds to a one electron oxidation in solution. From the amount of charge passed at the disc electrode (58.34C), it is calculated that approximately 3.5mM of cyclic trimer is formed if one assumes that approximately 3/4 of the electropolymerisation products are cyclic trimers. This assumption is consistent with the amount of trimer observed at the ring electrode in fig. 4.29. and the MALDI mass spectrum (fig. 5.11). Thus the electrochemical process which is observed at peak A is suggested to be due to a soluble solution species that undergoes a reversible one electron redox reaction and is apparent in a quantity expected for a cyclic trimer formed in a similar way to the 5-substituted indoles.

The Levich plot observed for the process at the chemically irreversible oxidation peak B also gives a very good straight line plot. The limiting currents produced from the polarogram observed at the peak A process are subtracted from the limiting currents obtained at peak B (which includes the current from A) to produce the resultant limiting currents for the process at B alone. It is likely that the process observed at B is due to the same species as that that undergoes the one electron redox reaction observed in peak A as peak B contains too much charge to be associated with one of the other 25% of electropolymerised soluble products that is in solution. The gradient of the Levich plot for Peak B is 50μA/s which is roughly twice the gradient for peak A. This indicates that twice as many electrons are passed in the peak B process than that for the peak A process. It is suggested, thereofre, that the peak B process is an irreversible 2 electron oxidation of the cyclic trimer species that undergoes an irreversible chemical reaction. This is consistent with a cyclic trimer that undergoes a further two electron oxidation which decomposes to another species, such as the loss of the methyl radical This would tend to lead to indole trimer which could precipitate on the electrode surface during polymerisation although no evidence could be found to support this. It is also possible that the N-methylindole trimer may undergo an additional linking reaction with the formation of two bonds through some other unidentified positions in the indole ring. However the product of this irreversible reaction could not be identified.

5.3.3.3 - Tafel analysis.

The polarogram obtained in the RDE experiment was examined by Tafel analysis, fig. 5.8. This shows a good straight line of gradient -39.6mV. Theory predicts that a one electron reversible process would have a gradient of 40 mV. Hence the Tafel plot is is consistent with peak A being a reversible one electron redox reaction of an N-methylindole cyclic trimer.

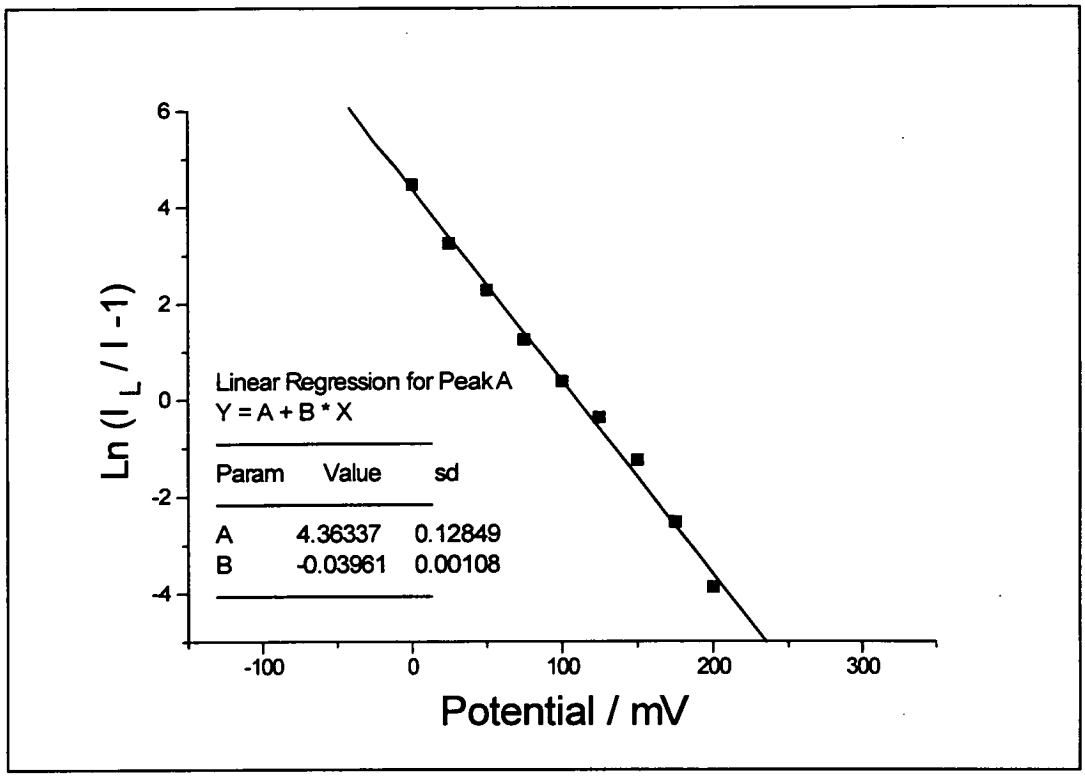

Fig. 5.8 - Tafel analysis of the 1Hz polarogram for the peak A process.

5.3.3.4 - Rotating ring-disc electrode experiments.

Similar rotating ring-disc electrode experiments to those described in section 4.2 & 4.3 were carried out a solution of 0.1M N-methylindole. The ring was swept from 350mV to -800mV and the ring polarogram recorded (fig. 5.9). It can be seen that the polarogram shows two distinct waves, the one at more positive potentials being due to soluble cyclic trimer, and the other being due to protons lost from the linking of N-methylindole radical cation monomers.

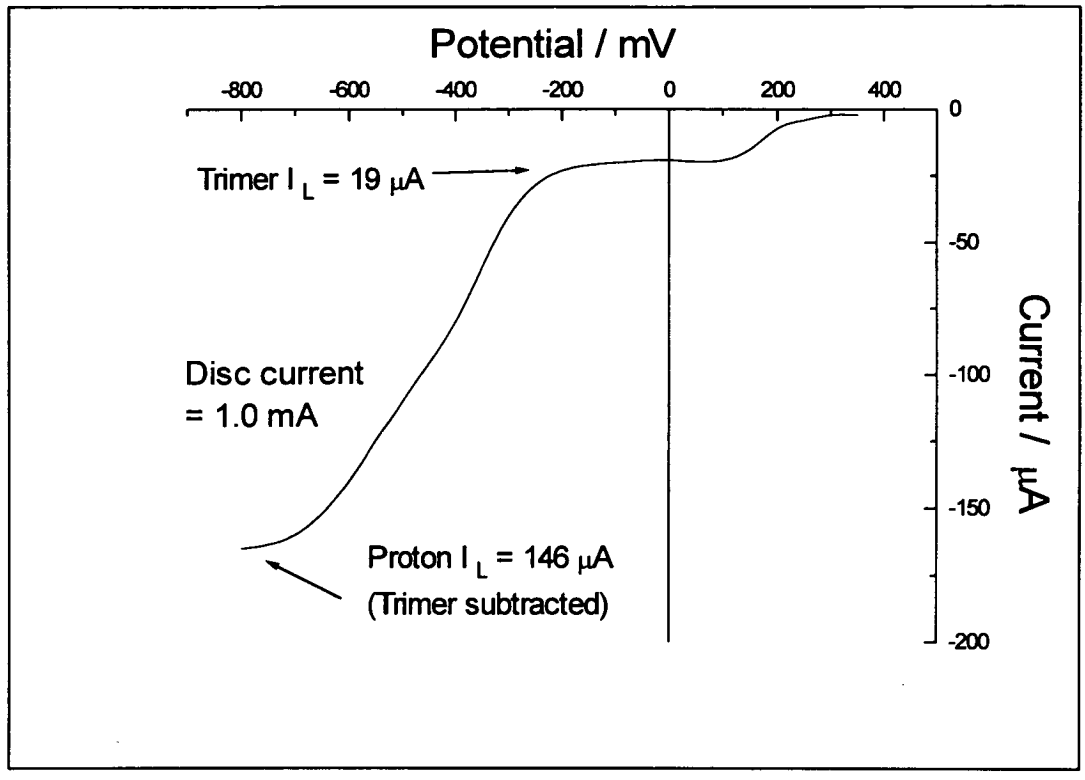

Fig. 5.9 - Ring polarogram produced from the electropolymerisation of 0.1M N-methylindole. Disc current = 1mA

5.3.3.4.1 - Proton wave.

Fig. 5.9 shows a similar proton wave to those that were observed for the 5-substituted indoles. The effective proton collection efficiency of the wave is 0.146 which is lower than 0.18 value obtained for the 5-substituted indoles. This indicates that less protons are being detected at the ring for a given amount of electrons passed at the disc, then for a 5-substituted indole; this is consistent with the observation that only 3/4 of the trimer is produced in this reaction and will be discussed in detail later.

5.3.3.4.2 - Trimer wave.

Fig. 5.10 shows the ring reduction wave at higher potentials to that of the proton wave in fig. 5.9.

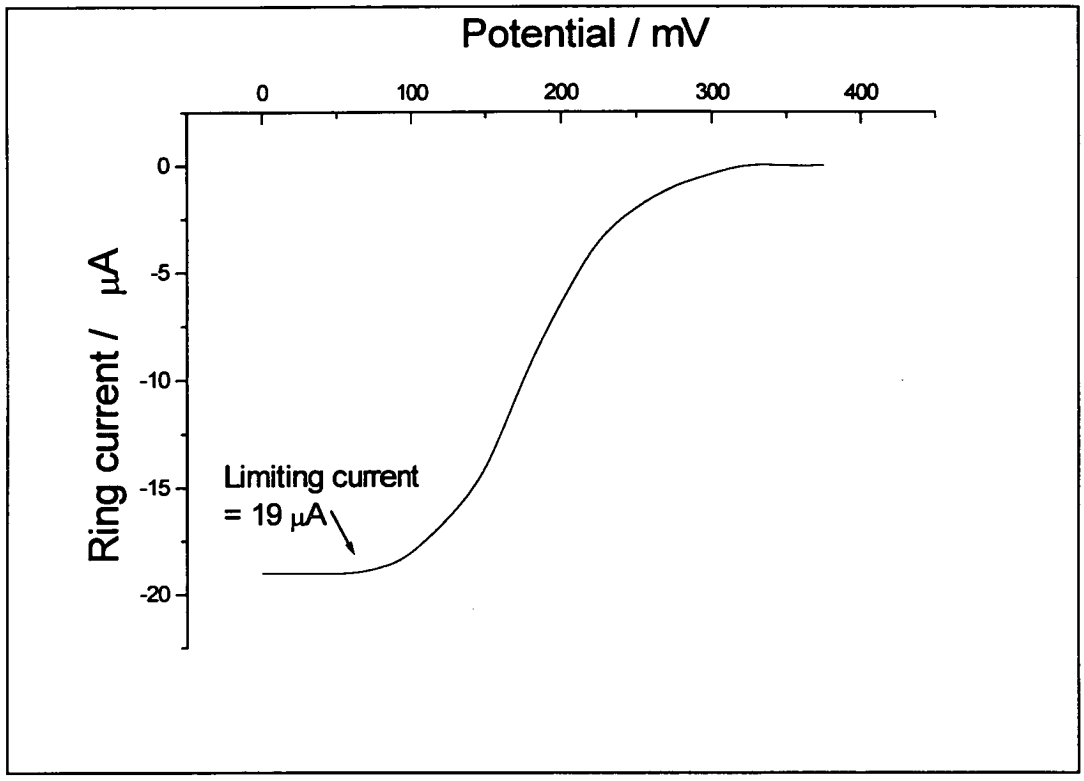

Fig. 5.10 - Ring polarogram observed for the electropolymerisation of 50mM N-methylindole. Disc current applied = 1000μA. Rotation rate = 2Hz. Sweep rate = 10mV/s.

The ring polarogram in fig. 5.10 shows a reduction wave at very similar potentials to the trimer waves observed in the electropolymerisation of 5-methylindole. It is suggested that this polarogram is due to the reduction of soluble N-methlyindole cyclic trimers. The $E_{1/2}$ value of this wave is very similar to that of 5-methylindole as they must both experience very similar electron-donating effects from their corresponding methyl substituents, even though they are substituted in different positions in the indole ring. Thus the potential at which the N-methylindole trimer wave was observed (180mV) is plotted on the Hammett substituent diagram in fig 4.16. It is comforting to note that the

potential at which this wave is observed is very similar to the potentials noted in fig. 5.6. This indicates that the loss of coplanarity of the N-substituent has little effect on the redox potential.

The observed ring current for the trimer wave was 19μA. From Equ^{n} 4.9, the observed ring current therefore corresponds to 63 % of the maximum theoretical value of trimer. This suggests that around 37% of the electrons that are being passed at the disc are going to produce some other soluble species that has not been detected at the ring electrode, as film formation was not observed for N-methylindole.

5.3.4 - MALDI mass spectroscopy.

The electrooxidised N-methylindole solution products were characterised further by matrix assisted laser desorption/ionisation mass spectroscopy (MALDI) with help from Dr Ian Mowat. The MALDI spectrum is reproduced in fig. 5.11. MALDI mass spectroscopy is known as a "soft" ionisation/desorption technique as it tends to produce mainly the parent ion peaks without much fragmentation. This is particularly useful for studies of indole polymers as it is the parent mass peaks that are of greatest interest. The technique uses a matrix of 1,8,9-trihydroxyanthracene-dithanol containing sodium and potassium salts, the matrix absorbs much of the laser energy and desorbs the polymer fragments without excessive fragmentation. The ionised polymer fragments are produced with the attachment of a cation from the salts present in the matrix and the time these fragments take to reach the detector is analysed and can be related to their mass[134]. The attached cation is usually a proton although sodium and potassium cation attachment also occurs to a lesser extent. The MALDI mass spectrum produced, therefore, often contains mass peaks which correspond to the mass of the polymer fragment, M, plus the mass of the attached cation. That is peaks consisting of M+1, M+23 and M+39 are often observed for the cation attachment of H^+, Na^+, and K^+ ions respectively.

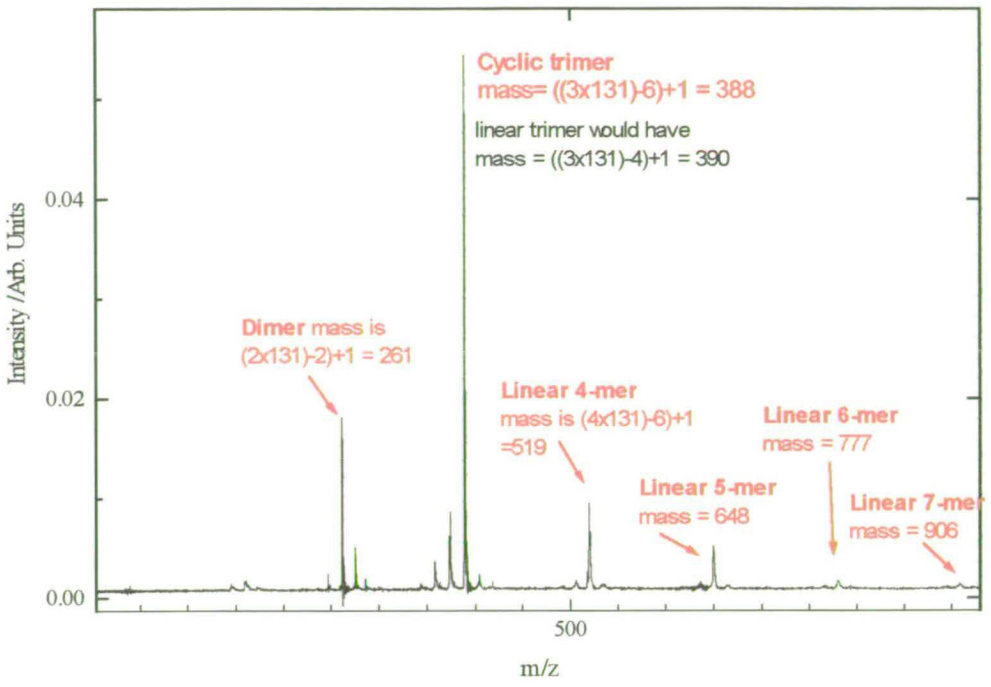

Fig. 5.11 - MALDI spectrum of electrooxidised N-methylindole solution products.

5.4.1 - Cyclic trimer.

The MALDI spectrum in fig. 5.11 shows a series of peaks that at first glance was rather unexpected. The main (base) peak is at a mass of 388, which corresponds to the mass of a cyclic N-methyindole trimer. This was expected to form from the molecular modelling calculations. The mass of an N-methylindole monomer is 131 Daltons (D), therefore the mass peak for a cyclic trimer mass would be 3x131 = 393, minus 6 D for the 6 protons lost in the linking of the three monomers, +1 for the proton (cation) attachment, which equals 388 D. Peaks corresponding to the loss of successive methyl substituents from the cyclic trimer can also be noted at mass units of 373, 358 and 343. Also the two small peaks immediately to higher mass than 388 correspond to potassium and sodium cation attachment.

5.4.2 - Linear polymer.

There are also some other, at first unexpected, mass peaks in the MALDI mass spectrum. These additional peaks were observed at masses of 261, 519, 648, 777 and 906 D. It is suggested that these peaks are due to **linear** polymer chains. This series of mass peaks correspond to [n(monomer mass)-2n+2]+1. Linear chain formation would result in the loss of two protons per monomer unit with the exception of the monomer units at the ends of the chain which would only lose one proton each. Taking in to account the MALDI proton (cation) attachment, the mass peaks correspond to a dimer, a linear 4-mer, a linear 5-mer and linear 6-mer and a linear 7-mer.

It was noted that the MALDI mass spectrum does **not** contain any mass peaks corresponding to multiples of the mass expected for linked cyclic trimers. For instance the mass of two cyclic trimers which have linked by the loss of two protons, would be expected to have been observed at a mass peak of (2x387-2)+1 = 773 AMU. However no such peak was observed. This suggests that linking of the cyclic trimers does not take place. This was predicted on the grounds that the steric bulk of the methyl groups would hinder the linking process of the cyclic trimers. Therefore, even though the electroxidation of N-methylindole results in the production of cyclic trimers, it is apparent that they do not link to form a polymer consisting of linked trimers. This is good indirect evidence to suggest that the cyclic trimers produced by the 5-substituted indoles link through the Nitrogen positions in the cyclic trimers.

The question arises of why the electropolymerisation of N-methylindole produces some linear chain polymer in conjunction with the cyclic trimers. Linear polymer formation has not been observed for indole or any of the other substituted indoles yet studied. It is believed that the first step in the formation of the all the substituted indole cyclic trimers is the linking of two of the monomer units through the 3 positions of the monomers with a loss of two protons (fig. 5.12). The linking is through the 3-positions (fig. 5.12) as these exhibit the greatest electron density[106].

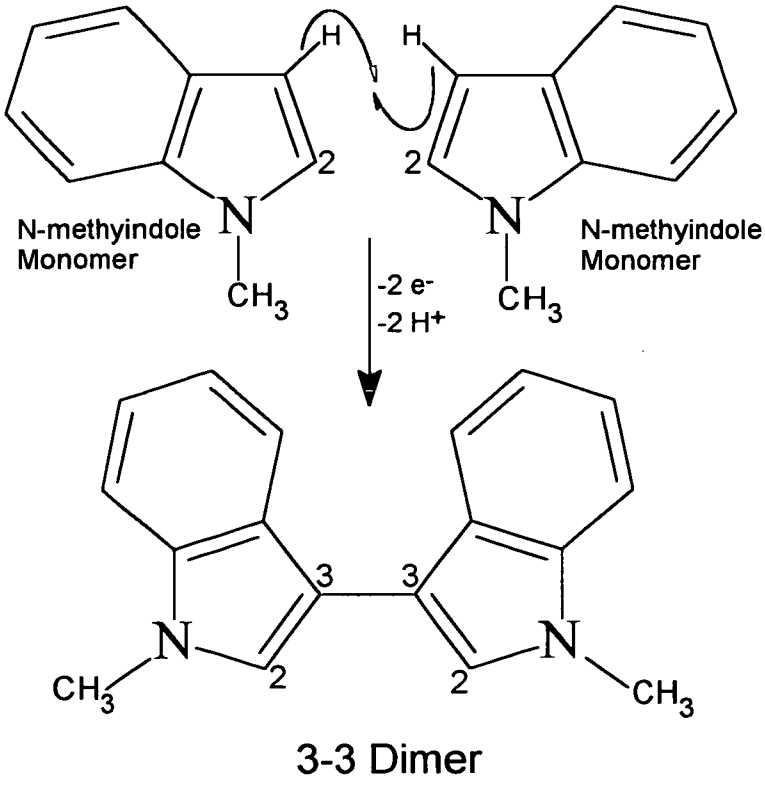

3-3 Dimer

Fig. 5.12 - Formation of 3-3 dimer.

Once this 3-3 dimer is produced, then there is a large driving force for the formation of a cyclic trimer due to the creation of an extended delocalised aromatic system. This can be achieved by linking a third monomer through its 2 and 3 positions to the available 2 positions in the dimer. This bond formation is shown by the blue lines in fig. 5.13.

By whatever orientation this third monomer is linked to the dimer, it results in the formation of an asymmetric trimer. This is believed to be the reason why only the asymmetric form of the trimer has ever been observed by electrochemical polymerisation, although the symmetric form has previously been noted as a minor product in a chemical synthesis[135].

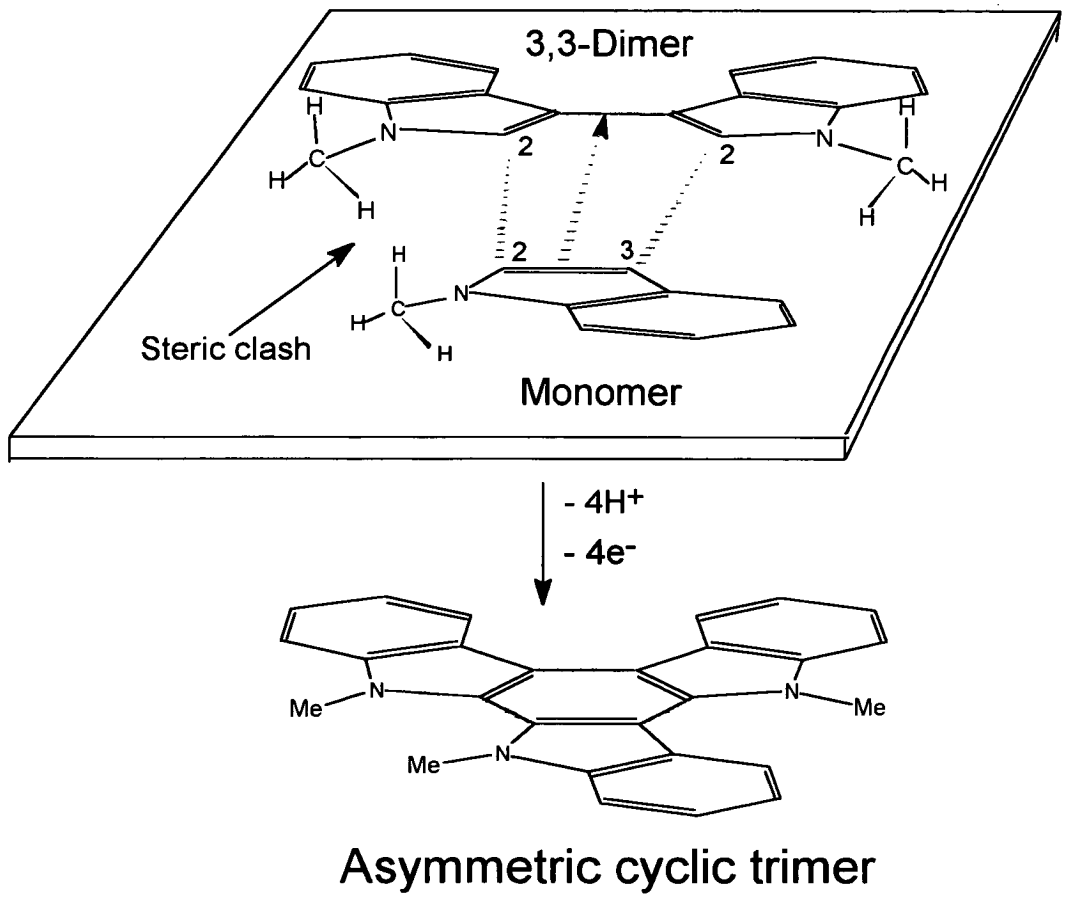

Fig. 5.13 - Linking of monomer to 3-3 dimer.

It can also be seen that as the third monomer approaches the dimer in fig. 5.13, there is a large amount of steric clash between one of the methyls on the dimer and the methyl on the monomer. This steric clash is believed to increase the activation energy sufficiently to hinder the cyclic trimer formation. This would result in an increased concentration of the 2,2'-dimer and monomer and coupling of these species may result in linear polymer formation (fig. 5.14). It is suggested that linear polymerisation occurs by succesive addition of an N-methylindole monomer from its 3-position to the available 2 position on the linear trimer, fig. 5.15.

Molecular Modelling calculations have shown that a linear polymer formed in this way is energetically more stable than that formed by -23-23-23- couplings or -32-23-32-23-32- couplings. Formation of the linear polymer must be controlled by the electron density of the monomer radical cation as the observed production of 5-mers and 7-mers in fig. 5.11 must have been due to the addition of succesive monomers on to dimer.

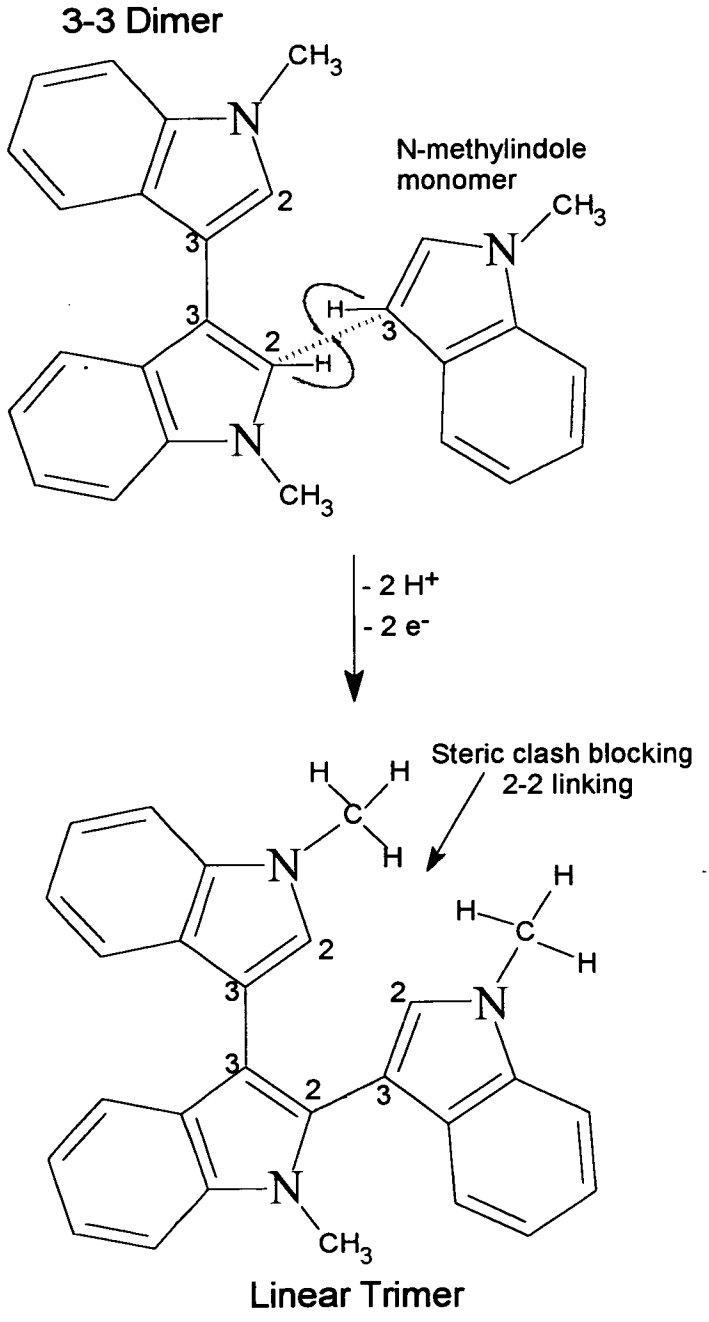

Fig. 5.14 - linear trimer formation.

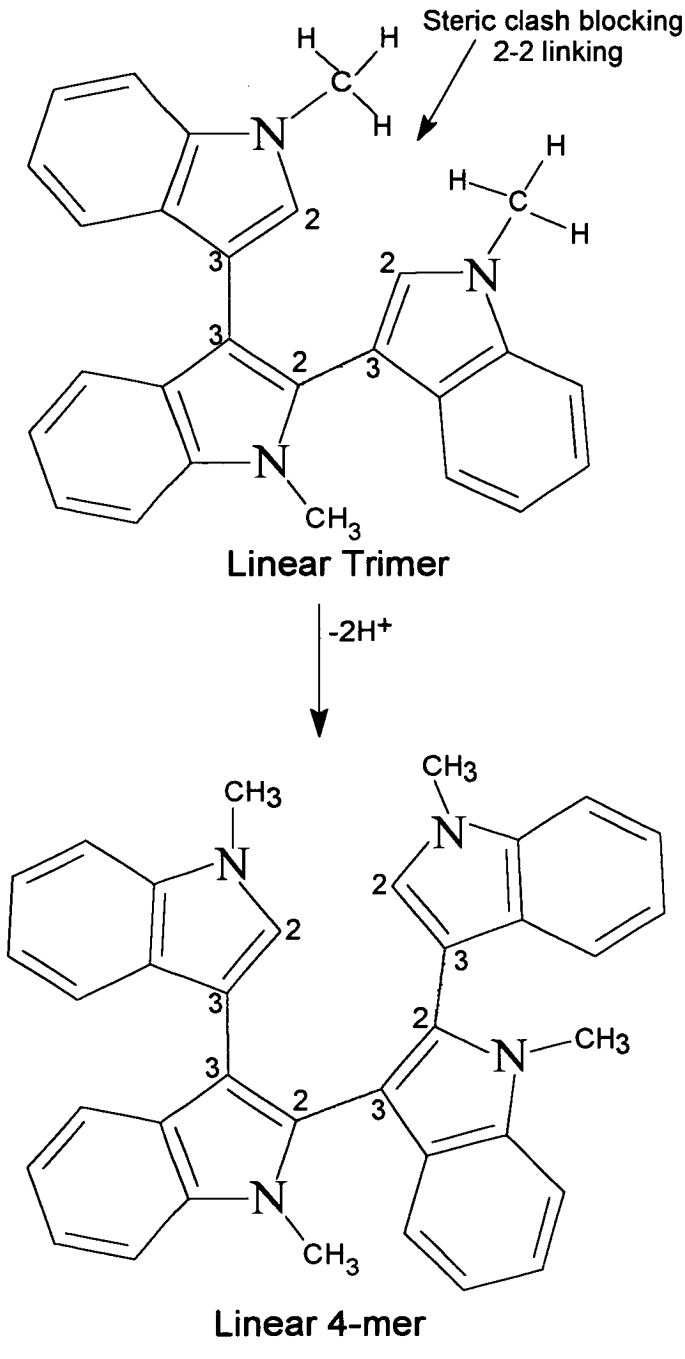

Fig. 5.15 - Proposed linear polymerisation formation.

5.5 - Conclusions.

The results presented in this chapter have given some insight in to the electropolymerisation mechanism of N-methylindole. In light of the results presented in the previous chapter, which showed that the 5-substituted indole trimers undergo similar redox redox reactions, these results also shed some light on the general electropolymerisation process of indole and the 5-substituted indoles.

1) Electropolymerisation of a solution of 50mM N-methylindole in background electrolyte, resulted in the production of soluble (probably asymmetric) cyclic trimer species with the addition of a small amount of linear chain polymerisation.

2) The linear polymerisation was attributed to the steric bulk of the methyl groups which destabilised the molecule sufficiently to partly hinder efficient trimer formation and allowed a less favoured linear polymerisation to occur.

3) No polymer (soluble or insoluble) consisting of linked N-methylindole cyclic trimers was observed which suggests that the methyl groups were hindering the linking of the N-methylindole cyclic trimers.

4) As the N-methyl groups were believed to hinder the linking of the cyclic trimers in forming polymer, this is strong indirect evidence to suggest that the 5-substituted indole cyclic trimers link through two of the Nitrogen positions to form a polymer consisting of linked cyclic trimers.

5) Despite the steric strain of the N-methyl group, the redox potential for the trimer was similar to that obtained for 5-methylindole, indicating little effect on the energy of the π-aromatic system.

Chapter 6 - Electrooxidation of 5-aminoindole.

6.1 - Introduction.

The results described in Chapter 4, showed it was possible to direct the formation and deposition of 5-hydroxyindole cyclic trimers with the use of a pre-formed electrodeposited poly(CI) or poly(NI) layer. The results presented in this chapter extend the use of this pre-formed polymer layer technique to facilitate the electropolymerisation of 5-aminoindole and characterise the subsequent 5-aminoindole films produced in this way.

6.2 - Electropolymerisation of 5-aminoindole.

6.2.1 - Electropolymerisation on platinum.

A cyclic voltammogram of 50mM 5-aminoindole in background electrolyte was carried out on a clean platinum electrode, fig. 6.1. The first cycle shows oxidation peaks at 350mV and 500mV. Successive cycles show a great reduction in current and a shift of the oxidation peaks to a more positive potential. This indicates that the 5-aminoindole oxidation reaction results in the deposition of a thin passivating or insulating film on the platinum electrode surface.

The oxidation peak potential (500mV) of the first sweep of the CV was applied as a potential pulse to the clean platinum electrode, and a current-time transient recorded, fig. 6.2. The 5-aminoindole current-time transient shows that the current dropped relatively rapidly with time eventually dropping to zero which indicates that a passivation or insulation of the platinum electrode was occurring. This may be due to the 5-aminoindole molecules chemisorbing via the amino groups on the platinum surface which hinders the electropolymerisation reaction. This type of passivation has previously been noted for pyridine.[136]

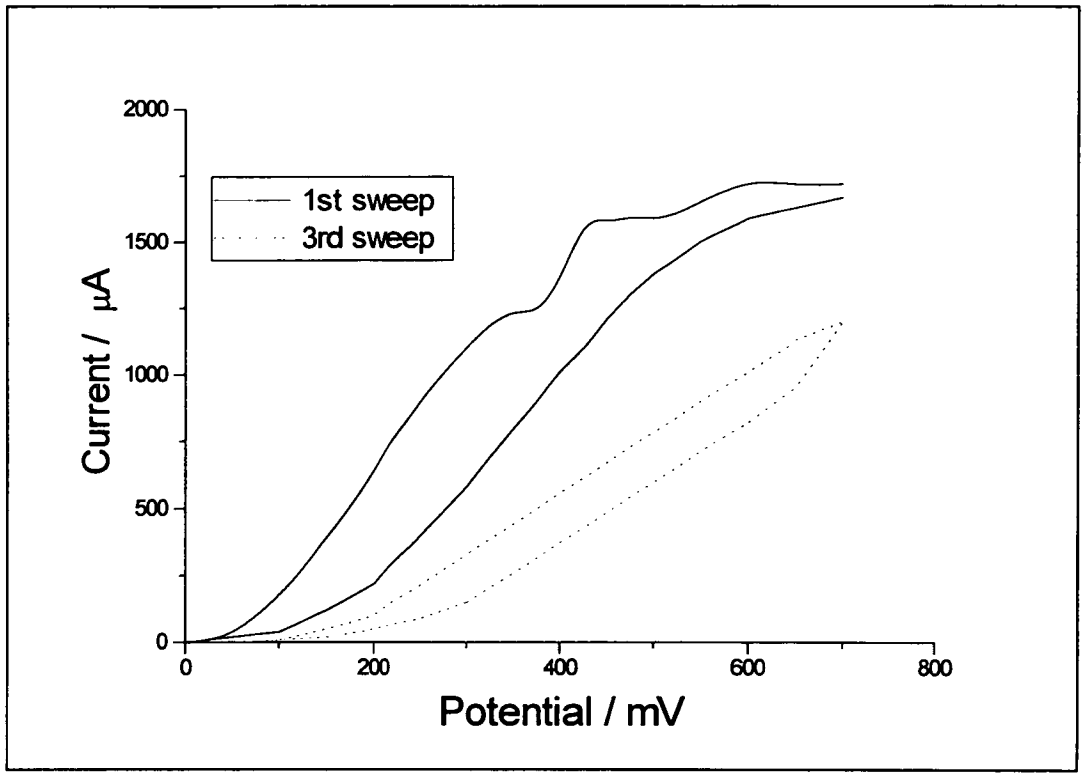

Fig 6.1 - CV of 50mM 5-aminoindole on Pt. Sweep rate = 10mV/s.

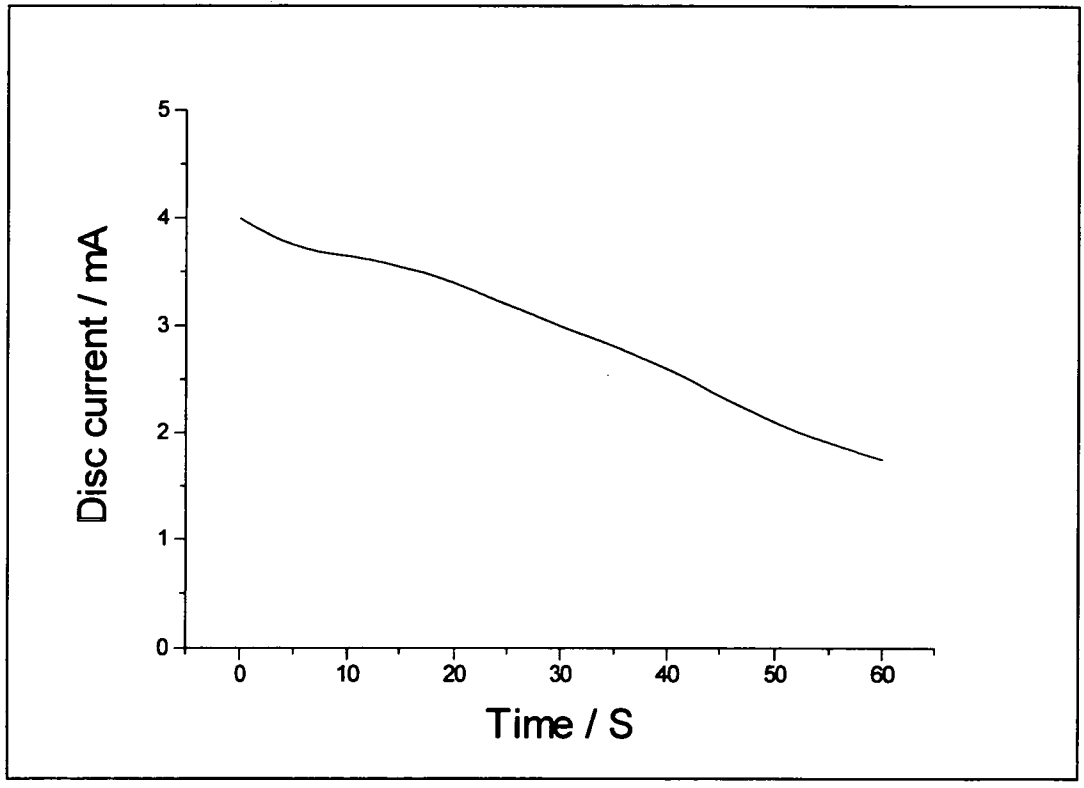

Fig. 6.2 - Current-time transient of 50mM 5-aminoindole on Pt. (0.575V)

A ring polarogram was recorded during the electrooxidation of 50mM 5-aminoindole at a clean platinum disc electrode (0.575 V). However the ring polarogram did not show any electroactivity between the potentials of +0.1V and - 0.5V, and the disc electrode current dropped rapidly towards zero. This indicated the formation of a passivating or insulating layer on the disc electrode.

6.2.2 - Electropolymerisation on a pre-formed poly(CI) layer.

A cyclic voltammogram of the 50mM 5-aminoindole solution was carried out using an electrode that had been modified by previously coating a poly(CI) layer on the platinum surface, fig. 6.3. It can be seen that the similar monomer oxidation peaks are observed in this CV as that carried out on a clean platinum surface (fig. 6.1). However, successive CV sweeps on the pre-formed poly(CI) layer reproduce the first sweep, this shows a great reduction of the passivation or insulation of the electrode surface that was observed on the clean platinum. The oxidation peaks are also better defined on top of the poly(CI) layer.

A current-time transient was recorded using a poly(CI) coated disc electrode for the electropolymerisation of 50mM 5-aminoindole at a potential of 0.575V, fig. 6.4. It can be seen that the current remains approximately constant at a value of 3mA without any of the passivation noted on the clean platinum surface. This suggests that the passivation reaction does not occur as readily on the pre-formed poly(CI) layer as that on pure platinum. Hence a pre-formed poly(CI) can be used to limit the unfavourable passivation reaction allowing the electropolymerisation reaction to proceed.

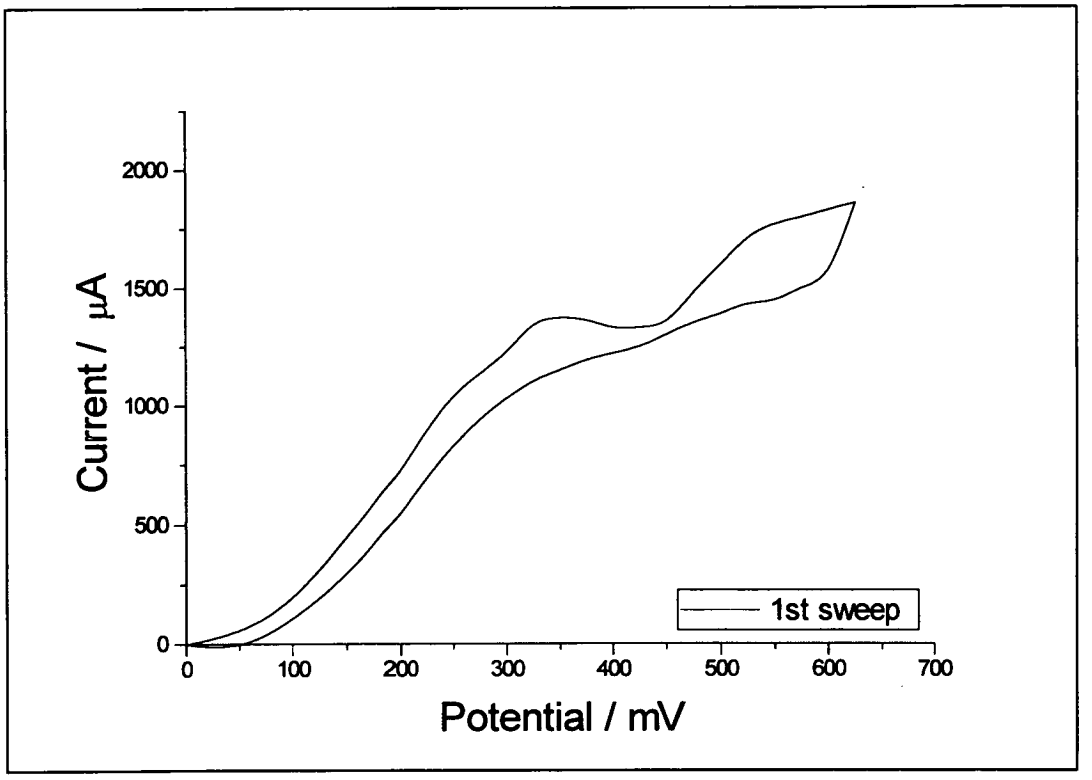

Fig 6.3 - CV of 50mM 5-aminoindole on a pre-formed poly(CI) film.

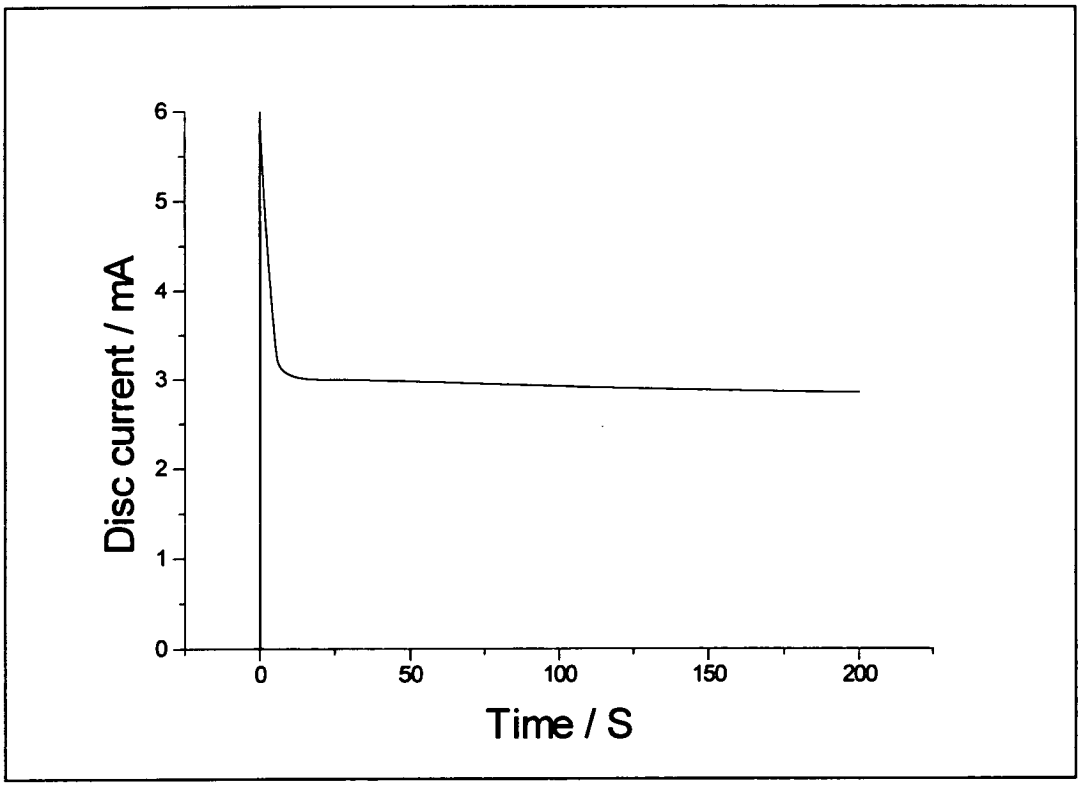

Fig. 6.4 - Current-time transient for the electrooxidation of 50mM 5-aminoindole on a poly(CI) layer. Electrode rotation = 2Hz. (0.575V)

A potential of close to 0.575V was applied to a solution of 50mM 5-aminoindole using a disc electrode that had been pre-coated with a poly(CI) layer and a ring polarogram was recorded at a constant disc current of 0.6mA. The ring polarogram is shown in fig. 6.5. It can be seen that a reduction wave is observed in the ring polarogram at an $E_{1/2}$ potential of approximately -0.25V. This is suggested to be due to the reduction of soluble 5-aminoindole trimers that had been produced on the poly(CI) layer on the disc. From Equ^{n}s 4.4 & 4.9, the amount of 5-amino trimer collected at the ring corresponds to approximately 36% of the total produced, assuming that Equ^{n} 4.1 applies. This indicates that either 64% of the trimer formed remains deposited on the disc electrode, or that some of the electrons passed at the disc are not all going to make trimers. In reality some of the product formed is probably not all trimer and much of this probably electrodeposits on the poly(CI) layer. It is suggested that the poly(CI) layer facilitates the formation of 5-aminoindole trimers on the surface of the poly(CI) film, a large proportion (up to 36 %) of which desorb from the surface of the film and can be detected at the ring electrode.

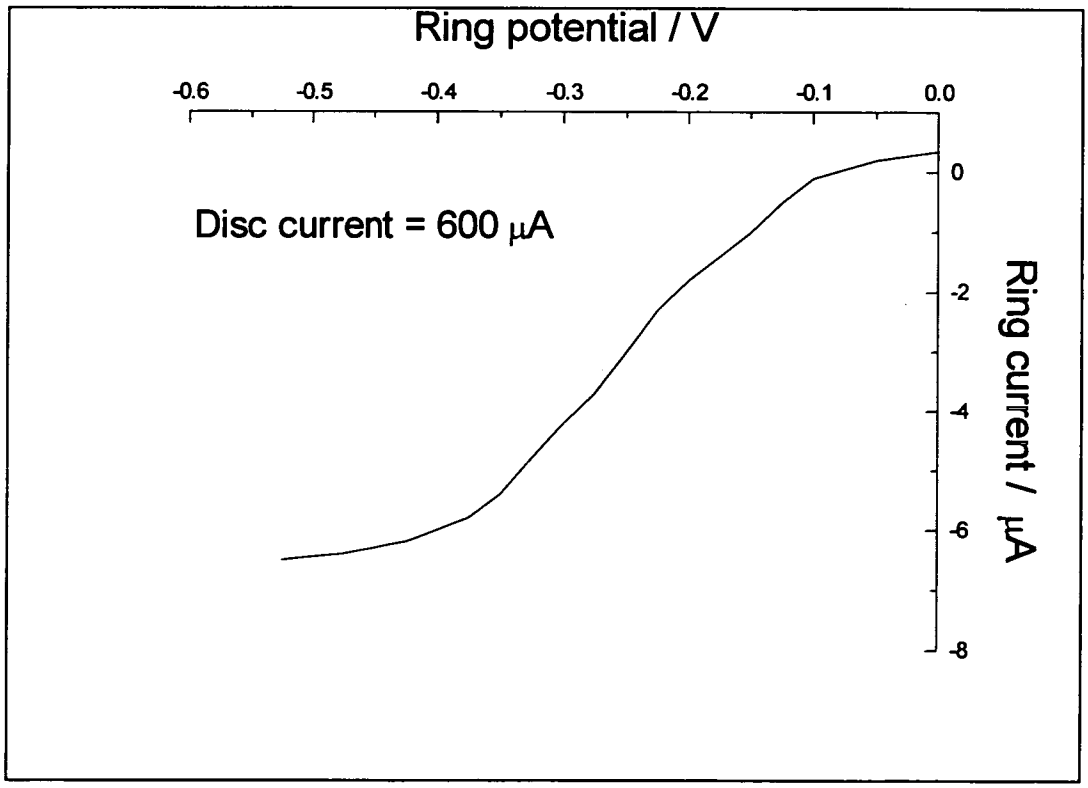

Fig. 6.5 - Ring polarogram of 50mM 5-aminoindole on poly(CI) layer.

Whilst carrying out this electropolymerisation, it was observed that a thin black layer had formed on top of the dark green poly(CI) layer. It was suggested that this was due to the formation of a 5-aminoindole trimer (and/or polymer) layer.

As with the 5-hydroxyindole electropolymerisation, described in section 4.5, further characterisation of this electrodeposited 5-aminoindole layer by various spectroscopic methods proved difficult as separation of the two layers could not readily be achieved. As this layer could not be studied as a whole by spectroscopic methods, due to the complicating similar spectroscopic characteristics produced by the poly(CI) in the layer, it was decided to attempt to polymerise the 5-aminoindole on top of a poly(NI) layer. As has previously been shown, poly(NI) does not show any fluorescence, this is often observed for nitro-substituted aromatics, and is attributed to the accessibility of the n-π^* transitions[137], which means that non-radiative pathways dominate in the decay of the excited states.

6.2.3 - Electropolymerisation on pre-formed poly(NI) layer.

Similar ring polarograms and current time transients to that obtained for the electrooxidation of 5-aminoindole on the poly(CI) layer were observed with the electrooxidation of 5-aminoindole on the poly(NI) layer. The electrooxidation of 5-aminoindole was accompanied with a similar build up of a dark secondary layer on top of the oxidised green poly(NI) layer. Fluorescence spectroscopy was then used to study the poly(NI)~5-aminoindole layer as a whole. Three emission spectra produced from excitation at 320, 350 and 380nm are displayed in fig. 6.6. These show three different emitting chromophores which suggest the presence of three different 5-aminoindole based products on the poly(NI) film.

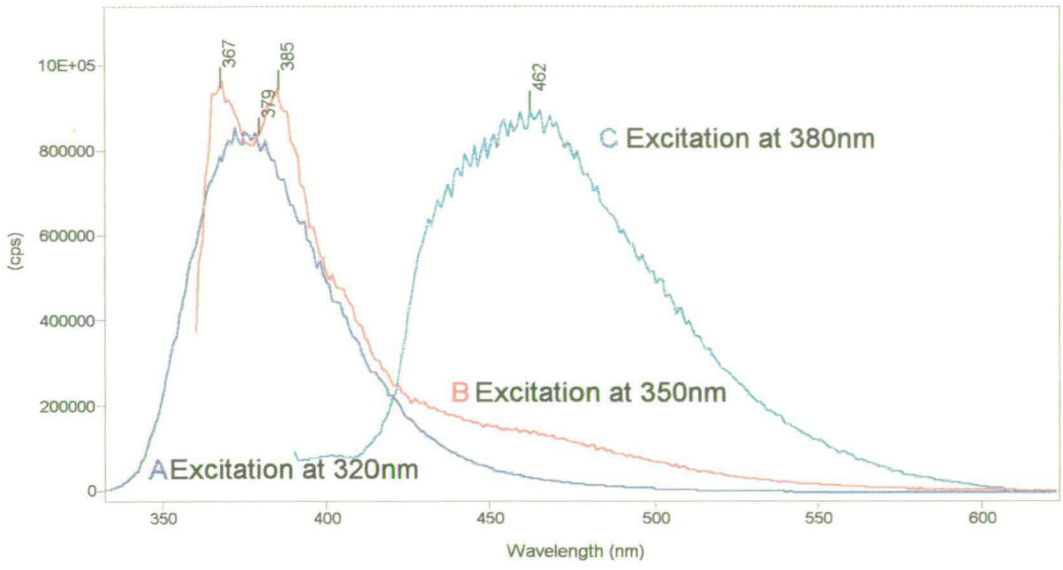

Fig. 6.6 - Fluorescence spectra of electrooxidised 5-aminoindole film on a poly(NI) layer.

The fluorescence spectrum (C) that peaks at 462nm in fig. 6.6 is at a higher wavelength and somewhat broader than the trimer species observed by other 5-substituted indoles. It was believed from other work[138] that the 5-aminoindole monomer and trimers may undergo aggregation in the ethanol solution used for the fluorescence experiment. It was decided to attempt to break up these aggregations by the addition of a small amount of acetic acid to the solution which was hoped to protonate the amino groups. It can be seen that on addition of the acetic acid this spectrum collapses to the characteristic trimer type spectrum observed by the other 5-substituted indoles, fig. 6.7.

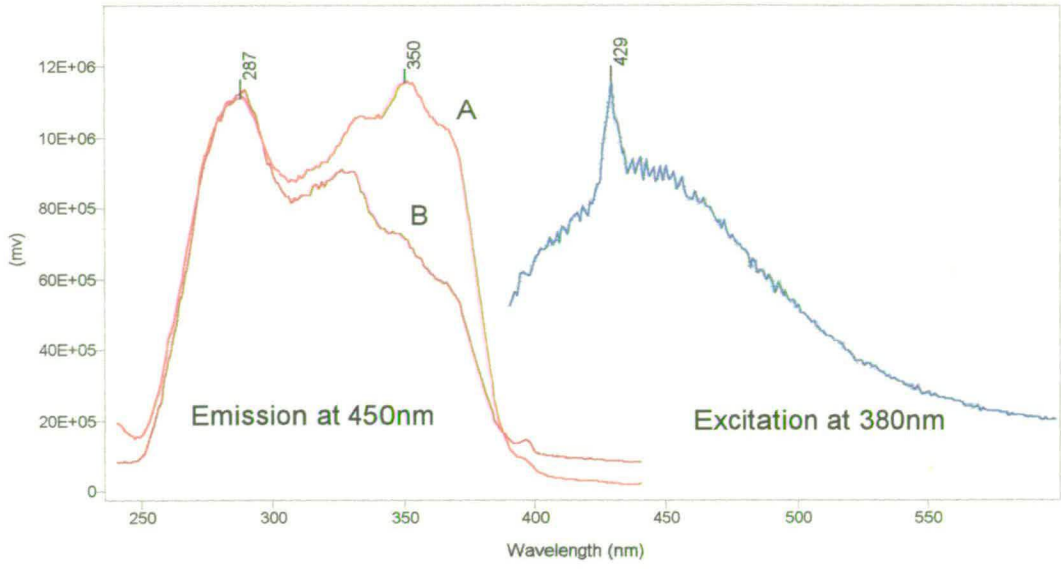

Fig. 6.7 - Fluorescence and excitation spectra after addition of acetic acid. A is addition of 1 aliquot of acetic acid. B is after addition of 2 aliquots.

Spectrum A in fig. 6.6 showed that there was a certain amount of fluorescence due to monomer observed at 377nm with an excitation of 320nm. It was also noted that there was possibly fluorescence due to a dimeric species with a peak at a wavelength of 385nm observed with an excitation at 335nm (spectrum B). These fluorescence spectra are strong evidence for the formation of a layer of 5-aminoindole trimer (and/or polymer), monomer and possibly a dimer species on top of the poly(NI) layer.

It was noted that the electropolymerisations of 5-aminoindole on the poly(CI) and poly(NI) layers often resulted in the bulk solution becoming coloured deeply red. It was thought that this colouration was most likely to be due to soluble products from the electropolymerisation of the 5-aminoindole, hence it was decided to also carry out a fluorescence study of this coloured bulk solution. This showed the characteristic fluorescence spectrum of a trimer like species with a very similar spectrum to that of fig. 6.6(C) as well as the large amount of expected monomer in solution. This finding is consistent with the RRDE experiment described in

section 6.2.2 that showed the presence of soluble 5-aminoindole trimer. From this it is apparent that 5-aminoindole trimer formation and a small amount of trimer/polymer film deposition can be directed through the use of a pre-formed 5-nitroindole or 5-cyanoindole polymer layer, although much of the 5-aminoindole trimer produced enters the bulk of solution.

6.3 - Rotating disc electrode studies of 5-aminoindole.

It was decided to study the electropolymerisation of 5-aminoindole on the pre-formed poly(CI) and poly(NI) layers in order to probe the mechanism of electropolymerisation on these layers further.

6.3.1 - Rotating disc electrode studies on poly(CI).

The electropolymerisation mechanism of 5-aminoindole on a poly(CI) layer was studied by examining the steady-state current produced by the electropolymerisation at the rotating disc electrode for a variety of bulk 5-aminoindole concentrations and electrode rotation speeds. The electropolymerisation was studied at a potential of 0.575V on a pre-formed poly(CI) layer. These data are plotted in fig. 6.8 according to the Koutecky-Levich equation (Equ^{n} 6.1) discussed in chapter 2.

$$\frac{1}{i} = \frac{0.643\upsilon^{1/6}}{nFAD^{2/3}c_{\infty}W^{1/2}} + \frac{1}{i_{\infty}} \qquad \text{--- Equ}^{n}\text{ 6.1 - Koutecky-Levich equation}$$

Where i is the oxidation current, w is the rotation speed in Hz,
n is the number of electrons transferred,
F is Faraday's constant,
D the diffusion coefficient,
c_{∞} the bulk concentration of the monomer,
υ is the kinematic viscosity of acetonitrile,
i_{∞} is the current which would be observed as the rotation

speed tends to infinity, when the current is independent of mass transport.

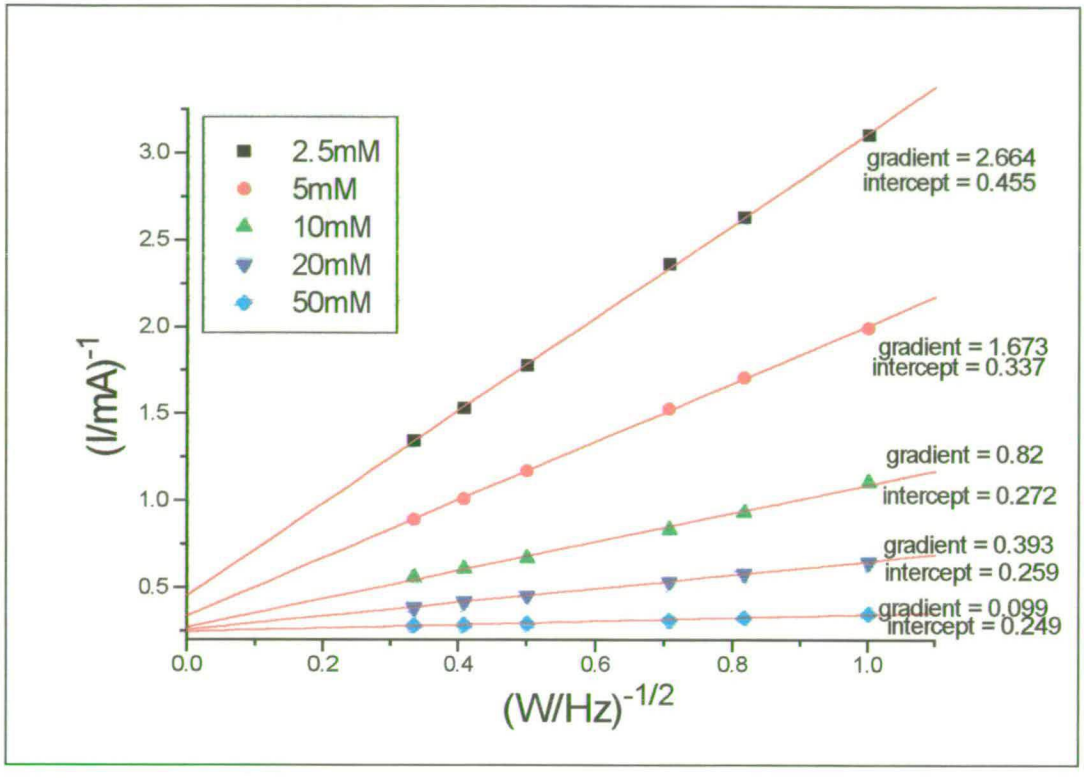

Fig. 6.8 - Koutecky-Levich plot of 5-aminoindole on a poly(CI) film (0.575V).

It can be seen that at each concentration of 5-aminoindole monomer, the data lie on a good straight line. This is indicative of the electro-oxidation being first order on monomer which is an assumption of the Koutecky-Levich theory. The gradient of each of the plots can give the number of electrons passed if the diffusion coefficient is known. The diffusion coefficient for I5CA has previously been estimated to be $1.5x10^{-5}$ cm^2s^{-1} [112], therefore the diffusion coefficient of 5-aminoindole is expected to have a very similar value. Using the estimated diffusion coefficient of $1.5x10^{-5}$, the calculated number of electrons passed for the different concentrations of 5-aminoindole are shown in fig. 6.9.

Concentration of 5-aminoindole / mM	Gradient of slope	Number of electrons passed
2.5	2.664	1.73
5	1.673	1.38
10	0.82	1.39
20	0.393	1.47
50	0.099	2.33

Fig. 6.9 - Table of number of electrons passed in electropolymerisation of 5-aminoindole on poly(CI).

It can be seen that only at a concentration of 50mM in monomer are there suffficient electrons passed to suggest the formation of 5-amino trimers. Theoretically there should be 2.33 electrons passed per monomer unit to form an oxidised trimer. At lower concentrations fewer electrons are passed indicating the formation of radical cations and a small amount of linking but not of a sufficient value to form cyclic trimers. This is consistent with the observation of monomer and dimer like species from the fluorescence experiemtns carried out in section 6.2.3.

For each of the plots, the y-intercept of the graph gives the i_∞ value which corresponds to the current observed at the electrode when the surface concentration of monomer is equal to the bulk concentration. It can be seen that as the concentration of monomer is increased the I_∞ values decrease, tending towards a constant value of 4mA for the 50mM monomer oxidation. At concentrations higher than 50mM mass transport is relatively high and the current is relatively insensitive to $W^{1/2}$, although the same I_∞ value 4mA is reached indicating that the same reaction is occuring. This suggests that the rate determining step for the oxidation of 5-aminoindole on the poly(CI) involves the reaction of an intermediate which fully covers the surface of the poly(CI) layer only at the higher concentrations (over 50mM) of monomer. At lower concentrations, this reaction intermediate does not fully cover the electrode. It is suggested that this intermediate may be 3-3' dimer which is produced from monomer radical cations that dimerise, the structure of which is postulated in fig. 6.10. This was anticipated to be the most likely dimer to form, as with all

the substituted indoles studied the greatest electron density resides in the 3 positions[106].

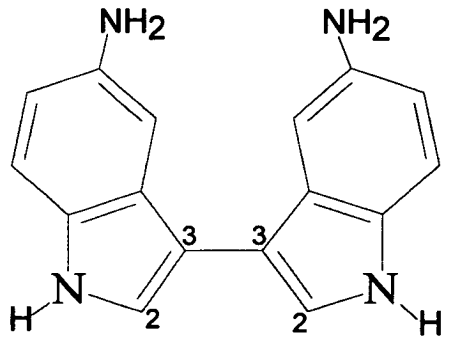

Fig. 6.10 - 3-3' aminoindole dimer.

The suggestion that the surface reaction intermediate may be the 3-3' dimer is in agreement with the fluorescence spectrum (fig. 6.6), which showed the probable presence of a dimer species in addition to the trimer and monomer spectra observed from the 5-aminoindole polymerisation on the poly(NI) surface.

It is proposed that the formation of cyclic 5-aminoindole trimers on the poly(CI) surface does not occur until it is fully covered with monomer radical cations. Only at concentrations of above 50mM is there sufficient oxidation and adsorption of the 5-aminoindole monomer on the surface to lead to linking and the formation of 5-aminoindole cyclic trimers.

The value of i_{∞} = 4mA for the oxidation of 5-aminoindole on poly(CI) can be compared with an i_{∞} values of 10mA and 20mA for the electropolymerisation on platinum of indole-5-carboxylic acid[114] and 5-cyanoindole respectively.[115] This suggests that the rate of linking of 5-aminoindole monomers to form a cyclic trimer is less than half the rate for I5CA and around a fifth of the rate for the trimer formation of 5-cyanoindole.

6.3.2 - Rotating disc electrode studies of 5-aminoindole on a poly(NI) layer.

It was decided to examine whether there were differences between the electropolymerisation reaction of 5-aminoindole on poly(CI) and that on poly(NI). The steady state currents were monitored for the electropolymerisation of 5-aminoindole monomer on a pre-formed poly(NI) film at a number of different concentrations and electrode rotation rates. These produced similar Koutecky-Levich plots to that observed on a poly(CI) and is shown in fig. 6.11.

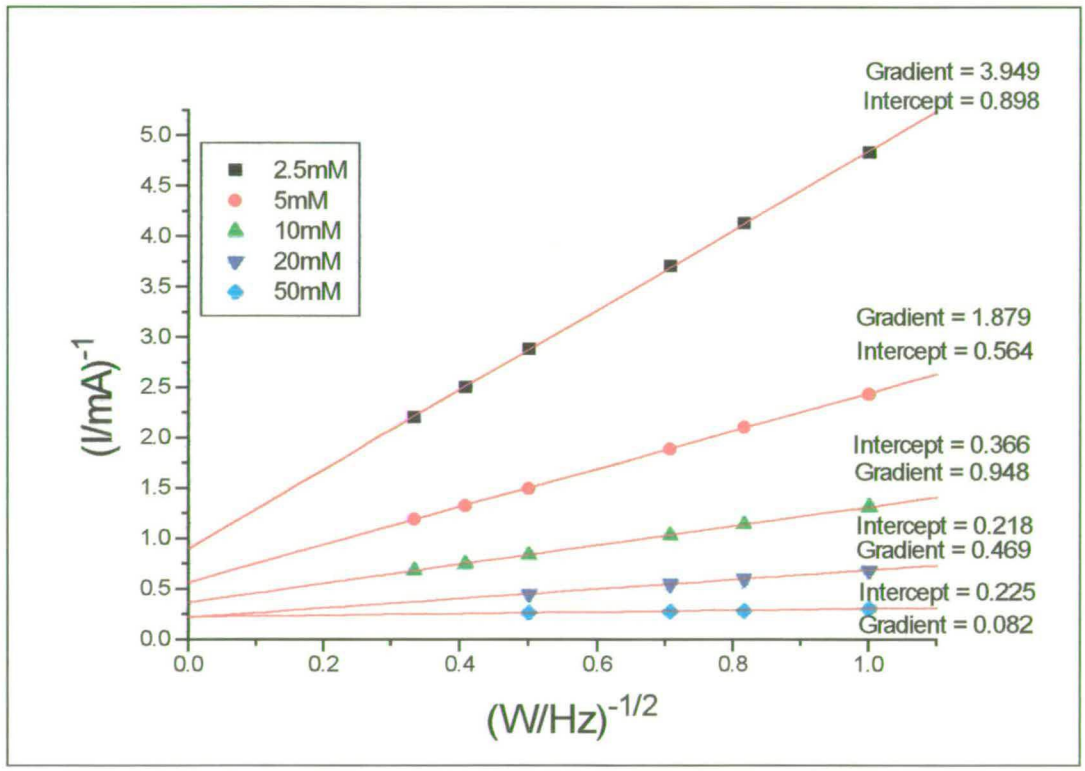

Fig. 6.11 - Koutecky-Levich plot of 5-aminoindole on poly(NI) (0.575V).

The Koutecky-Levich plot in fig. 6.11 is very similar in appearance to that for 5-aminoindole on a poly(CI) film. This indicates that the poly(NI) is a very similar surface to the poly(CI) layer. The Koutecky-Levich plots again show good straight lines for all the concentrations and tend towards a i_∞ value of 4.5mA. This surface rate of reaction is only slightly faster than that observed on the poly(CI) film which suggests that a very similar

mechanism is taking place. The number of electrons passed can again be estimated from the gradient of the various plots, assuming D to be 1.5×10^{-5} $cm^2 s^{-1}$, and are tabulated in fig. 6.12.

Concentration of 5-aminoindole / mM	Gradient of slope	Number of electrons passed
2.5	3.949	1.2
5	1.879	1.2
10	0.948	1.2
20	0.469	1.2
50	0.082	2.8

Fig. 6.12 - Table of number of electrons passed for the electropolymerisation of 5-aminoindole on poly(NI).

6.4 - Copolymerisation of 5-aminoindole with 5-cyanoindole and I5CA.

Examination of the 5-aminoindole layers that were produced on the poly(CI) of poly(NI), showed that they were very thin compared with the thick layers that could be grown from 5-cyanoindole and I5CA. Although the use of the pre-formed poly(CI) and poly(NI) layers directed some of the 5-aminoindole monomer to link to form trimers, the linking process and build up of the film was much slower and less efficient than that of the electropolymerisation of the other 5-substituted indoles. Most of the 5-aminoindole trimer formed desorbed from the poly(CI/NI) surface and entered the bulk solution, which is due to the relatively slow rate of linking and the solubilising nature of the amino groups.

6.4.1 - Copolymerisation of 5-aminoindole with 5-cyanoindole.

It was decided to attempt to copolymerise the 5-aminoindole with the much faster reacting 5-cyanoindole monomer to attempt to increase the efficiency of formation and decrease the solubility of any trimers formed that contained amino groups. This was hoped to result in a more efficient film formation and a much thicker copolymer film containing many amino groups. It was thought that the electropolymerisation of a solution containing 5-aminoindole and 5-cyanoindole would result in the formation of a series of mixed co-trimers containing both amino and cyano groups. The presence of the faster reacting and more lyophobic cyano groups was predicted to increase the rate of formation and decrease the rate of desorption of the mixed cyano:amino co-trimers.

It was found that it was necessary to carry out this electro-co-polymerisation on top of a thin pre-formed poly(CI) coat as the presence of even a small amount of 5-aminoindole monomer was found to passivate the surface of a clean platinum electrode sufficiently enough to disrupt the electropolymerisation reacton.

The current-time transients of the copolymerisation of 20mM 5-aminoindole and 20mM 5-cyanoindole is shown in fig. 6.13. The current-time transient for the formation of the poly(CI) under-coat is also shown in fig. 6.13. These transients record the total amount of charge passed at the disc electrode for the poly(CI) and cyano:amino copolymer formation.

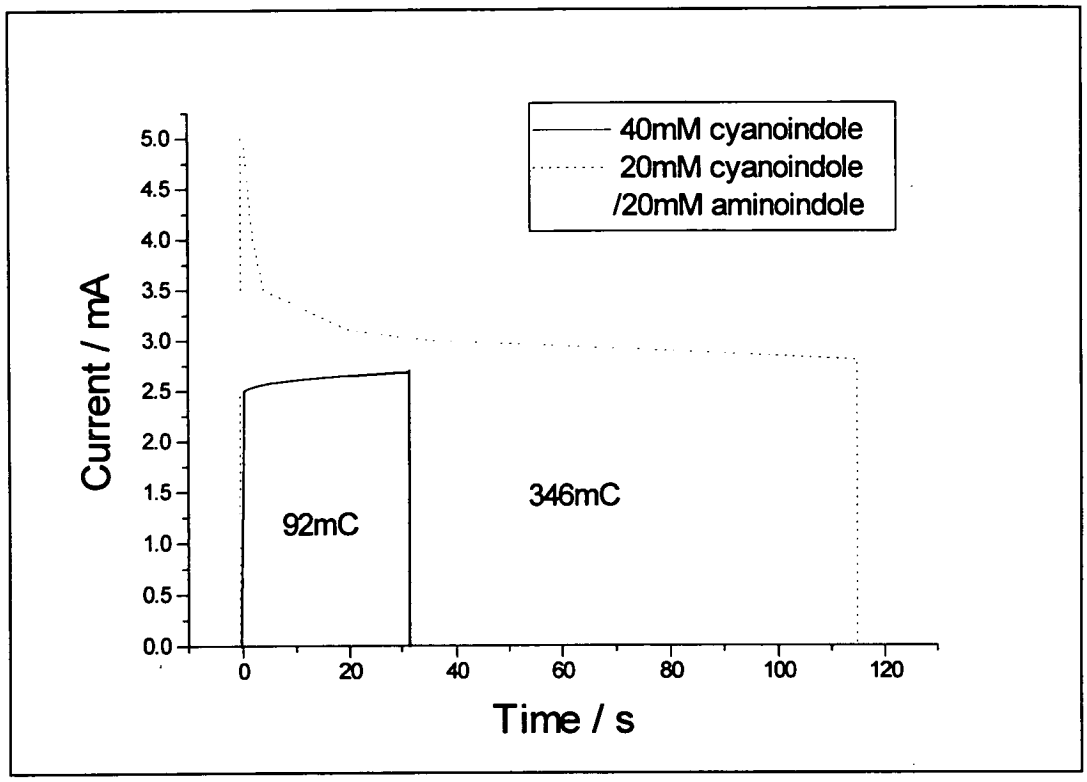

Fig. 6.13 - Current-time of copolymerisation of 20mM/20mM Amino:cyano and of poly(CI) undercoat. (Disc potential = 1.64V)

A Cyclic voltammogram of the poly(CI) film and the amino:cyano copolymer on top of the poly(CI) film formed after the current-time transient in fig. 6.13 was recorded is shown in fig. 6.14.

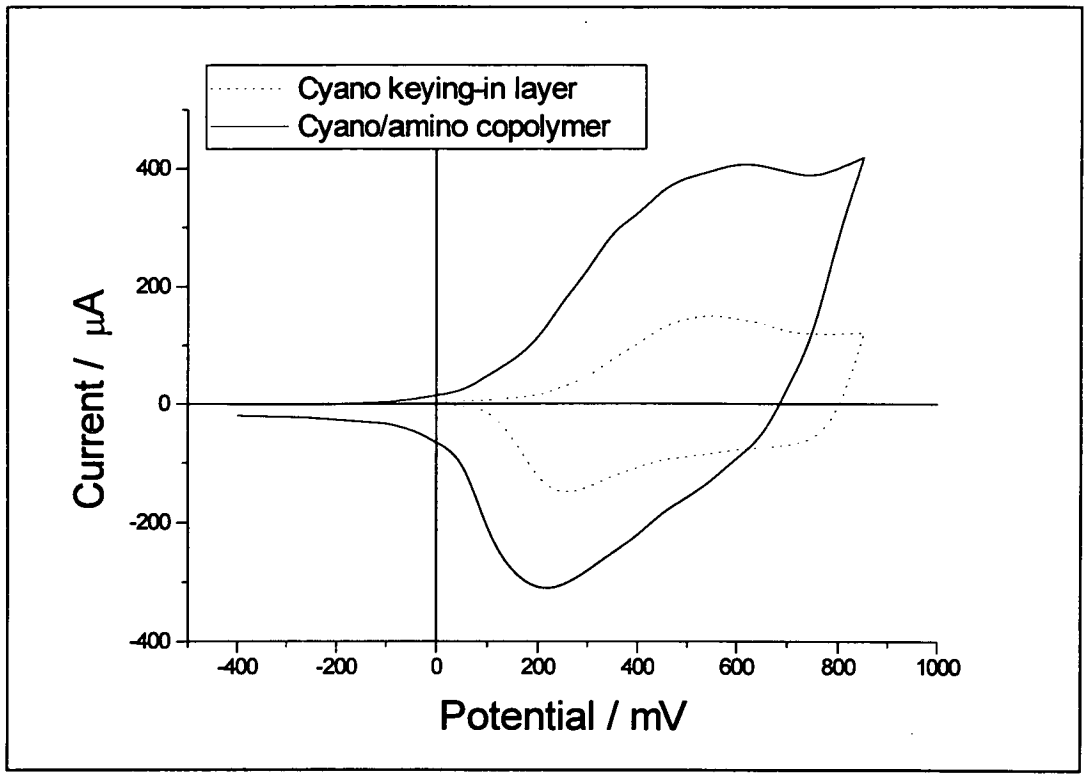

Fig. 6.14 - CVs of film poly(CI) undercoat and the copolymer produced from 20mM 5-cyanoindole / 20mM 5-aminoindole on the poly(CI) film. Sweep rate = 10mV/s.

The charge passed in the current-time transient (fig. 6.14) of the electro-co-polymerisation was compared with the amount of charge under the cyclic voltammogram of the resultant copolymer film produced at a number of different starting monomer concentrations of 5-cyanoindole and 5-aminoindole. It was found that the most efficient concentration range for the deposition of the copolymer was 20mM 5-cyanoindole to 20mM 5-aminoindole. In this case efficiency refers to the amount of charge in the CV of the polymer film compared with the amount of charge passed to form the polymer. The charge passed in forming the copolymer is due to the electrons passed in the oxidation and linking of the monomers and trimer to form polymer. The charge passed in the CV of the polymer is due to the electrons passed in the one electron redox reaction of the trimer units in the polymer. Therefore for free trimer, a 100% efficient electropolymerisation would be expected to lead to $1/7^{th}$ of the charge in

the CV of the polymer compared with that in forming it. For a fully linked polymer, a 100% efficient reaction would lead to $1/9^{th}$ of the charge in the CV compared with that of the polymer. Therefore the maximum efficiency observed would be expected to be between 11.1% and 14.3%. It has been found that the electropolymerisation of poly(CI) shows an efficiency of around 14 %.

The 20 / 20 cyano:amino copolymer had an efficiency of 5.5% of the charge in the CV of the copolymer film (fig. 6.14) compared with the charge passed to form the film in the current-time transient (fig. 6.13). This can be compared to efficiencies of less than 1% for the copolymer film produced from a solution of 40mM 5-aminoindole / 40mM 5-cyanoindole and less than 0.2% for the copolymer film produced from a starting solution of 100mM 5-cyanoindole /100mM 5-aminoindole.

6.4.2 - Copolymerisation of 5-aminoindole with I5CA.

It was decided to extend the copolymerisation studies to the copolymerisation of 5-aminoindole with indole-5-carboxylic acid. Similar experiments to that in section 6.4.1 were carried out to study the effect of concentration of the monomers with efficiency of deposition. The most efficient concentration range for the deposition of an I5CA:5-aminoindole copolymer film was again found to be 20mM for both monomers. This had an efficiency of approximately 3% for the electropolymerisation charge passed compared with the charge remaining on cycling the deposited film. Fig. 6.14 shows a CV of a copolymer produced by the electrocopolymerisation of 20mM 5-aminoindole and 20mM I5CA at 1.46V.

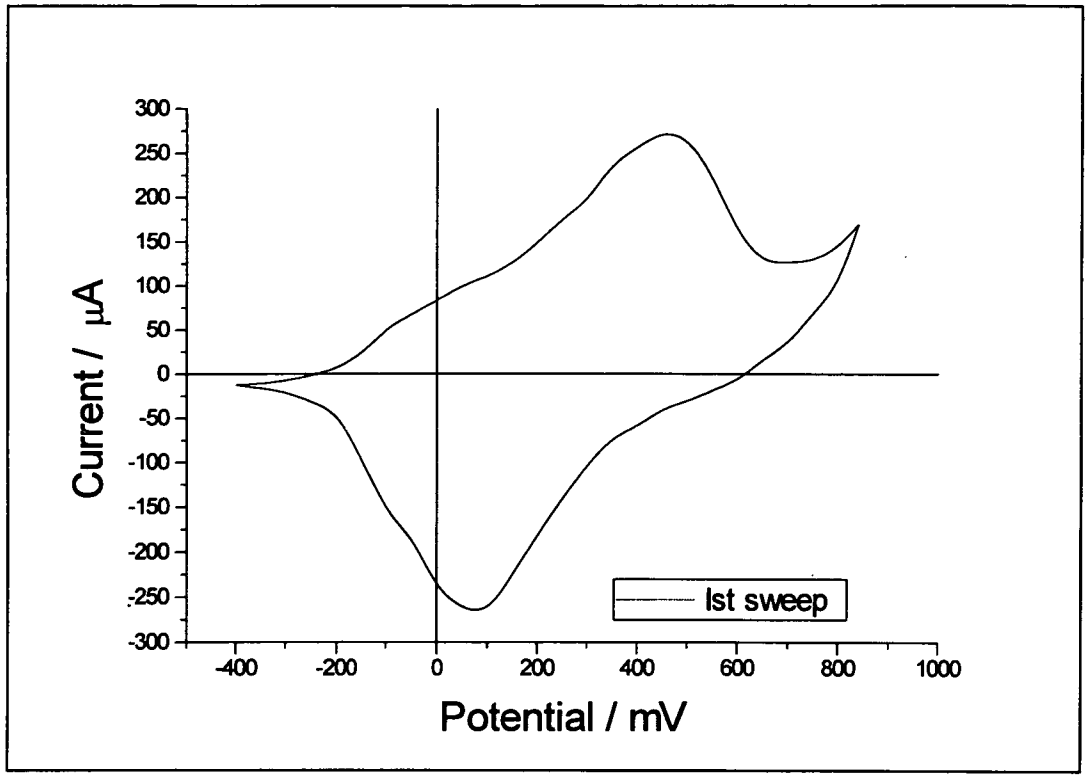

Fig. 6.15 - CV of copolymer of 20 / 20 amino:I5CA. Sweep rate = 10mV/s.

It can be seen that the first sweep of the amino:I5CA copolymer is very similar to a poly(I5CA) film that has been cycled around until a steady state has been reached. The 1st CV of a poly(I5CA) is generally found as that shown in fig. 6.15, as it is cycled, over typically a few days, it gradually develops in to a very similar CV that is shown by the 1st sweep of the I5CA:amino copolymer (fig. 6.15). This is suggested to be due to the increased lyophilicity of the amino:I5CA copoymer film which allows a much faster uptake of solvent by the film and is evidence to confirm the prescence of amino groups in the copolymer film.

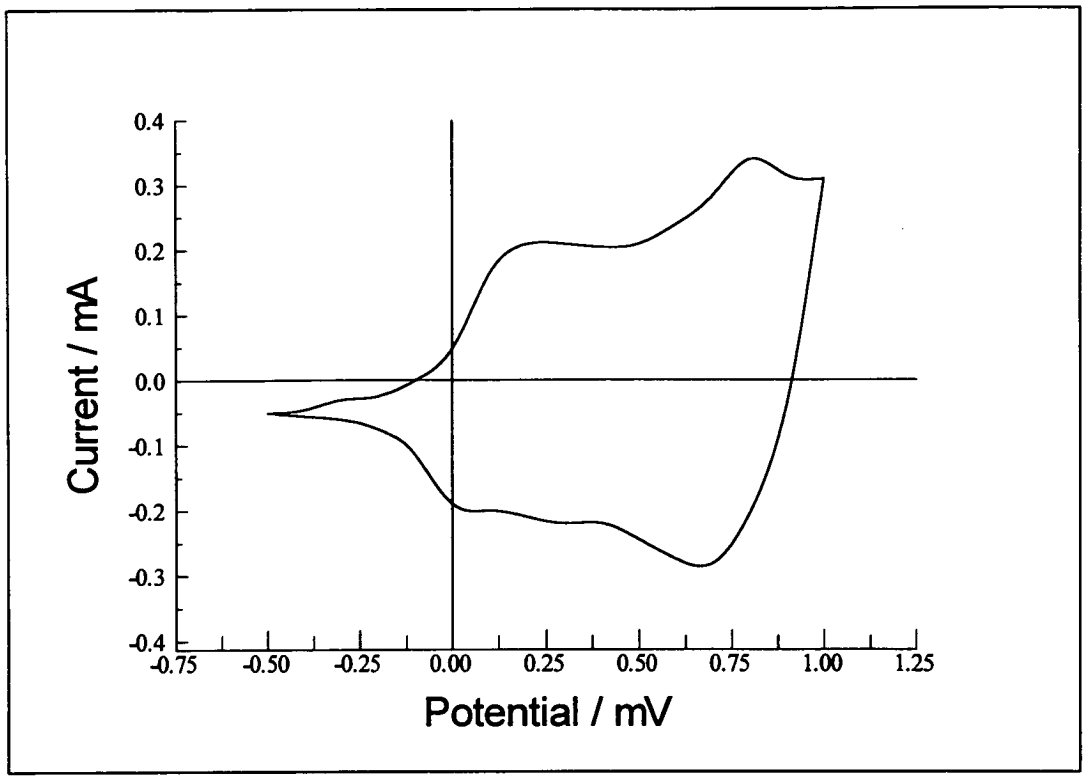

Fig. 6.16 - CV of Poly(I5CA) - 1st sweep. Sweep rate = 10mV/s

6.5 - pH studies.

To obtain further evidence that these copolymer films contained 5-substituted amino groups, it was decided to carry out some aqueous pH studies on these copolymer films. Previously linear sweep voltammetry studies on poly(I5CA) have reported a change in the polymer E^0 value, the standard potential of the polymer redox reaction, with a change in pH of the aqueous background electrolyte solution. Bartlett *et al*[119] originally attributed this effect to a "self-doping" reaction of the carboxylic acid groups. Self-doping arises when the charge on the polymer backbone is compensated by induced charges on the substituent. In this case the poly(I5CA) polymer backbones' positive charge being compensated by the negative charge from the dissociated carboxylate groups.

Later studies however, reported a similar pH dependence for poly(CI) and poly(indole)[112] which do not contain substituents which can undergo self-doping. It was therefore concluded that the pH dependence observed in poly(CI), poly(I5CA) and poly(indole) was solely dependent upon the redox process due to the loss of a proton from the free indole ring N-H functional group. In this work the polymers were studied potentiometrically, it was found that poly(CI) and poly(indole) have a potential shift of approximately -60mV per pH unit between the pH values of 2 and 10, fig. 6.16.

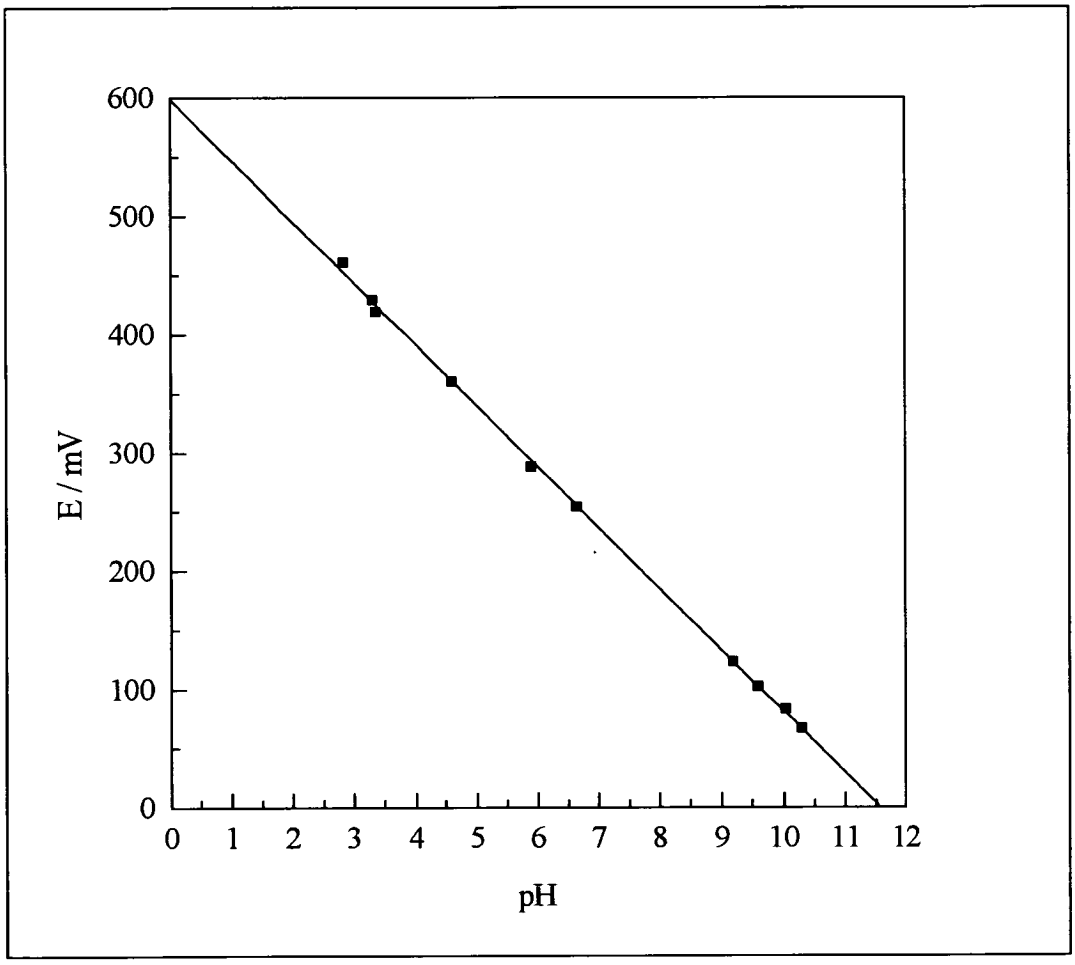

Fig. 6.17 - Plot of pH of aqueous solution vs E of poly(CI) film[112].

This behaviour was attributed to an equal ratio of protons to electrons being transferred in the polymer redox reaction, Equ^{n} 6.2.

$$[\text{Trimer}]_{red} \Leftrightarrow [\text{Trimer}]_{ox} + H^+ + e^- \qquad \text{--- Equ}^n\ 6.2$$

As $$E = E^\theta + \frac{RT}{F}\ln\frac{[H^+][\text{Trimer}]_{ox}}{[\text{Trimer}]_{red}} \qquad \text{--- Equ}^n\ 6.3$$

Then $$E = E^\theta - \frac{2.303RT}{F}pH \qquad \text{--- Equ}^n\ 6.4$$

$$E = E^\theta - 0.06pH \qquad \text{--- Equ}^n\ 6.5$$

Thus the poly(CI) was found to follow Nernstian behaviour. The proton lost in this redox reaction was believed to have come from the relatively labile indole ring N-H functional group. It can be seen that the proposed structure of these polymer films is consistent with this redox reaction as each linked trimer unit has one free indole N-H group remaining, fig. 6.18.

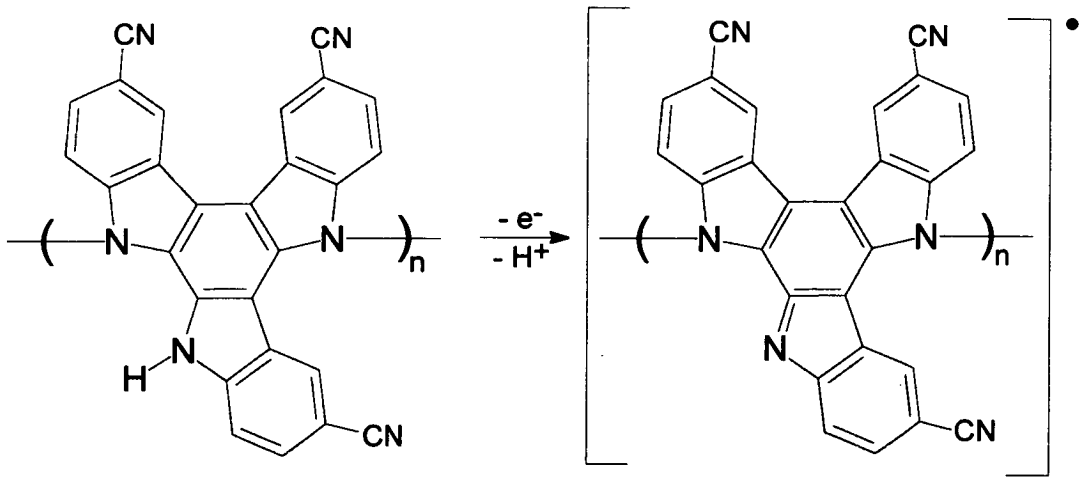

Fig. 6.18 - Poly(5-cyanoindole) redox reaction.

A very similar Nernstian response where a slope of -60mV per pH unit was observed for poly(indole). Studies undertaken on poly(I5CA), however, showed a markedly different response, fig. 6.19.

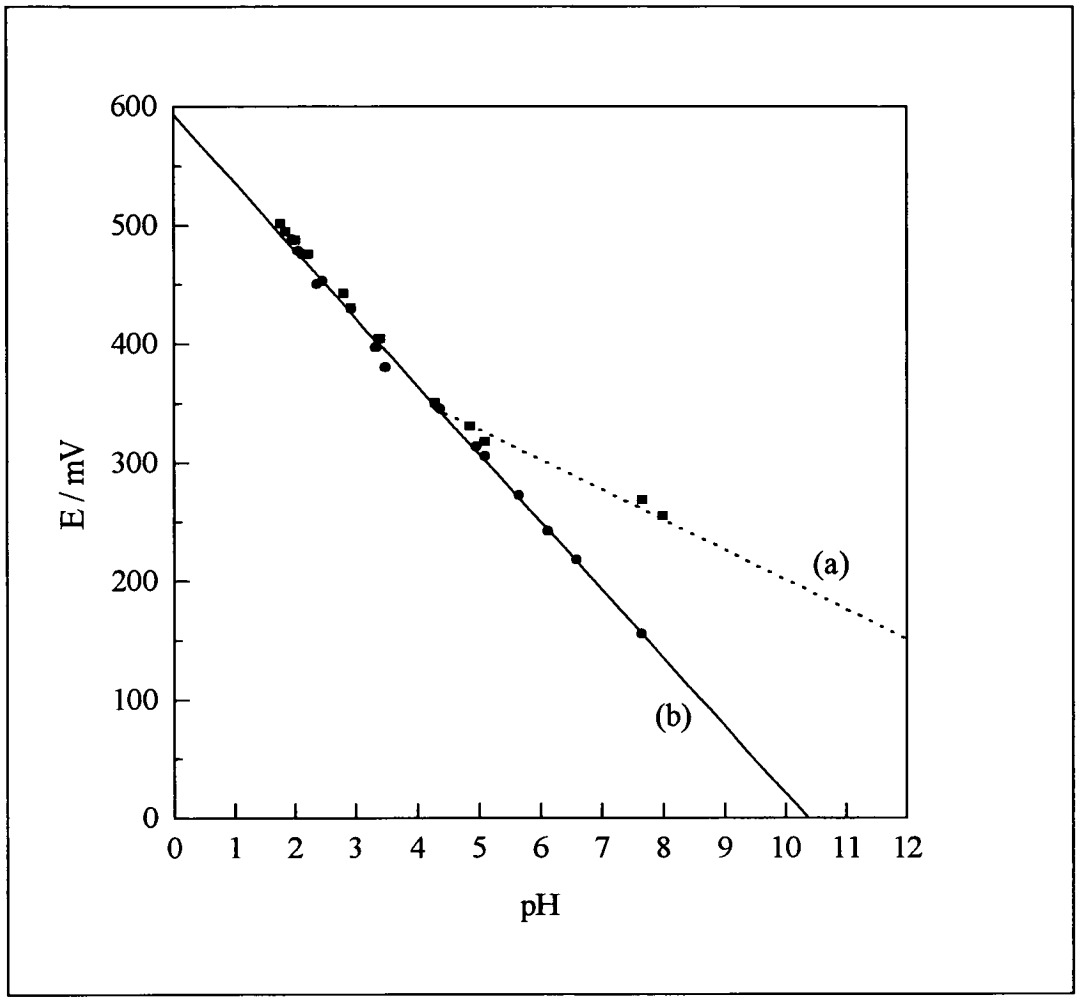

Fig. 6.19 - Plot of E *vs* pH for poly(indole-5-carboxylic acid). (a) with with no $PbCl_2$ added, (b) with $PbCl_2$ added.

The pH response of poly(I5CA) shows a similar one electron / one proton redox response to that observed for poly(CI) and poly(indole) up to a pH of approximately 4.2. On increasing the pH above 4.2, there is a break in the -60mV gradient to a lesser gradient. This was explained by the presence of the carboxylate groups, the break in gradient being due to the dissociation of the carboxylate groups. In the pH of 1 to 4.2, it was assumed that all the carboxylic acid groups would remain undissociated and the redox reaction is that found for poly(CI). In this pH range the electroneutrality is maintained in the layer by proton loss from the indole N-H group. At the pK_a for the acid group (in this case approximately 4.2), dissociation of the protons would take place with the result at higher pHs, the substituents are present as carboxylate anions. The indole N-H

the substituents are present as carboxylate anions. The indole N-H protons lost above a pH of 4.2, were suggested to re-protonate the carboxylate groups in the trimers, hence, as not all of the protons were lost from the polymer layer as a whole, there was a reduction in the gradient of the observed potential response. Lead ions are known to complex carboxylic acid groups[139], so lead ions were added to the solution to examine whether the complexation of the carboxy groups would stop the partial proton buffering effect of the carboxy groups. Indeed it can be seen that after the addition of lead, the pH response looks identical to that of poly(CI), i.e. the carboxy groups are complexed and the Nernstian potentiometric behaviour of the labile indole N-H group is restored.

All these pH studies on the poly(CI), poly(I5CA) and poly(indole) were carried out in aqueous electrolyte. It was found that it was necessary to transfer very slowly the polymer films produced in the electropolymerising acetonitrile solution in to the aqueous solution containing NaCl as an electrolyte. This was achieved by adding dropwise the 0.1M NaCl to the acetonitrile until around 90% of the solution was water. The polymer films could then be transferred in to a solution of pure 0.1M NaCl/H_2O. If this process was not carried out, the film would often peel off the electrode as soon as it was placed in the aqueous solution.

6.5.1 - pH studies of 5-aminoindole films.

It was clear from the pH studies described above that pH variations due to both the carboxylic acid groups, and the indole N-H groups could be detected. It was therefore thought possible that 5-substituted amino groups on an amino trimer or co-trimer would also show a pH-potential response. It was therefore decided to electropolymerise a number of 5-aminoindole copolymer films using a pre-formed poly(CI) or poly(NI) layers, and examine their pH response. A differing pH response to that observed for pure poly(CI) or poly(I5CA) would suggest the presence of 5-amino groups in the polymer film.

6.5.1.1 - pH response of 5-aminoindole:5-cyanoindole copolymer.

It was decided to first study the pH response of an amino:cyano indole copolymer which was produced from a solution containing 20mM 5-aminoindole and 20mM 5-cyanoindole. The copolymer was than slowly transferred in to an aqueous solution containing 0.1M NaCl as described in the experimental section.

The layer was allowed to equilibrate overnight and then the potential of the film, while passing zero current, was monitored with changes in the pH of the aqueous electrolyte. The pH of the solution was kept at a constant value by the addition of HCl and NaOH. The potential response to changes in the pH of the aqueous solution of this film is shown in fig. 6.20.

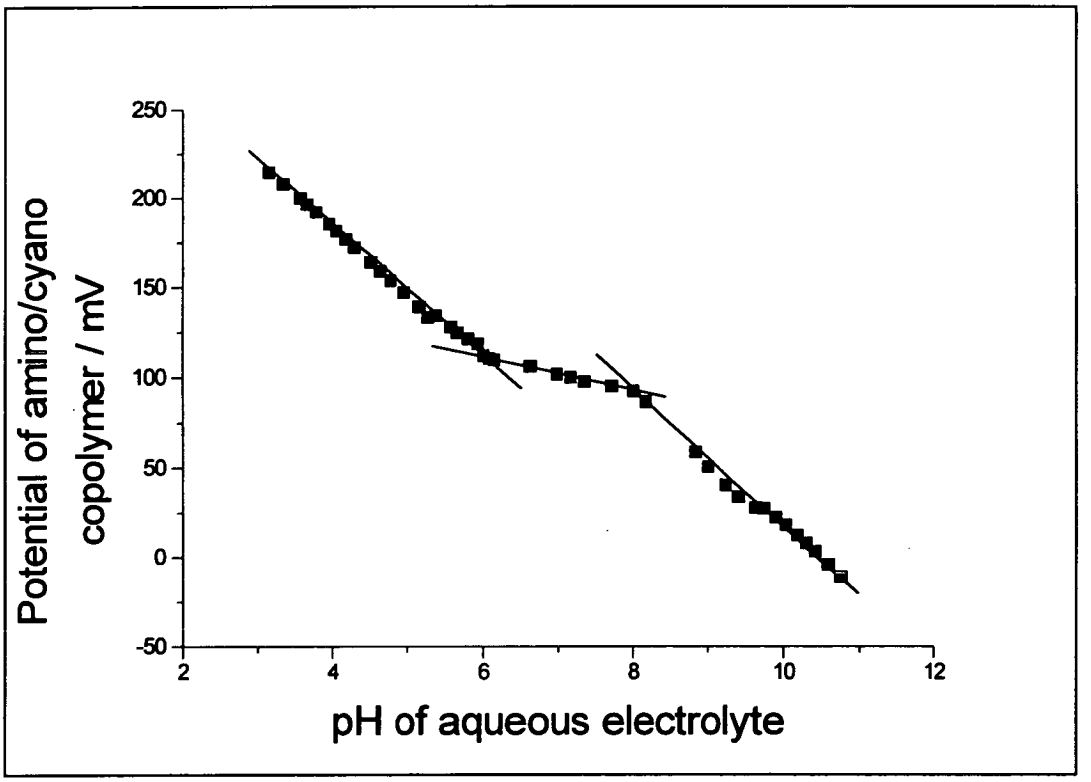

Fig. 6.20 - E *vs* pH of 20mM/20mM amino:cyano copolymer film.

It can be seen that there is a difference in this response to that observed for a pure poly(CI) film (fig. 6.17). This is suggested to be due to the presence of the amino groups covalently bound to linked co-trimers in the polymer film.

6.5.1.2 - Likely structure of the cyano:amino copolymer film.

Before an explanation of the potentiometric pH response of these films is proposed, it is helpful to reiterate what the structure of these films was likely to be. As the copolymer films were produced from solutions containing an equal amount of the two monomers, and the potential was set to ensure oxidation of all the monomers arriving at the electrode surface, it would be expected that an equal amount of each of the two monomer radical cations would be generated at the electrode surface. As the trimer formation was believed to involve statistical coupling of adsorbed monomer radical cations[150], the polymerisation was expected to be a first order reaction. Therefore on statistical grounds, it would expected that a series of mixed and unmixed co-trimers would form in the following ratio :-

Co-trimer-(5-substituents)	Ratio
Trimer-3(CN)	1
Co-trimer-1(CN),2(NH_2)	3
Co-trimer-2(CN),1(NH_2)	3
Trimer-3(NH_2)	1

This assumes the coupling is similar to that observed for the copolymerisation of 5-cyanoindole and 5-carboxyindole[112] This study found that the 5-cyanoindole and I5CA trimers and co-trimers were insoluble. The i_∞ value, which describes the rate of reaction of the monomers on the surface of the electrode was found to be 20mA for cyanoindole and 10mA for I5CA, i.e. I5CA radical cation monomers link at half the rate of the 5-cyanoindole radical cations on the electrode surface. This may have been expected to cause a skew in the statistical

distribution towards having more trimers containing cyano substituents, however the relative amount of the co-trimers observed followed the statistical distribution. This suggests that the rate of reaction of the monomers on the surface does not greatly affect the distribution of the trimers formed, as once adsorbed, trimerisation must occur to form a new adsorption site. Thus the relative reactivity of the trimers does not control the amount of trimer formed. It is is proposed that this mechanism of copolymerisation can also be applied to the amino - copolymer layers.

For the copolymerisation of 5-aminoindole and 5-cyanoindole however, there would be expected to be a skew towards trimers containing more cyano substituents in the film, as the solubility of the amino groups would be expected to cause most of the trimers containing 3 amino groups to desorb off the electrode surface and link to form polymer. Similarly any co-trimers formed containing two amino and one cyano groups would be expected to be more soluble than one amino or no amino co-trimers, with the majority desorbing from the electrode. From this consideration alone, there would be expected to be a large skew towards the film containing co-trimers with mostly cyano groups.

From the above arguments, it would therefore be expected that the amino:cyano and the amino:I5CA copolymers formed above would contain a majority of co-trimers with 2 cyano substituents and one amino substituent, with a lesser amount of tri-cyano substituted trimer. There may also be a very small amount of co-trimers containing two amino and one cyano groups. The following suggestions, to explain the pH-potential response that occurred in these films, are based on reactions of what was expected to be the majority co-trimer in the film, i.e. a co-trimer containing two cyano (or carboxy) substituents and one amino substituent.

The observed response in fig. 6.19, can be explained by consideration of the amino groups present in the copolymer film. The copolymer will contain both oxidised and reduced trimers as the 5-aminoindole monomer in the electropolymerising solution reduces much of the polymer as the oxidation potential of the 5-aminoindole monomer is lower than that of the redox potential for the trimers present. In addition to

this, the pK_a of most amino groups is around 9, so at a pHs lower than the pK_a of the amino groups, all the amino groups would be expected to be protonated. Thus in the pH range of 2 to 6 both the reduced and the oxidised co-trimers in the copolymer film would be expected to contain $-NH_3^+$ groups (fig. 6.21).

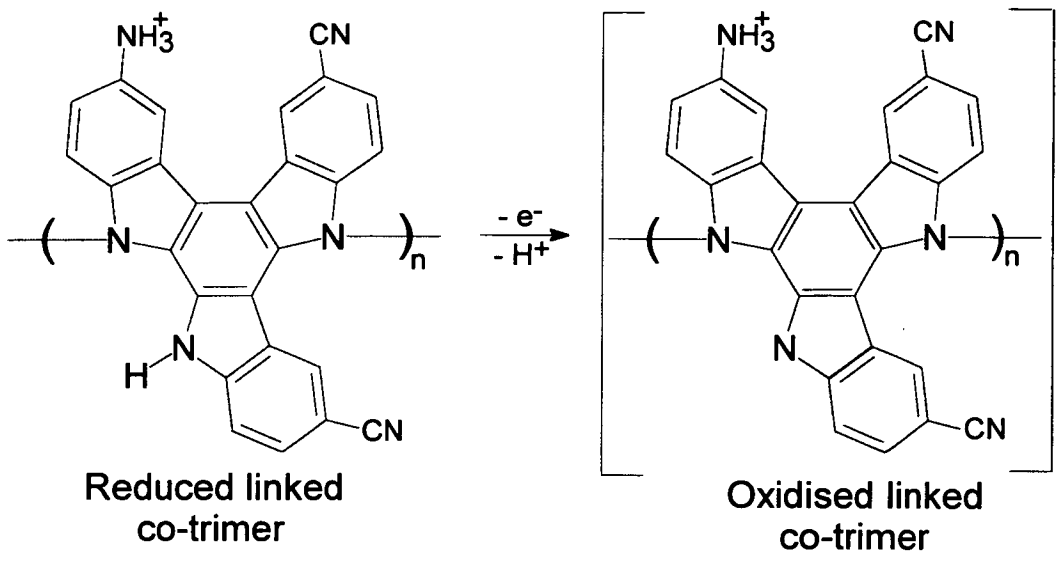

Fig. 6.21 - Redox reaction below a pH of 6.

As the pH is steadily increased, a pH response is noted which is suggested to have been due to the loss of protons from the indole ring N-H groups in the reduced co-trimers in the polymer film, similar to the response observed for poly(CI). The oxidised co-trimers present do not undergo any change in this pH range, but contain fully protonated 5-amino groups.

When the pH of approximately 6 is reached (where the first break in the gradient is observed) it is suggested that the $-NH_3^+$ group on the remaining reduced co-trimers reaches its pK_a and therefore deprotonates to form an NH_2 group. The oxidised co-trimers remain with protonated NH_3^+ groups. This is shown schematically in fig. 6.22.

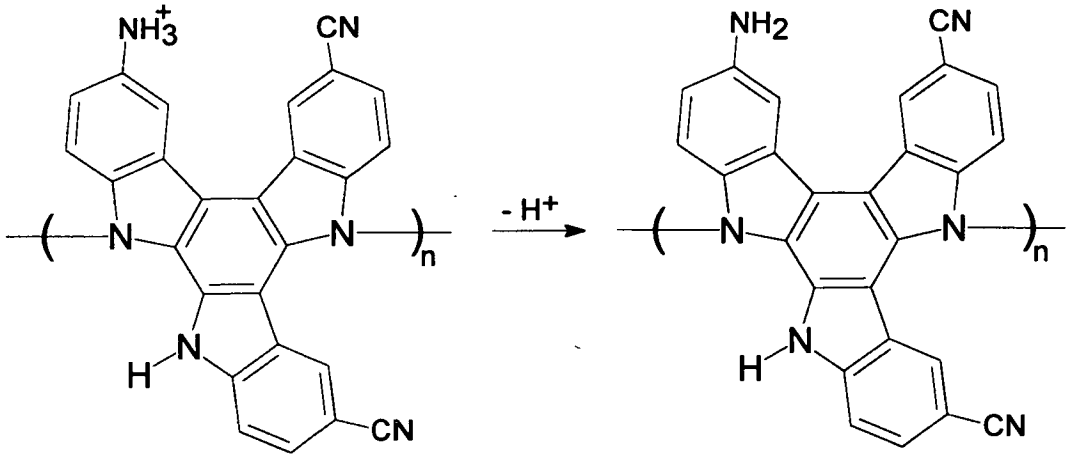

Reduced linked co-trimer

Reduced de-protonated linked co-trimer

Fig. 6.22 - Deprotonation reaction at pH of 6

In support of this from the Hammett plot (fig. 4.16), it is clear that the $-NH_2$ group is electronically coupled to the redox centre of the film, therefore it would be expected that the oxidised form would have a lower electron density in the Nitrogen atom of the 5-substituent, and hence a lower pK_a. In the low gradient region, between the pHs of 6 and 8, there is obviously very little change in film potential with a change in pH. This is suggested to be due to the reaction where any redox proton lost from the indole ring N-H group protonates the amino group on that or a neighbouring reduced co-trimer. This is shown schematically in fig. 6.23. As no protons are lost from the film as a whole, the Nernst Equation will show no pH dependence with this reaction which explains the almost zero gradient noted in this pH range.

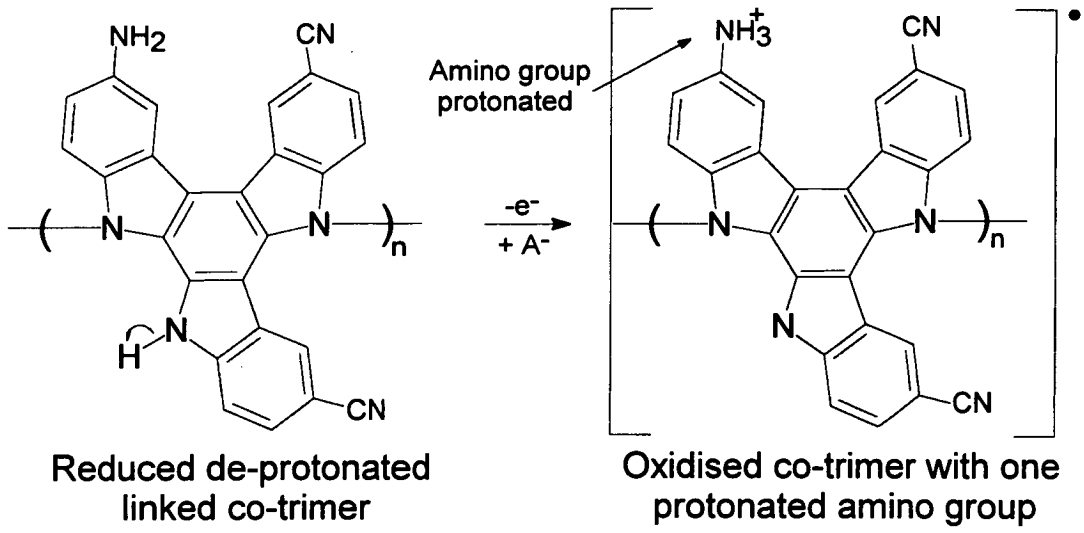

Fig. 6.23 - Redox reaction between pH of 6 and 8.

On reaching the pH of approximately 8 (the pK_a of the reduced species, the proton is lost from the amino group of the oxidised co-trimers, forming co-trimers that are oxidised and contain deprotonated NH_2 groups. The proposed reaction at the pH of approximately 8 is shown in fig. 6.24.

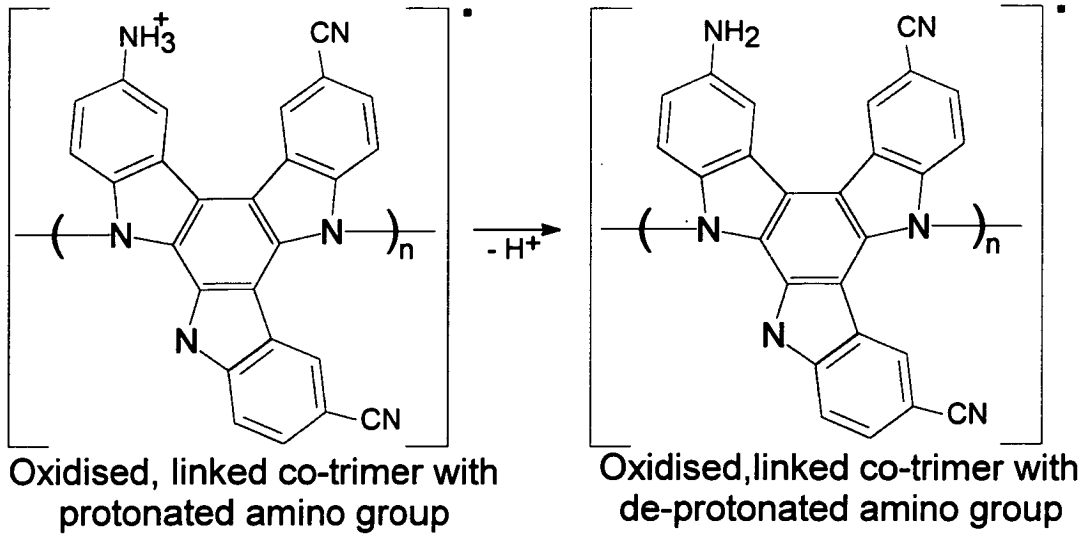

Fig. 6.24 - Redox reaction at pH of 8.

Above a pH of 8, it can be seen that there is again a pH dependence with a slope approaching that of 59mV. This is indicative of a transfer of one electron and one proton. This is suggested to be due to the indole ring N-H proton being lost and leaving the polymer film. Above the pH of eight, the pK_a of the amino groups is passed, so the N-H indole ring proton lost leaves the polymer film without reprotonating the NH_2 groups. The proposed redox reaction above the pH of 8 is shown in fig. 6.25.

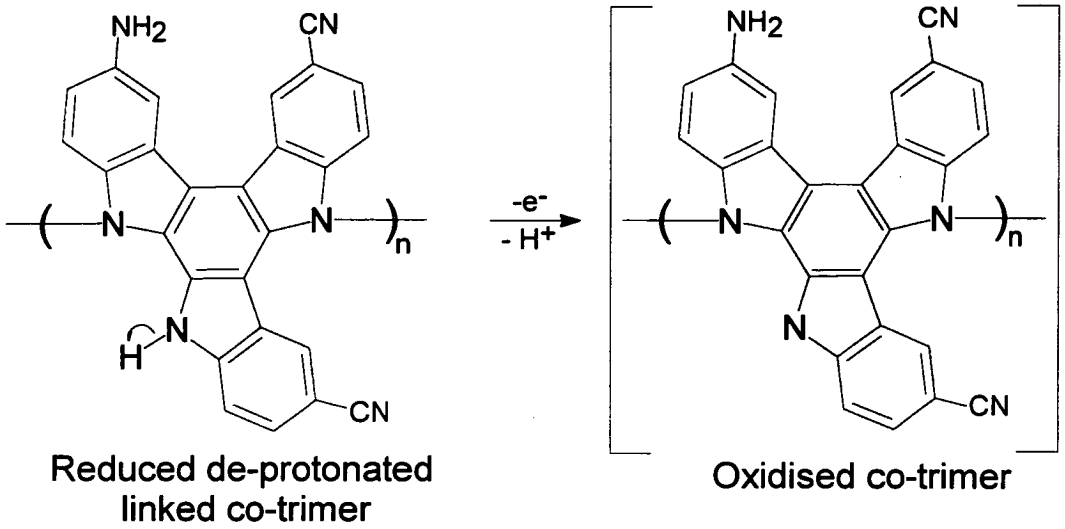

Reduced de-protonated linked co-trimer

Oxidised co-trimer

Fig. 6.25 - Redox reaction above pH of 8.

6.5.1.3 - pH response of cyano:amino copolymer containing low concentrations of amino groups.

The above picture of what is occurring in the cyano:amino copolymer film as the pH of the electrolyte is changed, is obviously simplified, as co-trimers containing two amino groups were expected to also be present, albeit in a smaller amount. It was therefore decided to attempt to form a copolymer from a solution containing 40mM cyanoindole and 1mM aminoindole monomer. At these concentrations, the greatest majority of trimers formed would be expected to be tri-cyano trimers with a much smaller amount of co-trimers containing one amino and two cyano groups also formed. On purely statistical grounds, trimers containing two

and three amino groups were not expected to form. The potential response of this copolymer film to changes in aqueous pH is reproduced in fig. 6.26.

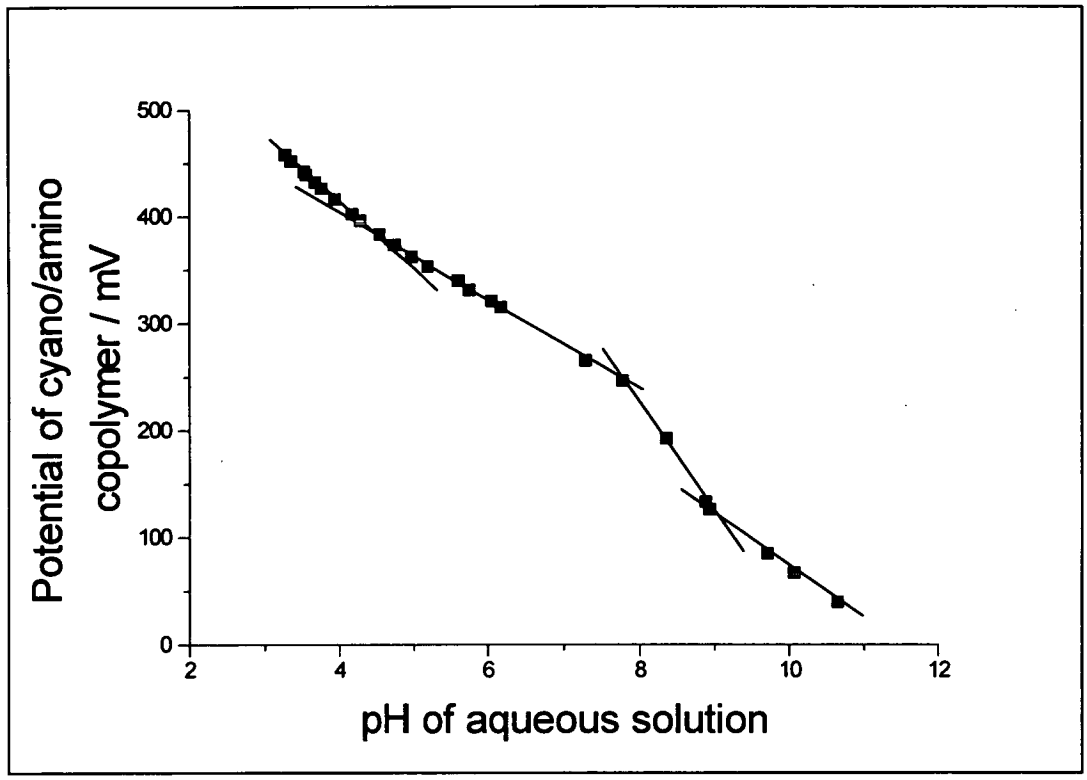

Fig. 6.26 - 40/1 cyano:amino copolymer E vs pH response.

It can be seen that this copolymer film shows four regions of response. This can be explained by the small amount of amino groups present in the copolymer film. At pHs lower than 4, a potential response is noted for the loss of a proton and electron from reduced trimers (similar to fig. 6.21). At a pH between 5 and 8, the gradient becomes shallower due to the protonation of the small amount of amino groups. The gradient of this response is not as shallow in this pH region as that of the 20/20 amino:cyano copolymer, as there are not as many amino groups to buffer all the protons produced in the reactions and some of the H^+ produced are lost from the coat. The overall response will therefore have a large contribution from the tri-cyano substituted trimers and produce a potential response that is between that of poly(CI) and the 20/20 cyano:amino copolymer. In the pH range between 8 and 9, these amino groups

deprotonate, in addition to the continuing deprotonation of the indole ring N-H protons to give an overall potential response of approximately 100mV / pH unit. This indicates that more protons are leaving the coat than electrons passed. Above the pH of 9, all the amino groups are deprotonated and the reduced trimers continue to lose their indole ring N-H proton with one electron reverting to a Nernstian slope of approximately 59mV.

6.5.1.4 - Copolymer of I5CA and aminoindole.

It was decided to examine the pH-potential dependence of the copolymer produced from the electropolymerisation of 20mM I5CA and 20mM 5-aminoindole, fig. 6.27.

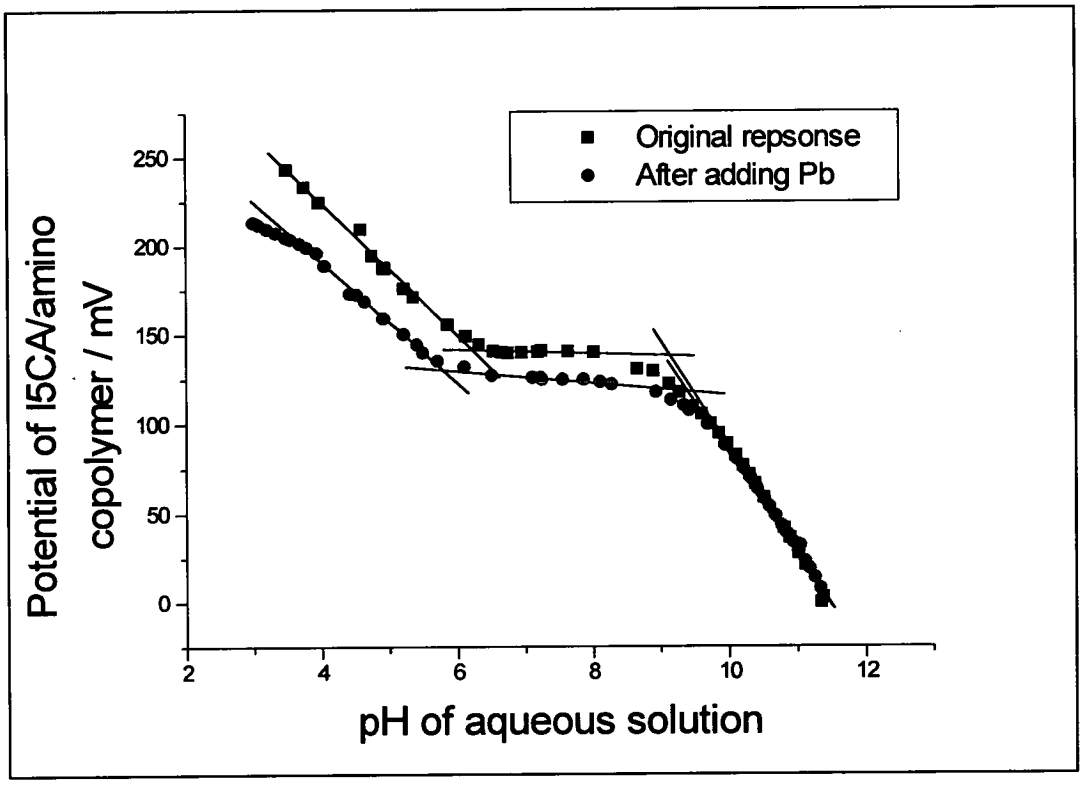

Fig. 6.27 - E vs pH response of 20mM/20mM I5CA:amino copolymer film.

It can be seen that the pH response is very similar to that for the cyano:amino copolymer although the intermediate section between the

pHs of 6 and 8 has a zero gradient whereas the copolymer produced from the electropolymerisation of 20mM 5-cyanoindole and 20mM 5-aminoindole, has a very shallow gradient in this pH range. At first sight this response was rather unexpected, as it was considered likely that the carboxylic acid groups present in the copolymer film would have a large contribution to the overall potential response, producing a potential response more similar to that observed for a pure poly(I5CA) film (fig. 6.19). It was decided to complex the carboxylic acid groups with the addition of lead ions and examine the pH response again to observe whether the pH response was affected. It can be seen that there is very little difference in the response after the addition of lead (fig. 6.26) which indicates that the carboxy groups are having very little effect on the pH-potential response of the film. It was therefore suggested that the amino groups were dominating the response. The observed response can therefore be explained by the same redox reactions that were suggested to occur in the 20/20 cyano:amino copolymer.

6.5.1.5 - pH response of aminoindole layer on top of poly(NI) layer.

It was decided to examine the pH-potential response of a film containing only 5-aminoindole trimers. 50mM 5-aminoindole was electropolymerised on top of a thin pre-formed poly(NI) layer and the potential response to changes in aqueous pH of the resultant bilayer measured (fig. 6.28).

It is reasonable to expect that the three amino groups in the same 5-aminoindole trimer would be affected by the presence of each other. For instance the protonation / deprotonation of one amino group was expected to affect the protonation / deprotonation of the other amino groups on the same trimer through electronic communication via the π-system. If this were the case then it was predicted there may be a shift of the observed pK_a to lower values with successive deprotonation, evident as a "spreading out" of the transitions between the different regions of potential response observed. However, the response observed was very similar to that observed for the 20 / 20 cyano:amino copolymer. The E vs pH response for this amino~nitro layer is shown in fig. 6.27. It contains three

regions associated with the protonation and deprotonation of the amino groups as described in figs 6.20 to 6.24. It can be seen that the response is qualitatively the same as that observed for the 20 / 20 cyano:amino and I5CA:amino copolymers. This suggests that the trimers containing three amino groups (as formed on top of the poly(NI) layer) undergo similar redox reactions to pH changes to co-trimers containing only one amino group. This may be an indication of the fact that once one amino group in a 5-aminoindole trimer undergoes protonation / deprotonation then the change in electron density on the amino group affects the other two groups and effectively prevents deprotonation. Although more likely, this result indicates that there are more than enough $-NH_2$ groups available to accept the H^+ lost from the indole N-H redox reaction.

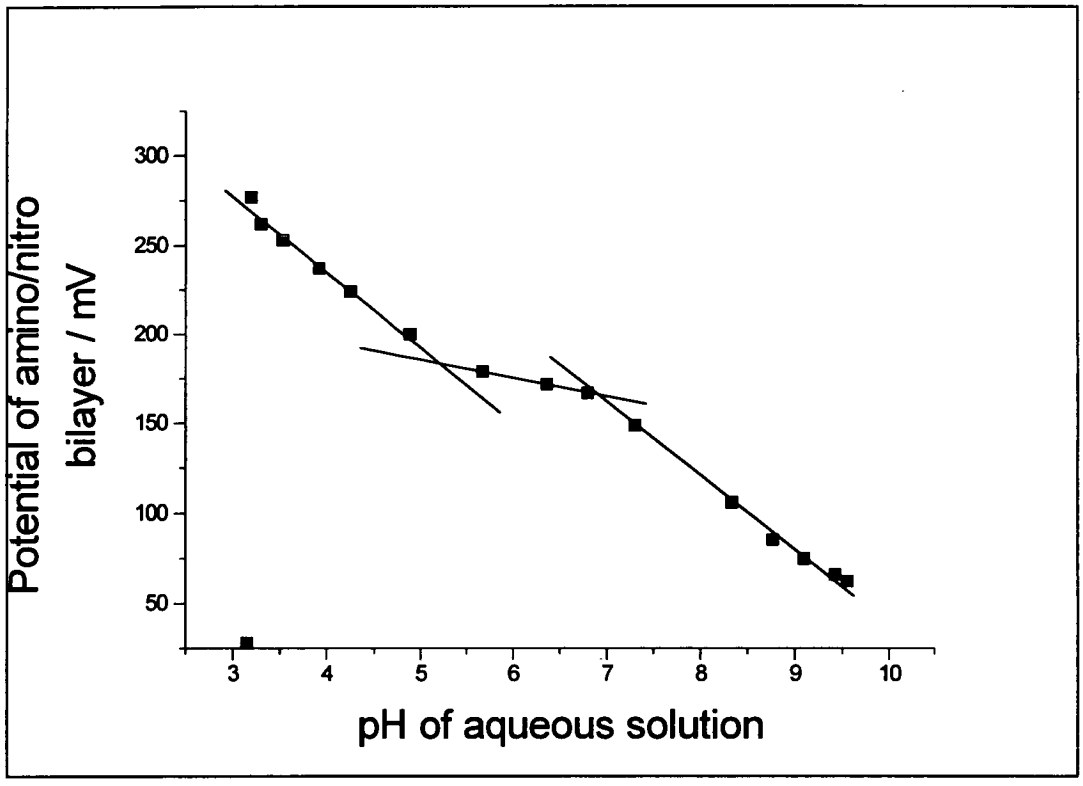

Fig. 6.28 - Potential response to changes in pH of electropolymerised 5-aminoindole on a poly(NI) layer.

6.6 - Conclusions.

This chapter has shown that 5-aminoindole can be electropolymerised or copolymerised on a pre-formed poly(CI) or poly(NI) layer to form an electrodeposited layer containing 5-aminoindole cyclic trimers or co-trimers. These layers show novel potential responses to changes in aqueous pH which can be explained by redox reactions of the amino groups and the indole N-H groups.

Chapter 7 - Copper ion sensor

7.1 - Introduction.

From the studies undertaken in the previous chapter, it was apparent that an electroactive polymer film containing amino groups could be formed by copolymerisation of 5-aminoindole with CI or I5CA. This was accomplished with the use of a pre-formed poly(CI) or poly(NI) layer to facilitate the formation and deposition of 5-aminoindole trimers and co-trimers. It was suggested that the amino groups in these copolymer films may be able to undergo co-ordination to certain metal ions. Chelation to metal ions has been observed by several other nitrogen containing ligands such as ethylenediamine[140] which is shown in fig. 7.1.

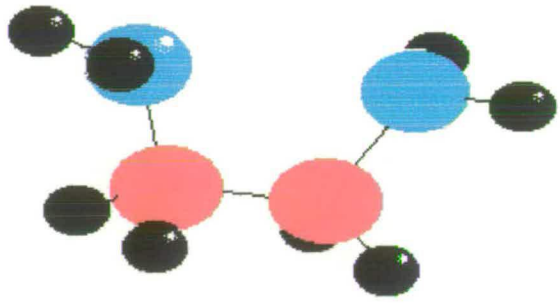

Fig. 7.1 - Ethylenediamine (en). Red = C, Blue = N, Black = H.

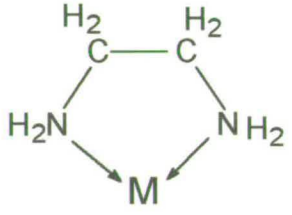

Fig. 7.2 - Metal chelation by en.

Ethylenediamine can co-ordinate to metal ions (fig. 7.2) through its ability to act as a π-acid, forming π-bonds with full metal d-orbitals and its vacant π^* orbitals[141]. It was thought likely that metal ions in an aqeuous solution would be able to permeate the amino copolymer film immersed in the solution, and that any chelation of the ions by the amino groups would result in a change in the redox potential of the layer which could be measured potentiometrically, producing a simple metal ion sensor device. This chapter describes work undertaken on similar amino group containing copolymers to those formed in the previous chapter, with the aim of developing such a metal ion sensing system.

Copolymer films were formed from the electropolymerisation of 5-aminoindole with both 5-cyanoindole and I5CA, and from the electropolymerisation of 5-aminoindole on top of a thin poly(NI) layer. The potential of these copolymer films was then monitored in a number of aqueous solutions containing 0.1M NaCl and varying concentrations of a large number of metal ions. These studies were undertaken at a constant pH as the results presented in the previous chapter showed that these films undergo potential changes with differences in pH. Changes in the pH of the solution would therefore complicate any potential changes observed due to chelation of metal ions. To accomplish this solutions of differing concentrations of the metal ions were prepared and pH adjusted to the same value. The copolymer coated electrode was then transferred between the different solutions of metal ions and the zero-current potential of the film recorded in each solution.

7.2 - Cyano:amino copolymer produced from a 40mM 5-cyanoindole / 1mM 5-aminoindole solution.

A copolymer film was produced from an electropolymerising solution consisting of 40mM 5-cyanoindole and 1mM 5-aminoindole resulting in the production of a copolymer film on the working electrode. The same method to that outlined in section 6.5.2.3 was used to form this copolymer. The first metal ion tested for this copolymer was $Cu(H_20)_6^{2+}$ ion which indeed showed a potential response.

7.2.1 - Potential response of copolymer to $CuCl_2$

The potential response of this film was then recorded in solutions consisting of varying concentrations of $CuCl_2$ in 0.1M NaCl / H_2O. The pH of these solution was held at a constant value of 4.3 by the addition of dilute HCl and NaOH as appropriate. The potential response versus the natural log of the [$CuCl_2$] is displayed in fig. 7.3.

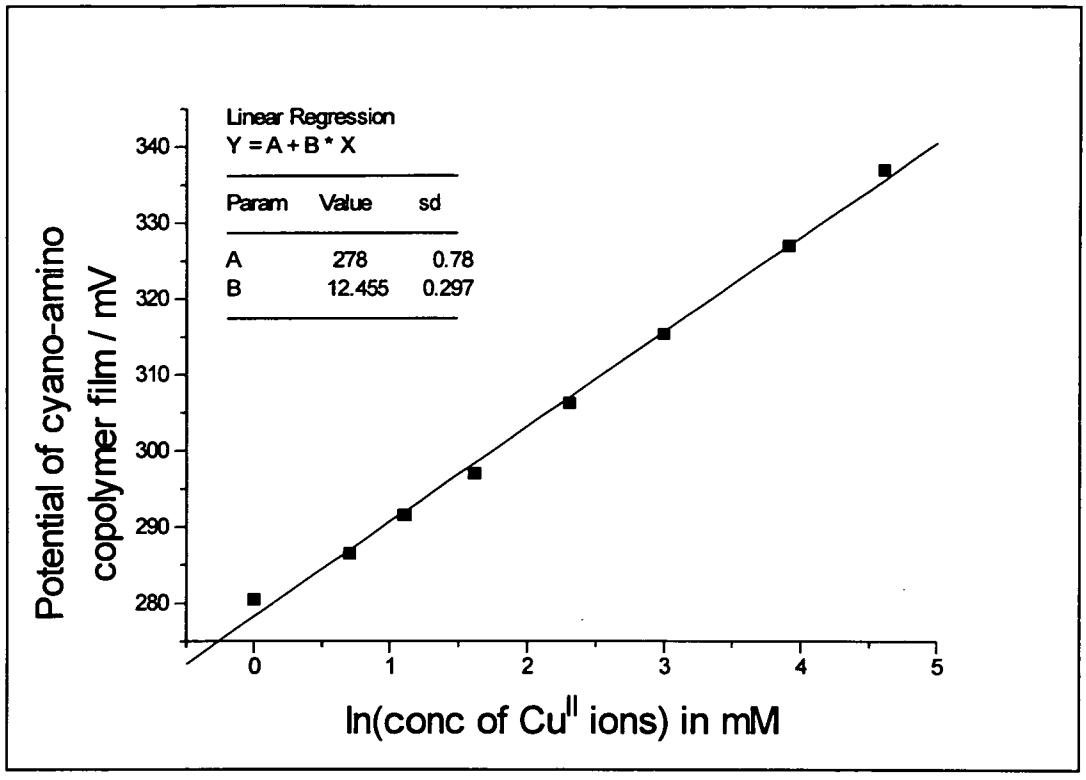

Fig. 7.3 - Potential *vs* ln[$CuCl_2$] for 40/1 Cyano:amino copolymer.

It can be seen from fig. 7.3 that the potential response to the $CuCl_2$ shows a good straight line of gradient 12.5 ± 0.6mV. It is suggested that this potential response is due to a redox reaction of the copolymer film due to chelation of the Cu^{II} ions at the 5-substituted amino groups.

7.2.2 - Control experiment - response of poly(Cl) to Cu^{II}.

It was thought likely that the observed potential response was due to Cu^{II} ions that had permeated the copolymer film and had undergone chelation with the amino groups. However, it was considered that the observed potential change may have arisen due to other factors, such as chelation of Cu^{II} at the indole N-H groups, or chemical oxidation of the copolymer film by the $CuCl_2$. To test that these factors were not controlling the potential response of the copolymer, a control experiment was carried out. This involved examining the potential response of a pure poly(Cl) film in identical aqueous solutions of $CuCl_2$ used in the copolymer experiments. However no potential changes of the poly(Cl) film were

observed with varying concentrations of $CuCl_2$. Both the amino copolymer and the poly(CI) film were expected to contain free indole N-H groups and have the possibility to undergo chemical oxidation; however as no potential response was observed, this suggests that the Cu^{II} ions were neither being chelated by the poly(CI) indole N-H groups nor were oxidising the poly(CI) film. This is good evidence to suggest that the potential response noted in the cyano:amino copolymer was not due to these factors and must have been due to the presence of the 5-substituted amino groups.

7.2.3 - Reasons for observed potential response in the cyano:amino copolymer film.

The results presented in chapter 6 showed that the cyano:amino copolymer produced from an electropolymerising solution of 40mM 5-cyanoindole and 1mM 5-aminoindole was expected to consist of mainly pure tri-cyano substituted trimers with a small amount of co-trimers containing two cyano and one amino groups. It is suggested that the reason for the observed response is due to the Cu^{II} ion undergoing bidentate chelation from two amino groups on neighbouring trimer units; this is shown in fig. 7.4.

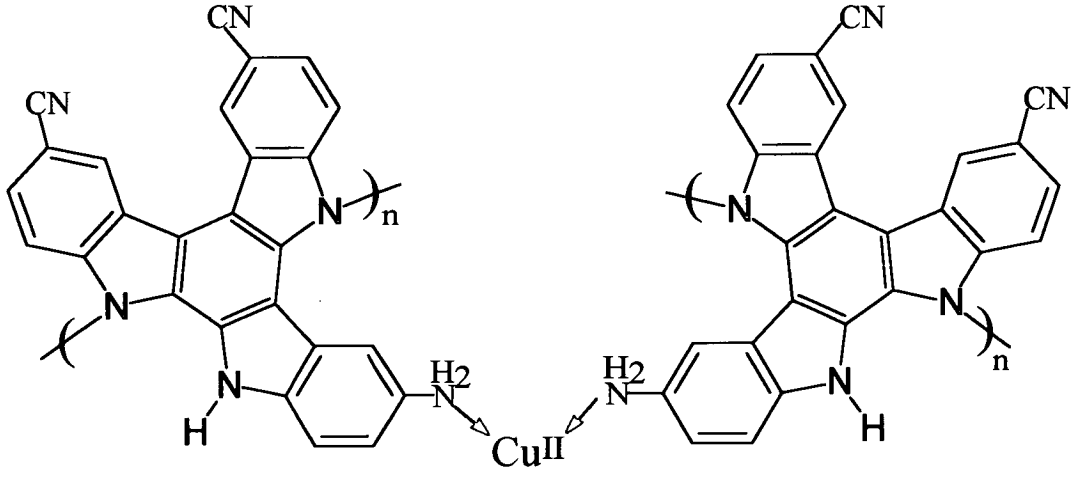

Fig. 7.4 - Chelation of Cu^{II} by amino groups on neighbouring amino:cyano co-trimers.

The chelation of Cu^{II} shown above in fig. 7.4 is suggested to undergo the following reaction :-

$$2[\text{Trimer-}(NH_2)]_{ox} + Cu^{II} + 2e^- \Leftrightarrow [2(\text{Trimer-}(NH_2))\text{-}Cu]^{2+}_{red} \quad \text{--- Equ}^n\ 7.1$$

The reason for the increased chelating ability of the reduced trimer over the oxidised trimer would again be the increased electron density at the Nitrogen atom of the 5-substituent.

The Nernst equation (neglecting activity coefficients, and assuming no effect due to Donnan potentials in the film) for this reaction is :-

$$E = E^0 + \frac{RT}{2F} \ln \frac{[\text{Trimer-}(NH_2)]^2_{ox}\ [Cu^{2+}]}{[2(\text{Trimer-}(NH_2))\text{-}Cu]^{2+}_{red}} \quad \text{--- Equ}^n\ 7.2$$

Which gives :-

$$= E' - \frac{RT}{2F} \ln\ [Cu^{2+}] \quad \text{--- Equ}^n\ 7.3$$

And :-

$$= E' - 0.0128 \ln\ [Cu^{2+}] \quad \text{--- Equ}^n\ 7.4$$

From the Nernstian theory presented above, this type of chelation of Cu^{II} would be expected to display a potential change of 12.8 mV per logarithmic decade of the concentration of Cu^{II}. The observed slope of 12.5 mV is within experimental error of this theoretical value and is good evidence that this type of bidentate chelation between two amino groups on neighbouring co-trimers is taking place. An alternative explanation is that the layer shows chelation of one Cu^{II} to one trimer unit, but that the response due to Cu^{II} ions is sub-Nernstain due to the interaction of trimer centres in the film. This can be dismissed because the pH response for

these layers discussed in the previous chapter was Nernstian and so the Cu^{II} response would also be expected to be Nernstian.

7.3 - Cyano:amino copolymer produced from 20mM 5-cyanoindole / 20mM 5-aminoindole.

A similar cyano:amino copolymer to that in section 6.5.1.1 was produced from a solution containing 20mM 5-aminoindole and 20mM 5-cyanoindole in background electrolyte. A number of solutions of differing concentrations of $CuCl_2$ in 0.1M NaCl were made up and pH adjusted to 4.3 with the addition of HCl and NaOH. As in the previous section, the pH of the solutions were held at a constant pH value to ensure that any potential changes noted in the film were not due to changes in pH. The amino:cyano copolymer film was then transferred to each of the $CuCl_2$ solutions in turn and the potential of the film recorded. The potential of the film was plotted against the ln [$CuCl_2$] and is reproduced in fig. 7.5.

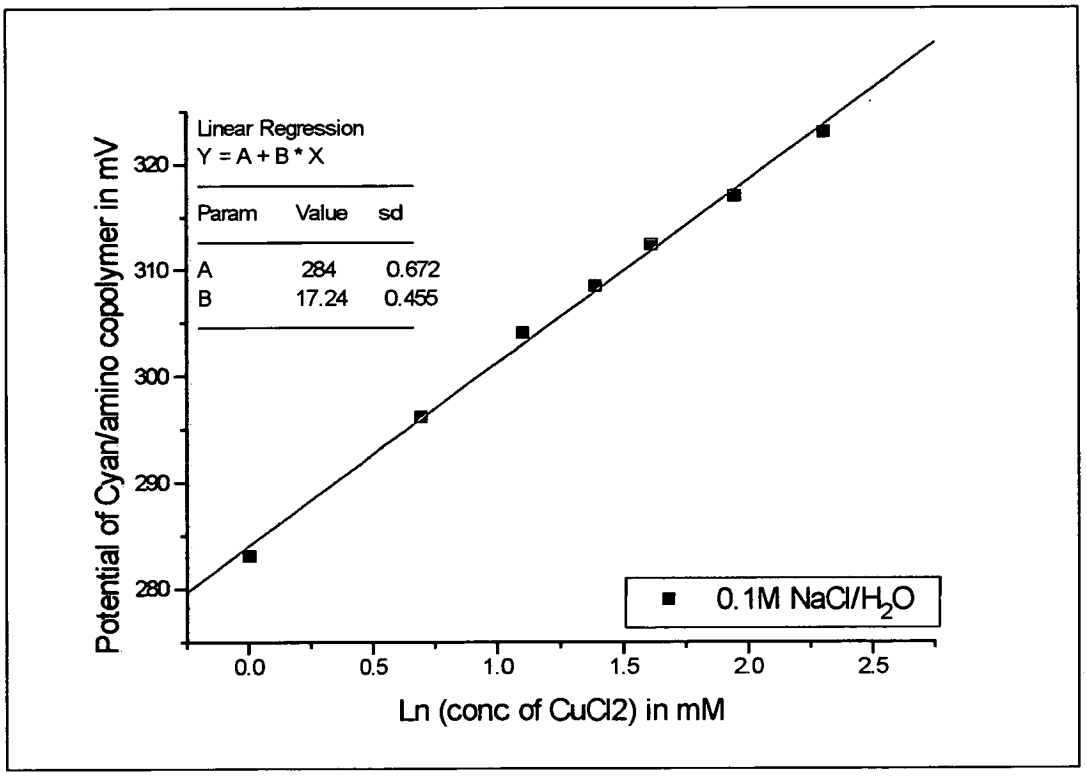

Fig. 7.5 - Potential *vs* ln[$CuCl_2$] response for 20/20 amino:cyano copolymer.

It can be seen that the potential response of the 20/20 cyano:amino copolymer to changes in the concentration of $CuCl_2$ shows a good straight line of gradient 17.2 ± 1 mV per ln decade. This gradient is somewhat higher than the 12.5mV slope observed for the 40/1 cyano/amino copolymer which contained only small amounts of amino groups. The higher gradient suggests that there is a different type of chelation taking place in the 20/20 cyano:amino copolymer. This was expected, as in chapter 6 it was suggested that a copolymer produced from a electropolymerising solution of 20mM 5-aminoindole and 20mM 5-cyanoindole would consist mainly of tri-cyano substituted trimers, co-trimers containing two cyano and one amino groups, and a smaller amount of co-trimers containing two amino and one cyano groups. It is reasonable to expect that the co-trimers containing two amino groups may undergo a different type of chelation of the Cu^{II} ions to co-trimers containing only one amino group, and would therefore be expected to produce a diferent potential response.

7.3.2 - Reasons for Cu^{II} ion potential response in 20 / 20 cyano:amino copolymer.

It was suggested that the co-trimers containing two amino and one cyano groups may be able to chelate a Cu^{II} ion between the two amino groups, fig. 7.6.

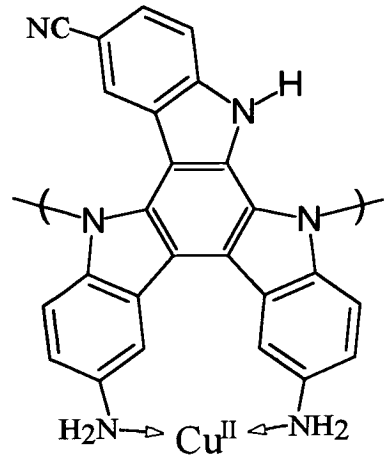

Fig. 7.6 - Chelation of the Cu^{II} by co-trimer containing two amino groups.

From the proposed chelation in fig. 7.6, it is suggested that the co-trimer containing two amino groups undergoes the following reaction :-

$$[\text{Trimer-}(NH_2)_2]_{ox} + Cu^{II} + e^- \Leftrightarrow [(\text{Trimer-}(NH_2)_2)\text{-}Cu]^{2+}_{red} \quad \text{--- Equ}^n\ 7.5$$

The Nernst equation for this reaction is :-

$$E = E^0 + \frac{RT}{F} \text{Ln} \frac{[\text{Trimer-}(NH_2)_2]_{ox}\ [Cu^{2+}]}{[(\text{Trimer-}(NH_2)_2)\text{-}Cu]^{2+}_{red}} \quad \text{Equ}^n\ 7.6$$

$$= E' - \frac{RT}{F} \text{Ln}[Cu^{2+}] \quad \text{--- Equ}^n\ 7.7$$

$$= E' - 0.0256\ \text{Ln}[Cu^{2+}] \quad \text{--- Equ}^n\ 7.8$$

The expected slope would be 25.6mV if all the Cu^{II} ions were chelating in a bidentate way described above. In this copolymer film however, it is believed that a combination of chelation sites are available, i.e. some of the Cu^{II} ions were undergoing chelation by the co-trimers containing two amino groups, producing a local potential response of 25.6 mV. Other Cu^{II} ions were thought to be undergoing chelation between two neighbouring co-trimers containing only one amino group leading to a local potential response of 12.8 mV (as in section 7.3.1). For this 20 / 20 cyano:amino copolymer as a whole therefore, it was expected to observe a slope with a gradient between 25.6 and 12.8 mV. The observed slope of 19mV suggests that both these types of chelation are taking place in this 20 / 20 cyano:amino copolymer, and that 50% of the Cu^{II} is complexed to one trimer unit with 50% to two trimer units.

7.4 - Cu^{II} response of electropolymerised 5-aminoindole on a pre-formed poly(NI) film.

It was decided to extend the Cu^{II} - potential study to an electropolymerised 5-aminoindole film. A poly(NI) layer was deposited and a 5-aminoindole layer polymerised on top from a 50mM solution of 5-aminoindole (0.575V). The resultant nitro~amino bilayer was then transferred in to a 0.1M NaCl aqueous solution and the potential of the film monitored with varying concentrations of $CuCl_2$. The observed potential response is shown in fig. 7.7.

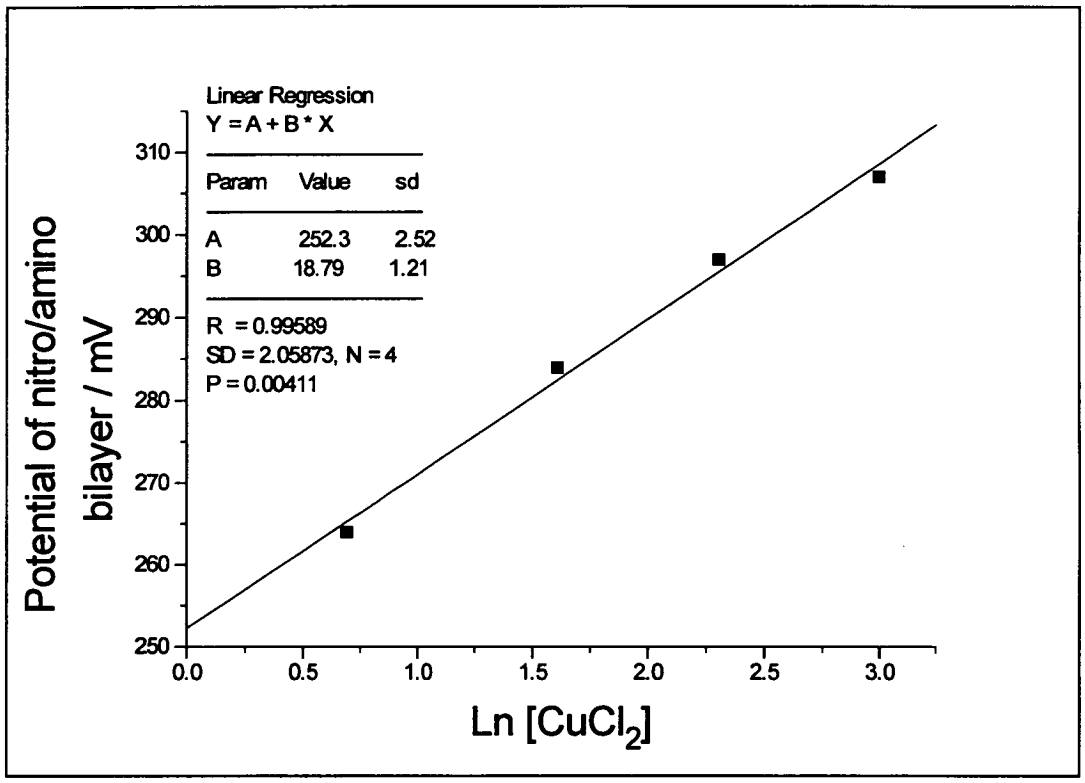

Fig. 7.7 - Potential vs ln[$CuCl_2$] of amino~nitro bilayer.

It can be seen that the potential response of the amino~nitro bilayer shows a straight line response to the natural log of $CuCl_2$ with a gradient of 18.7 ± 2.4mV. The gradient suggests that there is again a combination of different types of chelation occurring in the 5-aminoindole layer. This layer was thought to consist of trimers containing three amino groups. The Cu^{II} ions were thought to undergo chelation in **both** an inter-trimer

trimer bidentate and intra-trimer bidentate fashion, leading to mixed chelation behaviour (fig. 7.8). Therefore the macroscopic response of the whole film would be expected to lead to a slope of between 12.8mV and 25.6mV.

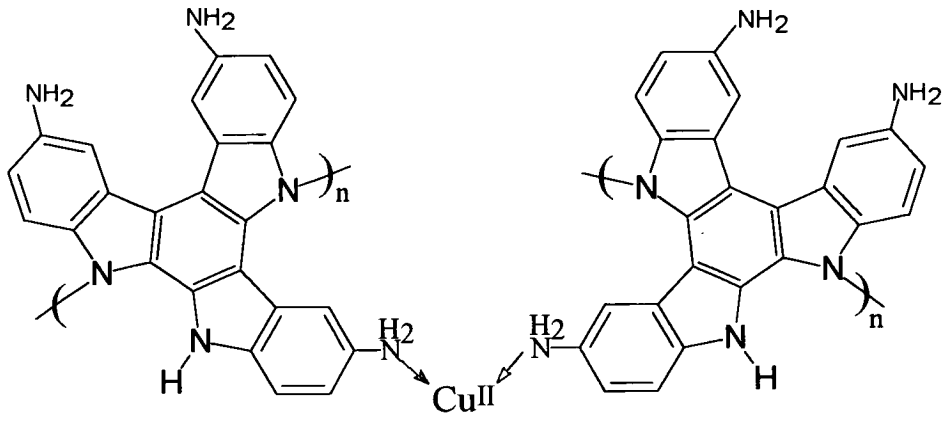

Inter bidentate chelation

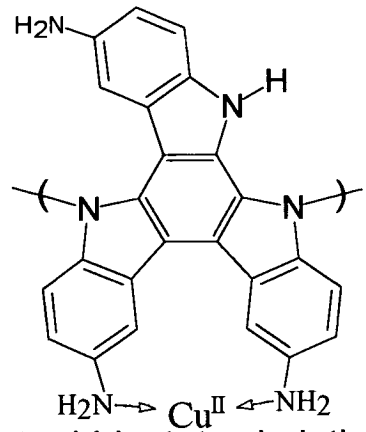

Intra bidentate chelation

Fig 7.8 - Intra- and inter- trimer chelation of Cu^{II} in 5-aminoindole trimers.

It is reasonable to expect that a slope of close to 25 mV may have been observed for this nitro~amino bilayer, as every 5-aminindole trimer contains an intra-trimer bidentate chelation site. The reason that the mixed chelation behaviour was observed is proposed that once a Cu^{II} ion is chelated in-between the amino groups on two neighbouring trimers, it is sufficiently destabilised to inhibit the chelation of Cu^{II} in-between the other two amino groups in the same trimer. By the same argument, if a Cu^{II} ion

inhibits any chelation at the third amino group. This results in the mixed chelation behaviour that is suggested by the observed slope of 19mV.

7.5 - Selectivity of the copolymer layers to Cu^{II}.

These copolymer layers were tested for a potential response to a number of other metal ion solutions in a similar way to the $CuCl_2$. The metal compounds tested were Pb $(NO_3)_2$, $NiSO_4$, $CdCl_2$, $CoCl_3$, $NiCl_2$, $MgCl_2$, $CrCl_3$ and $CaCl_2$. The copolymer films did not show any potential changes in solutions of any of these metal compounds. However a potential response was noted on the addition of $FeCl_3$. This response was believed not to be due to chelation of the Fe^{III}, but to be due to a redox reaction of the $Fe^{III} + e^- \Leftrightarrow Fe^{II}$ which oxidises the copolymer film. This hypothesis was tested by observing whether a pure poly(CI) film showed a similar potential change to the addition of $FeCl_3$ as that observed for the amino:cyano copolymers. In a solution of 0.1M NaCl / H_2O at a pH of 2.87 the poly(CI) film showed a zero current potential of 358 mV. In a solution of 1mM $FeCl_3$ / 0.1M NaCl / H_2O at the same pH, the potential rose to 525 mV. If the concentration was increased to 2mM $FeCl_3$, the potential increased again to 552 mV. As the poly(CI) film did not contain any chelating groups, it was believed that the Fe^{III} was oxidising the Poly(CI) film. To show that this was the case, 2mM $FeCl_2$ was added to the solution containing the Fe^{III}. The potential of the film immediately dropped and reached a value of 455mV. This is due to the fact that the Fe^{II} is in equilibrium with the Fe^{III} which retards the oxidation of the poly(CI) film. This is good evidence that the potential change observed in the amino:cyano copolymer with the addition of $FeCl_2$ was due to the redox reaction $Fe^{III} + e^- \Leftrightarrow Fe^{II}$ which oxidised the copolymer film, and that this was also therefore observed for the aminoindole films.

The amino:cyano copolymer films produced seem to be very selective to the bidentate chelation of Cu^{II} ions which is a very useful property for an ion sensor device. It is suggested that the reason for this

selectivity of the copolymers can be found by examination of the Irving - Williams series[151]. The Irving - Williams series plots the formation constants for the first d-series of metal atoms by bidentate chelating ligands. For all these types of ligands, the formation constant for Cu^{II} is several orders of magnitude greater than all the other metals in the first d-series and increases across the row of transition metals Cr, Fe, Ni, Cu as the size of the 2+ ion decreases. The reason for this is mainly due to electrostatic effects where the stabilisation is proportional to the ligand field stabilisation energy. Cu^{II} complexes have by far the greatest stabilisation energies because of the additional stabilising influence of Jahn-Teller distortion; after Cu^{II}, the binding energy decreases markedly. Moreover, whatever the size of the chelation site, the chelation of Cu^{II} is considerably stronger than that for any other metal ions.

7.6 - Reversibility of Cu^{II} complexation.

The complexation of Cu^{II} in these amino:cyano copolymer films was found to be reversible. The Cu^{II} ions were observed to dissociate by placing the Cu^{II}-complexed copolymer films back in to a solution of pure 0.1M NaCl / H_2O. The potential of the film drops very rapidly back to a potential very close to that for the film before undergoing chelation with the Cu^{II}. Fig. 7.9 shows the fall of potential with time of an amino:cyano copolymer film produced from an electropolymerising solution of 40mM 5-cyanoindole and 1mM 5-aminoindole. In this figure the copolymer was transferred from a solution of 1mM $CuCl_2$ to a pure 0.1M NaCl / H_2O. Both solutions were recorded at a pH of 4.45.

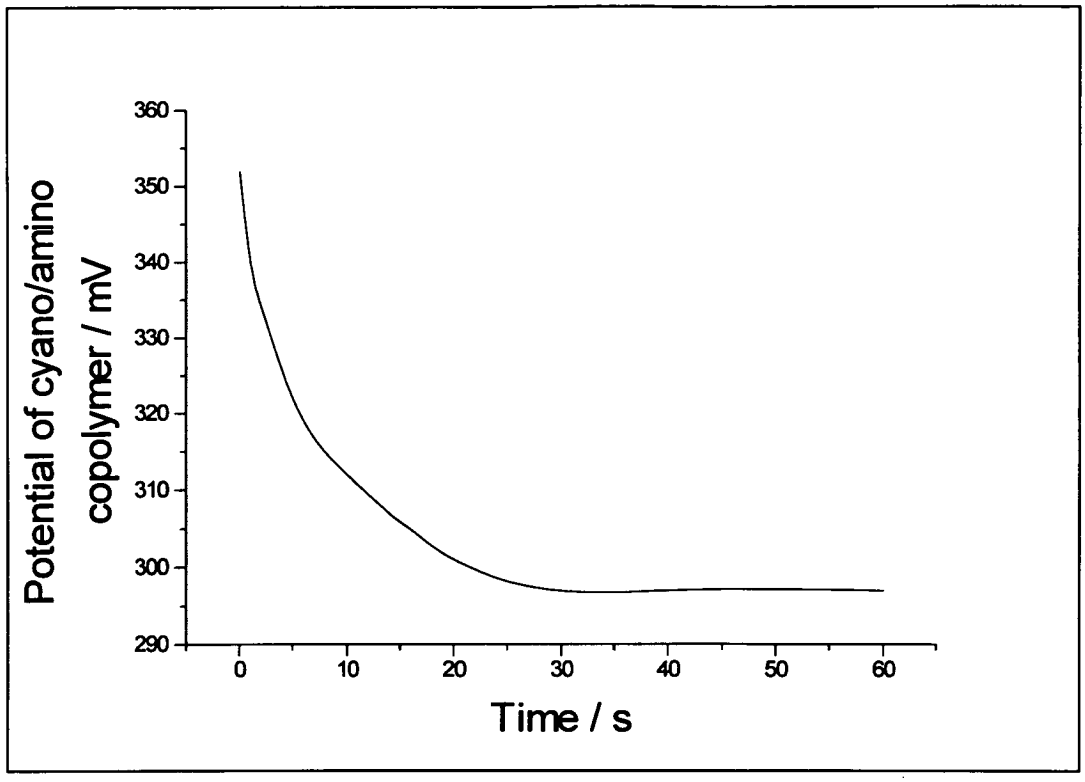

Fig. 7.9 - Potential time response of Cu^{II} complex dissociation.

It can be seen that within 30 seconds the potential of the film returns to a steady state value. This is very close to the potential value recorded before being transferred in to solution containing Cu^{II}. This suggests that although the Cu^{II} ions are relatively strongly bound, an equilibrium is established and the dissociation reaction is relatively facile.

7.7 - Conclusions.

This chapter has shown that the production of a Cu^{II} ion sensor device is possible using the amino groups in a cyano:amino copolymer to chelate the Cu^{II} ions. Potential changes were observed due to redox reactions due to chelation of the Cu^{II} ions by the amino groups. These potential changes can be explained by consideration of the structure of the copolymer films. Although very selective to Cu^{II} ions, these polymers

are sensitive to both redox active ions and pH changes. Further testing of the copolymers reproducibility and effects of other metal ions is needed before a useful commercial device can be developed.

Chapter 8 - Ferrocene incorporation

8.1 - Introduction.

In view of the results discussed in the previous chapters, where it was found that all of the 5-substituted indoles studied could be directed to form cyclic trimer and polymer species, it was decided to probe the methodolgy of chemical functionalisation at the 5-position. As all the other studied 5-substituted indoles could be directed to form cyclic trimer and polymer films (and electronic communication between a 5-substituent and the redox centre was likely), to test this, the polymerisation of a chemically functionalised indole monomer to form an electrochemically active, functionalised conducting polymer was attempted.

It was decided to attempt to functionalise an indole monomer in the 5-position with a ferrocene functional group (fig. 8.1). Ferrocene consists of an iron atom capped by two cyclopentadienyl (Cp) ligands. Ferrocene was chosen as it has been extensively studied electrochemically and shows a well defined, completely reversible one electron redox reaction in cyclic voltammetry experiments.[142] Thus if it were possible to produce a conducting polymer film from a ferrocene functionalised indole monomer, it was thought likely that the redox reaction of the ferrocene groups would be electrochemically observable in the copolymer. Because of ferrocene's well defined redox behaviour, it was hoped that it would be a useful substituent in establishing the method of functionalisation and to probe the electronic communication between the 5-position and the trimer/polymer backbone.

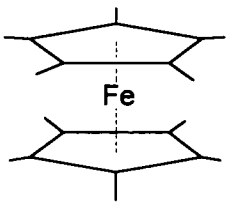

Fig. 8.1 - Ferrocene.

Previously, ferrocene has also been identified for use as an electron transfer mediator to a large number of redox enzymes such as Glucose oxidase[143], cytochrome C[144] and NADH[145]. Efficient electron transfer to redox enzymes is essential for the use of such enzymes in the rapidly expanding research area of bio-technology, biosensors and biocatalysis. However most redox enzymes lack pathways that can transport an electron from their embedded redox site to an electrode, thus a mediator is often used to facilitate the electron transfer without the destruction of the enzyme.[146] The mediator is usually an electrochemically reversible redox system which can accept (or donate) electrons from the electrode and then donate (or accept) electrons to the redox site in the enzyme. The use of ferrocene as a mediator for electron transfer has widely been reported[2,3,4]. Thus if an indole monomer containing a covalently bound ferrocene group could be electropolymerised to form a polymer film containing ferrocene groups, the system may also have a use as an electron transfer mediator for various enzymes.

8.2 - Synthesis of a ferrocene substituted indole.

Having examined the available starting materials, it was decided that the most facile way to form an indole based molecule with a 5-substituted ferrocene group was to form an amide bond, with a condensation reaction, between the amino group of the commercially available 5-amino indole, and the carboxylic acid group of the commercially available ferrocene-mono-carboxylic acid. The amide link would be expected to be planar with a high π-electron density, and would be a suitable link for preserving the electronic communication between trimer and substituent. As carboxylic acids have only a limited reactivity, it was decided to first convert it to the acid chloride which has an increased reactivity to nucleophilic attack. The reaction scheme is shown in fig. 8.2. Full experimental details can be found in chapter 3.

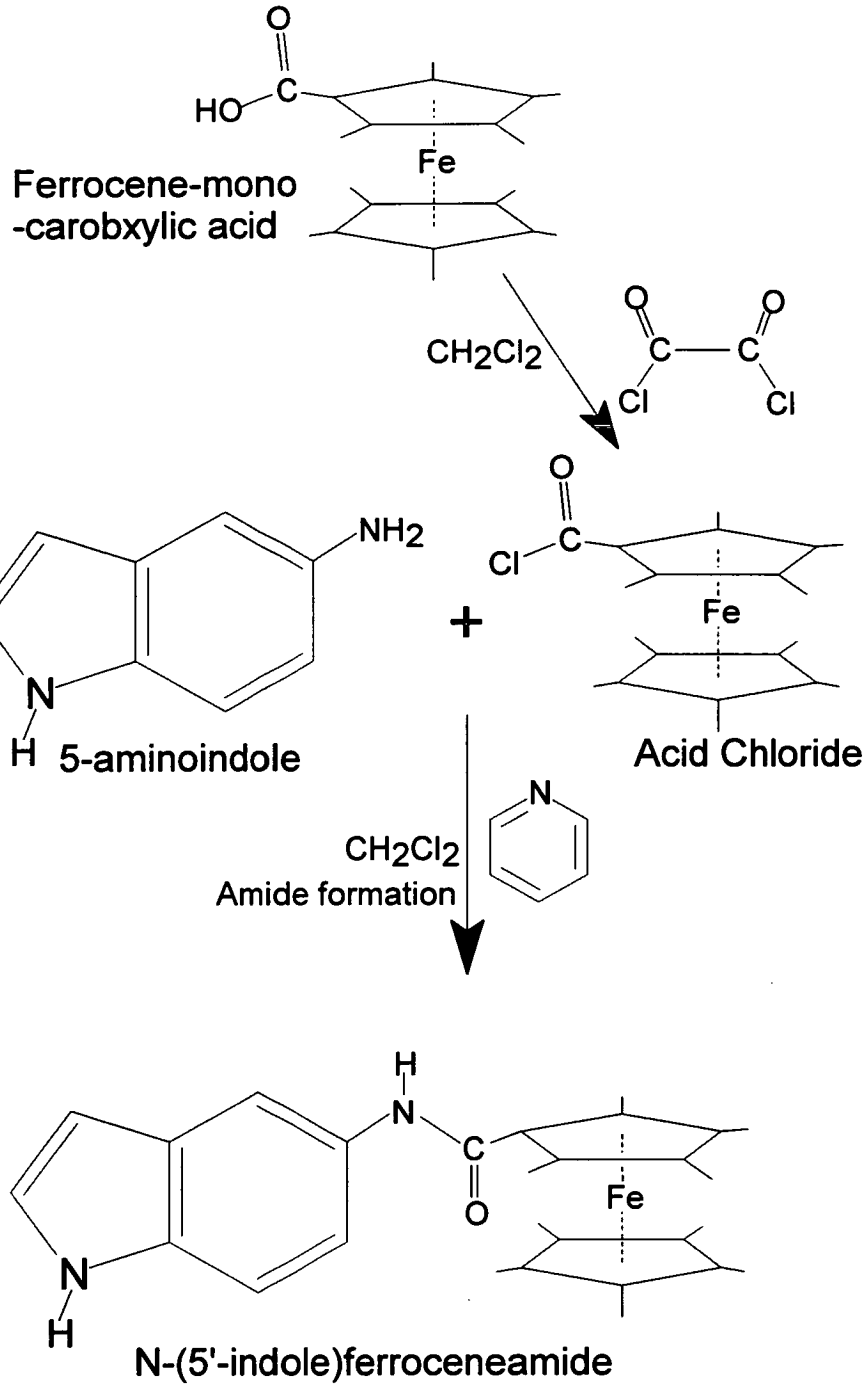

Fig. 8.2 - Reaction scheme for ferrocene derivatisation.

The product was purified by column chromatography (silica) and recrystallised from toluene to produce orange-red crystals of N-(5'-indole)ferroceneamide, (NIFA). The NIFA was then studied by a number of spectroscopic methods described as follows.

8.2.1 - Infra-red spectroscopy (I.R.)

The I.R. spectrum of the reaction product is reproduced in fig. 8.3.

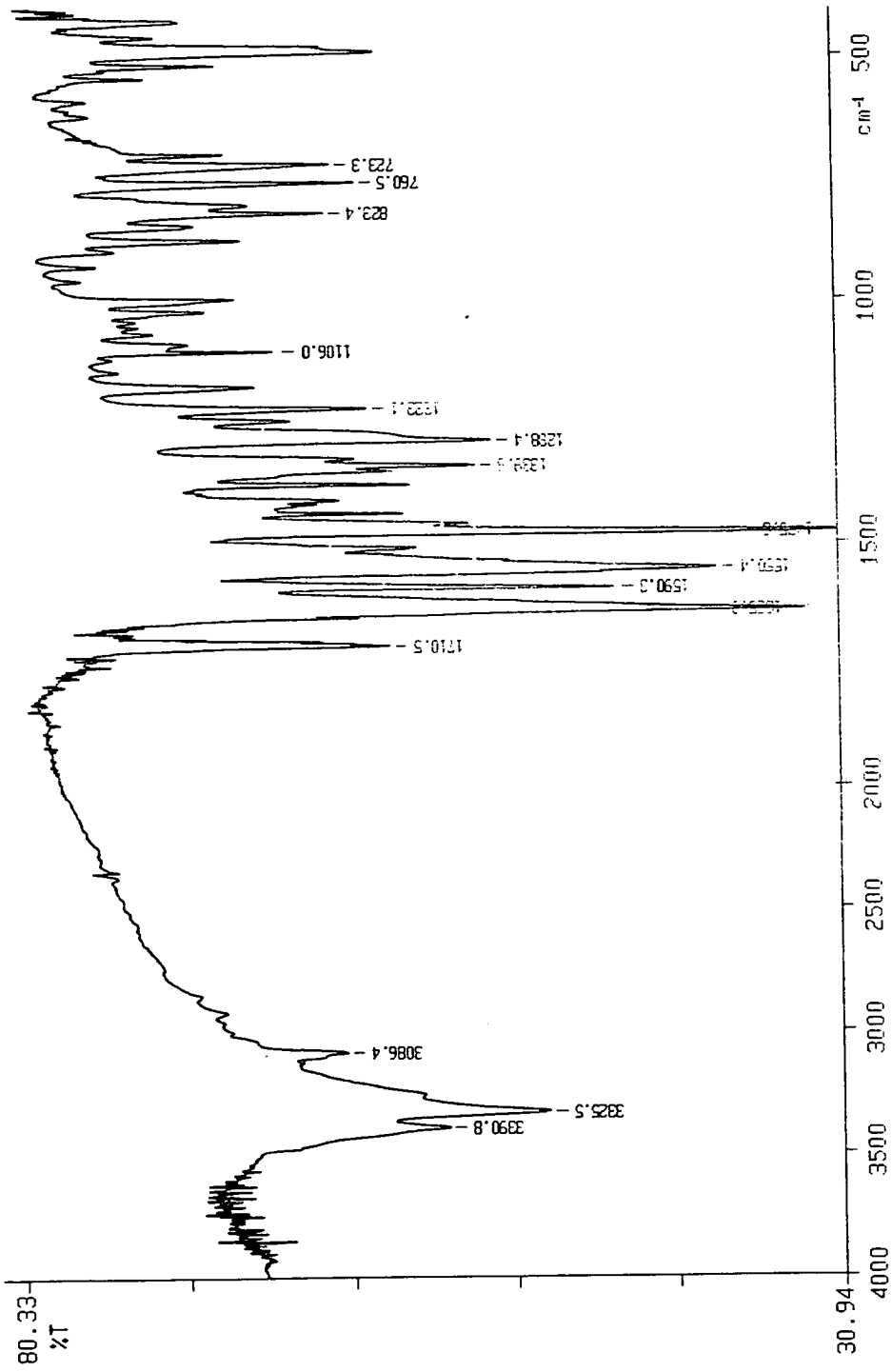

Fig. 8.3 - I.R. Spectrum of NIFA reaction product.

A selection of the important I.R. peaks are tabulated in fig. 8.4 with their assignment. The I.R. spectrum shows all of the main indole, amide and ferrocene functional group peaks expected for the proposed NIFA product.

Peak position / cm^{-1}	Assignment
3391	Indole N-H
3325, 3087	Secondary amide
1711	Saturated ketone
1636	Possibly aryl
1590, 1550	Aromatic C-H stretches
1475	Ferrocene peaks of unknown origin
823	2 adjacent aromatic C-H's

Fig. 8.4 - Table of I.R. peaks and group assignment for NIFA product.

8.2.2 - N.M.R. spectroscopy.

The product was recrystallised from Toluene and submitted for proton ^{1}H and carbon 13 ^{13}H NMR in deuterated acetone. The proton NMR spectrum is reproduced in fig. 8.5.

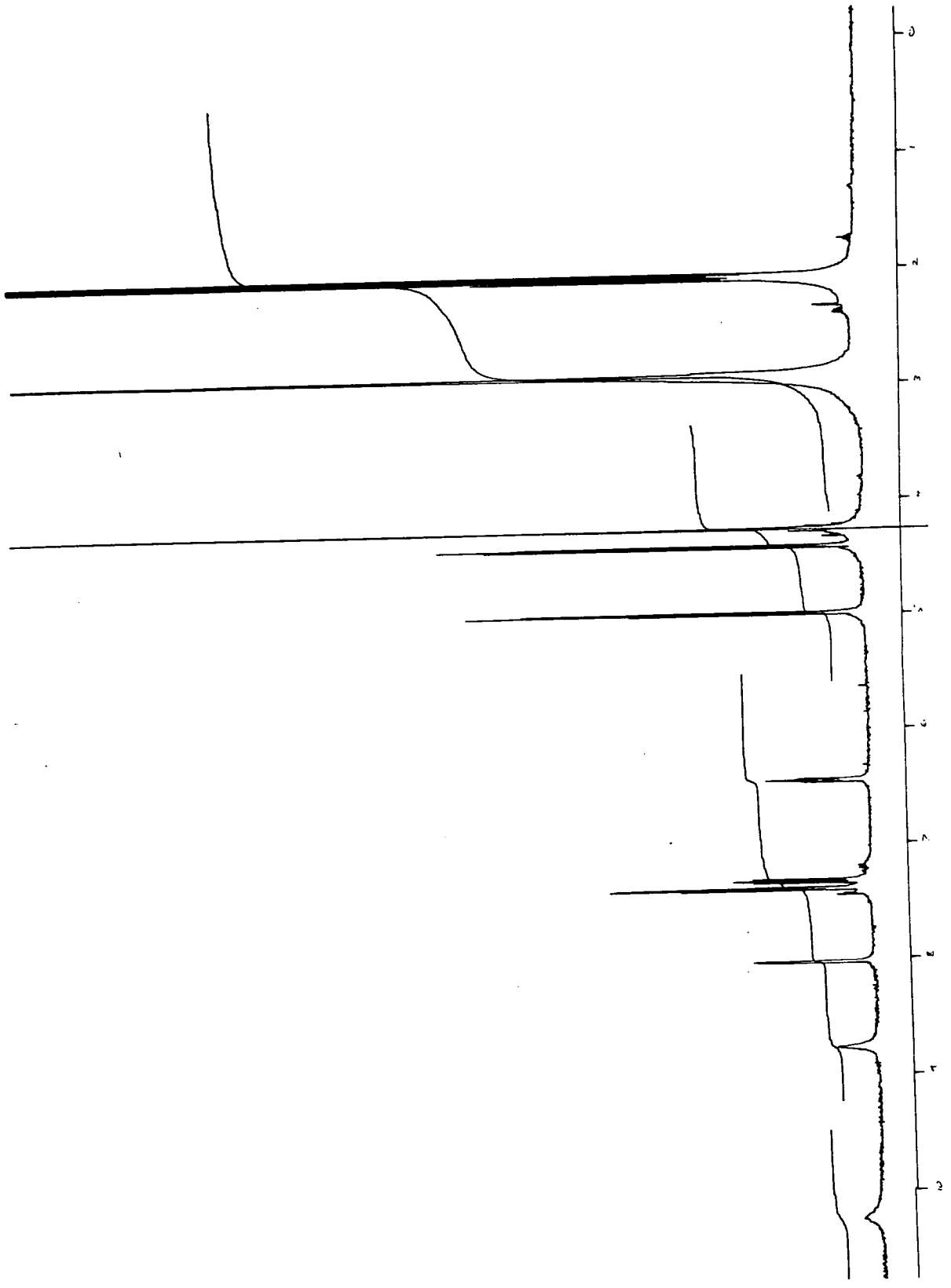

Fig. 8.5 - Proton NMR of NIFA reaction product.

The peaks produced in the proton NMR and their assignments are tabulated in fig. 8.6. The NMR spectrum shows all the expected proton peaks, shifts and couples for the structure of the NIFA product indicated.

Proton peak shifts / ppm	Assignment
10.24 Broad singlet	Amide N-H
8.759 Broad singlet	Indole N-H
8.02, 7.4-6.4	Indole ring protons
4.99, 4.4 doublet of triplets	Substituted ferrocene ring H's
4.25 singlet	Unsubstituted ferrocene ring H's

Fig. 8.6 - Table of ^{1}H NMR peak assignment.

The sample was also submitted for a proton decoupled ^{13}C NMR and this is reproduced in fig. 8.7.

The peaks produced in the ^{13}C NMR and their assignments are tabulated in fig 8.8.

^{13}C shifts / ppm	Assignment
166.7	Amide carbon
132.4, 130.8, 127.2	3 quaternary indole carbons
124.5, 115.2, 111.2, 110, 100.6	5 tertiary indole carbons
76.7	1 quaternary ferrocene ring carbon
69.3	2 equivalent substituted ferrocene ring tertiary carbons
68.6	5 equivalent unsubstituted ferrocene ring tertiary carbons
67.5	2 equivalent substituted ferrocene ring tertiary carbons

Fig. 8.8 - Table of ^{13}C NMR peak assignments.

The proton-decoupled ^{13}C NMR spectrum shows all of the expected carbon atoms for the NIFA molecule.

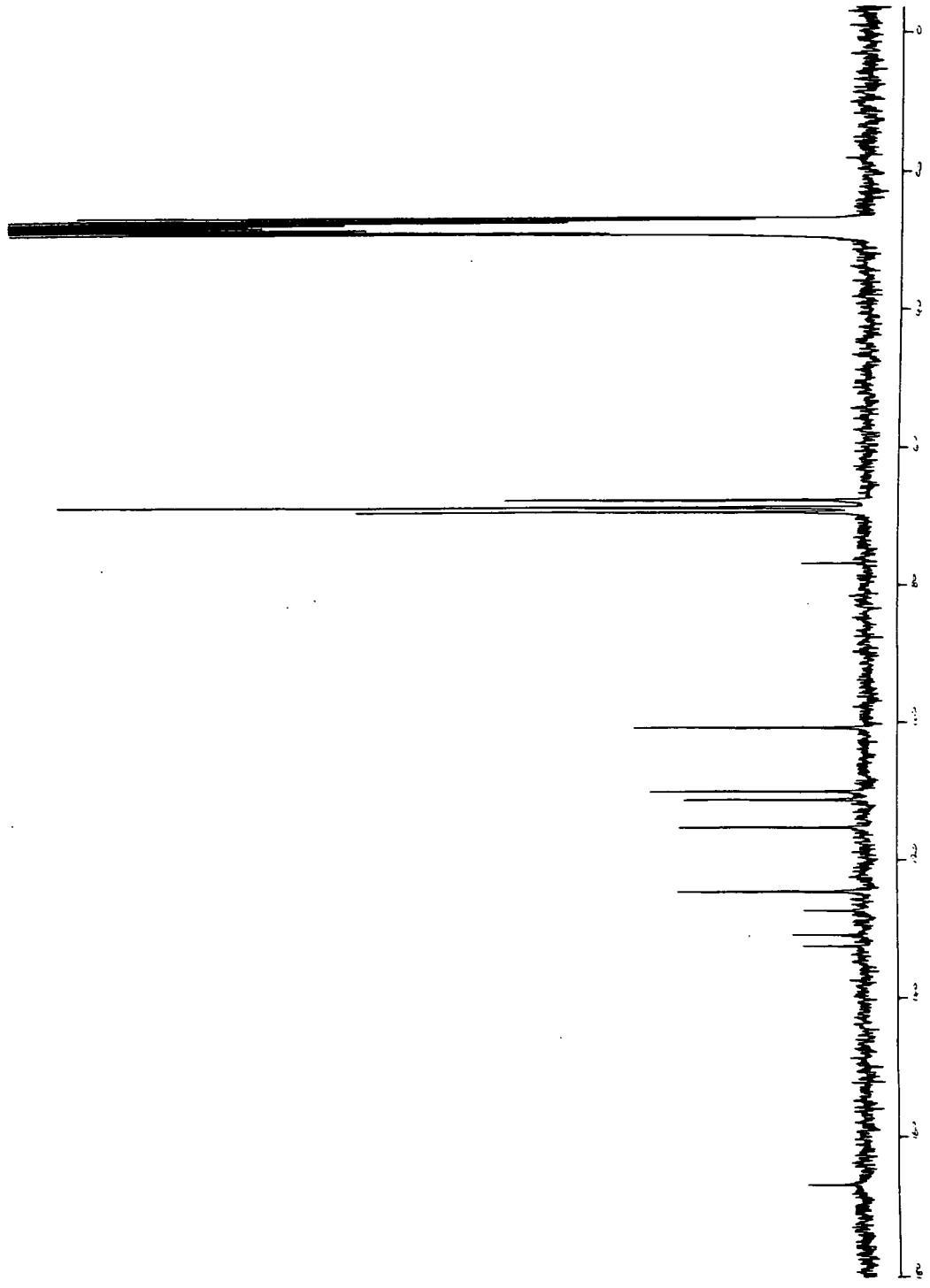

Fig. 8.7 - Proton decoupled ^{13}C NMR of ferrocene sample.

8.2.3 - Elemental analysis.

Elemental analysis was carried out on the product. If the product produced was indeed the proposed NIFA (molecular formula of $C_{19}H_{16}N_2OFe$), then the formula weight would be 344.19 D. The expected and actual compositions for the percentage carbon, nitrogen and oxygen are shown in fig. 8.9. The results obtained were within experimental error of the expected composition.

	% Carbon	% Nitrogen	% Hydrogen
Expected composition	66.3	4.69	8.14
Results of analysis	67.1	4.77	7.94

Fig. 8.9 - Table of CHN data.

8.2.4 - X-ray crystallography.

A number of good single crystals were grown from the vapour diffusion of hexane into a solution of acetone containing the NIFA product. The resultant crystal structure is shown in fig 8.10.

The crystal structure confirms the structure of the NIFA product conclusively as that in fig. 8.2. The packing diagram shows the molecules to be intermolecularly hydrogen-bonded at the relatively short distance of 1.84 Å between the oxygen in the amide moiety and the indole N-H. This is interesting because similar hydrogen-bonding may also take place in a polymer layer formed from the NIFA monomer. The full data set is shown in Appendix 1.

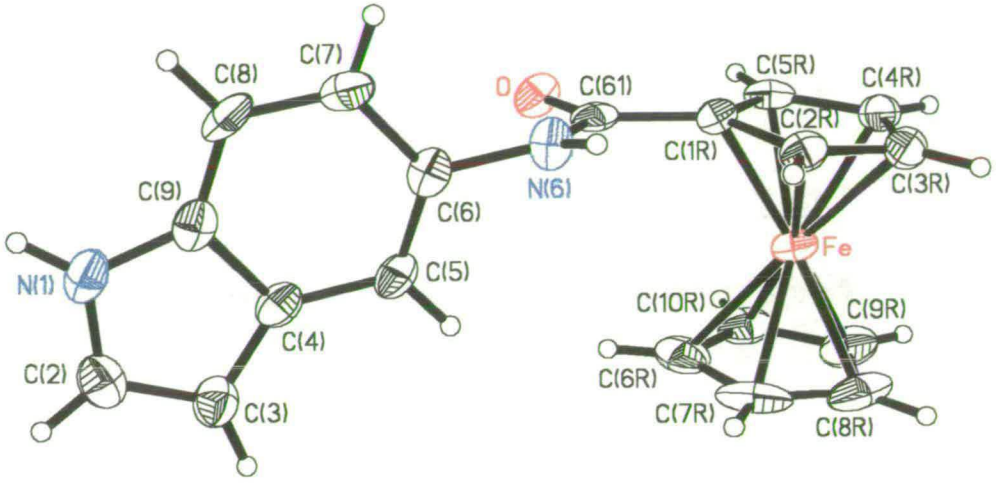

Fig 8.10 - Crystal structure of N-(5'-indole)ferroceneamide (NIFA).

8.3 - Electrochemistry of NIFA.

With the synthesis of the required indole based monomer functionalised with a ferrocene group having been successful, it was decided to study the NIFA product electrochemically. It was hoped that it would be possible to electropolymerise the NIFA to form a conducting polymer containing covalently bound redox active ferrocene groups.

8.3.1 - Cyclic voltammetry of 1mM NIFA.

The NIFA was dissolved in background electrolyte to form a 1mM NIFA / 0.1M $LiClO_4$ / MeCN solution and a cyclic voltammogram recorded, fig. 8.12.

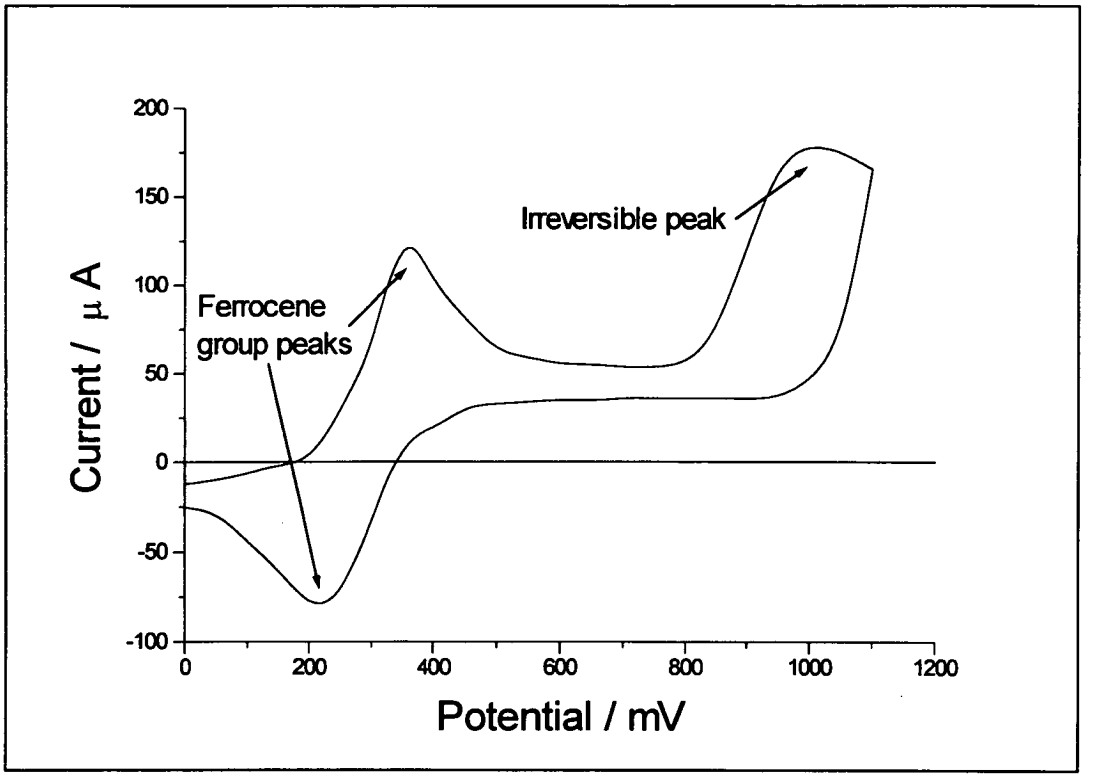

Fig. 8.12 - CV of 1mM NIFA / 0.1M $LiClO_4$ / MeCN. Sweep rate = 10mV/s.

This CV shows an electrochemically reversible redox couple at a potential ca 290mV with another irreversible peak to higher potentials (at approximately 1000mV). The reversible couple is at higher potentials than that for the reversible redox couple observed for a solution of unsubstituted 1mM ferrocene in background electrolyte which occurs at around 90mV. The reversible couple observed in fig. 8.12 is suggested to be due to the one electron redox reaction of the ferrocene functional groups in the NIFA molecule. The peak separation of these peaks is approximately 100mV, which is higher than the theoretical 59mV expected for a fully reversible one electron redox reaction. The greater peak separation is suggested to be due to iR drop in the solution. The potential at where this redox reaction occurs would be expected to be higher than that of free ferrocene in solution, as the covalent attachment in the NIFA molecule increases the redox potential of the ferrocene group through the inductive effect of the amide group.

The irreversible peak is suggested to be due to the oxidation of the NIFA monomers to form NIFA monomer radical cations which then undergo a chemical reaction (most likely linking). The potential at which the irreversible peak was observed (1000mV) suggests that the formation of the ferrocinium cation has a substantial electron-withdrawing effect on the indole monomer, as Chapter 4 showed that the potential at which the radical-cation is formed has been shown to be dependent upon the electronic nature of the substituent (Hammett plot). Therefore the cyclic voltammogram of the NIFA monomer shows there to be substantial electronic communication between the ferrocene group and the indole ring. To elucidate the reversible redox couple in fig. 8.12 further, a rotating disc electrode (RDE) study was carried out on the solution.

8.3.2 - Rotating disc electrode study.

A rotating disc electrode study was carried out on the 1mM NIFA solution over the potential range where the reversible couple was observed in fig. 8.12 (0 - 400 mV). A number of polarograms were produced at varying rotation rates and the limiting current values were plotted against the electrode rotation rate, $W^{1/2}$, to produce a Levich plot, fig. 8.13.

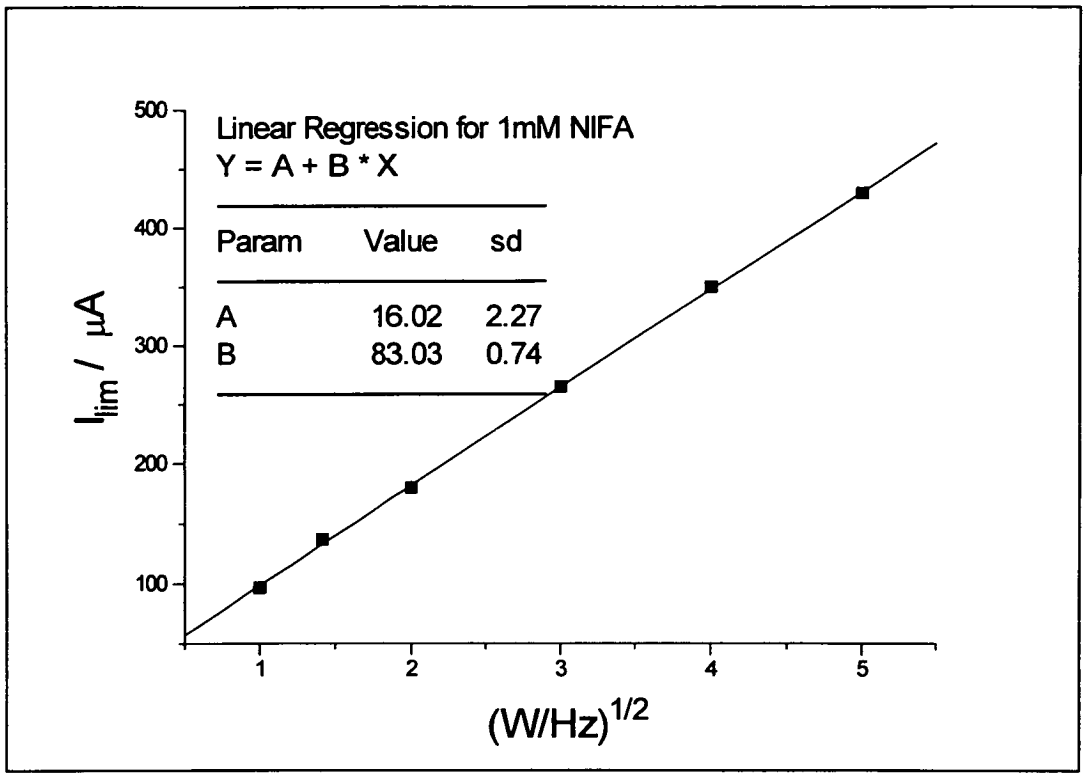

Fig. 8.13 - Levich plot of 1mM NIFA / 0.1M $LiClO_4$

The Levich plot in fig. 8.13 shows a good straight line which is indicative of simple mass transport control of a solution species. The gradient of the best fit line is given by equation 2.1, with c_∞ equal to the bulk concentration of NIFA. Therefore for a one electron oxidation (expected for the ferrocene / ferrocinium couple), the gradient of 83µA/s$^{1/2}$ corresponds to a diffusion coefficient (D) of $1.41 \times 10^{-5} \pm 0.05 \times 10^{-5}$ cm^{2}s^{-1}. This value is in agreement with diffusion coefficients measured for other substituted ferrocenes[147], whose values are tabulated in fig. 8.14. It can be seen that as the substituent size increases, the diffusion coefficient decreases as expected. From the trend shown by these substituted ferrocenes the diffusion coefficient calculated for NIFA is entirely reasonable for its size.

Molecule	Diffusion coefficient
Ferrocene	3.1×10^{-5}
1'1-Dimethylferrocene	2.1×10^{-5}
2-methyl-4nitrophenylferrocene	1.7×10^{-5}
NIFA	$\mathbf{1.41 \times 10^{-5} \pm 0.05 \times 10^{-5}}$
Tetrakis(phenlymethyl)ferrocene	1.2×10^{-5}

Fig. 8.14 - Diffusion coefficients of substituted ferrocenes in MeCN.

8.3.3 - Tafel plot.

A Tafel plot was obtained from the 4Hz polarogram from the RDE study of 1mM NIFA in section 8.3.2. This is reproduced in fig. 8.15.

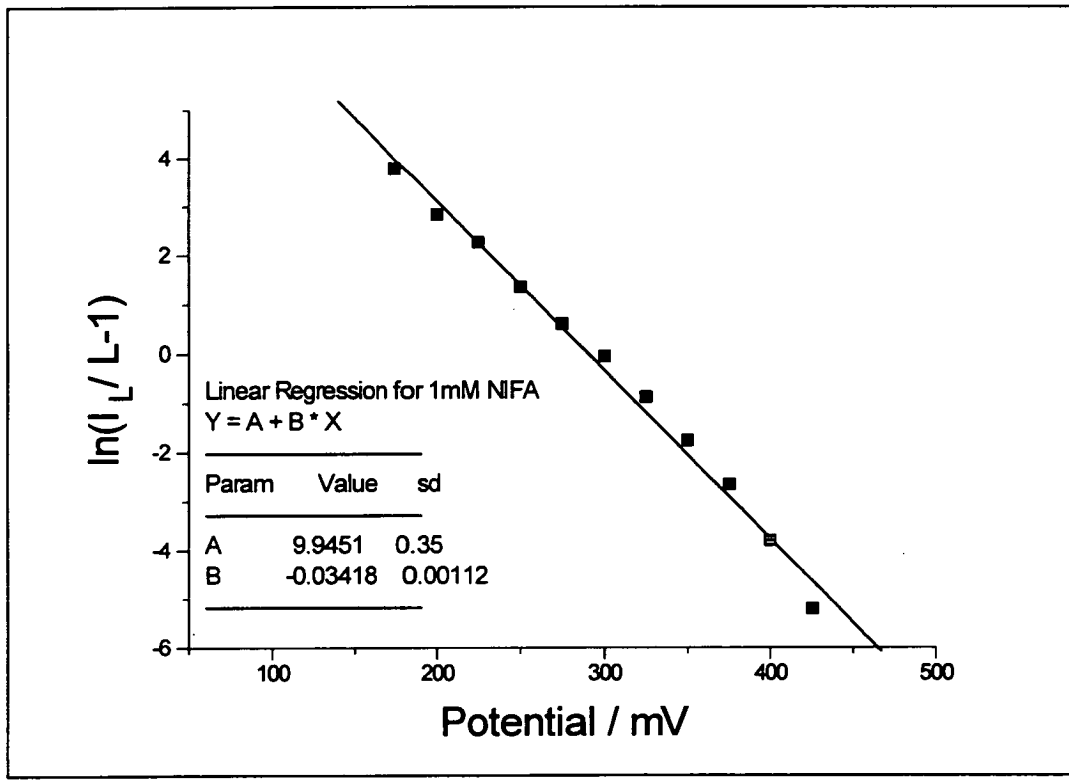

Fig. 8.15 - Tafel plot of reversible peaks from 1mM NIFA.

The Tafel plot shows a gradient of 34.2mV. In theory a fully reversible one electron system would exhibit a Tafel plot gradient of 39mV, however any iR drop in solution will cause the gradient to be slightly lower, this type of iR drop was also observed in the CV of the NIFA film which showed a peak separation larger than that expected by theory. The observed Tafel slope of 34mV, although slightly lower than the theoretical value of 39mV, is therefore attributed to a reversible one electron redox system, i.e. the expected redox reaction of the ferrocene group.

8.3.4 - Polymerisation of NIFA on a platinum electrode.

It was suggested that the second irreversible peak observed in fig. 8.12 was due to the linking reaction of the NIFA radical cations. It was thought likely that these radical cations may be forming ferrocene substituted cyclic trimers species similar to that observed by the other 5-substituted indoles. Thus it was decided to attempt to polymerise the NIFA monomers by applying a potential slightly above that observed for the irreversible peak, i.e. at 1.1V, to ensure full mass transport control.

The current-time transient produced from the applied potential pulse of 1.1V is shown in fig. 8.16.

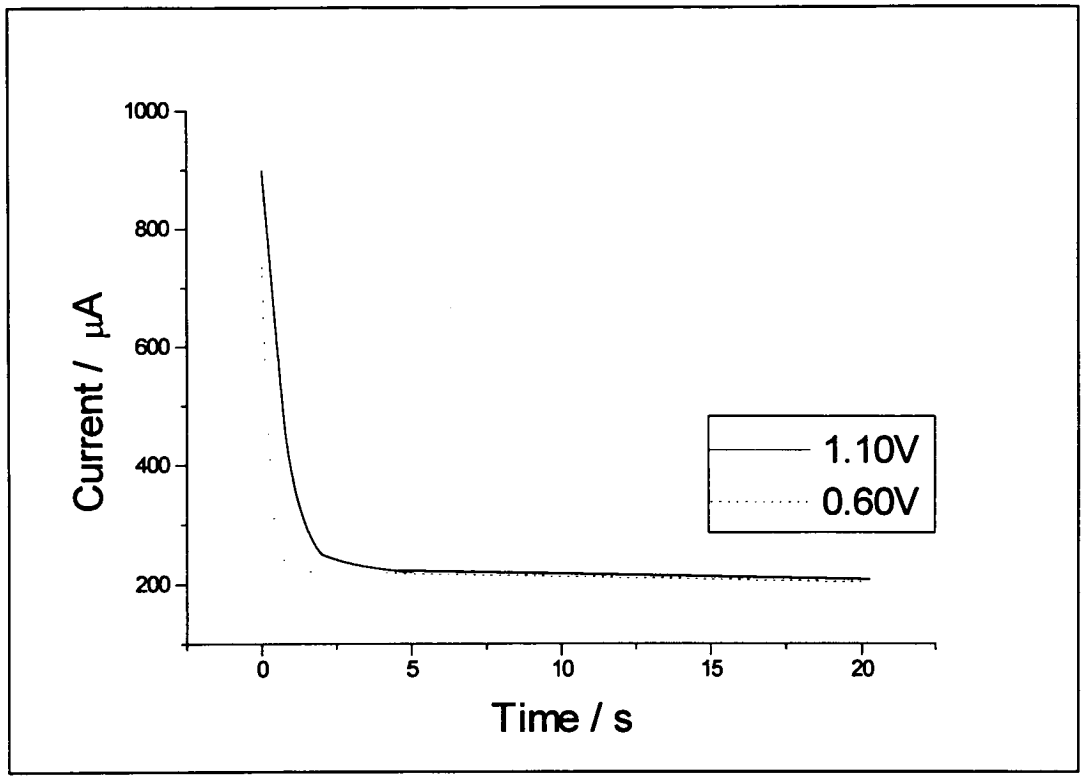

Fig. 8.16 - Current-time transients for the electropolymerisation of 1mM NIFA on Pt at 1.10V and 0.60V. W=2Hz.

It can be seen in fig. 8.16 that the current drops rapidly to a relatively low current where it reaches a steady state value of 220μA. Examination of the electrode showed there to be no film formation on the electrode during this potential pulse. This steady state current may be due to the oxidation of the NIFA ferrocene groups in solution and not the formation and linking of radical cations. This hypothesis was tested by applying a potential pulse at a lower potential (600mV) which is just past the oxidation potential of the ferrocene groups. This would not be sufficient to oxidise the NIFA-indole monomers to form radical cations, although it would still be high enough to oxidise all of the NIFA ferrocene groups in solution. The current-time transient recorded at a potential pulse of 600mV is also plotted in fig. 8.16 This shows an immediate drop of current to the same steady state value observed for the current-time transient observed with a potential pulse of 1100mV. This indicates that the steady state current of 220μA observed in these transients is indeed due to the oxidation of the ferrocene substituents. The extra charge (≈400

μC) observed at the start of the current-time transient at 1100mV compared with the I - t transient at 600mV, it is likely that this is due to the formation of NIFA radical cations which link to form a thin film upon which nothing else deposits. This extra charge (≈400 μC) corresponds to a film thickness of approximately $2x10^{-9}$ moles of trimer or roughly ten layers at most, although there is likely to be less, as soluble plumes of darker material were observed to drift away from the electrode surface during this polymerisation. The reason the film does not grow beyond these few layers may be due to the adsorption of the ferrocene groups on the platinum surface which inhibits the formation of radical cations. This has been observed previously.[148] The concentration of the NIFA monomer is relatively low, at 1mM, so the concentration of radical cations produced in the diffusion layer for this short time is probably too low to facilitate their linking to form trimers and polymer. It was decided to attempt to increase the concentration of radical cations produced by increasing the NIFA monomer concentration to 10mM. The current-time transient obtained for 10mM NIFA (potential of 1.1V) is shown in fig. 8.17.

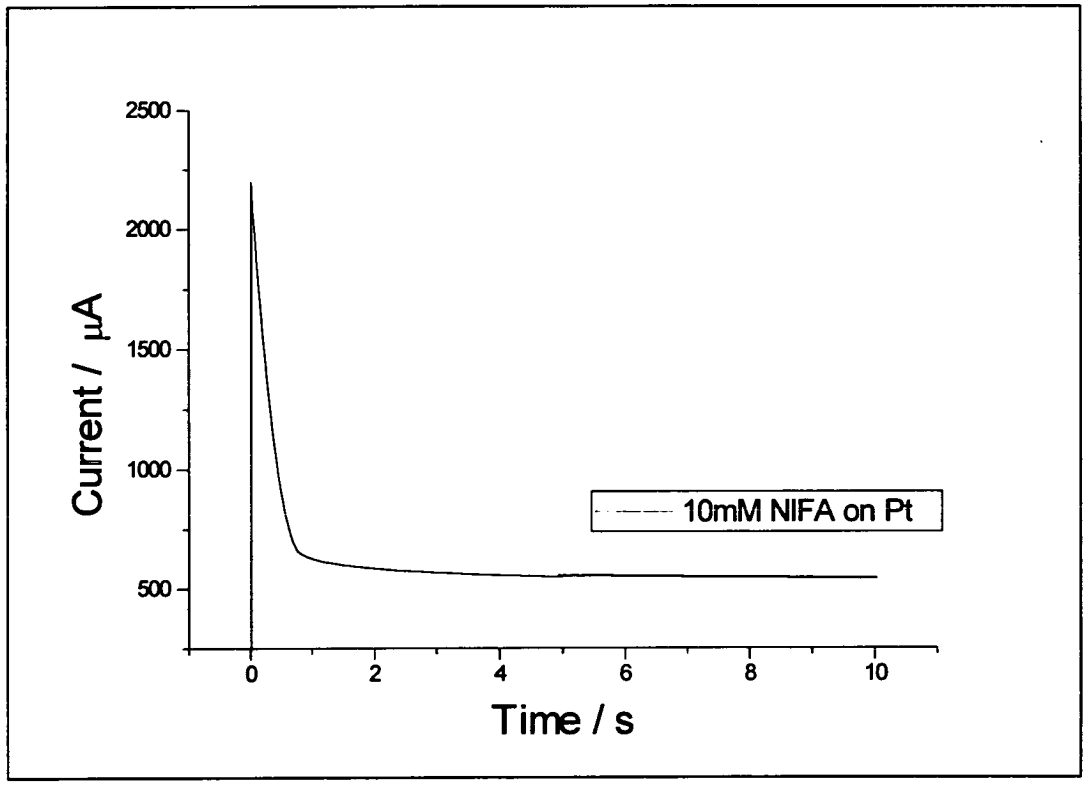

Fig. 8.17 - Current-time transient of 10mM NIFA at 1.1V.

Fig. 8.17 shows a higher current for the polymerisation of 10mM NIFA although it still falls rapidly to a steady state value, indicating the production of only a very thin film. The current spike in the first second of polymerisation has a very similar charge to that observed for the 1mM polymerisation indicating the formation of a similar film thickness of less than 10 layers of NIFA trimer. While this experiment was being carried out some darker plumes of soluble products were observed drifting away from the electrode surface in to the bulk of solution. Thus it seems that some electropolymerisation may be taking place at the electrode, although the products are mostly soluble and the deposition reaction passivates quickly. Fe^{+} would also be expected to be a solubilising side group.

In light of the results discussed in chapter 4, where passivation of the electropolymerisation of 5-aminoindole was reduced, and formation and deposition of the trimers facilitated, with the use of a pre-formed poly(CI), poly(NI) or poly(I5CA) layer, it was decided to use this technique to attempt to combat the problems that arose in electropolymerising the NIFA monomer to produce an electroactive film.

8.3.5 - Electropolymerisation of NIFA using a pre-formed poly(I5CA) layer.

It was decided to use poly(I5CA) as the pre-formed polymer layer as it forms a good, electroactive polymer film with a lower redox potential than poly(CI) or poly(NI). A film of poly(I5CA) was grown on the working electrode and a cyclic voltammogram experiment carried out in a solution of 10mM NIFA / 0.1M $LiClO_4$ using the poly(I5CA) coated electrode. The CV obtained is reproduced in fig. 8.18.

On successive cycles, an increase in the current can be observed which indicates the laying down of the NIFA on top of the poly(I5CA) layer. However as the layer becomes thicker with additional cycles, it can be seen that the ferrocene group redox peaks become more separated. This

This peak separation may be due to the redox reaction of the ferrocene groups being hindered until the poly(I5CA) layer underneath has been oxidised or reduced. As the NIFA film is deposited, the peaks become larger indicating that the film is growing. The ferrocene groups on any NIFA trimers formed are relatively sterically bulky groups, these would be likely to substantially decrease the likelihood of the NIFA trimers linking and also reduce the efficient packing of the trimer centres. This would dramatically decrease the conductivity of the NIFA film which may explain the increasing peak separation observed.

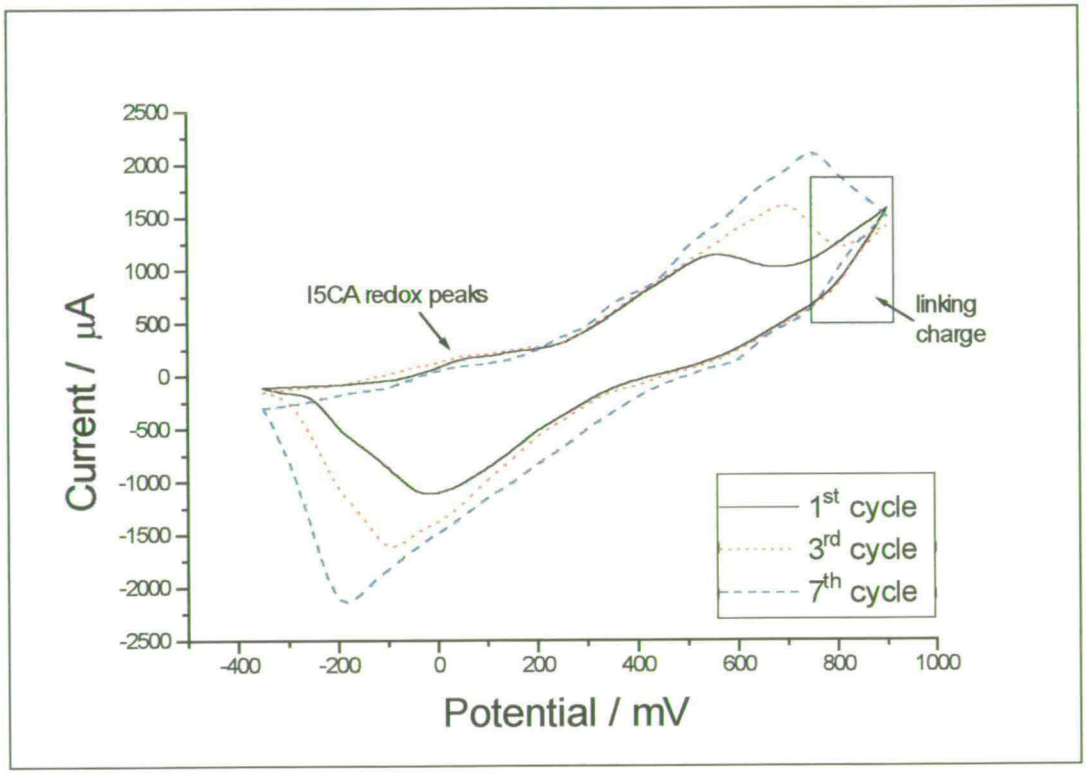

Fig. 8.18 - CV of 10mM NIFA on poy(I5CA) layer showing build up of charge in film.

The potential range of this cyclic voltammogram was sufficient to only form a small amount of NIFA radical cations for each cycle, however it can be seen that the small amount of linking charge in the CV corresponds well with the increased amount of charge observed in successive cycles. This indicates that the majority of the NIFA radical cations formed were linking and depositing on the pre-formed poly(I5CA)

layer. This constitutes an almost complete elimination of the production of the soluble products observed on the clean platinum electrode.

8.3.6 - Copolymerisation of NIFA and I5CA.

The peak separation was thought to have been due to the formation of a more insulating NIFA layer due to the interactions of the bulky ferrocene groups. The large steric bulk of the ferrocene groups, which would be very close to each other in a cyclic trimer/polymer layer, would force the trimers increasingly out of plane leading to a lower conductivity and greater resistivity. The large ferrocene groups would also be expected to hinder the π-stacking interactions of the trimer which would also hinder efficient conductivity. In an attempt to reduce this steric effect, it was decided to attempt to copolymerise NIFA with I5CA in the hope that this would result in a copolymer containing ferrocene groups with greater spatial separation. It was decided to copolymerise the NIFA with I5CA, as on electropolymerisation, I5CA forms an electroactive insoluble coat and would therefore be expected to facilitate the deposition of the NIFA:I5CA copolymer on top of the pre-formed poly(I5CA) layer.

A 30mM I5CA solution was used to form the preformed I5CA undercoat with an applied potential of 1.46V. After this, a 15mM 15CA / 15mM NIFA solution was electropolymerised at 1.46V on top of the pre-formed I5CA layer. A potential of 1.46V was chosen to ensure full oxidation of all the I5CA and NIFA monomers arriving at the polymer surface. The current-time transients for these are shown in fig. 8.19.

A cyclic voltammogram for the 15CA:NIFA copolymer layer produced from the applied potential is shown in fig. 8.20 with a CV of the the I5CA undercoat. This shows that the ferrocene peaks are slightly closer together than those observed after the electropolymerisation of NIFA on its own (fig. 8.18) which constitutes a reduction in the resistance although the redox peaks are still ca. 450mV apart.

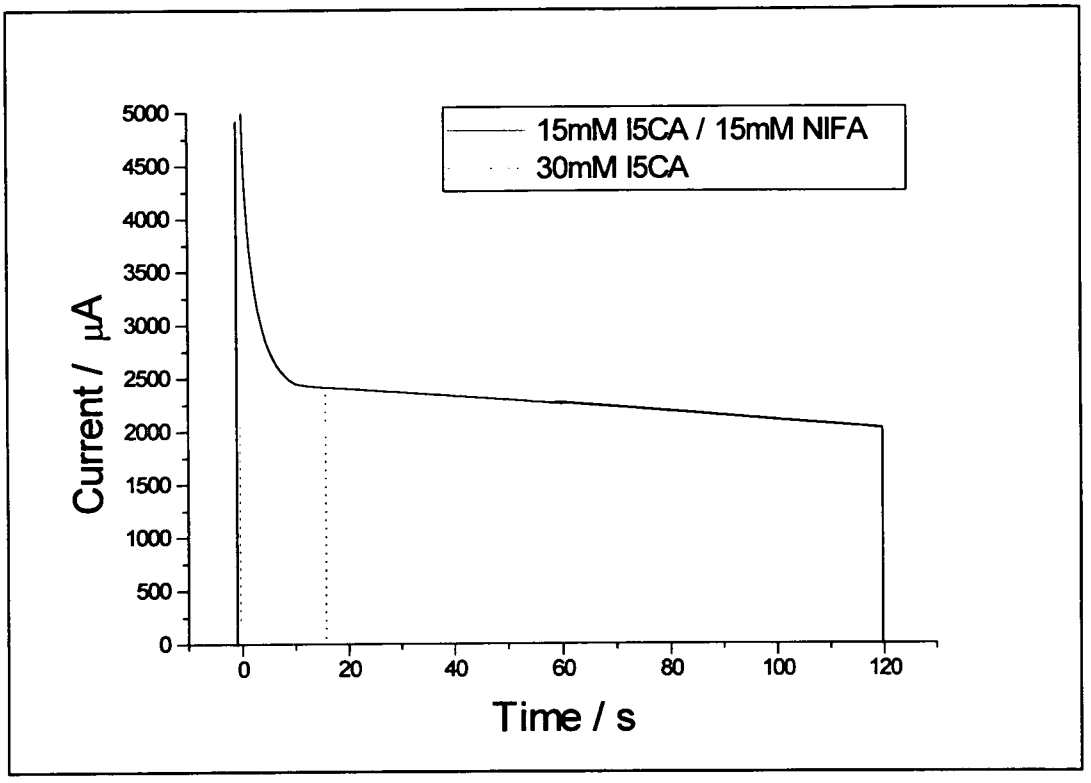

Fig 8.19 - Current-time transients for I5CA / NIFA copolymer formation.

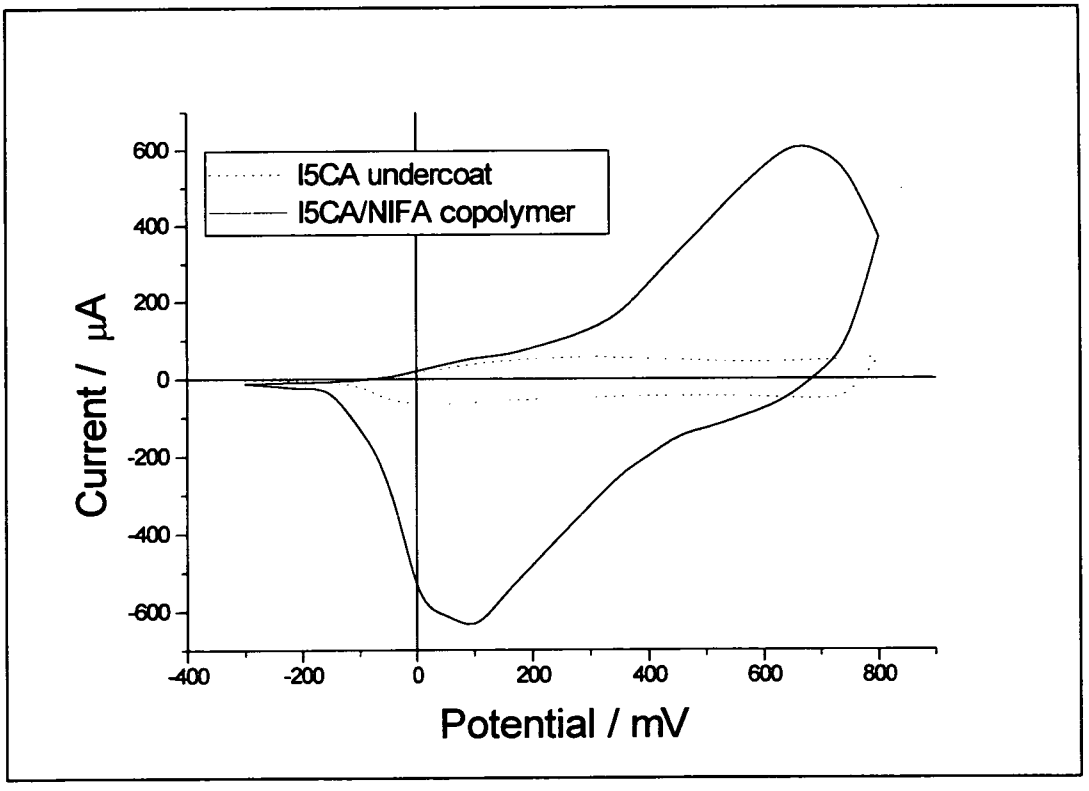

Fig. 8.20 - CV of !5CA/ NIFA copolymer. Sweep rate = 10mV/s.

8.3.6.1 - Control experiment.

It was considered possible that on polymerisation the amide bond may break in the NIFA molecule, leaving free ferrocene groups trapped in the layer. It is possible that this may have produced the type of peaks observed although it is unlikely as the solution electrochemistry does not show any free ferrocene peaks on the reverse sweep (fig. 8.12). A control experiment was run to ascertain if either the redox peaks observed were due to free ferrocene groups that had been trapped in the coat during the polymerisation, or if they were indeed due to covalently bound ferrocene groups in the NIFA molecules. The control experiment consisted of electropolymerising a solution of 15mM I5CA / 15mM ferrocene on top of a preformed I5CA layer (1.46V). The CV obtained, fig. 8.21, showed an increase in charge after electropolymerising the 15CA / ferrocene solution on top of the poly(I5CA) layer. However there is no hint of any free ferrocene redox type peaks in the resultant polymer layer. This suggests that the extra charge is due to the deposititon of further poly(I5CA) on top of the poly(I5CA) already deposited. This indicates that the ferrocene-type redox peaks observed in the previous CVs of NIFA polymerisation, were not due to ferrocene groups trapped in the poly(I5CA) layer, but were due to covalently bound ferroene groups from the electropolymerised NIFA molecules.

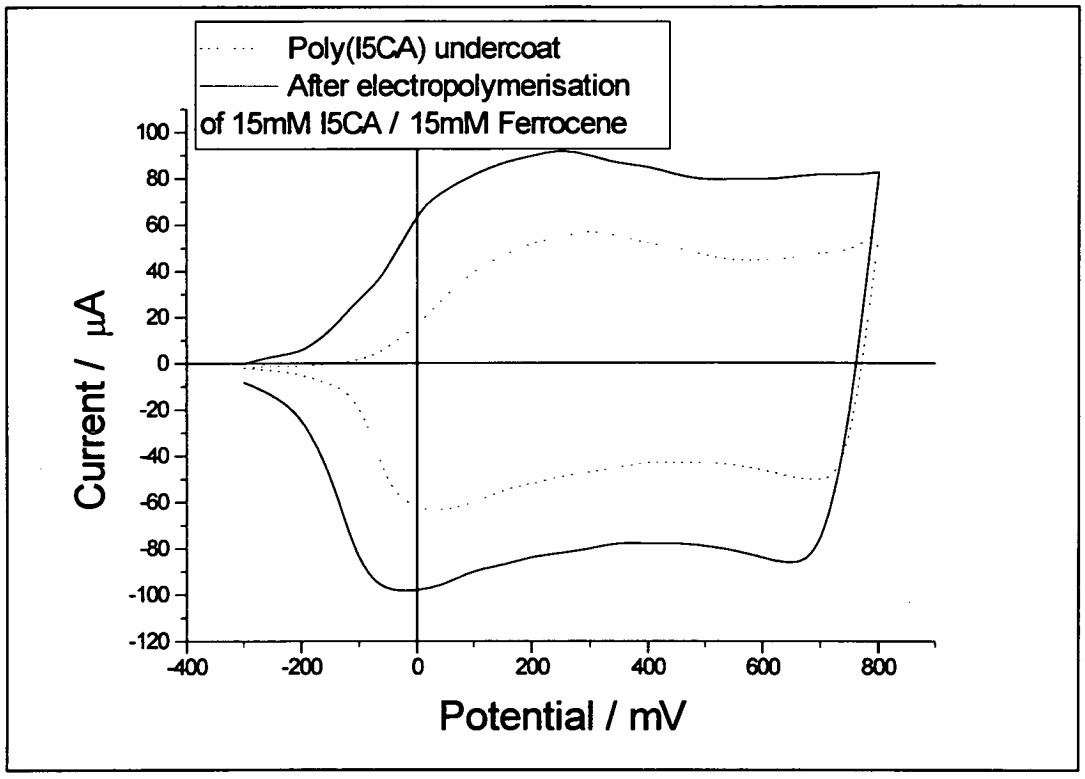

Fig. 8.21 - CVs of poly(I5CA) and I5CA/ferrocene polymerised on top. Sweep rate = 10mV/s.

8.3.6.2 - Drop-coated I5CA / NIFA copolymer.

The layer was washed and ultra-sonicated in dichloromethane and drop-coated on to the working electrode allowing the solvent to evaporate off slowly. The I5CA portion of the layer is not soluble in dichloromethane leaving the soluble NIFA:I5CA copolymer to be dropcoated on to the electrode. A cyclic voltammogram of this drop-coated layer is shown in fig. 8.23.

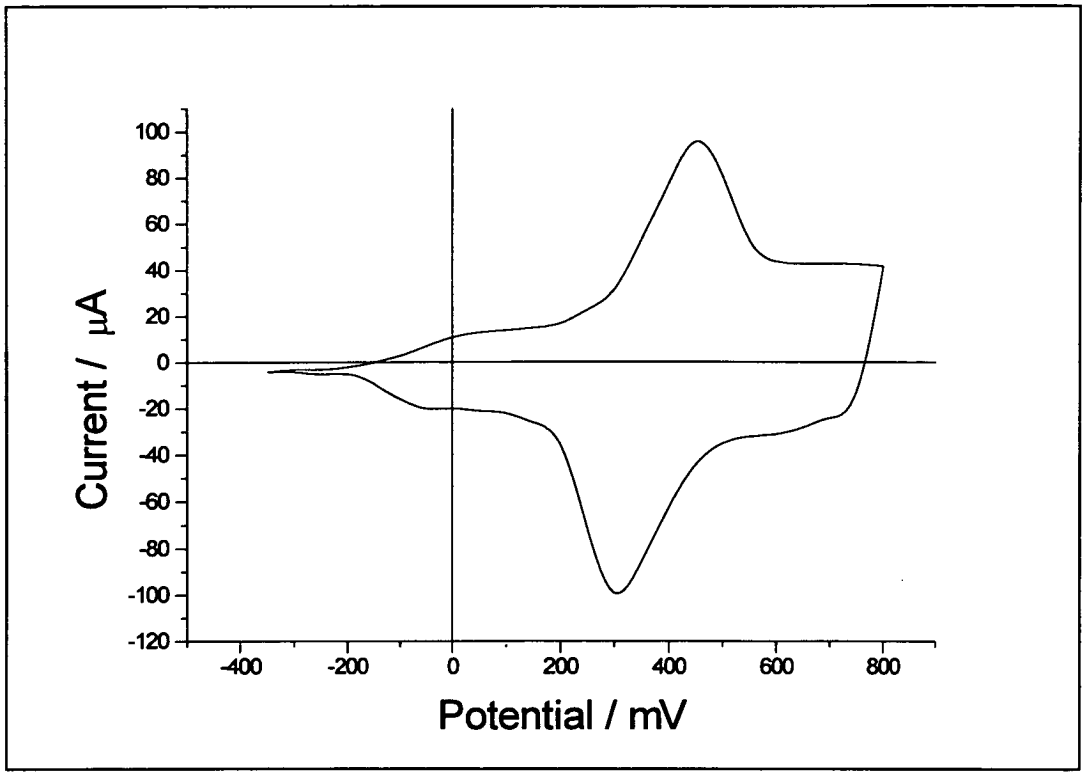

Fig. 8.23 - CV of drop-coated NIFA:I5CA copolymer in background electrolyte. Sweep rate = 10 mV/s.

Fig. 8.23 interestingly shows a CV with the ferrocene group peaks much closer together (peak separation of ca. 100mV) than that for the copolymer on top of the I5CA layer. This is suggested to be due to the fact that the ferrocene groups are present in a much more homogeneous layer that is less resistive. As the film is cycled, the redox peaks remain which shows that the ferrocene groups in the NIFA:I5CA copolymer remain electroactive. The redox reaction peak separation is now equivalent to that observed for the NIFA monomer (ca. 100mV in fig. 8.12) which suggests that there is very little resistance in this film. The half wave potential of the ferrocene groups in this copolymer is approximately 375 mV, this compares with potentials of approximately 290 mV in the NIFA monomer and around 90mV for pure ferrocene. This indicates that the ferrocene groups observed in the copolymer, are probably linked to a different species than in either the NIFA monomer, or pure ferrocene. As the potential of these redox peaks is somewhat higher, it suggests that the ferrocene groups experience a greater electron-withdrawing effect than an

indole ring monomer. This is consistent with a ferrocene group linked to an oxidised trimer species.

The charge in the CV under the ferrocene redox peaks compared with the I5CA redox peaks, shows that there is approximately one ferrocene group per trimer centre which would be expected for the 1:1 copolymerisation undertaken. This is a relatively high concentration of ferrocene groups which is an important result for the possible use in certain bio-technology applications that require a large concentration of electron transfer sites.

The formation of a conducting polymer film with redox active ferrocene groups that are covalently bound to the polymer backbone has now been achieved. The ferrocene groups are delocalised in to the copolymer to a large extent, which suggests a wide scope for this type of functionalisation method for the realisation of tailored sensor devices. The NIFA:I5CA conducting copolymer may also be useful for the mediated electron transfer to certain redox active enzymes although testing of this was beyond the scope of this work.

8.4 - Conclusions.

(1) It was shown that a 5-substituted monomer could be chemically derivitised to form an indole molecule with a covalent attachment to a ferrrocene molecule, N-(5'-indole)ferroceneamide, (NIFA).

(2) The NIFA was copolymerised with I5CA to form a copolymer containing REDOX active ferrocene groups. The potential at which the redox reaction of the ferrocene groups was observed was shifted by approximately by 85mV relative to the NIFA monomer and 285mV relative to ferrocene. This indicated that there was a substantial electronic communication between the ferrocene groups and the indole trimer centres. It was estimated that there was approximately one ferrocene group per trimer centre in the copolymer which results in a large concentration of ferrocene groups.

References

1 C.K.Chiang, C.R.Fincher,Y.W.Park, A.J.Heeger, H.Shirakawa, E.J.Louis, S.C.Gau and A.G. MacDiarmid.; *Phys. Rev. Lett.*, 1977, **39**, 1098.

2 T. Ito, H. Shirakawa and S. Ikada.; *J. Polym. Sci. Polym. Chem. Ed,* 1974, **12**, 11.

3 J.H.Edwards, W.J.Feast and D.C.Bott.; *Polymer*, 1984, **25**, 395-398

4 J.W. Lin and L.P. Dudek.; *J. Polym. Sci.* 1980, **18**, 2869.

5 M. Kobayashi, J. Chen, T.C. Maraes, A.J. Heeger, F. Wudl.; *Synth. Met.* 1984, **9**, 77.

6 J.Prejza, I.Lundstrom and T.Skotheim.;*J. Electrochem. Society*, 1981, **128**, 1625.

7 E.M.*Genies, G.Bidan and A.F.Diaz.;J. Electroanal. Chem*, 1983, **149**, 101-113.

8 Instrumental Methods in Electrochemistry.; Southampton Electrochemistry Group, Ellis Horwood, 1985.

9 C.P. Andrieux, P. Audebart, P. Hapiot, J.M. Saveant.; *J. Am. Chem. Soc.* 1990, **112**, 2439.

10 K. Tanaka, T. Shichiri, S. Wang, and T. Yamabe.; *Synth. Met.* 1988, **24**, 203.

11 G.B. Street, T.C. Clarke, M. Icrounbi, K.K. Kanazawa, V. Lee, P.Pfluger, J.C. Scott and G.Weiser.; *Mol. Cryst. Liq. Cryst.* 1982, **83**, 253.

12 E. Genies, G. Bidan, A.F. Diaz.; *J. Electroanal. Chem.* 1983, **149**, 113.

13 J.L.Bredas, B.Themas, J.G.Fripat, J.M.Andre and R.R.Chance.; *Phys. Rev. B*, 1984, **29**, 6761

14 S.H.Glarum and J.H.Marshall.; *J. Physical Chemistry*, 1988, **92**, 4210-4217

15 G.B.Street.; *Handbook on Conducting Polymers*, Marcel Dekker, New York, 1986

16 J.C.Scott, P.Fluger, M.T.Krounbi and G.B.Street.; *Physical Rev B - Condensed Matter*, 1983, **28**(4), 2140-2145

17 K. Yakushi, L.J. Lauehlan, T.C. Clarke, G.B. Street, *J. Chem. Phys.* 1983, **79**, 4774.

18 J.L. Bredas and G.B. Street.; *Acc. Chem. Res.* 1985, **18**, 309.

19 N.E. Mott and E.A. Davis.; *Electronic processes in non-crystalline materials*, Oxford Clarendon Press, 2nd edition, 1979.

20 P. Sheng.; *Phys. Rev.* 1980, **1321**, 2180.

21 R.R. Chance, J. L. Bredas and R. Silbey.; *Phys. Rev.* 1984, **B29**, 449.

22 S.J. Xie, L.M. Mie, D.L. Lin,; *Phys.-Conden. Matter,* 1994, **50**, 13364

23 A. Bhattacharya, A. De, S. Das,; *Polymer,* 1996, **37**, 4375.

24 W.J.Albery and C.C.Jones.; *Faraday. Discussions of the Chemical Society*, 1984, **78**, 193-201

25 W.R.Salaneck, R.Eriandson, J.Prezja, I.Lunsdstrom and O.Inganas.; *Synthetic Metals*, 1983, **5**(2), 125-139

26 F.Garnier, G.Tourillon, J.Y.Barraud and H.Dexpert.; *J. Materials Science*, 1985, **20**(8), 2687-2694

27 F.Genoud, M.Guglielmi, M.Neichstein, E.Genies and M.Slamon.; *Phys. Rev. Lett.*, 1985, **55**, 118

28 E.M.Genies and M.Lapkowski.; *J. Electroanal. Chem.*, 1987, **220**, 67-82

29 E.M.Genies and M.Lapkowski.; *J. Electroanal. Chem.*, 1987, **236**, 199-208

30 K.K.Kanazawa, A.F.Diaz, W.D.Gill, P.M.Grant, G.B.Street, G.P.Gardini and J.F.Kwak.; *Synthetic Metals*, 1980, **1**, 329

31 A.F.Diaz, K.K.Kanazawa and G.P.Gardini.; *J. Chem. Soc. Chem. Comm.*, 1979, 635-636

32 K.K.Kanazawa, A.F.Diaz, R.H.Geiss, W.D.Gill, J.F.Kwak, J.A.Logan, J.F.Rabolt and G.B.Street.; *J. Chem. Soc. Chem. Comm.*, 1979, 854

33 A.F.Diaz, J.I.Castillo, J.A.Logan and W-Y.Lee.; *J. Electroanal. Chem.*, 1981, 129, 115-132

34 M.Saloma, M.Aguilar, M.Salmon.; *J. Electrochemical Society*, 1985, **132**, 2379

35 D. Delabouglise, J. Roncali, M. Lemaire, F. Garnier,; *J. Chem. Soc. Comm,* 1989, 475-477.

36 M.Salmon, M.E.Carbajal, M.Aguilar, M.Saloma and J.C.Juarez.; *J. Chem. Soc. Chem. Comm.*, 1983, 1532-1533

37 A.F.Diaz, J.I.Crowley, J.Bargon, G.P.Gardini and J.B.Torrance.; *J. Electroanal. Chem.*, 1981, **121**, 355-361

38 R.J. Waltman, J. Bargon.; *J. Tetrahedron*, 1984, **40**, 3963.

39 G. Tourillon, F. Garnier.; *J. Phys. Chem.* 1983, **87**, 2289.

40 M.Sato, S.Tanaka and K.Kaeriyama.; *J. Chem. Soc. Chem. Comm.*, 1986, 873-874

41 M.R.Bryce, A.Chissel, P.Kathirgamanathan, D.Parker and N.R.M.Smith.; *J. Chem. Soc. Chem. Comm.*, 1987, 466-467

42 W.Büchner, R.Garreau, M.Lemaire and J.Roncali.; *J. Electroanal. Chem*, 1990, **277**, 355

43 J. Roncali, F. Garnier, R. Garreau, M. Lemaire.; *J. Chem. Phys.* 1989, **86(1)**, 93

44 F. Wudl, M. Kobayashi, A.J. Heeger.; *J. Org. Chem.* 1984, **44**, 3382

45 T.C. Laubet, J.P. Ferraris.; *J. Chem. Soc. Chem. Commun.* 1991, 752

46 A. Bolognesi, M. Catellani, S. Desti, R. Zamboni, T. Taliani.; *J. Chem. Soc. Chem. Commun.* 1988, 246.

47 R.J. Waltman, J. Bargon, A.I. Diaz, *J. Phys. Chem.* 1983, **87**, 2289.

48 J. Roncali , P. Marque, R. Garreau, F. Garnier, M. Lemaire.; *Macromolecular.* 1990, **23**, 1347.

49 B. Zinger, Y. Greenwald, I. Rubinstein.; *Synth. Met.* 1991, **41-43**, 583.

50 M.Lemaire, R.Garreau, D.Delabouglise, J.Roncali, K.Youssoufi and F.Garnier.; *New. J. Chemistry*, 1990, **14**, 359

51 O. Vogl, G.D. Jaycox.; *Chemtech.* 1986, **Nov**, 698.

52 J.Roncali.; *Chemical Reviews*, 1992, **92**, 711-738

53 D.Delabouglise and F.Garnier.; *New. J. Chemistry*, 1991, **15**, 233-234

54 R.J. Waltman, A.F. Diaz, J. Bargon.; *J. Electrochem. Soc.* 1985, **132**, 632

55 J. Bargon, S. Mohmand, R.J. Wlatman.; *IBM. J. Res. Dev.* 1983, **27**, 330

56 M. Sato, K. Kaeriyama, K. Someno.; *Macromol. Chem.* 1983, 2241-2249

57 A.K. Bakhshi and J. Cadik.; *Synth. Met.* 1989, **30**, 115

58 P. Bauerle, K. U. Gaudl.; *Synth. Met.* 1991, **41-43**, 3037

59 P. Bauerle, K. U. Gaudl.; *Adv. Mater.* 1990, **2**, 185.

60 R. Mirrazaei, D. Parker, M.S. Munro.; *Synth. Met.* 1989, **30**, 265

61 D.Delabouglise and F.Garnier.; *Synthetic Metals*, 1989, **39**, 117

62 J.M. Cooper, D.G. Morris, K.S. Ryder.; *J. Chem. Soc. Chem. Commun.* 1995, 697-698

63 E.E.Havinga, W.Hoeve and H.Wynnberg.; *Polymer Bulletin*, 1992, **29**, 119-126

64 E.E. Havinga, L.W. Horssen,; *Macromol.* 1989, **24**, 67.

65 P.Novák and W.Vielstich.; *J. Electroanal. Chem.*, 1991, **300,** 99-110

66 J.P. Ferraris, R.T. Hanlon.; *Polymer.* 1989, **30**, 1319.

67 Q.Pei, O.Inganäs, J. Österholm and J.Laakso.; *Polymer*, 1993, **34**(2), 247-252

68 J. Roncali, F. Garnier.; *J. Phys. Chem.* 1988, **92**, 833.

69 S.E. Lindsey, G.B. Street.; *Synth. Met.* 1985, **10**, 67.

70 X.H. Yin, K. Yoshino, H. Yamamoto, T. Watanuki, I. Isa, S. Nakagawa, M. Aduchi,; *Jap. J. Appl. Phys.* 1994, **33**, 6a, 3597.

71 V. Mano, M.I. Felisberti, T. Matencio, M.A. Depaoli,; *Polymer*, 1996, **37**, 5165.

72 G. Nagosubramanian, S. Di Stefano, J. Moacoanin.; *J. Phys. Chem.* 1986, **90**, 4447-4451

73 K. Imanshi, M. Satoh, Y. Yasuda, R. Tsushima, S. Aoki,; *J. Electroanal. Chem.* 1988, **242**, 203.

74 F. Garnier, G. Tourillon, J. Y. Barroud, H. Dexpert.; *J. Mater. Sci.*

75 R. John, G.G. Wallace.; *Polymer International,* 1992, **27**, 255-260

76 S. Roth, H. Bleir, W. Pukacki.; *Faraday Discuss. Chem. Soc.* 1989, **88**, 223.

77 A.R. Hillman, E. Mallen.; *J. Electroanal. Chem.* 1987, **220**, 351.

78 D. Delabouglise, R. Garreau, M. Lemaire, J. Roncali.; *New. J. Chem.* 1988, **12**, 155.

79 J. Roncali, F. Garnier, M. Leamaire, R. Garreau.; *Synth. Met.* 1986, **15**, 323.

80 Z. Deng, W.H. Smyrl, H.S. White.; *J. Electrochem. Soc.* 1989, **136**, 2152.

81 S. Aeiyach, A. Kone, M. Dieng, J.J. Aaron, P.C. Lacaze. *J. Chem. Soc. Chem. Commun.* 1991, 852.

82 Y. Lin, G.G. Wallace, *Electrochimica Acta.* 1994, **39**, 1409.

83 M. Gratzl, H. Duan-Fu, A.M. Riley, J. Janata.; *J. Phys. Chem.* 1990, **94**, 1594.

84 J. Roncali, F. Garnier.; *New J. Chem.* 1986, **4-5**, 237.

85 A. Watanabe, K. Mori, Y. Iwasaki, Y. Nakmura,; *J. Chem. Soc. Chem. Comm.,* 1987 3-4.

86 A. Nazzal, G.B. Street,; *J. Chem. Soc. Chem. Comm.,* 1984, 83-84

87 D. Beljonne, Z Shuai, J.L. Bredas, *J. Chem. Phys.* 1993, **98**, 11, 8819 - 8828.

88 E.M. Genies,; *New J. Chem.* 1991, **15**, 373.

89 C.G. Smith, R.A. Nyquist, P.B. Smith, A.J. Pasztor, S.J. Martin,; *Anal. Chem.* 1991, **63**, 11R-32R.

90 H.J. Zhao, A. Mirmoseni, W.E. Price, A. Talaie, G.G. Wallace.; *J. Intelligent Mater. systems.* 1994, **5**, 605.

91 J.P. Nigrey, A.G. Macdirmid, A.J. Heeger.; *J. Chem. Soc. Chem. Commun.* 1979, 594.

92 J.Y. Lee, L.H. Ong, G.K. Chuah,; *J. Appl. Electrochem.* 1992, **22**, 738-742.

93 R.J.Waltman, A.F.Diaz and J.Bargon.;*J. Electrochemical Society*, 1984, **131**, 1452

94 H. Yaschima, M. Kobayashi, K.B. Lee, D. Chung, A.J. Heeger, F. Wudl.; *J. Electrochem. Soc.* 1987, **W4**, 46.

95 K. Yoshiro, S. Hayashi, Y. Kohno, K. Kareto, J. Okube, T. Moniya, J. Pu.; *J. Appl. Phys.* 1984, **23**, 2198.

96 R.B.Bjorklund and I.Lundström.; *J.Electronic Materials*, 1984, **13**, 211

97 T.C. Pearce, J.W. Gardner, S. Friel, P.N. Bartlett, N. Blair.; *Analyst,* 1993, **118**, 371-377.

98 J.H. Burroughes, C.D.D. Bradley, A.R. Brown, R.N. Marks, K Mackay, R.H. Friend, P.L. Burn, A.B. Holmes,; *Nature*, 1990, **347**, 539.

99 R.Noufi, A.J.Frank and A.J.Novik.; *J. American Chemical Society*, 1981, **103**, 849

100 A.S. Sarac, B. Ustamehmetoglu, E. Sezer, C. Erbil,; *Turkish J. Chem.* 1996, **20**, 80-87.

101 W.H. Meyer, H. Kiess, B. Binggeli, E. Meier, G. Harbeke.; *Synth. Met.* 1985, **10**, 255.

102 G.Tourillon and F.Garnier.; *J. Electroanal. Chem*, 1982, **135**, 173-178

103 C.J. Nielsen, R. Stotz, G.T. Cheek, R.F. Nelson.; *J. Electroanal. Chem.* 1978, **90**, 127.

104 D.Billaud, E.B.Maarouf and E.Hannecart.; *Materials Research Bulletin*, 1994, **29**(12), 1239-1246

105 J.M.Bobbitt, C.L.Kulkarni and J.P.Willis.; *Heterocycles*, 1981, **15**(1), 495-516

106 R.J.Waltman, A.F.Diaz and J.Bargon.;*J.Physical Chemistry*, 1984, **88**, 4343-4346

107 R.J.Waltman and J.Bargon.; *Canadian J.Chemistry*, 1986, **64**(1), 76-95

108 P.N.Bartlett, D.H.Dawson and J.Farrington.; *J.Chem.Soc.Faraday Trans.*, 1992, **88**(18), 2685-2695

109 G.Zotti, S.Zecchin, G.Schiavon, R.Sergaglia, A.Berlin and A. Canavesi.; *Chem. Materials*, 1994, **6**, 1742-1748

110 K. Jackowska and J. Bukowska,; *Polish J. of Chem.* 1992, **66**, 1477

111 H. Tabli, E.B. Maarouf, B. Humbert, M. Alnot, J.J. Ehrhardt, J. Ghanbaja, D. Billaud,; *J. Phys. Chem. Solids.* **57**, 1145-1151.

112 J.G. Mackintosh.; *PhD Thesis*, 1996, University of Edinburgh.

113 J.G. Mackintosh, C.R. Redpath, A.C. Jones, P.R.R. Langridge-Smith, A.R. Mount.; *J. Electroanal. Chem.* 1995, **388**, 179-185.

114 J.G. Mackintosh, C.R. Redpath, A.C. Jones, P.R.R. Langridge-Smith, A.R. Mount, D. Reed.; *J. Electroanal. Chem,* 1994, **374**, 163.

115 D. Billaud, E.B. Maarouf, E. Hannecart.; *Synth. Met.* 1995, **69**, 571.

116 T. Kaneko, M. Matsuo.; *Heterocycles*, 1979, **12(4)**, 471.

117 J. Bergman, N. Eklund.; *Tetrahedron,* 1980, **36**, 1445.

118 E.B. Maarouf, D. Billand, E. Hannecart.; *Materials Res. Bull.* 1994, **29(6)**, 637.

119 P.N. Bartlett, J. Farrington.; *Bulletin of Electrochemistry.* 1992, **8(5)**, 208.

120 S.W. Kong, K.M. Choi, K.H. Kim.; *J. Phys. Chem. Solids.* 1992, **53(5)**, 657.

1 21 Southhampton Electrochemistry group, *"Instrumental Methods in Electrochemstry"* , 1985, Ellis Horwood.

122 V.G. Levich,; *Acta Phys. Chim. USSR,* 1942, **17**, 257.

123 C.M.A. Brett, A.M.O. Brett,; *" Electrochemistry: Principles, Methods and Applications".* 1993, Oxford Science Publications.

124 A.J. Bard, L.R. Faulkner,; *"Electrochemical Methods". 1980, J. Wiley & Sons.*

125 S.A. Soper, L.B. McGown, I.M. Warner,; *Anal. Chem.* 1994, **66** 428R- 444R.

126 E.A.V. Ebsworth, D.W.H. Rankin, S. Cradock, *Structural Methods In Inorganic Chemistry.* 1987, Blackwell Scientific Publications

127 W.G. Jenkins, S.S.H. Sadeghi, J.P. Wikswo,; *J. Physics and App. Physics.* 1997, **30(3)**, 293-323.

128 A.R.Mount; *PhD Thesis,* Imperial college. London, 1987.

129 M.J. Dale, A.C. Jones, P.R.R. Langridge-Smith, K.F. Costello, P.G. Cummins,; *Analytical Chemsitry,* 1993, **65**, 793-801.

130 I.A. Mowat, *PhD Thesis,* University of Edinburgh, 1996

131 J. Daschbach, D. Blackwood, J.W. Pons, S. Pons,; *J. Electroanal. Chem.* 1987, **237(2)**, 269-273.

132 K. Pekmez, A. Yildiz,; *International J. Research Phys. Chem.* 1996, **196(1)**, 109-123.

133 G. Tourillon, D. Gouriez, F. Garnier, D. Vivien,; *J. Phys. Chem.* 1984, **88**, 1049.

134 I.A. Mowat, R.J. Donovan, RRJ Maier,; *Rapid Comm. Mass Spec.* 1997, **11(1)**, 89-98.

135 T. Kaneko, M. Matsuo, Y. Iitaka, *Chem. Pharm. Bull.* 1981, **29**, 12, 499-3506

136 P. Li, J.Y. Lin, K.L. Tan, J.Y. Lee,; *Electrochimica Acta.* 1997, **42(4)**, 60-615.

137 J.P. Morgan, M. Daniels, *J. Phys. Chem,* 1982, **86**, 20, 4004-4007.

138 A. Wildeberg,; *ERASMUS Project.* 1997, University of Edinburgh.

139 N. Kitamura, K. Nakatani, H.B. Kim, *Pure and applied Chemsity,* 1995, **67**, 1, 79-86.

140 A. Deronzier, J.C. Moutet,; *Coord. Chem. Rev.* 1996, **147**, 339-371.

141 D.F. Shriver, P.W. Atkins, C.H. Langford,; *Inorganic chemistry,* 1990, OUP.

142 A.J. Zara, S.S. Machado, L.O.S. Bulchoes, A.V. Benedetti, T. Rabockai,; *J. Electroanal. Chem.* 1987, **221(1-2)**, 165-174.

143 W. Schuhmann,; *Biosensors and Bioelectronics*, 1995, **10(1-2)**, 181-193.

144 S.J. Sadeghi, A.E.G. Cass,; *Biochemical Soc. Trans.* 1995, **23(2)**, 153.

145 Y. Kashiwagi, T. Osa,; *Chem. Lett.* 1993, **4**, 677-680.

146 G.W. Harwood, C.W. Pouton,; *Advanced Drug Delivery Reviews,* 1996, **18(2)**, 163-191.

147 *Chem. Rev.* 1991, **91**, 165-195

148 J. Dschbach, D. Blackwood, J.W. Pons, S. Pons,; *J. Electroanal. Chem.* 1987, **237(2)**, 269-273.

149 A.Badia, R. Carlini, A. Fernandez, F. Bataglini, S.R. Mikkelsen, .M. English. *J. Am. Chem. Soc.* 1993, **115**, 16, 7053-7060.

150 J.G. Mackintosh, S.W. Wright, P.R.R. Langridge-Smith and A.R. Mount,; *J.Chem. Soc. Farraday Trans.* 1996, **92**(20), 4109-4114.

151 F.A. Cotton and G. Wilkinson,; *Advanced Inorganic Chemistry,* 4th Edition, John Wiley & Sons.

152 A.J. Bard and L.R. Faulkner,; *Electrochemical Methods*, 1980, John Wiley & Sons.

153 K.M. Mackay and R.A. Mackay,; *Introduction to Modern Inorganic Chemistry,* 4th Edition, Blackie.

Appendix

Crystal structure data

Empirical formula of N-(5'-indole)ferroceneamide = $C_{19}H_{16}N_2FeO$

Formula weight	344.19	
Temperature	150 K	
Wavelength	0.71073 Å	
Crystal system	Orthorhombic	
Space group	P2(1)2(1)2(1)	
Unit cell dimensions	a = 9.7889(12) Å	alpha = 90°
	b = 11.4799(14) Å	beta = 90°.
	c = 13.548(2) Å	gamma = 90°.
Volume	1526.5(3) A^3	
Z	4	
Density	1.498 Mg/m^3	
Absorption coefficient	0.993 mm^{-1}	
F(000)	712	
Crystal size	0.51 x 0.31 x 0.12 mm	
Theta range	2.56 to 25.03 deg.	
Reflections collected	3263	
Independent reflections	1920 [R(int) = 0.0203}	
Refinement method	Full matrix least squares on F^2	

Data / restraints / parameters	1918 / 0 / 208	
Goodness of fit on F^2	1.057	
Final R indices [I>2sigma(I)]	R1 = 0.0320,	wR2 = 0.0655
R indices (all data)	R1 = 0.0392,	wR2 = 0.0692
Absolute strucure parameter	0.05(3)	
Lagest diff. peak and hole	0.261 and -0.324 e.A^{-3}	

Atomic coordinates (x 10^4) and equivalent isotropic displacement parameters (A^2 x 10^3) for 1.
U(eq) is defined as one third of the trace of the orthogonalized Uij tensor.

n	x	y	z	U(eq)
N(1)	4058(4)	772(3)	5810(2)	36(1)
C(2)	5145(5)	245(4)	6236(3)	38(1)
C(3)	6088(5)	1048(3)	6523(3)	35(1)
C(4)	5544(4)	2165(3)	6262(2)	28(1)
C(5)	5985(4)	3320(3)	6384(2)	28(1)
C(6)	5156(4)	4205(3)	6080(3)	27(1)
N(6)	5608(3)	5395(3)	6216(2)	29(1)
C(61)	6504(4)	5900(3)	5604(2)	25(1)
O	6792(3)	5479(2)	4790(2)	30(1)
C(7)	3878(5)	3987(3)	5646(2)	33(1)
C(8)	3431(4)	2865(4)	5511(2)	35(1)
C(9)	4258(4)	1962(4)	5821(2)	30(1)
Fe	8965(1)	6981(1)	6652(1)	25(1)
C(1R)	7147(4)	6999(3)	5938(2)	23(1)
C(2R)	7015(4)	7534(3)	6892(2)	27(1)
C(3R)	7920(4)	8489(3)	6921(3)	29(1)
C(4R)	8617(4)	8560(3)	6001(3)	28(1)
C(5R)	8143(4)	7650(3)	5400(2)	28(1)
C(6R)	9690(4)	5308(3)	6713(3)	39(1)
C(7R)	9456(5)	5746(4)	7672(3)	49(1)
C(8R)	10263(5)	6741(4)	7804(3)	49(1)
C(9R)	11000(4)	6932(4)	6930(3)	44(1)
C(10R)	10665(4)	6053(4)	6257(3)	37(1)

Bond lengths [Å] and angles [deg.]

N(1)-C(2)	1.354(5)	N(1)-C(9)-C(4)	107.1(4)	C(3R)-C(2R)-C(1R)	107.4(3)
N(1)-C(9)	1.381(5)	C(1R)-Fe-C(9R)	162.14(14)	C(3R)-C(2R)-Fe	70.0(2)
C(2)-C(3)	1.362(5)	C(1R)-Fe-C(5R)	41.24(14)	C(1R)-C(2R)-Fe	68.8(2)
C(3)-C(4)	1.432(5)	C(9R)-Fe-C(5R)	123.7(2)	C(2R)-C(3R)-C(4R)	108.7(3)
C(4)-C(5)	1.405(5)	C(1R)-Fe-C(8R)	156.6(2)	C(2R)-C(3R)-Fe	69.6(2)
C(4)-C(9)	1.413(5)	C(9R)-Fe-C(8R)	40.5(2)	C(4R)-C(3R)-Fe	69.6(2)
C(5)-C(6)	1.363(5)	C(5R)-Fe-C(8R)	160.4(2)	C(5R)-C(4R)-C(3R)	108.0(3)
C(6)-C(7)	1.405(6)	C(1R)-Fe-C(2R)	41.48(13)	C(5R)-C(4R)-Fe	69.3(2)
C(6)-N(6)	1.448(4)	C(9R)-Fe-C(2R)	154.0(2)	C(3R)-C(4R)-Fe	69.5(2)
N(6)-C(61)	1.340(5)	C(5R)-Fe-C(2R)	69.22(14)	C(4R)-C(5R)-C(1R)	108.5(3)
C(61)-O	1.239(4)	C(8R)-Fe-C(2R)	120.3(2)	C(4R)-C(5R)-Fe	70.4(2)
C(61)-C(1R)	1.482(5)	C(1R)-Fe-C(7R)	122.6(2)	C(1R)-C(5R)-Fe	69.2(2)
C(7)-C(8)	1.373(5)	C(9R)-Fe-C(7R)	67.9(2)	C(7R)-C(6R)-C(10R)	107.2(4)
C(8)-C(9)	1.381(5)	C(5R)-Fe-C(7R)	157.6(2)	C(7R)-C(6R)-Fe	69.4(2)
Fe-C(1R)	2.026(3)	C(8R)-Fe-C(7R)	40.2(2)	C(10R)-C(6R)-Fe	69.6(2)
Fe-C(9R)	2.028(4)	C(2R)-Fe-C(7R)	109.2(2)	C(8R)-C(7R)-C(6R)	108.5(4)
Fe-C(5R)	2.032(3)	C(1R)-Fe-C(3R)	68.7(2)	C(8R)-C(7R)-Fe	69.7(2)
Fe-C(8R)	2.035(4)	C(9R)-Fe-C(3R)	118.8(2)	C(6R)-C(7R)-Fe	70.1(2)
Fe-C(2R)	2.039(4)	C(5R)-Fe-C(3R)	68.3(2)	C(7R)-C(8R)-C(9R)	108.0(4)
Fe-C(7R)	2.039(4)	C(8R)-Fe-C(3R)	106.8(2)	C(7R)-C(8R)-Fe	70.1(2)
Fe-C(3R)	2.044(4)	C(2R)-Fe-C(3R)	40.42(14)	C(9R)-C(8R)-Fe	69.5(2)
Fe-C(4R)	2.045(3)	C(7R)-Fe-C(3R)	125.8(2)	C(10R)-C(9R)-C(8R)	108.6(4)
Fe-C(10R)	2.047(4)	C(1R)-Fe-C(4R)	68.8(2)	C(10R)-C(9R)-Fe	70.6(2)
Fe-C(6R)	2.049(4)	C(9R)-Fe-C(4R)	105.6(2)	C(8R)-C(9R)-Fe	70.0(2)
C(1R)-C(5R)	1.429(5)	C(5R)-Fe-C(4R)	40.29(14)	C(9R)-C(10R)-C(6R)	107.8(4)
C(1R)-C(2R)	1.440(4)	C(8R)-Fe-C(4R)	123.8(2)	C(9R)-C(10R)-Fe	69.1(2)
C(2R)-C(3R)	1.410(5)	C(2R)-Fe-C(4R)	68.7(2)	C(6R)-C(10R)-Fe	69.7(2)
C(3R)-C(4R)	1.426(5)	C(7R)-Fe-C(4R)	161.6(2)	O-C(61)-N(6)	122.3(4)
C(4R)-C(5R)	1.404(5)	C(3R)-Fe-C(4R)	40.81(14)	O-C(61)-C(1R)	120.6(3)
C(6R)-C(7R)	1.415(6)	C(1R)-Fe-C(10R)	126.4(2)	N(6)-C(61)-C(1R)	117.1(3)
C(6R)-C(10R)	1.423(5)	C(9R)-Fe-C(10R)	40.2(2)	C(8)-C(7)-C(6)	120.4(4)
C(7R)-C(8R)	1.400(7)	C(5R)-Fe-C(10R)	107.4(2)	C(7)-C(8)-C(9)	118.4(4)
C(8R)-C(9R)	1.407(5)	C(8R)-Fe-C(10R)	67.9(2)	C(8)-C(9)-N(1)	131.0(4)
C(9R)-C(10R)	1.401(5)	C(2R)-Fe-C(10R)	164.9(2)	C(8)-C(9)-C(4)	121.9(4)
C(2)-N(1)-C(9)	109.0(4)	C(7R)-Fe-C(10R)	68.0(2)	C(10R)-Fe-C(6R)	40.7(2)
N(1)-C(2)-C(3)	110.6(4)	C(3R)-Fe-C(10R)	153.4(2)	C(5R)-C(1R)-C(2R)	107.4(3)
C(2)-C(3)-C(4)	106.5(4)	C(4R)-Fe-C(10R)	118.9(2)	C(5R)-C(1R)-C(61)	125.3(3)
C(5)-C(4)-C(9)	118.6(4)	C(1R)-Fe-C(6R)	109.5(2)	C(2R)-C(1R)-C(61)	126.9(3)
C(5)-C(4)-C(3)	134.6(3)	C(9R)-Fe-C(6R)	68.1(2)	C(5R)-C(1R)-Fe	69.6(2)
C(9)-C(4)-C(3)	106.8(3)	C(5R)-Fe-C(6R)	121.7(2)	C(2R)-C(1R)-Fe	69.7(2)
C(6)-C(5)-C(4)	119.0(4)	C(8R)-Fe-C(6R)	68.0(2)	C(61)-C(1R)-Fe	120.7(2)
C(5)-C(6)-C(7)	121.6(3)	C(2R)-Fe-C(6R)	127.6(2)	C(61)-N(6)-C(6)	121.9(3)
C(5)-C(6)-N(6)	118.8(3)	C(7R)-Fe-C(6R)	40.5(2)	C(4R)-Fe-C(6R)	154.9(2)
C(7)-C(6)-N(6)	119.5(4)	C(3R)-Fe-C(6R)	163.7(2)		

Symmetry transformations used to generate equivalent atoms:

Appendix II

List of figure legends

Chapter 1 - Introduction

Chapter 2 - Theory

Chapter 3 - Experimental

Chapter 4 - Polymerisation of 5-substituted indoles

Chapter 5 - Electrooxidation of N-methylindole

Chapter 6 - Electroxidation of 5-aminoindole

Chapter 7 - Copper ion sensor

Chapter 8 - Ferrocene incorporation